

INTERNATIONAL THEORY, RESEARCH AND REVIEWS IN

ENGINEERING

October 2023

EDITORS

PROF. DR. COŞKUN ÖZALP
ASSOC. PROF. DR. SELAHATTİN BARDAK

Genel Yayın Yönetmeni / Editor in Chief • C. Cansın Selin Temana

Kapak & İç Tasarım / Cover & Interior Design • Serüven Yayınevi

Birinci Basım / First Edition • © Ekim 2023

ISBN • 978-625-6760-12-7

© copyright

Bu kitabın yayın hakkı Serüven Yayınevi'ne aittir.

Kaynak gösterilmeden alıntı yapılamaz, izin almadan hiçbir yolla çoğaltılamaz.

The right to publish this book belongs to Serüven Publishing. Citation can not be shown without the source, reproduced in any way without permission.

Serüven Yayınevi / Serüven Publishing

Türkiye Adres / Turkey Address: Kızılay Mah. Fevzi Çakmak 1. Sokak

Ümit Apt No: 22/A Çankaya/ANKARA

Telefon / Phone: 05437675765

web: www.serüvenyayınevi.com

e-mail: serüvenyayınevi@gmail.com

Baskı & Cilt / Printing & Volume

Sertifika / Certificate No: 47083

INTERNATIONAL THEORY, RESEARCH AND REVIEWS IN ENGINEERING

October 2023

Editors

Prof. Dr. Coşkun ÖZALP
Assoc. Prof. Dr. Selahattin BARDAK

CONTENTS

Chapter 1

DEEP LEARNING-BASED CHROMATIC FILTERING AND CLASSIFICATION OF OBJECTS WITH A 4-DOF ROBOTIC ARM

İbrahim SHAMTYA, Batıkan Erdem DEMİR, Funda DEMİR 1

Chapter 2

MACHINE LEARNING MODELLING OF ISENTROPIC COMPRESSIBILITY OF BINARY BLENDS OF OXYGENATED ADDITIVES AND HYDROCARBONS

Mert GULUM, Yunus Emre KARABACAK..... 21

Chapter 3

HYDROXYAPATITE SYNTHESIS AND COATING METHODS

Safiye İPEK AYVAZ 33

Chapter 4

MANY-TO-ONE MODE LSTM APPROACH TO PREDİCT THE Z0 BOSON'S MASS

Jale BEKTAŞ 49

Chapter 5

TIME COMPLEXITY OF MACHINE LEARNING METHODS: A REVIEW

Celalettin ARSLAN, Volkan KAYA 61

Chapter 6

MASS TRANSPORT AND UARBAN RAILWAYS IN THE CONTEXT OF SUSTAINABILITY

Mehmet Çağrı KIZILTAŞ, Vail KARAKALE 93

Chapter 7

CLAY MINERALS IN NANOTECHNOLOGY: IMPORTANCE AND APPLICATIONS IN ENGINEERING

Dilek ŞENOL ARSLAN..... 109

Chapter 8

**CURRENT APPROACHES ON THE USE OF BIODIESEL AS AN
ALTERNATIVE FUEL IN INTERNAL COMBUSTION ENGINES**

Hicri YAVUZ 123

Chapter 9

**ALTERNATIVE FUELS IN THE FUTURE OF THE MARITIME
INDUSTRY**

Ayfer ERGİN, M. Fatih ERGİN..... 147

Chapter 10

**EFFECTS OF EARTHQUAKES ON GROUNDWATER: THE CASE OF
KAHRAMANMARAŞ**

Göknur KAYATAŞ ONGUN, Arda YALÇUK..... 165

Chapter 11

HEATERS USED FOR ENGINEERING SYSTEMS

Hatice Aylin KARAHAN TOPRAKCI, Sertan TURAN

Varol KORKMAZ..... 189

Chapter 12

**GENETIC PROGRAMMING MODEL FOR PREDICTION OF WEAR BY
MEANS OF HARDNESS VALUES OF STEEL MATERIAL**

Yenal ARSLAN 203

Chapter 13

**EVALUATION OF MASS TRANSPORTATION SYSTEMS IN ISTANBUL
AND MODAL SELECTION**

Mehmet Çağrı KIZILTAŞ, Vail KARAKALE 225

Chapter 14

**THE ROLE OF GEOPOLYMERS IN MINING AND THEIR
CONTRIBUTIONS TO A SUSTAINABLE FUTURE**

Kemal ŞAHBUDAK 237

Chapter 15

**THE EFFECT OF NORMALIZATION ON THE SUCCESS OF
FORECASTING ENERGY CONSUMPTION**

Ahmet GÖKÇE, Fulya ASLAY 251

Chapter 16

RENEWABLE ENERGY AND SUSTAINABLE LIVING

Abdullah YİNANÇ 271

Chapter 17

**GREEN BUILDING CONCEPT: AN OVERVIEW FROM THE WORLD
AND TURKEY PERSPECTIVE**

Mirac Nur CİNER, Emine ELMASLAR ÖZBAŞ

H. Kurtulus OZCAN 289

Chapter 18

**A MACHINE LEARNING BASED RECEIVER SCHEME FOR VARIABLE
ON-OFF KEYING MODULATION TECHNIQUE**

Methmet SÖNMEZ 301

Chapter 19

**A COMPREHENSIVE REVIEW ON THE DESIGN AND
PERFORMANCE OF SOLAR DRYING METHODS**

Mesut YAZICI, Ramazan KÖSE 319

Chapter 20

BIOCOMPUTING AND BIOCOMPUTERS

Esra ŞATIR 347

Chapter 21

**MATLAB/SIMULINK SUPPORTED ANALYSIS OF RL AND RC
CIRCUITS**

Hilmi ZENK, Birol ERTUĞRAL 359

Chapter 1

DEEP LEARNING-BASED CHROMATIC FILTERING AND CLASSIFICATION OF OBJECTS WITH A 4-DOF ROBOTIC ARM

İbrahim SHAMTYA¹

Batıkan Erdem DEMİR²

Funda DEMİR³

1 Karabuk University. Technology Faculty Karabuk, TURKEY. ORCID ID: 0009-0003-1280-679X

2 Dr. Öğr.Ü., Karabuk University Technology Faculty Karabuk, TURKEY. ORCID ID: 0000-0001-6400-1510

3 Dr. Öğr.Ü. Karabuk Univ. TOBB. Vocational School of Technical Sciences. Karabuk, TURKEY. ORCID ID: 0000-0001-7707-8496

One of the fundamental objectives of computer vision is the comprehension of visual scenes. This understanding encompasses various tasks such as the recognition of existing objects, determination of the 2D and 3D coordinates of objects, detection of object and scene attributes, characterization of relationships among objects, and providing a semantic description of the scene. Present-day object classification and detection datasets play a significant role in pursuing this objective. Image processing through robot technology and deep learning algorithms constitutes one of the most crucial applications utilized in industries and various other fields by scientists and engineers (Lin et al., 2014; Xiao, Hays, Ehinger, Oliva, & Torralba, 2010).

With the advancements in the field of artificial intelligence, the design of autonomous and efficient robots equipped with image classification and processing capabilities has become feasible. The fusion of robot technology and deep learning algorithms in image processing enables a wide array of applications across various domains, including but not limited to industrial applications such as automated product inspection and sorting, quality control procedures, the high-precision analysis of medical images and disease diagnosis within the medical field, as well as the analysis of plant images and the prediction of harvest outcomes in the agricultural sector (Deng et al., 2010; Everingham, Van Gool, Williams, Winn, & Zisserman, 2010).

The integration of robot technology and deep learning algorithms into image processing mitigates human errors, enhances accuracy and efficiency, leads to time and effort savings, and elevates both productivity and quality. Consequently, the utilization of this technology across diverse domains represents a pivotal stride towards achieving superior outcomes and advancing the industrial and service sectors. Object detection and classification constitute fundamental pillars of Computer Vision (CV). Image perception, serving as an intelligent attribute in autonomous systems, has the potential to imbue autonomous vehicles with intelligent capabilities. In a broad sense, a system capable of identifying any object through CV can be deemed an intelligent system. Within the scholarly literature, numerous applications abound within the realms of computer vision and robotics (Chen, Yang, Liu, Tian, & Zhou, 2023; De-An, Jidong, Wei, Ying, & Yu, 2011; Everingham et al., 2010; Everingham, Zisserman, Williams, & Van Gool Leuven, 2006; Schneiderman, 2004).

One of these studies is conducted by Zhao et al. in 2011. In this research, an automated robotic system capable of performing apple picking tasks is developed. This robot device achieves its task with an average picking time of approximately 15 seconds and high accuracy. The robotic device consists of components such as a manipulator, end-effector, image-based vision, and a servo control system. The manipulator, which has a 5 Degrees of Freedom (DOF) PRRRP structure, is optimized to reduce nonlinear behavior and simplify control strategy. The spoon-shaped end-effector, designed to meet apple picking requirements, is utilized in conjunction with a pneumatic actuated gripper. For the automated detection of apples on trees and determination of their positions, an image-based module is employed to develop a fruit recognition algorithm using Support Vector Machines and Radial Basis Function. The control system, comprising an industrial computer and AC servo driver, manages the manipulator and end-effector to facilitate apple picking. The functionality of the prototype robotic device is validated through laboratory tests as well as field experiments conducted in open terrain (De-An et al., 2011).

In his 2017 study, Sachdeva proposes a solution for the robotic sorting of colored objects in the industry using a robotic arm. The system utilizes the TCS3200 color sensor to detect the objects' colors and reposition them to specific locations on a conveyor belt. DC motors are employed to manipulate the conveyor belt, holder, and lifter. The system is controlled by an Arduino Nano microcontroller. The L293D motor driver and LCD screen contribute to enhancing the user-friendliness of the system (Sachdeva, 2017).

In a study conducted by Chen et al. in 2023, a modified method based on YOLOv5 is employed. This method enables the automatic and rapid classification of source types, identification of detection signs, and determination of the Region of Interest (ROI) for the source. Detection requirements are transformed into a unified target localization task to obtain three results through a single inference path. Experimental results demonstrate that the presented method achieves improvements in both accuracy and computation speed. The provided method for source type classification, source point recognition, and source ROI determination is accurate and swift. This method attains precision and recall rates of 100%, a pixel center deviation of 2.41, and inference times of 18 ms for original-sized images (Chen et al., 2023).

The primary objective of the study conducted by Shetty et al. is to design an efficient system capable of accurately picking colored objects and placing them in the correct location, aiming to reduce product costs, optimize efficiency, and minimize human errors. The research presents an application for separating colored objects using a robotic arm. This robotic arm can select different colored objects and place them into specific containers. Communication with the TCS3200 color sensor and control of the arm's movements are facilitated using various motor modules (Shetty, Tambe, Zurkale, & Dange, n.d.).

In this study, a method is presented for chromatic filtering and classification of shapes using a 4-DOF robotic arm, a webcam, an NVIDIA embedded artificial intelligence computer, and the Jetson Nano developer kit. The materials employed and the methods applied are detailed in the subsequent section, while the experimental results are elucidated through graphs in the results section. The findings indicate that the method and techniques presented in the study can effectively classify objects based on their colors. When combined with the Jetson Nano developer kit and YOLOV8 and YOLOV5 algorithms, the 4-DOF robotic arm can offer a higher degree of accuracy in applications where processes are automated, such as food processing facilities.

2. Materials and Methods

2.1. Hardware Components of the System

The hardware architecture of the system consists of the Camera System, Jetson Nano Developer Board, Robotic Arm, and Visualization sections, as illustrated in the block diagram in Figure 1.

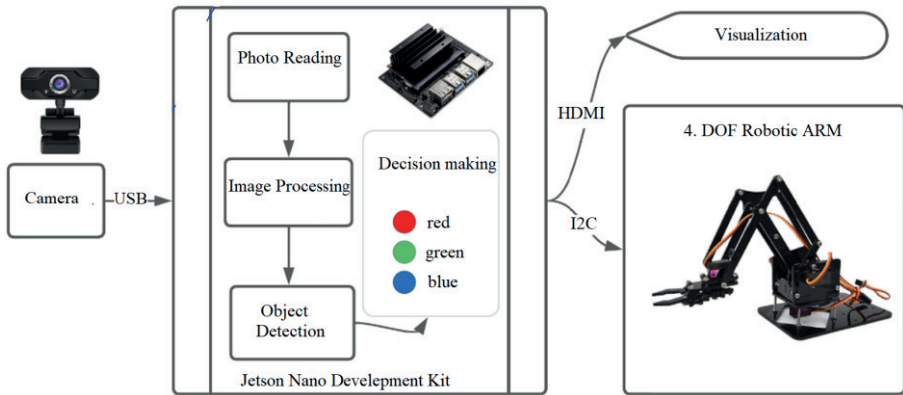


Figure 1. Block Diagram of the 4-DOF Robotic Arm

2.1.1. Developer Kit (NVIDIA Jetson Nano)

The NVIDIA® Jetson Nano™ Developer Kit is a compact yet powerful computing platform designed for various applications in parallel execution of multiple neural networks, such as image classification, object detection, segmentation, and speech processing. These capabilities are facilitated within an easily accessible and user-friendly platform, characterized by a power consumption of less than 5 watts. The specifications of the board are outlined in Table 1 (Nvidia, 2014).

Table 1. Technical Specifications of the NVIDIA® Jetson Nano™ Developer Kit.

GPU	128-core Maxwell
CPU	4-core ARM A57 @1.43 GHz
Memory	4GB 64 Bit LPDDR4 25.6 GB/s
Storage	microSD
Connectivity	Gigabit Ethernet, M.2 Key E
Camera	2x MIPI CSI-2 DPHY lanes
Video Encoding	4K @ 30 4x 1080p @ 30 9x 720p @ 30 (H.264/H.265)
Video Decoding	4K @ 60 2x 4K @ 30 8x 1080p @ 30 18x 720p @ 30 (H.264/H.265)
Screen	HDMI 2.0 ve eDP 1.4
Max. Operating Frequency	1.43 GHz

2.1.2. Webcam

The Trax TWC 1080p camera utilized in the study is a type of video camera system that offers high-definition image quality. This camera is equipped with

a CCD (Charged-coupled device) sensor capable of recording 1080p resolution video at 30 frames per second and capturing 12-megapixel photographs. Featuring an integrated microphone and speaker, this camera facilitates not only video recording but also real-time audio and visual communications. Moreover, this camera is suitable for both indoor and outdoor use, and it is supplied with the requisite image processing software ('TRAX 2 Mp 1080 P Web Kamera Fiyatı, Yorumları - Trendyol', n.d.).

2.1.3. 4- DOF ARM Robotic-ARM

A robot arm possessing four degrees of freedom is suitable for uncomplicated applications. This arm incorporates four micro servo motors. While the base motor allows for a 360-degree rotation, the first joint angle motor can move within the range of 0 to 90 degrees. Similarly, the second joint angle motor can also move within the range of 0 to 90 degrees. The head (claw) motor, on the other hand, exhibits a working range of 60 degrees. With the capacity to lift weights up to 200 grams, this arm can reach a maximum distance of 20 centimeters ('robot arm 4dof - Bing - Shopping', n.d.).

2.1.4. Driver Kit

The Adafruit PCA9685 16-Channel Servo Driver module is a component that can be connected to Raspberry Pi, Jetson Nano, and other small computers. This module employs 16 channels for connecting and precisely maneuvering servo motors. Utilizing Pulse Width Modulation (PWM) technology, the module achieves high precision in motor movement and is utilized to control both speed and angle. The control board is equipped with I2C interface connectors and is compatible with most programming languages commonly used in electronic projects. This module finds applicability in a wide range of use cases, including propelling robots and electronic projects, as well as facilitating various applications such as small and large-scale automation projects (By ALLDATASHEETCOM, n.d.).

2.1.5. Servo Motor

The micro servo SG90 is one of the most commonly employed motors in hobby electronics and robot projects. It stands out for its compact size, low cost, and commendable performance. Operating through servo technology, the motor's movement can be precisely controlled with high accuracy. The motor's motion angle and speed are determined by a Pulse Width Modulation

(PWM) signal. SG90 is powered by 5 volts of electricity and possesses a rotational range between 0 and 180 degrees. It finds suitability for applications demanding precise motion ('sg90_datasheet', n.d.).

2.2. Deep Learning-Based Image Processing

Deep learning is a machine learning approach based on artificial neural networks that focuses on obtaining appropriate data representations to achieve desired outcomes. The term "deep" implies that hierarchical concepts are learned directly from raw data (Ketkar & Moolayil, 2017). In this learning structure, there exist an input layer, hidden layers, and an output layer, with each layer sequentially functioning as the input to the subsequent layer (Sözen, Bardak, Aydemir, & Bardak, 2018). The schematic representation of the deep learning method is provided in Figure 2.

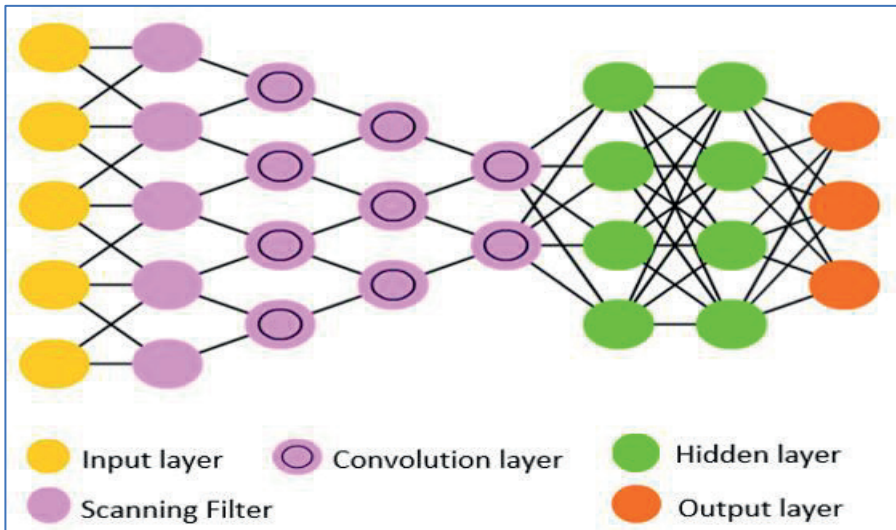


Figure 2. Deep Learning network architecture

Unlike conventional machine learning, predictions here cannot be manually adjusted; the accuracy of predictions in deep learning is determined by foundational algorithms (Aalami, 2020).

2.2.1. YOLO Algorithm

YOLO (You Only Look Once) algorithms are robust and innovative techniques employed for object detection in images and videos. These

algorithms distinguish themselves through their ability to conduct real-time object detection at high speeds, positioning them as among the fastest algorithms employed in the field of computer vision. YOLO exhibits commendable performance in detecting objects of varying dimensions and in complex environments. However, it may not achieve the same level of success in detecting very small objects. Developed in 2016 by researcher Joseph Redmon and his team at the University of Washington, YOLO employs an output format termed "Bounding Box" to represent and ascertain the locations of detected objects.

The algorithm employs an approach that initially partitions the image into sections and subsequently provides predictions for each section in a single pass. However, this approach encounters challenges in detecting small objects and objects with high levels of occlusion (Redmon, Divvala, Girshick, & Farhadi, 2015). With the development of the second version in 2017, the detection performance of small objects and overlapping instances was significantly improved. Additionally, the inclusion of the Darknet-19 network and the fusion of ImageNet and COCO databases enhanced detection and classification accuracy. This version utilizes Spatial Pyramid Pooling to handle objects of varying sizes (Redmon & Farhadi, 2016). In the third iteration developed in 2018, new layers were introduced for detailed detection, resulting in a substantial enhancement in both detection speed and accuracy. Multiple scale predictions were incorporated within the network to enhance broad-scale detection. The foundational model for object detection and classification utilized 53 Darknet layers (Redmon & Farhadi, 2018). The fourth version, released in 2020, amalgamates techniques from previous versions, such as multi-scale detection and detail layers. Darknet-53 and enhanced CSPDarknet53 layers were employed for detection and classification. YOLOv4 encompasses techniques like Mish Activation, CIOU Loss, SAM, and PANet, resulting in improved performance and a substantial advancement in detection speed and accuracy compared to previous versions (Bochkovskiy, Wang, & Liao, 2020).

YOLOv5: The fifth iteration of YOLO, YOLOv5, was introduced to the market in 2020 by Glenn Jocher and others. This version stands as an independent implementation based on PyTorch, rather than an official continuation of the preceding editions. The algorithm employs a novel network architecture named YOLOv5s, which is smaller and faster compared

to YOLOv4. Additionally, new features such as automatic model scaling, label smoothing, class probability calibration, and model ensembling have been incorporated. YOLOv5 achieves a mean average precision (mAP) of 88.9% on the COCO dataset and operates at a speed of 140 frames per second (FPS) on a GPU (Shenoda, 2023).

YOLOv8, leveraging an advanced architecture that combines high-level features and contextual information through the C2f unit, enhances detection accuracy. Its reference-free model structure processes object presence, classification, and regression tasks independently, contributing to an overall accuracy boost. Object detection performance, particularly concerning small objects, has been enhanced using the CIoU (Completed Intersection over Union) and DFL (Distribution Focal Loss) loss functions. YOLOv8 also introduces a semantic segmentation model with the CSPDarknet53 feature extractor through the C2f unit. Operating at a high speed and efficiency, it achieves 280 FPS on NVIDIA A100 and TensorRT platforms. YOLOv8 is an impressive algorithm, characterized by its advanced architecture, reference-free model structure, improved loss functions, semantic segmentation capability, and high speed and efficiency features (Terven & Cordova-Esparza, 2023). YOLOv8 is indicated as the latest version of this algorithm ('YOLOv8 Ultralytics: State-of-the-Art YOLO Models', n.d.).

2.2.2. Dataset

The preparation of training data is a critical aspect for achieving accurate results in the training and object detection process. For each category, several images were captured, and these data were grouped based on colors (red, green, blue) to enable the algorithm to classify shapes accordingly. Each group consists of 75 images composed of three distinct colors, as depicted in Figure 3. The dataset has been partitioned into training (80%), validation (17%), and testing (3%) subsets.

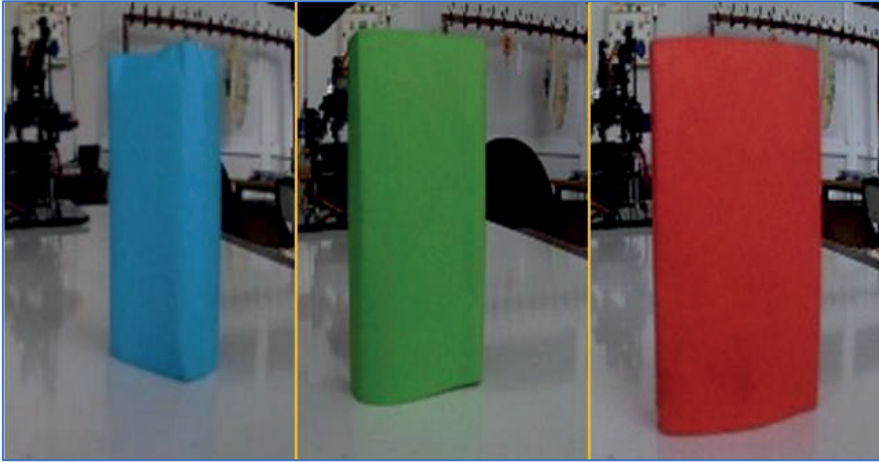


Figure 3. Sample Images

2.2.3. Utilized Model in the Study

In this research, the YOLOv5 and YOLOv8 algorithms have been employed and their performances are comparatively presented. Training parameters for both models have been set with a training step of 16, an iteration count of 100, and an image size of 460.

2.2.4. Motion Mechanism

The proposed system classifies objects based on their colors and carries out the task of placing each color into distinct compartments. This procedure occurs over several stages. In the initial step, the coordinates for capturing the object and the current coordinates of each compartment (red, blue, and green) are established. To accomplish this, a user interface has been created, allowing for direct manipulation of the robot's angles and the ability to save important coordinates. This interface, shown in Figure 4, includes four interactive sliders corresponding to each motor. These sliders make it easier to directly control the motors in real-time, all while simultaneously displaying the angle values.

During the Object Detection phase, the operational field of the camera connected to Jetson Nano is analyzed to discern the present elements. The detected object, as per the trained model, undergoes processing to determine its color in the subsequent stage. Subsequently, the object is approached, captured, and placed in the relevant compartment. Following this, the system returns to the center point, and the process continues by iterating through object detection and classification. Figure 5 illustrates the flowchart depicting the operational process of the motion mechanism. Subsequently, a return to

the center point is executed, and the procedure continues by iteratively repeating the object detection and classification process. Figure 5 provides a flowchart illustrating the operational workflow of the motion mechanism.

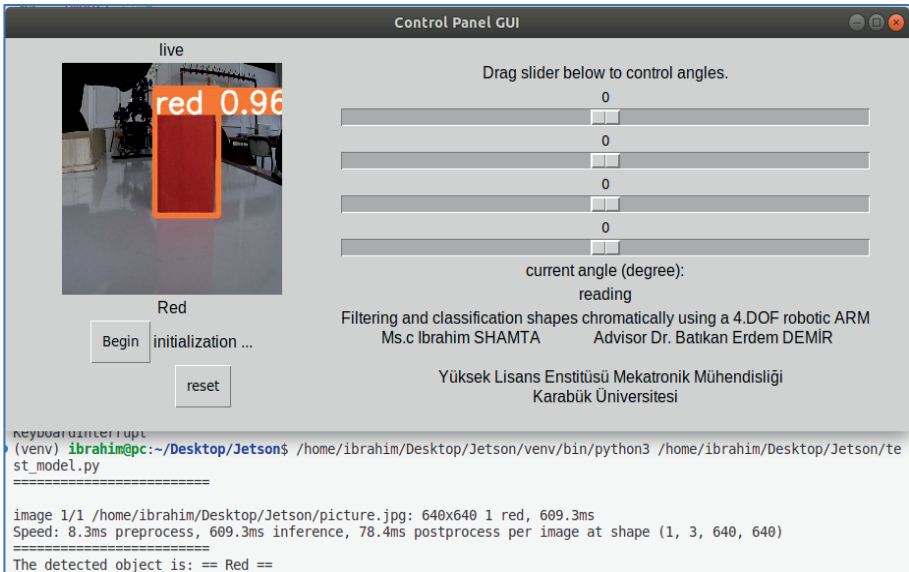


Figure 4. User interface of the proposed system

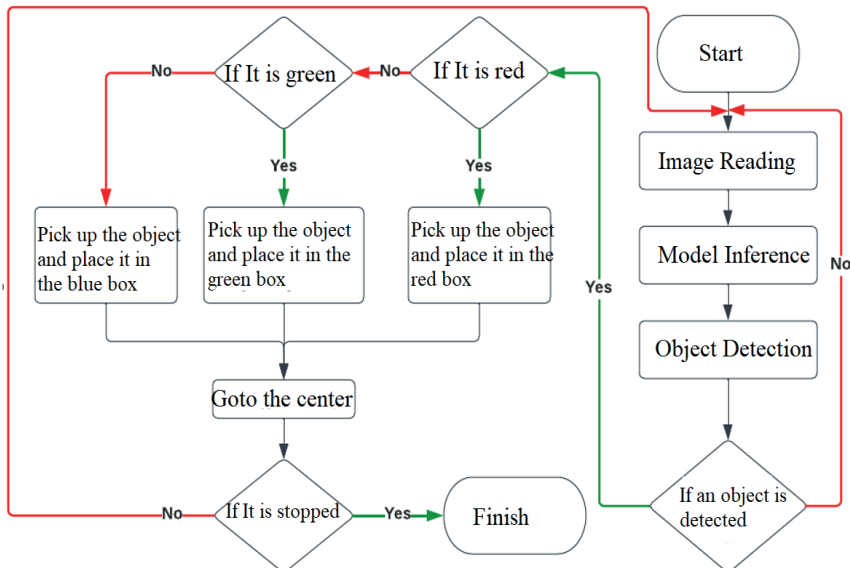


Figure 5. Flowchart depicting the operation of the motion mechanism.

2.2.5. Analysis of Arm Movement

Figure 6 illustrates a two-dimensional analysis of arm movement. Following the determination of the radius, the angles θ_1 and θ_2 of the arm, which have lengths L_1 and L_2 , need to be determined through inverse analysis.

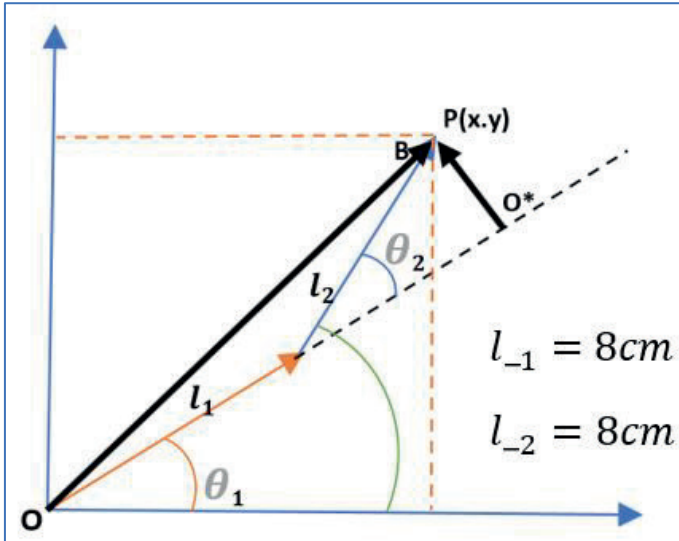


Figure 6. Radial shape of the moving arm.

$$x^2 + y^2 = OB^2$$

Equation 1

$$OB^2 = OO^{*2} + O^*B^2$$

$$OB^2 = (l_1 + l_2 \cos \theta_2)^2 + (l_2 \sin \theta_2)^2$$

$$\begin{aligned} &= l_1^2 + l_2^2 + 2l_1l_2 \cos \theta_2 = x^2 + y^2 \\ 2l_1l_2 \cos \theta_2 &= x^2 + y^2 - l_1^2 - l_2^2 \\ \cos \theta_2 &= \frac{x^2 + y^2 - l_1^2 - l_2^2}{2l_1l_2} \end{aligned}$$

Therefore, the positional angles can be calculated from the equations in Equation 2:

$$\theta_2 = \arccos\left(\frac{x^2 + y^2 - 128}{128}\right)$$

Equation 2

$$\theta = \operatorname{atan} \frac{y}{x}$$

$$\theta_1 = \theta - \theta_2$$

Once the equations are entered into the processing unit, angles are generated for transitioning to the desired point. In the scope of this study, the position of the held object is determined to be fixed along the Z-axis (Lynch & Park, n.d.; Roshanianfard & Noguchi, 2018).

3. Experimental Results and Findings

After the training and testing of the model were completed, the results were presented comparatively as shown in Table 2. The training parameters were as follows: Pretrained: Yes, Epochs: 100, Image Size: 640, Patience: 100, Cache: RAM, Device: GPU (NVIDIA Tesla T4), Batch Size: Set to automatic. The evaluation metrics are as follows:

Table 2. The table of evaluation metrics

	Evaluation Metrics			
	mAP50	mAP50-95	Precision	Recall
YOLOV5	99.5%	90.5%	99.2%	100%
YOLOV8	99.5%	92.4%	99.4%	100%

The evaluation of the detection system in YOLO involves the use of several metrics and their corresponding explanations, as outlined below (Bochkovskiy et al., 2020):

1. **mAP50:** It is the average precision calculated with a union threshold of 50% for bounding boxes (i.e., when an item is detected with an accuracy of 50% or higher, it is considered positive).
2. **mAP50-95:** It is the average precision calculated with a union threshold between 50% and 95% for bounding boxes.
3. **Precision:** Precision is the ratio of true positive results to all positive predictions (i.e., correctly detected instances within all instances predicted as positive) for bounding boxes.

4. **Recall:** Recall is the number of true positive results detected within bounding box B, divided by the total number of actual positive instances.

These metrics collectively provide a comprehensive assessment of the performance of the detection system, considering different levels of accuracy and precision in bounding box predictions.

In Figure 7, the confusion matrices of both models are presented

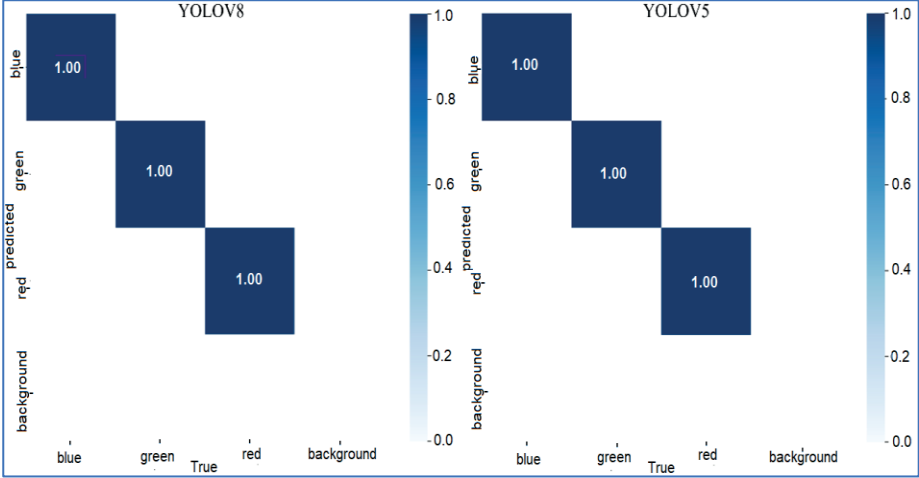


Figure 1. The confusion matrices

These matrices can be utilized to compute performance metrics such as accuracy, precision, specificity, and sensitivity of the model. These metrics illustrate how well the classification model manages the relationship between actual and predicted classes.

Differences between the YOLOV5 and YOLOV8 algorithms can be observed through the curves provided in Figure 8

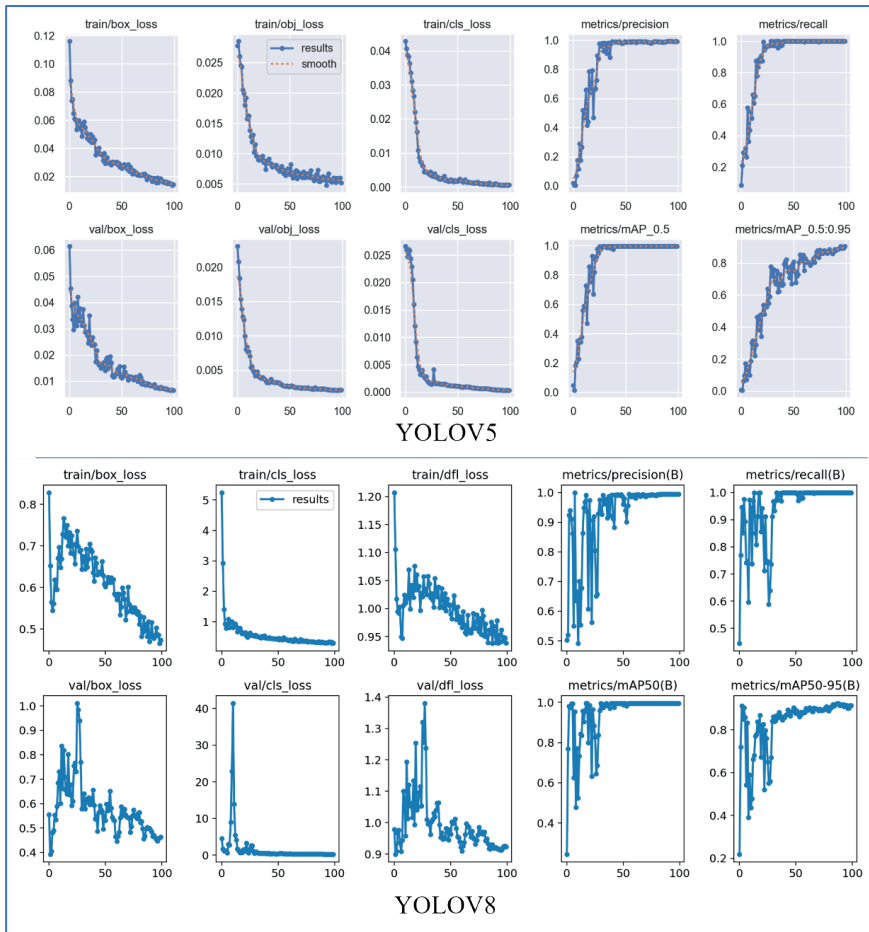


Figure 8. Curves illustrating the differences and disparities in the YOLOv5 and YOLOv8 algorithms.

4. Conclusion

In this study, a novel model is proposed for sorting and classifying objects based on their colors within a four-degree-of-freedom robotic system, utilizing the NVIDIA Jetson Nano development board and deep learning methodology. When the color of an object is identified, the robotic arm captures the object and places it in the appropriate color-coded area. This method has demonstrated high accuracy results in terms of detection and classification. Two models were trained using the same dataset and standards, and the YOLOv8 model outperformed YOLOv5 by 1.9% in mAP50-95

standard and by 0.2% in Precision standard. In a new data experiment, both models achieved a 100% accuracy in open object detection. Additionally, this study emphasizes the significance of utilizing deep learning algorithms for object or shape detection. Future developments will involve designing a comprehensive application that offers significant advantages for this purpose and facilitating the industrial utilization of this robot. The system's operation can be observed through the following link: https://youtube.com/shorts/POEIN7e_bi0.

REFERENCES

- Aalami, N. (2020). Analysis of Images Using Deep Learning Methods. *Journal of ESTUDAM Information*, 1(1), 17–20.
- Bochkovskiy, A., Wang, C.-Y., & Liao, H.-Y. M. (2020). YOLOv4: Optimal Speed and Accuracy of Object Detection. Retrieved from <http://arxiv.org/abs/2004.10934>
- By ALLDATASHEETCOM, P. (n.d.). PCA9685 NXP | *Alldatasheet*.
- Chen, S., Yang, D., Liu, J., Tian, Q., & Zhou, F. (2023). Automatic weld type classification, tacked spot recognition and weld ROI determination for robotic welding based on modified YOLOv5. *Robotics and Computer-Integrated Manufacturing*, 81. doi:10.1016/j.rcim.2022.102490
- De-An, Z., Jidong, L., Wei, J., Ying, Z., & Yu, C. (2011). Design and control of an apple harvesting robot. *Biosystems Engineering*, 110(2), 112–122. doi:10.1016/j.biosystemseng.2011.07.005
- Deng, J., Dong, W., Socher, R., Li, L.-J., Kai Li, & Li Fei-Fei. (2010). *ImageNet: A large-scale hierarchical image database* (pp. 248–255). Institute of Electrical and Electronics Engineers (IEEE). doi:10.1109/cvpr.2009.5206848
- Everingham, M., Van Gool, L., Williams, C. K. I., Winn, J., & Zisserman, A. (2010). The pascal visual object classes (VOC) challenge. *International Journal of Computer Vision*, 88(2), 303–338. doi:10.1007/s11263-009-0275-4
- Everingham, M., Zisserman, A., Williams, C., & Van Gool Leuven, L. K. (2006). *The Pascal Visual Object Classes Challenge 2006 (VOC2006) Results*.
- Ketkar, N., & Moolayil, J. (2017). *Deep Learning with Python. Deep Learning with Python*. doi:10.1007/978-1-4842-5364-9
- Lin, T.-Y., Maire, M., Belongie, S., Bourdev, L., Girshick, R., Hays, J., ... Dollár, P. (2014). Microsoft COCO: Common Objects in Context. Retrieved from <http://arxiv.org/abs/1405.0312>
- Lynch, K. (Kevin M.), & Park, F. C. (n.d.). *Modern robotics : mechanics, planning, and control*.
- Nvidia. (2014). *DATA SHEET NVIDIA Jetson Nano System-on-Module Maxwell GPU + ARM Cortex-A57 + 4GB LPDDR4 + 16GB eMMC*. Retrieved from www.khronos.org/conformance.

- Redmon, J., Divvala, S., Girshick, R., & Farhadi, A. (2015). You Only Look Once: Unified, Real-Time Object Detection. Retrieved from <http://arxiv.org/abs/1506.02640>
- Redmon, J., & Farhadi, A. (2016). YOLO9000: Better, Faster, Stronger. Retrieved from <http://arxiv.org/abs/1612.08242>
- Redmon, J., & Farhadi, A. (2018). YOLOv3: An Incremental Improvement. Retrieved from <http://arxiv.org/abs/1804.02767>
- robot arm 4dof - Bing - Shopping. (n.d.). Retrieved 10 June 2023, from <https://www.bing.com/shop/productpage?q=robot+arm+4dof&filters=scenari o%3a%2217%22+gType%3a%2212%22+gId%3a%22144713953673%22+gIdH ash%3a%220%22+gGlobalOfferIds%3a%22144713953673%22+AucContextGu id%3a%220%22+GroupEntityId%3a%22144713953673%22+NonSponsoredOf fer%3a%22True%22&productpage=true&FORM=SHPPDP&browse=true>
- Roshanianfard, A., & Noguchi, N. (2018). Kinematics analysis and simulation of a 5DOF articulated robotic arm applied to heavy products harvesting. *Tarım Bilimleri Dergisi*, 24(1), 91–104. doi:10.15832/ankutbd.446396
- Sachdeva, A. (2017). Development Of Industrial Automatic Multi Colour Sorting and Counting Machine Using Arduino Nano Microcontroller and TCS3200 Colour Sensor. *The International Journal of Engineering and Science*, 06(04), 56–59. doi:10.9790/1813-0604025659
- Schneiderman, H. (2004). *Feature-centric evaluation for efficient cascaded object detection*. In *Proceedings of the IEEE Computer Society Conference on Computer Vision and Pattern Recognition* (Vol. 2). doi:10.1109/cvpr.2004.1315141sg90_datasheet. (n.d.).
- Shenoda, M. (2023). Lighting and Rotation Invariant Real-time Vehicle Wheel Detector based on YOLOv5. Retrieved from <http://arxiv.org/abs/2305.17785>
- Shetty, P., Tambe, S., Zurkale, S., & Dange, K. (n.d.). *Color Sorting Robotic Arm Using Arduino*.
- Sözen, E., Bardak, T., Aydemir, D., & Bardak, S. (2018). Estimation of Deformation in Nanocomposites Using Artificial Neural Networks and Deep Learning Algorithms. *Journal of Bartın Faculty of Forestry*, 20(2), 223–231. doi:10.24011/barofd.449563

Terven, J., & Cordova-Esparza, D. (2023). A Comprehensive Review of YOLO: From YOLOv1 and Beyond. Retrieved from <http://arxiv.org/abs/2304.00501>

TRAX 2 Mp 1080 P Web Kamera Fiyatı, Yorumları - Trendyol. (n.d.). Retrieved 10 June 2023, from <https://www.trendyol.com/trax/2-mp-1080-p-web-kamera-p-89662101>

Xiao, J., Hays, J., Ehinger, K. A., Oliva, A., & Torralba, A. (2010). *SUN database: Large-scale scene recognition from abbey to zoo*. In *Proceedings of the IEEE Computer Society Conference on Computer Vision and Pattern Recognition* (pp. 3485–3492). doi:10.1109/CVPR.2010.5539970

YOLOv8 Ultralytics: State-of-the-Art YOLO Models. (n.d.). Retrieved 4 June 2023, from <https://learnopencv.com/ultralytics-yolov8/>



Chapter 2

MACHINE LEARNING MODELLING OF ISENTROPIC COMPRESSIBILITY OF BINARY BLENDS OF OXYGENATED ADDITIVES AND HYDROCARBONS

*Mert GULUM*¹

*Yunus Emre KARABACAK*²

1 Assist. Prof. Dr., Karadeniz Technical University, Faculty of Engineering, Department of Mechanical Engineering, Trabzon, TURKEY, ORCID: 0000-0002-1792-3499

2 Assist. Prof. Dr., Karadeniz Technical University, Faculty of Engineering, Department of Mechanical Engineering, Trabzon, TURKEY, ORCID: 0000-0002-0268-3656

1. Introduction

The increase in global energy demand can be attributed to the effects of population, industrialization, and urbanization. Fossil fuels play a dominant role in the transportation and power generation sectors, which contributes to the rapid depletion of fossil fuel reserves. Moreover, the emissions resulting from the operation of an internal combustion engine adversely affect the natural environment [1]. To address these challenges, renewable biofuels and oxygenated additives (ethers, alcohols, etc.) have emerged as potential alternatives.

Dibutyl ether (DBE) is mainly derived from lignocellulosic biomass and is considered a favorable substitute for diesel engines. DBE is a colorless liquid immiscible with water. It is flammable and can form oxides during storage. In terms of human health, it is considered toxic and irritant. DBE is commonly derived from butanol, although it can also be synthesized from ethanol, making it a renewable oxygenated additive. DBE is a diesel cetane enhancer (~100). DBE has high volatility and low viscosity (~0.824 mm²/s). DBE exhibits a high oxygen content (~12% mass), resulting in notably reduced soot emissions during combustion. DBE has a somewhat lower calorific value (~42.8 MJ/kg) than diesel fuel (~43 MJ/kg). The production of DBE from butanol is widely recognized and typically involves the dehydration of butanol using sulfuric acid or catalytic dehydration using ferric chloride, copper sulfate, silica, or silica-alumina at high temperatures. Based on the superior fuel properties of DBE, in recent years, experimental and numerical studies have been performed to investigate the effects of DBE blends on the combustion, auto-ignition, and exhaust emission characteristics of diesel engines [2-7].

Over the past decade, butanol derived from lignocellulosic feedstocks has emerged as a promising and sustainable source of green energy for diesel engines. This is attributed to its superior fuel properties compared to other alcohols. For example, butanol has a higher heating value (~33 MJ/kg) than ethanol (~27 MJ/kg) and methanol (20 MJ/kg). Butanol exhibits good solubility with diesel fuel, and has a higher cetane number (~25), flash point temperature (~ 35°C), and kinematic viscosity (2.22 mm²/s at 40°C), which makes it a better choice for diesel engines than ethanol and methanol. The oxygen molecule present in butanol (~21 wt.%) facilitates improved diffusion during the combustion [8-13]. Owing to its superior fuel properties, many researchers have tested diesel engines using mixtures of butanol [14-16].

The analysis of the changes in the fuel properties under different conditions plays a crucial role in comprehending the spray, combustion, and emission characteristics in internal combustion engines. Some of these fuel properties serve as essential input data for multi-dimensional engine simulations. That is

why, an accurate knowledge of the fuel properties under different conditions is required for the proper development of engine simulations. Moreover, it is essential to determine whether the fuels and their blends meet the standard specifications. However, experimental measurements of the fuel properties can be time-consuming and expensive under all conditions of interest. Therefore, the ability to calculate these properties using prediction methods is highly beneficial. Such an approach enables a priori estimation of the properties [17-19]. Among the properties, isentropic compressibility is an important property in the studies of internal combustion engines.

The isentropic compressibility, the inverse of the isentropic bulk modulus, is a crucial indicator of the space between molecules within a substance or its compressibility potential. It informs us about a substance's ability to undergo compression [20]. The isentropic bulk modulus can be calculated using the density and speed of sound in the sample. The isentropic compressibility along with density and viscosity play a significant role in the injection process in diesel engines. The compressibility affects not only the wave amplitude but also its velocity, thereby influencing the fuel injection timing and NO_x emissions [21, 22]. For example, Tat et al. reported that the isentropic bulk modulus and speed of sound are higher for soybean oil biodiesels than diesel fuel, which increases NO_x emissions [22]. A number of studies have presented measured data and predictive models (empirical or thermodynamic) for the isentropic compressibilities of biodiesel blends [23-26]. Most isentropic compressibility measurements and their predictions are either for a specific blend or within a narrow composition range. Few studies have focused on the use of machine learning algorithms to correlate the isentropic compressibility over a wider composition range of oxygenated additives. To overcome this limitation and to increase prediction accuracy, machine learning algorithms, namely Artificial Neural Networks (ANN) and Linear Regression (LR), are employed in this research to model isentropic compressibility data of binary blends (including oxygenated additives (DBE and butanol) and hydrocarbons (toluene and cyclohexane)) depending on the mole fraction of oxygenated additives.

2. Materials and Methods

2.1. Artificial Neural Networks (ANN) and Linear Regression (LR) Algorithms

Machine learning algorithms driven by data have been widely adopted to solve various engineering problems, including classification, analysis, prediction, and optimization. Among these algorithms, artificial neural networks (ANN) and linear regression (LR) have emerged as robust and efficient options. These algorithms have attracted considerable attention, especially in the areas of renewable and sustainable energy [27]. Hence, this

study focuses on the use of machine learning algorithms (ANN and LR) in predicting isentropic compressibility. Although both algorithms are utilized for predicting continuous dependent variable values, they exhibit unique characteristics and employ distinct methodologies. For a short comparison of ANN and LR, Table 1 provides an overview of their features and distinctions.

Table 1. *Some properties of ANN and LR algorithms [28-30]*

Property	Artificial Neural Networks (ANN)	Linear Regression (LR)
Model Type	Non-linear	Linear
Function approximation	ANN can approximate highly complex functions and capture non-linear relationships between variables.	LR assumes a linear relationship between the independent and dependent variables.
Flexibility	ANN can handle a wide range of input features and is flexible in adapting to different problem domains.	LR is more suitable for problems where the relationship between variables is linear and assumptions of linearity hold.
Training	ANN requires iterative training using techniques like backpropagation and gradient descent.	LR can be solved analytically using closed-form equations or iteratively using optimization algorithms.
Complexity	ANN can have multiple layers and numerous neurons, resulting in complex architectures.	LR has a simple and interpretable model with coefficients representing the impact of variables.
Interpretability	ANN is often considered black boxes, making it challenging to interpret the learned relationships.	LR allows for easy interpretation as coefficients indicate the magnitude and direction of variable impacts.
Handling outliers	ANN can be more robust to outliers as it captures non-linear patterns and is less influenced by extreme values.	LR is sensitive to outliers and can be heavily influenced by their presence.
Performance	ANN can provide high accuracy and predictive power, particularly in complex and non-linear tasks.	LR performs well when assumptions of linearity are met and the relationship between variables is simple.
Computational requirements	ANN typically requires more computational resources (memory, processing power) for training and inference compared to linear regression.	LR is computationally less demanding and can be solved efficiently.
Data size	ANN can handle large datasets effectively and can benefit from big data.	LR is less affected by data size and can handle small to moderate datasets efficiently.

2.2. Details of the Datasets and Machine Learning Algorithms

In this study, machine learning algorithms are used to predict the isentropic compressibility values of binary blends containing oxygenated additives (DBE and butanol) and hydrocarbons (toluene and cyclohexane) depending on the mole fraction of the first (1) component. The isentropic compressibility data measured by Abala et al. [31] are used to establish a predictive model in ANN and LR algorithms. The input and output variables used in these algorithms are listed in Table 2. The input and output data are randomly divided into three separate sets: training (70%), validation (15%), and test (15%) to provide the reliability and robustness of these algorithms. The root mean square error (RMSE) and regression parameters are calculated to evaluate the predictive capabilities of the machine learning algorithms. Table 3 shows the hyperparameters of the machine learning algorithms in this study.

Table 2. *Input and output variables used in ANN and LR [31]*

Input Parameters		Output Parameter
Temperature, T/K (Kelvin)	298.15	Isentropic compressibility (k_s) ($10^{12} \times \text{Pa}^{-1}$)
Pressure, P/MPa	0.1	
Dibutyl ether (DBE) (1) + Butanol (2)	1	
Dibutyl ether (DBE) (1) + Toluene (2)	2	
Butanol (1) + Toluene (2)	3	
Dibutyl ether (DBE) (1) + Cyclohexane (2)	4	
Mole fraction of the first component (x_1)	0-1	

Table 3. *Hyperparameters of ANN and LR*

ANN	LR
Preset: Trilayered neural network	Preset: Interactions linear
Number of fully connected layers: 3	Terms: Interactions
First layer size: 10	Robust option: Off
Second layer size: 10	PCA disabled
Third layer size: 10	
Activation: ReLU	
Iteration limit: 1000	
Regularization strength (Lambda): 0	
Standardize data: Yes	

3. Results and Discussion

Table 4 shows the performance indicators of the ANN and LR algorithms for predicting the isentropic compressibility of the binary blends. Figure 1 depicts the validation and testing outcomes of these machine learning algorithms, respectively. For the ANN, the RMSE values indicate that the

predicted values deviate from the measured data by 1.8343 and 2.5156 for the validation and test sets, respectively. Moreover, R^2 is calculated as 1.00 for both the validation and test sets. In contrast, the LR exhibits higher RMSE values (31.12 for the validation set and 32.886 for the test set), compared to the ANN. R^2 scores for the LR are 0.93 for the validation set and 0.85 for the test set. For DBE+Butanol, DBE+Toluene, Butanol+Toluene, and DBE+Cyclohexane binary blends, the relative errors coming from ANN and LR vary in the following range: 0.0003%-0.2434% and 0.0750%-3.0071%; 0.0009%-0.8653% and 0.3145%-9.7351%; 0.0002%-0.2412% and 2.5794%-6.5749%; and 0.0002%-0.2565% and 1.6474%-3.6375%, respectively. According to the regression results, because the ANN achieves lower RMSE values and a perfect fit ($R^2 = 1.00$) for both the validation and test sets, it demonstrates excellent quantitative agreement between the measured data and calculated values, compared to the LR. On the other hand, LR shows higher RMSE values and lower R^2 scores, suggesting that it does not capture the complexities of the data as effectively as ANN.

Table 4. Training results of ANN and LR

Algorithm	RMSE Validation	R^2 Validation	RMSE Test	R^2 Test
ANN	1.8343	1.00	2.5156	1.00
LR	31.12	0.93	32.886	0.85

Figure 2 illustrates the measured isentropic compressibility data at different mole fractions along with the predicted isentropic compressibility values from the ANN and LR for different binary blends. These findings indicate that an increase in the mole fraction corresponds to an increase in the isentropic compressibility. Moreover, the isentropic compressibility values differ for distinct binary blends. In other words, the ANN and LR models exhibit different performance characteristics in the prediction of the isentropic compressibility across different mole fractions. As depicted in Figure 2, the ANN model is qualitatively more consistent with the experimental data than the LR model.

After a thorough analysis of the results presented in both tabular and graphical forms, it can be noted that the ANN model outperforms the LR model in terms of prediction performance. These findings may have significant implications across various fields, including fuel and combustion science as well as in renewable energy research. By harnessing the capabilities of machine learning algorithms, researchers can enhance their understanding of the intricate interplay between input and output parameters.

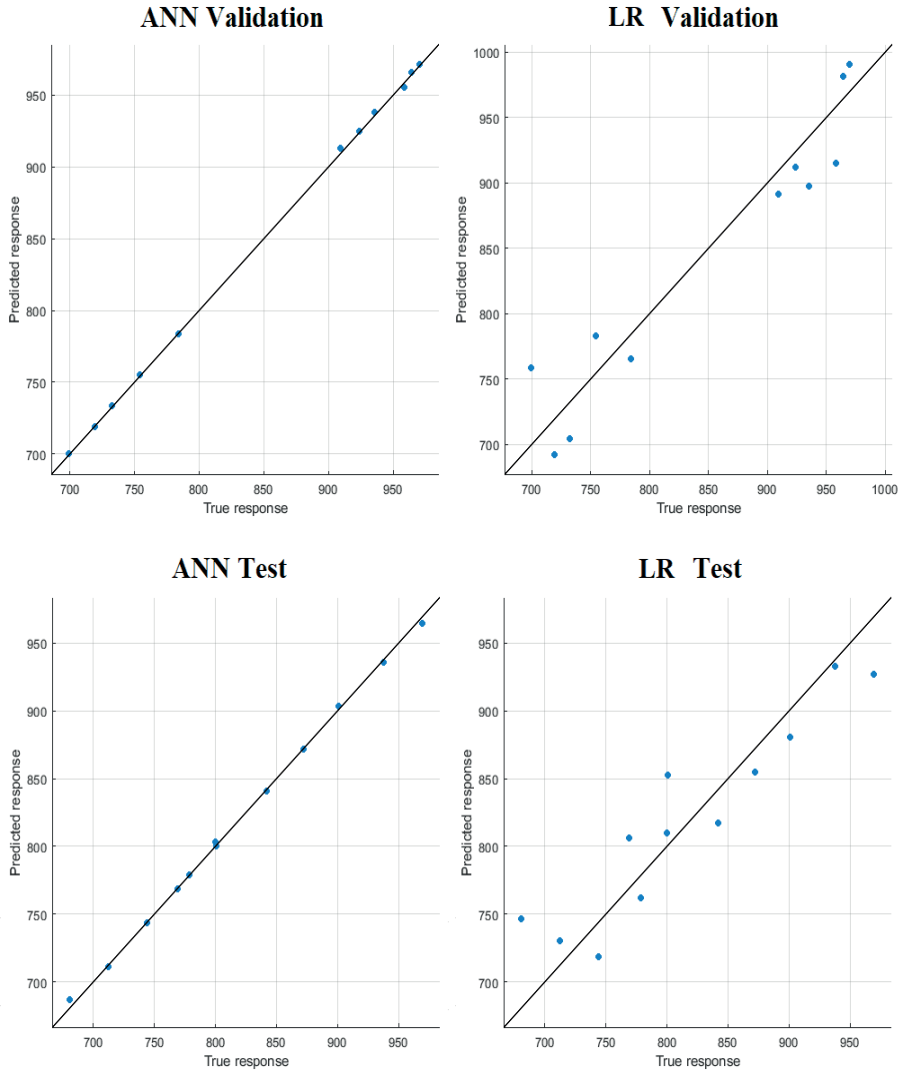


Figure 1. Validation and test results of ANN and LR

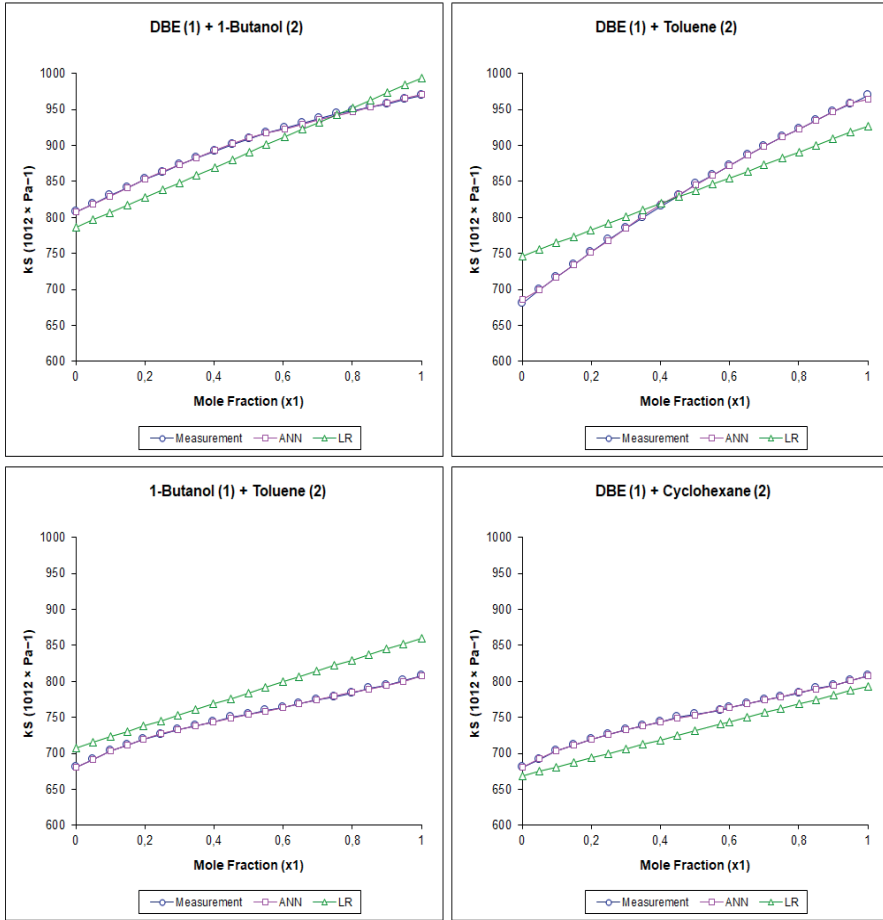


Figure 2. Comparison of the measured isentropic compressibility data with the predicted isentropic compressibility values from ANN and LR for different binary blends

4. Conclusion

The objective of this study is to predict the isentropic compressibility of binary blends containing oxygenated additives (DBE and butanol) and hydrocarbons (toluene and cyclohexane). Traditional methods for estimating isentropic compressibility rely on empirical correlations or thermodynamic models. However, these approaches can suffer from limited accuracy, particularly over a wider composition range. To overcome this limitation, advanced machine learning algorithms, namely ANN and LR, are employed in this study to predict the isentropic compressibility of the binary blends. The prediction performance of the machine learning algorithms is evaluated by comparing the root mean square error and R^2 values.

The results obtained from the ANN and LR models show that the ANN model qualitatively and quantitatively outperforms the LR model in predicting the isentropic compressibility of binary blends under different mole fractions. The ANN model demonstrates superior accuracy owing to its lower RMSE values (1.8343 for the validation dataset and 2.5156 for the test dataset) and a perfect fit ($R^2 = 1.00$) for both the validation and test datasets. This underlines the capability of the ANN model to reflect the complex relationships in isentropic compressibility data. These outcomes may benefit fuel and combustion science, renewable energy research, and other related fields, offering researchers a useful tool for understanding the fuel components and their isentropic compressibilities. Machine learning algorithms can enable improved predictions and enhance knowledge of the interactions between variables, thereby contributing to fuel science progress and sustainable energy solution development.

REFERENCES

- [1] Dubey, A., Prasad, R.S., Singh, J.K., & Nayyar, A. (2022). Optimization of diesel engine performance and emissions with biodiesel-diesel blends and EGR using response surface methodology (RSM). *Cleaner Engineering and Technology*, 8, 100509.
- [2] Arteconi, A., Mazzarini, A., & Di Nicola, G. (2011). Emissions from ethers and organic carbonate fuel additives: a review. *Water, Air, & Soil Pollution*, 221, 405–423.
- [3] Manzer, L.E., D'Amore, M.B., & Miller, E.S. (2008). Process for making dibutyl ethers from dry ethanol. WO2008069981.
- [4] Karas, L., & Piel, W.J.E. (2005). Kirk-othmer encyclopedia of chemical technology, Fifth Ed., vol. 10, section 5.3, 576-597.
- [5] Wang, J., Sun, L., Luan, P., Wu, Y., Cheng, Z., Zhang, Z., Kong, X., Liu, H., & Chen, G. (2022). Effect of diesel blended with di-n-butyl ether/1-octanol on combustion and emission in a heavy-duty diesel engine. *Environmental Pollution*, 311, 119976.
- [6] Zhong, A., & Han, D. (2022). Experimental and kinetic modelling studies on di-n-butyl ether (DBE) low temperature auto-ignition. *Combustion and Flame*, 237, 111882.
- [7] Rahiman, M.K., Santhoshkumar, S., Subramaniam, D., Avinash, A., & Pugazhendhi, A. (2022). Effects of oxygenated fuel pertaining to fuel analysis on diesel engine combustion and emission characteristics. *Energy*, 239, 122373.
- [8] Tipanluisa, L., Thakkar, K., Fonseca, N., & López, J.M. (2022). Investigation of diesel/n-butanol blends as drop-in fuel for heavy-duty diesel engines: combustion, performance, and emissions. *Energy Conversion and Management*, 255, 115334.
- [9] Karthick, C., & Nanthagopal, K. (2021). A comprehensive review on ecological approaches of waste to wealth strategies for production of sustainable biobutanol and its suitability in automotive applications. *Energy Conversion and Management*, 239, 114219.
- [10] Lapuerta, M., Hernández, J.J., Rodríguez, D.F., & Bonillo, A.C. (2017). Auto-ignition of blends of n-butanol and ethanol with diesel or biodiesel fuels in a constant-volume combustion chamber. *Energy*, 118, 613-621.
- [11] Nanthagopal, K., Kishna, R.S., Atabani, A.E., Al-Muhtaseb, A.H., Kumar, G., & Ashok, B. (2020). A compressive review on the effects of alcohols and nanoparticles as an oxygenated enhancer in compression ignition engine. *Energy Conversion and Management*, 203, 112244.
- [12] Lapuerta, M., Rodríguez-Fernández, J., Fernández-Rodríguez, D., & Patiño-Camino, R. (2017). Modeling viscosity of butanol and ethanol blends with diesel and biodiesel fuels. *Fuel*, 199, 332-338.

- [13] Ning, L., Duan, Q., Chen, Z., Kou, H., Liu, B., Yang, B., & Zeng, K. (2020). A comparative study on the combustion and emissions of a non-road common rail diesel engine fueled with primary alcohol fuels (methanol, ethanol, and n-butanol)/diesel dual fuel. *Fuel*, 266, 117034.
- [14] Lujaji, F., Kristóf, L., Bereczky, A., & Mbarawa, M. (2011). Experimental investigation of fuel properties, engine performance, combustion and emissions of blends containing croton oil, butanol, and diesel on a CI engine. *Fuel*, 90(2), 505-510.
- [15] Kumar, K.S., Babu, J.M., & Venu, H. (2022). Performance, combustion and emission characteristics of a single-cylinder DI diesel engine fuelled with lotus biodiesel-diesel-n-butanol blends. *International Journal of Ambient Energy*, 43(1), 7941-7951.
- [16] Zhang, Z., Tian, J., Xie, G., Li, J., Xu, W., Jiang, F., Huang, Y., & Tan, D. (2022). Investigation on the combustion and emission characteristics of diesel engine fueled with diesel/methanol/n-butanol blends. *Fuel*, 314, 123088.
- [17] Benjumea, P., Agudelo, J., & Agudelo, A. (2008). Basic properties of palm oil biodiesel-diesel blends. *Fuel*, 87(10-11), 2069-2075.
- [18] Ramírez-Verduzco, L.F., García-Flores, B.E., Rodríguez-Rodríguez, J.E., & Jaramillo-Jacob, A.D.R. (2011). Prediction of the density and viscosity in biodiesel blends at various temperatures. *Fuel*, 90(5), 1751-1761.
- [19] Mejía, J.D., Salgado, N., & Orrego, C.E. (2013). Effect of blends of diesel and palm-castor biodiesels on viscosity, cloud point and flash point. *Industrial Crops and Products*, 43, 791-797.
- [20] Krisanangkura, P., Lilitchan, S., Phankosol, S., Aryusuk, K., & Krisanangkura, K. (2018). Gibbs energy additivity approaches to QSPR in modelling of isentropic compressibility of biodiesel. *Journal of Molecular Liquids*, 249, 126-131.
- [21] Ndiaye, E.H.I., Bazile, J.P., Nasri, D., Boned, C., & Daridon, J.L. (2012). High pressure thermophysical characterization of fuel used for testing and calibrating diesel injection systems. *Fuel*, 98, 288-294.
- [22] Tat, M.E., Van Gerpen, J.H., Soylu, S., Canakci, M., Monyem, A., & Wormley, S. (2000). The speed of sound and isentropic bulk modulus of biodiesel at 21°C from atmospheric pressure to 35 MPa. *Journal of the American Oil Chemists' Society*, 77, 285-289.
- [23] Daridon, J.L., Coutinho, J.A.P., Ndiaye, E.H.I., & Paredes, M.L.L. (2013). Novel data and a group contribution method for the prediction of the speed of sound and isentropic compressibility of pure fatty acids methyl and ethyl esters. *Fuel*, 105, 466-470.
- [24] Habrioux, M., Nasri, D., Coutinho, J.A.P., & Daridon, J.L. (2023). Measurement and prediction of the volumetric and acoustic properties of two biodiesel fuels up to 200 MPa. *Fuel*, 349, 128677.
- [25] Habrioux, M., Nasri, D., & Daridon, J.L. (2018). Measurement of speed of

- sound, density compressibility and viscosity in liquid methyl laurate and ethyl laurate up to 200 MPa by using acoustic wave sensors. *The Journal of Chemical Thermodynamics*, 120, 1-12.
- [26] Sirimongkolgal, N., Phankosol, S., & Chum-in, T. (2022). Gibbs energy additivity approaches for isentropic compressibility of biodiesels (ethyl ester). *International Journal of Mechanical Engineering*, 7(8), 231-241.
- [27] Amasyali, K., & El-Gohary, N.M. (2018). A review of data-driven building energy consumption prediction studies. *Renewable and Sustainable Energy Reviews*, 81(1), 1192-1205.
- [28] Sarker, I.H. (2021). Machine learning: algorithms, real-world applications and research directions. *SN Computer Science*, 160, 1-21.
- [29] Tosun, E., Aydin, K., & Bilgili, M. (2016). Comparison of linear regression and artificial neural network model of a diesel engine fueled with biodiesel-alcohol mixtures. *Alexandria Engineering Journal*, 55(4), 3081-3089.
- [30] Kadnár, M., Káčer, P., Harničárová, M., Valíček, J., Tóth, F., Bujna, M., Kušnerová, M., Mikuš, R., & Boržan, M. (2023). Comparison of linear regression and artificial neural network models for the dimensional control of the welded stamped steel arms. *Machines*, 11, 376, 1-18.
- [31] Abala, I., Lifi, M., Alaoui, F.E.M., Muñoz-Rujas, N., Aguilar, F., & Montero, E.A. (2021). Density, speed of sound, isentropic compressibility, and refractive index of ternary mixtures of oxygenated additives and hydrocarbons (dibutyl ether + 1-butanol + toluene or cyclohexane) in fuels and biofuels: experimental data and PC-SAFT equation-of-state modeling. *J. Chem. Eng. Data*, 66, 3, 1406-1424.

A circular graphic with a green top half and a white bottom half, surrounded by a green outline. The text is centered within the circle.

Chapter 3

HYDROXYAPATITE SYNTHESIS AND COATING METHODS

Safiye İPEK AYVAZ¹

¹ Manisa Celal Bayar University, Turgutlu Vocational School, Department of Machinery and Metal Technologies, 45140 Manisa, Turkey
E-mail: safiye.ipek@cbu.edu.tr
Orcid id: orcid.org/0000-0001-7385-7388

1. HYDROXYAPATITE

Metal biomaterials are generally coated with bioceramics to improve their biocompatibility and chemical stability (Yilmaz et al., 2014). Some of the ceramic biomaterials, such as alumina and zirconia, are bioinert. In other words, they do not interact with the tissue in which they are implanted. However, some bioceramics such as hydroxyapatite (HAp) are classified as bioactive. These ceramic biomaterials accelerate the recovery process by increasing the formation of cells of the transplanted tissue (Korkusuz & Korkusuz, 1997).

Many solutions have been sought throughout history for the regeneration and fracture healing of bone, which is inorganic and composed of calcium and phosphate. As a result of many years of research, which accelerated in the 20th century, HAp, which is bioactive and osteoconductive, has shown to be the best artificial bone material. (Korkusuz & Korkusuz, 1997). HAp composed of calcium and phosphate apatites is represented by the formula $\text{Ca}_{10}(\text{PO}_4)_6(\text{OH})_2$ (Bogdanoviciene et al., 2006; Hung et al., 2012; Kong et al., 2002; Nayak, n.d.; Poštić, 2014). The physicochemical, mechanical and some biological properties of HAp are also shown in Table 1.

Table 1. *Physicochemical, Mechanical and Biological Properties of HAp (Çağlayan E, 2016).*

Properties	
Molecular Formula	$\text{Ca}_{10}(\text{PO}_4)_6(\text{OH})_2$
Ca/P Ratio	1.67
Crystal Structure	Hexagonal
Modulus of Elasticity (GPa)	4.0-117
Compressive Strength (MPa)	400 - 900
Flexural Strength (MPa)	147
Tensile Strength (MPa)	115 - 200
Density (g/m^3)	3.16
Fracture Toughness ($\text{MPa m}^{1/2}$)	0.7 - 1.2
Sertlik (Vickers, GPa)	3.43
Poisson Ratio	0.27
Decomposition Temperature ($^{\circ}\text{C}$)	>1000
Melting Temperature ($^{\circ}\text{C}$)	1614
Dielectric Constant	7.40
Thermal Conductivity (W/cmK)	0.013
Bioactivity	High
Biocompatibility	High
Biodegradation	Low
Cellular Compatibility	High
Bone Conductivity	High

Figure 1 shows the similarity between bone and HAp in SEM images. As can be seen, both HAp and bone have a porous structure. This porous structure of HAp provides two advantages. The first one is that it allows the passage of blood and other body fluids that the bone needs during the healing and development process. Secondly, it allows these new developing cells to grow into the pores of HAp, allowing the formation of a bond between the implant and the tissue. (ENGIN F, 2017). Bone development in porous structure is shown in Figure 2.

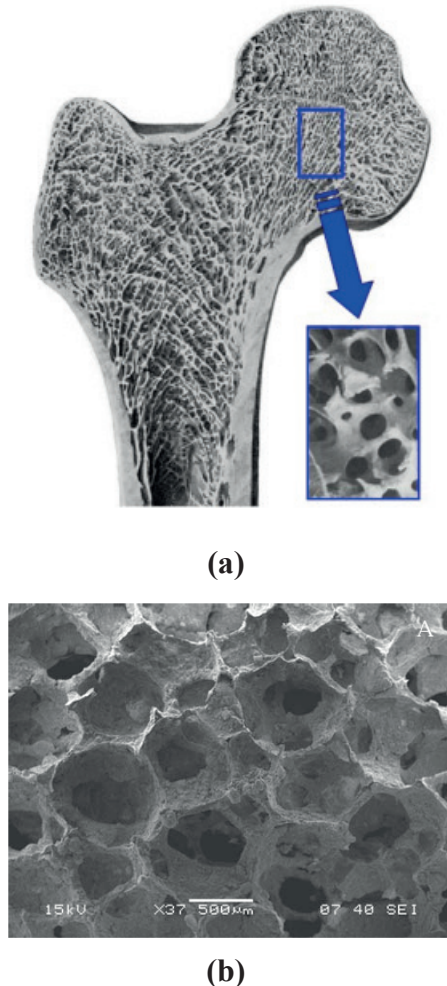


Figure 1. SEM image of bone and HAp: (a) Bone (Tsuchiya et al., 2008), (b) HAp (Swain, n.d.).

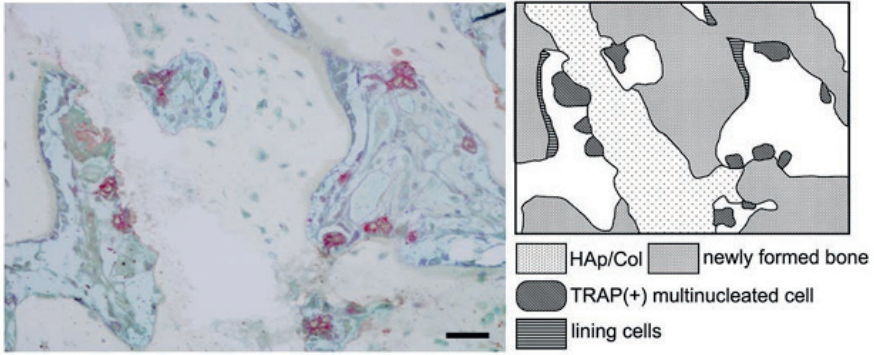


Figure 2. New Bone Tissue Formation in Porous HAp (Tsuchiya et al., 2008).

In addition, HAp is intensively studied and researched in different branches due to the fact that different cations such as Mg^{2+} , Zn^{2+} , La^{3+} , Y^{3+} , In^{3+} , Al^{3+} and Bi^{3+} can be added instead of calcium (Piattelli et al., n.d.).

2. HYDROXYAPATITE SYNTHESIS AND COATING METHODS

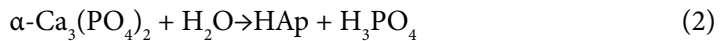
Despite HAp's high biological and chemical biocompatibility, they cannot be used alone in implant areas where strength is required due to their low mechanical properties. Instead, metallic biomaterials are coated with HAp.

HAp powders can be synthesized by wet chemical method, hydrothermal method, sol-gel method, continuous and thermal precipitation methods and solid state reactions. Some example reactions are given below (Evcin A et al., 2009):

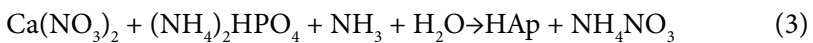
Solid state reaction;



Hydrolysis reaction;



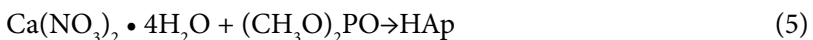
Precipitation process;



Hydrothermal synthesis;



Sol-gel process;



Mechanochemical process;



2.1. Plasma Spray Coating Method

Plasma spray coating is one of the methods of coating metals with different metal and ceramic powders to increase their corrosion, wear and fatigue resistance and to make them heat resistant. Due to its ease of application and low cost, plasma spray coating is the most common application for HAp and Calcium phosphate (Ca-P) coatings (Evcin A et al., 2009). The application has two disadvantages. The first one is that the coating is not homogeneous in terms of thickness and density. The other disadvantage is the stresses and cracks caused by the coefficient of thermal expansion between the substrate and the coating material (Çağlayan E, 2016).

2.2. Thermal Spray Coating Method

Thermal spray coating method, which is widely used to protect the coated material from wear, corrosion and temperature, is also used in biomedical applications. In thermal spray coating, the coating powder is melted by electric arc, plasma or flame or sprayed onto the workpiece in semi-melted form with inert gas. The schematic image of the coating is given in Figure 3 (Yang et al., 2005). Thermal spray method has lower cost compared to plasma spray method (Chean & Khors, 1996; Yang et al., 2005). In the literature, it has been reported that in HA coating with thermal spray, coating thicknesses up to 200 μm can be achieved, but non-uniform crystallization may occur in the HAp coating and the bond between the HAp coating and the implant is weak (Hamdi et al., 2000; Hanyaloglu et al., n.d.).

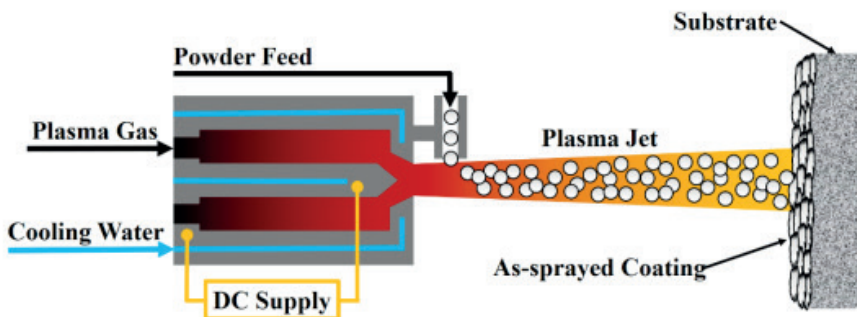


Figure 3. Schematic View of Thermal Spray Coating (L.-H. Chen et al., 2017).

2.3 Coating by Hot Isostatic Pressing

Porous HAp implant coatings are made by powder metal sintering under high pressure and temperature or by hot isostatic pressing method used as coating method (Hanyaloglu et al., n.d.). A schematic image of the hot isostatic pressing method is shown in Figure 4.

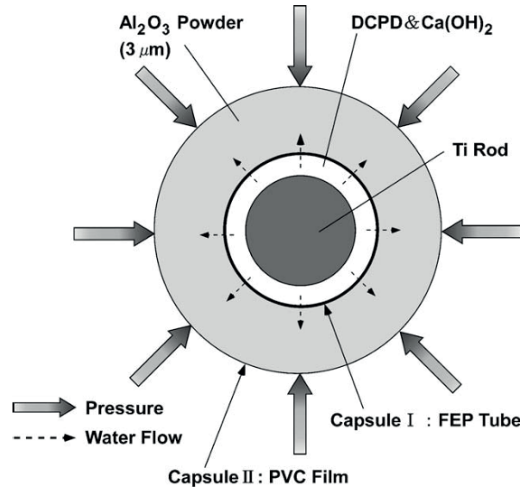


Figure 4. Schematic Image of Hot Isostatic Pressing Method (Onoki & Hashida, 2006).

2.4. Sol-Gel Coating Method

Sol-gel is a method of coating on glass or metal, usually ceramics, in the form of one or several very thin films. In this process, starting chemicals are converted into nano-sized particles to generate a colloidal suspension (sol). These colloidal nanoparticles are then bonded together in a three-dimensional liquid-filled net (gel) (ENGİN F, 2017). Sol-gel coating is an easy, economical, effective and low sintering temperature method, but the abrasion resistance of the final sample is low and porosity control is very difficult (Olding et al., 2001).

2.5. Biomimetic Coating Method

The systems that people design by taking the systems found in nature as an example, inspiration and imitation are called biomimetics. The aim of HAp coating with biomimetic method is to develop biomaterials compatible with human tissues and cells. For this purpose, artificial body fluids (ABFs) that are fully compatible with the human body are produced in a laboratory environment. In this ABF, HAp is deposited on the activated surface of the substrate material and the surface is coated. This process is also carried out in a biomimetic environment (37 °C ve 7,4 pH).

HA coating with the biomimetic method is carried out in three stages:

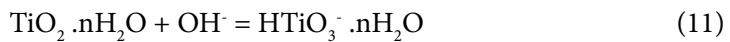
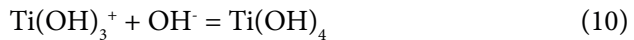
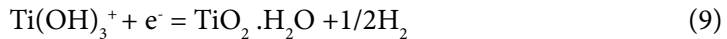
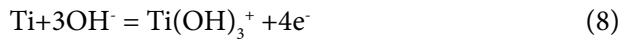
1. The surface of the substrate is cleaned and activated with the help of chemicals.
2. Heat treatment is applied to the substrate material for apatite nucleation to take place.
3. The substrate is kept in ABF and coated.

The chemical reactions of apatite formation on the titanium substrate surface are as follow

1. Titanium oxide (TiO_2) on the surface of titanium is reacted in an alkaline aqueous solution:



2. Ti under TiO_2 reacts as follows:



3. After the negatively charged $\text{HTiO}_3^- \cdot \text{nH}_2\text{O}$ absorbs sodium ions into its structure, heat treatment is applied in the chemical environment necessary for the initiation of apatite nuclea (Çağlayan E, 2016; ENGİN F, 2017).

2.6. Comparison of HA Coating Methods

Table 2 shows a comparison of different coating methods in terms of coating thickness, advantages and disadvantages. In most of the methods, cracks can be seen due to the high temperature input and the coefficient of thermal expansion during cooling. In the electrochemical method, although the coating thickness was high, it was noted that there was not a good bond strength between the coating and the substrate. The biomimetic method stands out with a coating thickness of up to 30 μm and helps bone healing.

Table 2. Comparison of Different Hydroxyapatite Coating Methods (Asri et al., 2016; Mohseni et al., 2014).

Method	Coating Thickness	Advantage	Disadvantage
Biomimetics	< 30 μm	Acceleration of bone healing with low production temperature, formation of apatite similar to bone structure	Difficulty in creating ABF liquid, time consuming process.
Sol-Gel	< 1 μm -2 μm	Economical, extremely thin, high purity film coatings.	Thermal expansion coefficient mismatch, low wear resistance and difficult pore control in high temperature sintering
Hot Isostatic Pressing	0.2-2 mm	Production in desired dimensions and surface properties	High temperature, high pressure and high cost requirement
Plasma Spray	< 20 μm	Fast and cheap	Poor bonding and residual stress generation between HA and implant
Thermal Spray	30-200 μm	Achieving fast, cheap and thick coating	Low porosity HA coating formation, crack formation due to rapid cooling
Electrochemical	0.05-0.5 mm	Fast, inexpensive and uniform thickness coating	Weak bonds between the substrate and HA coating

3. LITERATURE REVIEW

In recent years, there have been many studies in which magnesium alloys (AZ31, AZ91D, Mg-9Li-7Al-1Si, Mg-9Li-5Al-3Sn-1Zn etc.), CoCrMo alloys, titanium alloys (Ti-6Al-4V, Ti-13Nb-13Zr, Ti-6Al-7Nb etc.), stainless steels and zirconium have been coated with HAp using different coating methods. (Aktug et al., 2017; Al-Rashidy et al., 2017; Ayu et al., 2017; Blanda et al., 2016; Coşkun et al., 2015; İbrahim Coşkun et al., 2016; Jia et al., 2016; Jugowiec et al., 2017; Kulpetchdara et al., 2016; Maurya et al., 2017; Tang et al., 2017; Tang & Gao, 2016; Yu et al., 2017).

In their study, Kokubo et al. coated different biomaterials with HAp in ABF for the first time using a Tris-HCl buffer system. However, it was observed that the ABF fluid used was not fully compatible with human blood plasma (Kokubo et al., n.d.).

In his study, Taş used artificial body fluid that is closer to blood plasma in terms of ion values than Kokubo et al. In the study, nano-sized HAp (n-HAp) was synthesized by biomimetic method using $\text{Ca}(\text{NO}_3)_2 \cdot 4\text{H}_2\text{O}$ and $(\text{NH}_4)_2\text{HPO}_4$ salts (Tas A C, 2000).

Hamadouche et al. reported in their study that the surface roughness of the substrate, the chemical composition of the biomaterial and the coating thickness are important for a suitable biocoating (McEntire et al., 2015).

In their study, Wang et al. fabricated composites with polyamide (PA) matrix and needle-shaped n-HAp reinforcement. Homogeneous dispersion and interfacial bonding were observed in the PA/n-HAp composite, which enhanced bioactivity and mechanical properties (Wang et al., 2002).

Chen ve ark., çalışmalarında sulu çözeltilerden HA üretimini gerçekleştirmişlerdir. Aktifleştirme işlemi $\text{Ca}(\text{NO}_3)_2$ ve $\text{NH}_4\text{H}_2\text{PO}_4$ çözeltisinde pH 10'dan fazla ve Ca/P oranı 1.67'de gerçekleştirildi. Daha sonra pH 7'ye düşürüldü ve kurutma işlemi 80°C 'de yapıldı. Bu çalışmada, 20-30 nm genişlikte ve 50-60 nm uzunlukta n-HAp nanopartikülleri üretilmiştir. (F. Chen et al., n.d.).

Şerbetçi et al. applied in-vivo tests to bone cement prepared by adding HAp in their study. As a result of the tests, it was observed that HAp addition increased the biocompatibility of bone cement and it was stated that it could be used in medical applications (Şerbetçi K et al., 2002).

Kim et al. produced amorphous n-HAp powders in the size range of 50-150 nm in $\text{Ca}(\text{NO}_3)_2 \cdot 4\text{H}_2\text{O}$ and P_2O_5 solution using sol-gel method (Kim & Kumta, 2004).

Cao et al. produced n-HAp with a size of 20 nm by ultrasonic heating using $\text{Ca}(\text{NO}_3)_2$ and Na_2HPO_4 . They used carbamide (NH_2CONH_2) for the precipitation process (Cao et al., 2005).

Feng et al. produced single phase, 10-15 nm sized n-HAp in P_2O_5 and $\text{Ca}(\text{NO}_3)_2 \cdot 4\text{H}_2\text{O}$ solution using sol-gel method and 600-700 °C sintering temperature (Feng et al., 2005).

Guo et al. produced n-HAp using microemulsion method in their study. The analysis showed that the n-HA powders produced were 20-100 nm in size (Guo et al., 2005).

In their study, Han et al. realized n-HAp production by microwave-hydrothermal method. The production was carried out by holding H_3PO_4 and $\text{Ca}(\text{OH})_2$ under 600 bar at a temperature of 300 °C for 30 min. It was reported that when 550 W was used in the microwave, two different types of n-HAp were formed: needle-like with a width of 4-15 nm and a length of 10-50 nm and spherical with a diameter of 10-30 nm. (Han et al., 2006).

In their study, Wei et al. performed HAp coating process by keeping Ti6Al4V alloy samples in ABF at 37 °C for 24 hours. It was reported that the strength of the coating with the substrate was strong and allowed new bone cells to grow (Hu et al., 2017).

In their study, Leena et al. synthesized nano HAp by biomimetic method in ABF. In the study, it was reported that biomimetic nano HAp synthesis took 3-24 hours shorter than classical synthesis (Leena et al., 2016).

Avcı et al. coated Ti6Al4V titanium alloy with HA using biomimetic method in their study. Titanium alloy samples were kept in 5 M NaOH solution at 600 °C for 24 hours in order to activate their surfaces. NaCl, NaHCO₃, KCl, K₂HPO₄-3H₂O, MgCl₂-6H₂O, CaCl₂ and Na₂SO₄ were used as ABF. Two separate solutions were prepared by adding 0.15 and 1 mM Sr²⁺. The samples coated with 0.15 mM ABF showed better cell growth (Avcı et al., 2017).

Bayrak et al. synthesized HA using microwave heating in ABF 10 times more concentrated than human plasma. The method was reported to be faster (Kaynak Bayrak et al., 2017).

In their study, Ruiz et al. coated Ti alloy samples with ABF solution using biomimetic method. Collagens were added to the ABF and their effects were analyzed (Ruiz et al., 2017).

Gabriela and Octavian Ciobanu prepared ABF from CaCl₂-2H₂O, NaH₂PO₄-H₂O and NaHCO₃ solution and coated Ti samples with HAp. Vitamins A and D3 were added to the prepared ABF solution in order to examine the effect of vitamins. It was determined that the added vitamins accelerated the formation of apatite and the apatites formed were in smaller crystalline structures. (Ciobanu & Ciobanu, 2013).

In their study, Ou et al. coated Ti6Al4V alloy with HAp by biomimetic method. In the study, collagens were used to examine their effects on mechanical properties. As a result, it was observed that the modulus of elasticity of the samples to which collagen was added increased from 3.6 GPa to 7.5 GPa. It was stated that the method can be used in severe injuries (Ou et al., 2011).

In their study, Faure et al. coated Ti6Al4V alloy with bone-like apatites using a biomimetic method. Amino acids and vitamins were added to the artificial body fluid used to help cell formation. The coating was reported to be successful (Faure et al., 2009).

In order to prevent infections that may occur after the implantation process, Stigter et al. coated Ti6Al4V alloy samples with HAp by biomimetic method by adding Tobramycin antibiotic active substance into the ABF they prepared. As a result, the coating was found to be very effective against *Staphylococcus aureus* bacteria (Stigter et al., 2002).

4. RESULTS

Hydroxyapatite can be obtained by different synthesis methods and coated on biometals, especially those used as orthoses/prostheses, to improve

their biocompatibility. Studies have focused on synthesizing and coating hydroxyapatite coatings more easily, in a short time and at lower cost. In addition, mechanical, microstructural, chemical and tribological properties of the coatings are investigated. In addition to these, the antibacterial activity of hydroxyapatite coatings is also tried to be improved. With the studies carried out and various properties developed, hydroxyapatite coating applications are increasing.

REFERENCES

- Aktug, S. L., Kutbay, I., & Usta, M. (2017). Characterization and formation of bioactive hydroxyapatite coating on commercially pure zirconium by micro arc oxidation. *Journal of Alloys and Compounds*, 695, 998–1004. <https://doi.org/10.1016/j.jallcom.2016.10.217>
- Al-Rashidy, Z. M., Farag, M. M., Ghany, N. A. A., Ibrahim, A. M., & Abdel-Fattah, W. I. (2017). Aqueous electrophoretic deposition and corrosion protection of borate glass coatings on 316 L stainless steel for hard tissue fixation. *Surfaces and Interfaces*, 7, 125–133. <https://doi.org/10.1016/j.surfin.2017.03.010>
- Asri, R. I. M., Harun, W. S. W., Hassan, M. A., Ghani, S. A. C., & Buyong, Z. (2016). A review of hydroxyapatite-based coating techniques: Sol-gel and electrochemical depositions on biocompatible metals. In *Journal of the Mechanical Behavior of Biomedical Materials* (Vol. 57, pp. 95–108). Elsevier Ltd. <https://doi.org/10.1016/j.jmbbm.2015.11.031>
- Avci, M., Yilmaz, B., Tezcaner, A., & Evis, Z. (2017). Strontium doped hydroxyapatite biomimetic coatings on Ti6Al4V plates. *Ceramics International*, 43(12), 9431–9436. <https://doi.org/10.1016/j.ceramint.2017.04.117>
- Ayu, H. M., Izman, S., Daud, R., Krishnamurthy, G., Shah, A., Tomadi, S. H., & Salwani, M. S. (2017). Surface Modification on CoCrMo Alloy to Improve the Adhesion Strength of Hydroxyapatite Coating. *Procedia Engineering*, 184, 399–408. <https://doi.org/10.1016/j.proeng.2017.04.110>
- Blanda, G., Brucato, V., Pavia, F. C., Greco, S., Piazza, S., Sunseri, C., & Inguanta, R. (2016). Galvanic deposition and characterization of brushite/hydroxyapatite coatings on 316L stainless steel. *Materials Science and Engineering C*, 64, 93–101. <https://doi.org/10.1016/j.msec.2016.03.088>
- Bogdanoviciene, I., Beganskiene, A., Tõnsuaadu, K., Glaser, J., Meyer, H. J., & Kareiva, A. (2006). Calcium hydroxyapatite, Ca₁₀(PO₄)₆(OH)₂ ceramics prepared by aqueous sol-gel processing. *Materials Research Bulletin*, 41(9), 1754–1762. <https://doi.org/10.1016/j.materresbull.2006.02.016>
- Çağlayan E. (2016). *Alanin-Alanin Sodyum Tuzu Ortamında Ti Bazlı Ti-Alaşımlarının Hidroksiapatit İle Kaplanması Ve Kaplamanın Bazı Özelliklerinin İncelenmesi*. Celal Bayar Üniversitesi.
- Cao, L. Y., Zhang, C. B., & Huang, J. F. (2005). Synthesis of hydroxyapatite nanoparticles in ultrasonic precipitation. *Ceramics International*, 31(8), 1041–1044. <https://doi.org/10.1016/j.ceramint.2004.11.002>
- Chean, P., & Khors, K. A. (1996). Addressing processing problems associated with plasma spraying hydroxyapatite coatings * of. In *Biomaterials* (Vol. 17).
- Chen, F., Wang, Z.-C., & Lin, C.-J. (n.d.). *Preparation and characterization of nano-sized hydroxyapatite particles and hydroxyapatite/chitosan nano-composite for use in biomedical materials*. www.elsevier.com/locate/matlet
- Chen, L.-H., Chen, Y.-R., Chou, C.-Y., Chen, C.-H., Ko, C.-C., & Tung, K.-L. (2017).

Inorganic Membranes in Water and Wastewater Treatment (pp. 121–154). https://doi.org/10.1007/978-981-10-5623-9_5

- Ciobanu, G., & Ciobanu, O. (2013). Investigation on the effect of collagen and vitamins on biomimetic hydroxyapatite coating formation on titanium surfaces. *Materials Science and Engineering C*, 33(3), 1683–1688. <https://doi.org/10.1016/j.msec.2012.12.080>
- Coşkun, M. I., Karahan, I. H., & Golden, T. D. (2015). Computer assisted corrosion analysis of hydroxyapatite coated CoCrMo biomedical alloys. *Surface and Coatings Technology*, 275, e1–e9. <https://doi.org/10.1016/j.surfcoat.2015.05.037>
- ENGİN F. (2017). *Glikolik Asit-Sodyum Glikolat Tampon Sistemi Kullanılarak Oluşturulan Hidroksiapatit Kaplamanın Mekanik Özelliklerinin İncelenmesi*. Celal Bayar Üniversitesi.
- Evcin A, Kepekçi D B, & Barut İ. (2009, May 13). Coating Of Hydroxyapatite Powder By Plasma Spraymethod On Stainless Steel. *IATS'09*. <https://www.researchgate.net/publication/280304812>
- Faure, J., Balamurugan, A., Benhayoune, H., Torres, P., Balossier, G., & Ferreira, J. M. F. (2009). Morphological and chemical characterisation of biomimetic bone like apatite formation on alkali treated Ti6Al4V titanium alloy. *Materials Science and Engineering C*, 29(4), 1252–1257. <https://doi.org/10.1016/j.msec.2008.09.047>
- Feng, W., Mu-Sen, L., Yu-Peng, L., & Yong-Xin, Q. (2005). A simple sol-gel technique for preparing hydroxyapatite nanopowders. *Materials Letters*, 59(8–9), 916–919. <https://doi.org/10.1016/j.matlet.2004.08.041>
- Guo, G., Sun, Y., Wang, Z., & Guo, H. (2005). Preparation of hydroxyapatite nanoparticles by reverse microemulsion. *Ceramics International*, 31(6), 869–872. <https://doi.org/10.1016/j.ceramint.2004.10.003>
- Hamdi, M., Hakamata, S., & Ektessabi, A. M. (2000). Coating of hydroxyapatite thin film by simultaneous vapor deposition. In *Thin Solid Films* (Vol. 377378).
- Han, J. K., Song, H. Y., Saito, F., & Lee, B. T. (2006). Synthesis of high purity nano-sized hydroxyapatite powder by microwave-hydrothermal method. *Materials Chemistry and Physics*, 99(2–3), 235–239. <https://doi.org/10.1016/j.matchemphys.2005.10.017>
- Hanyaloglu, C., Aksakal, B., & Bolton, J. D. (n.d.). *Production and indentation analysis of WC/Fe-Mn as an alternative to cobalt-bonded hardmetals*.
- Hu, C., Aindow, M., & Wei, M. (2017). Focused ion beam sectioning studies of biomimetic hydroxyapatite coatings on Ti-6Al-4V substrates. *Surface and Coatings Technology*, 313, 255–262. <https://doi.org/10.1016/j.surfcoat.2017.01.103>
- Hung, I. M., Shih, W. J., Hon, M. H., & Wang, M. C. (2012). The properties of sintered calcium phosphate with [Ca]/[P] = 1.50. *International Journal of Molecular Sciences*, 13(10), 13569–13586. <https://doi.org/10.3390/ijms131013569>
- İbrahim Coşkun, M., Karahan, İ. H., Yücel, Y., & Golden, T. D. (2016). Optimization of electrochemical step deposition for bioceramic hydroxyapatite coatings on

- CoCrMo implants. *Surface and Coatings Technology*, 301, 42–53. <https://doi.org/10.1016/j.surfcoat.2015.12.076>
- Jia, L., Liang, C., Huang, N., Zhou, Z., Duan, F., & Wang, L. (2016). Morphology and composition of coatings based on hydroxyapatite-chitosan-RuCl₃ system on AZ91D prepared by pulsed electrochemical deposition. *Journal of Alloys and Compounds*, 656, 961–971. <https://doi.org/10.1016/j.jallcom.2015.09.223>
- Jugowiec, D., Łukaszczyk, A., Cieniek, Ł., Kowalski, K., Rumian, Ł., Pietryga, K., Kot, M., Pamuła, E., & Moskalewicz, T. (2017). Influence of the electrophoretic deposition route on the microstructure and properties of nano-hydroxyapatite/chitosan coatings on the Ti-13Nb-13Zr alloy. *Surface and Coatings Technology*, 324, 64–79. <https://doi.org/10.1016/j.surfcoat.2017.05.056>
- Kaynak Bayrak, G., Demirtaş, T. T., & Gümüşderelioğlu, M. (2017). Microwave-induced biomimetic approach for hydroxyapatite coatings of chitosan scaffolds. *Carbohydrate Polymers*, 157, 803–813. <https://doi.org/10.1016/j.carbpol.2016.10.016>
- Kim, I. S., & Kumta, P. N. (2004). Sol-gel synthesis and characterization of nanostructured hydroxyapatite powder. *Materials Science and Engineering B: Solid-State Materials for Advanced Technology*, 111(2–3), 232–236. <https://doi.org/10.1016/j.mseb.2004.04.011>
- Kokubo, T., Kim, H.-M., Miyaji, F., Takadama, H., & Miyazaki, T. (n.d.). *Ceramic-metal and ceramic-polymer composites prepared by a biomimetic process*.
- Kong, Y. M., Kim, D. H., Kim, H. E., Heo, S. J., & Koak, J. Y. (2002). Hydroxyapatite-based composite for dental implants: An in vivo removal torque experiment. *Journal of Biomedical Materials Research*, 63(6), 714–721. <https://doi.org/10.1002/jbm.10392>
- Korkusuz, F., & Korkusuz, P. (1997). Kalsiyum hidroksiapatit seramiklerin ortopedide kullanımı*. In *Acta Ortop Traumatol Turc* (Vol. 31).
- Kulpetchdara, K., Limpichaipanit, A., Rujijanagul, G., Randorn, C., & Chokethawai, K. (2016). Influence of the nano hydroxyapatite powder on thermally sprayed HA coatings onto stainless steel. *Surface and Coatings Technology*, 306, 181–186. <https://doi.org/10.1016/j.surfcoat.2016.05.069>
- Leena, M., Rana, D., Webster, T. J., & Ramalingam, M. (2016). Accelerated synthesis of biomimetic nano hydroxyapatite using simulated body fluid. *Materials Chemistry and Physics*, 180, 166–172. <https://doi.org/10.1016/j.matchemphys.2016.05.060>
- Maurya, R., Siddiqui, A. R., & Balani, K. (2017). In vitro degradation and biomineralization ability of hydroxyapatite coated Mg-9Li-7Al-1Sn and Mg-9Li-5Al-3Sn-1Zn alloys. *Surface and Coatings Technology*, 325, 65–74. <https://doi.org/10.1016/j.surfcoat.2017.06.027>
- McEntire, B. J., Bal, B. S., Rahaman, M. N., Chevalier, J., & Pezzotti, G. (2015). Ceramics and ceramic coatings in orthopaedics. *Journal of the European Ceramic Society*, 35(16), 4327–4369. <https://doi.org/10.1016/j.jeurceramsoc.2015.07.034>

- Mohseni, E., Zalnezhad, E., & Bushroa, A. R. (2014). Comparative investigation on the adhesion of hydroxyapatite coating on Ti-6Al-4V implant: A review paper. *International Journal of Adhesion and Adhesives*, 48, 238–257. <https://doi.org/10.1016/j.ijadhadh.2013.09.030>
- Nayak, A. K. (n.d.). Hydroxyapatite Synthesis Methodologies: An Overview. In *International Journal of ChemTech Research CODEN* (Vol. 2, Issue 2).
- Olding, T., Sayer, M., & Barrow, D. (2001). Ceramic sol-gel composite coatings for electrical insulation. In *Thin Solid Films*.
- Onoki, T., & Hashida, T. (2006). New method for hydroxyapatite coating of titanium by the hydrothermal hot isostatic pressing technique. *Surface and Coatings Technology*, 200(24), 6801–6807. <https://doi.org/10.1016/j.surfcoat.2005.10.016>
- Ou, K. L., Chung, R. J., Tsai, F. Y., Liang, P. Y., Huang, S. W., & Chang, S. Y. (2011). Effect of collagen on the mechanical properties of hydroxyapatite coatings. *Journal of the Mechanical Behavior of Biomedical Materials*, 4(4), 618–624. <https://doi.org/10.1016/j.jmbbm.2011.02.001>
- Piattelli, A., Trisi, P., Passi, P., Piattelli, M., & Cordioli, G. P. (n.d.). *Histochemical and confocal laser scanning microscopy study of the bone-titanium interface: an experimental study in rabbits*.
- Poštić, S. D. (2014). INTERNATIONAL JOURNAL OF BIOMEDICINE X-Ray Diffraction Technique in the Analysis of Phases of Hydroxylapatite and Calcium Phosphate in a Human Jaw. In *International Journal of BioMedicine* (Vol. 4, Issue 2).
- Ruiz, G. C. M., Cruz, M. A. E., Faria, A. N., Zancanela, D. C., Ciancaglini, P., & Ramos, A. P. (2017). Biomimetic collagen/phospholipid coatings improve formation of hydroxyapatite nanoparticles on titanium. *Materials Science and Engineering C*, 77, 102–110. <https://doi.org/10.1016/j.msec.2017.03.204>
- Şerbetci K, Orhun S, Korkusuz F, & Hasırcı N. (2002). Hidroksi Apatit İçeren Kemik Çimentosunun In-Vivo Biyouyumluluğu. *Jour. of Arthroplasty & Arthroscopic Surgery*, 13(13), 259–263.
- Stigter, M., De Groot, K., & Layrolle, P. (2002). Incorporation of tobramycin into biomimetic hydroxyapatite coating on titanium. In *Biomaterials* (Vol. 23).
- Swain, S. K. (n.d.). *Processing of Porous Hydroxyapatite Scaffold*.
- Tang, H., & Gao, Y. (2016). Preparation and characterization of hydroxyapatite containing coating on AZ31 magnesium alloy by micro-arc oxidation. *Journal of Alloys and Compounds*, 688, 699–708. <https://doi.org/10.1016/j.jallcom.2016.07.079>
- Tang, H., Han, Y., Wu, T., Tao, W., Jian, X., Wu, Y., & Xu, F. (2017). Synthesis and properties of hydroxyapatite-containing coating on AZ31 magnesium alloy by micro-arc oxidation. *Applied Surface Science*, 400, 391–404. <https://doi.org/10.1016/j.apsusc.2016.12.216>
- Tas A C. (2000). Synthesis of biomimetic Ca-hydroxyapatite powders at 373C in synthetic body fluids. In *Biomaterials* (Vol. 21).

- Tsuchiya, A., Sotome, S., Asou, Y., Kikuchi, M., Koyama, Y., Ogawa, T., Tanaka, J., & Shinomiya, K. (2008). Effects of pore size and implant volume of porous hydroxyapatite/collagen (HAp/Col) on bone formation in a rabbit bone defect model. In *J Med Dent Sci* (Vol. 55).
- Wang, X., Li, Y., Wei, J., & De Groot, K. (2002). Development of biomimetic nano-hydroxyapatite/ poly(hexamethylene adipamide) composites. In *Biomaterials* (Vol. 23).
- Yang, Y., Kim, K. H., & Ong, J. L. (2005). A review on calcium phosphate coatings produced using a sputtering process - An alternative to plasma spraying. In *Biomaterials* (Vol. 26, Issue 3, pp. 327–337). <https://doi.org/10.1016/j.biomaterials.2004.02.029>
- Yılmaz, B., Eviş, Z., Doğu Teknik Üniversitesi, O., Fakültesi, M., & Mühendisliği Bölümü, B. (2014). Titanyum Alaşımının Selenat Eklenmiş Hidroksiapatit ile Kaplanması. In *AKU J. Sci. Eng* (Vol. 14).
- Yu, N., Cai, S., Wang, F., Zhang, F., Ling, R., Li, Y., Jiang, Y., & Xu, G. (2017). Microwave assisted deposition of strontium doped hydroxyapatite coating on AZ31 magnesium alloy with enhanced mineralization ability and corrosion resistance. *Ceramics International*, 43(2), 2495–2503. <https://doi.org/10.1016/j.ceramint.2016.11.050>

Chapter 4

MANY-TO-ONE MODE LSTM APPROACH TO PREDICT THE Z0 BOSON'S MASS

Jale BEKTAŞ¹

¹ Department of Computer Engineering, Faculty of Engineering, Mersin University, Mersin, Turkey

1. Introduction

The Standard Model (SM) is a mathematical theory describing the identification of the fundamental particles and the carriers of their interactions as shown in the following figure (Shupe, 1979).

mass→	2.4 MeV	1.27 GeV	171.2 GeV	0
charge→	$\frac{2}{3}$	$\frac{2}{3}$	$\frac{2}{3}$	0
spin→	$\frac{1}{2}$	$\frac{1}{2}$	$\frac{1}{2}$	1
name→	u up	c charm	t top	γ photon
Quarks	4.8 MeV $-\frac{1}{3}$ $\frac{1}{2}$ d down	104 MeV $-\frac{1}{3}$ $\frac{1}{2}$ s strange	4.2 GeV $-\frac{1}{3}$ $\frac{1}{2}$ b bottom	0 0 1 g gluon
	<2.2 eV 0 $\frac{1}{2}$ ν_e electron neutrino	<0.17 MeV 0 $\frac{1}{2}$ ν_μ muon neutrino	<15.5 MeV 0 $\frac{1}{2}$ ν_τ tau neutrino	91.2 GeV 0 1 Z⁰ weak force
	0.511 MeV -1 $\frac{1}{2}$ e electron	105.7 MeV -1 $\frac{1}{2}$ μ muon	1.777 GeV -1 $\frac{1}{2}$ τ tau	80.4 GeV ± 1 1 W[±] weak force
Leptons				Bosons (Forces)

Figure 1. The Standard Model particles

According to the SM, all particles in the universe are either bosons or fermions. While fermions are matter particles, bosons are the force carriers like the Z^0 boson which is an intermediate vector boson of electroweak interaction introduced by Salam who received the Nobel prize (Salam, 1968). It was observed at the large electron-positron (LEP) collider (Brooks & Preuss, 2021) and has a mass of about 91.18 GeV (Tanabashi, 2018). Actually, it is not directly detected at the detector since its lifetime is extremely short (10^{-25} sec) (Tanabashi, 2018) and therefore, it immediately decays into a particle and its antiparticle as shown in the following Fig.2. (Fontes & Romão, 2020).

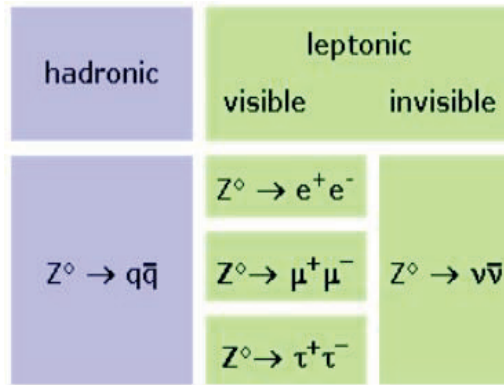


Figure 2. The decay channels of the Z boson

Experimentally, the probability of hadronic decay is three times greater than leptonic decay because of the possible decay channels of the color-charged particles (Taga and Peak, 1996). Here, the visible leptonic decay channels are selected apart from the tau particle for producing the Z^0 events.

With Deep Learning applications found in every field in recent years, the strengths of their methods have emerged, and their success has surpassed other Machine Learning methods. While in a traditional CNN, it is assumed that all inputs and outputs are independent of each other, the RNN (Mullainathan and Spiess, 2017; Zacharaki et al., 2009) architecture performs the same work for each element of a sequence based on previous outputs. RNN strengthens algorithms that work in the temporal field, where transitions about data order are at a significant level. RNNs have the ability to provide likelihood probability estimation to represent many multi-body dynamics and to optimize variable parameters by maintaining a strong stochastic approximation (Hibat-Allah et al., 2020). The RNN consists of a network of neurons for modeling sequential data. The types of RNNs in the literature are visualized in the following Fig.3.(Luo, 2017).

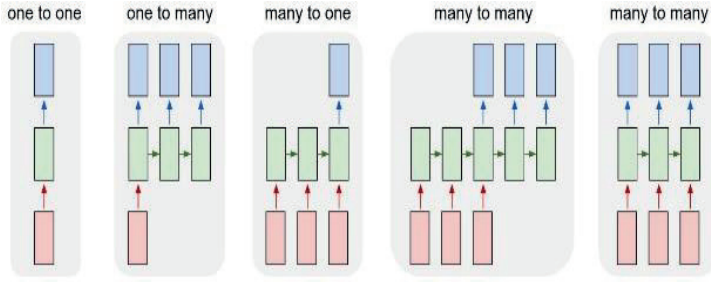


Figure 3. Type of RNN

According to Figure 3., input vectors are represented with red color, output vectors are associated with blue color and green vectors hold the RNN's state. Here, a form of the RNN architecture is chosen with a many-to-one mode that is used when an input sequence is mapped onto a single output. Hochreiter & Schmidhuber introduce the architecture of Long Short-Term Memory (LSTM) to overcome the weakness of the traditional RNN arising from long-term dependencies (Tilaver et al, 2021). The architecture of LSTM is shown in the following Fig.4.

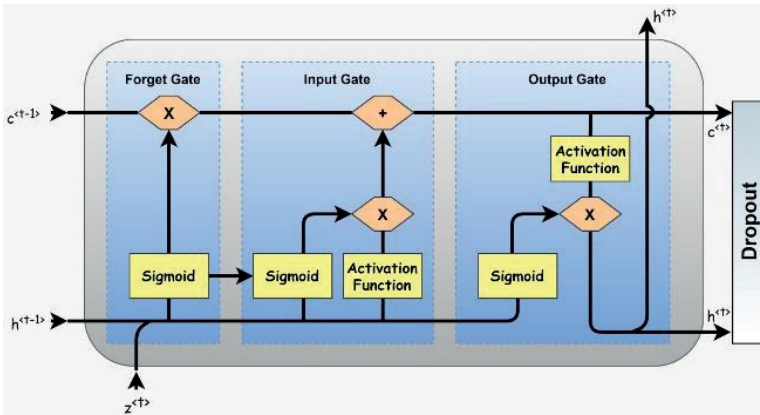


Figure 4. Schematic representation of LSTM.

Mathematically, the relationship between the hidden state and output in the LSTM mechanism is represented by Zaremba and Sutskever, 2015.

$$h^{<t>} = \theta_f(W_{hh} \odot h^{<t-1>} + W_{zh} \odot z^{<t>} + b_h) \quad (1.1)$$

$$H^{<t>} = \theta_f(W_{hH} \odot h^{<t>} + b_H) \quad (1.2)$$

Here, $h^{<t>}$ and $h^{<t-1>}$ determines the hidden layer value and the previous one, $H^{<t>}$ indicates the output layer and θ_f is an activation function. W_{hh} , W_{zh} and W_{hH} are weights that regulate the connection between the input layer and the hidden layer. Also, $\langle \rangle$ and \odot denote the symbol of a vector and a matrix product, respectively. Then, t corresponds to time and b indicates the corresponding bias.

With the ability of Long Short-Term Memory (LSTM) networks to have sequence processing and gated repetitive units (GRU), the behavior of the Z Boson containing temporal dependencies can be modeled. The LSTM method is used for modeling of voltage time series of the Large Hadron Collider (LHC) superconducting magnets (Wielgosz et al., 2017), and also in another study, the background rejection reaches 100 for 50 signal efficiency of the LSTM network (Egan, 2017). The hybrid use of LSTM-CNN networks is configured to learn comparative local and global emotion-related properties from the log-mel spectrogram and speech, respectively, achieving a satisfactory recognition accuracy of 95.33 (Zhao et al., 2019). Another study uses a sequence of classification problems, RNN, to obtain the nonlinear relationship between short-term price returns and the space-time representation of order-quota-constrained data (Dixon, 2018). LSTM network is used to mine temporal dependencies and removes important eigenvectors from damaged inertial sensor traces (Wang et al., 2020). Another example of the Sequence application is the development of Particle Flow Networks (Komiske et al., 2019). These networks feature per-particle secret representation, and the sum of all particles provides an overall event-level hidden representation. This integration processes and combines these events by handling active data from detector images and radiation moments.

This work has been completed in the following stages. In the first section, by adjusting some Monte Carlo parameters in the MadGraph, the Z boson events were simulated by decaying into two electrons or two muons. In the second section, the architecture of LSTM with many-to-one mode was designed and then the Z boson mass was calculated with the help of the LSTM.

2. Materials and Methods

2.1. The Production Process of Events

MadGraph is a Monte Carlo event generator used to simulate events at the Large Hadron Collider (LHC). Given a model, it generates all Feynman

diagrams to compute the corresponding helicity amplitudes for any physical process with the help of a rule specified by the model. However, before running, there is a need to configure some input files in the MadGraph (Alwall et al., 2021) according to the model. After all the necessary steps are performed automatically, it produces a file whose format is a Les Houches Event (henceforth, LHE) file in which the data such as the total production cross section and the center-of-mass energy should be listed. In this study, to simulate the associated production of visible leptonic decays, the default Standard Model existing in the MadGraph package is used. The structure of the MadGraph package is illustrated by the following Figure 5.

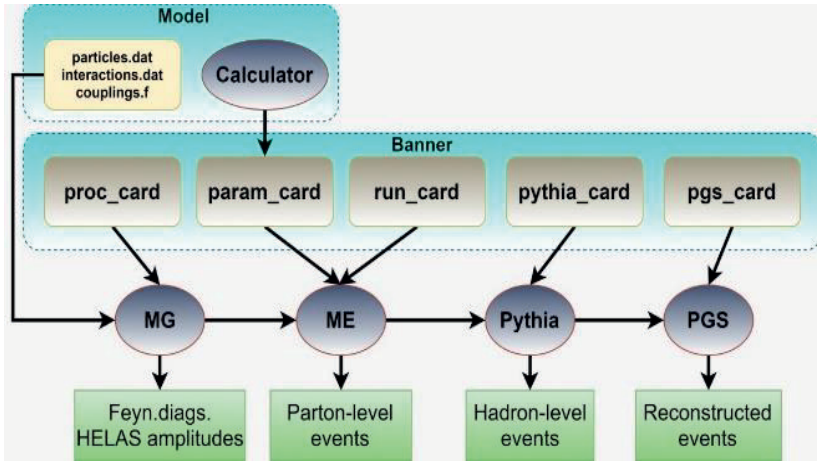


Figure 5. Event generation progress

From Fig.5, there are four steps for event production in Madgraph and it is considered in the first two steps to evaluate the parton level analysis. The first step is to directly define the physical interaction requested by the user to the process card. The second step is to fill the numerical values of parameters into both the parameter and run cards. Once the filling process of cards are done, the event generation process can be automatically started, and the obtained results will be directly printed into the LHE file as the unweighted events. Phenomenologically, a fermion-antifermion decay of the Z boson is given in Fig.6.

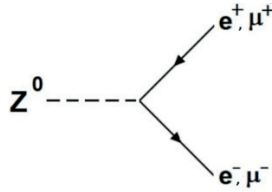


Figure 6. Feynman diagram of leptonic decay of Z bosons

In this study, 10000 events at a center-of-mass energy of 13 TeV were obtained from proton-proton collisions and each event generally includes two opposite-sign isolated electrons or two opposite-sign isolated muons which satisfy both transverse momentum $P_T > 10\text{GeV}$ and pseudo rapidity $|\eta| < 2.5$ requirement. Here, the mass values of the Z bosons were calculated with the following mathematical equation (Bora and Scholar, 2019).

$$M_{Z^0} = \sqrt{2P_T^1 P_T^2 [\cosh(\eta_1 - \eta_2) - \cos(\varphi_1 - \varphi_2)]} \tag{2.1}$$

Where the symbols 1 and 2 indicate the fermion and anti-fermion states, respectively. The obtained mass value was sequentially stored with a csv extension and then, by reading the saved csv file with the help of panda’s library one gets the following Fig.7.

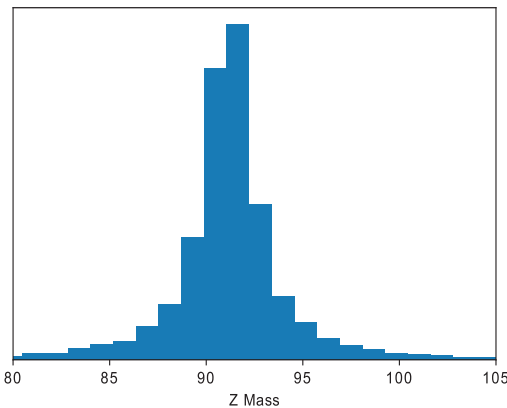


Figure 7. The mass distribution of Z boson

As seen in Fig. 7, the mean value of the mass distribution is around 90.18GeV as expected from the theoretical point view. Moreover, if a box plot of the kinematic distribution of electrons is made and muons

obtained from the parton level production, the following Fig.8. is obtained.

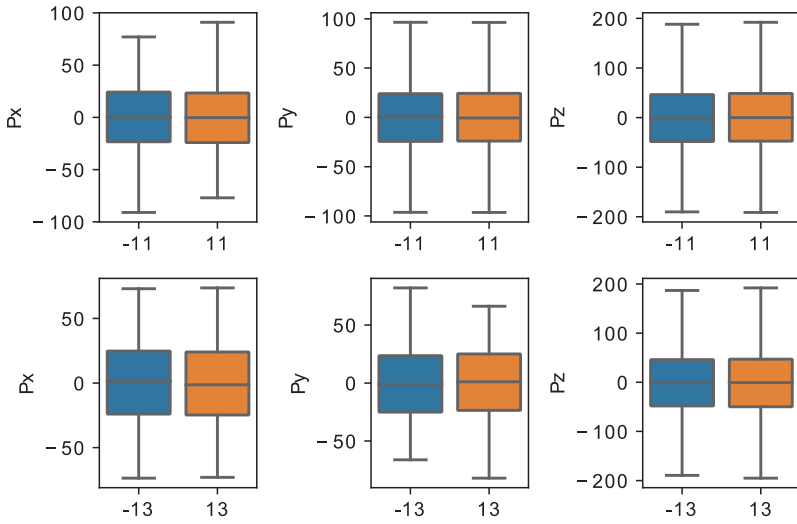


Figure 8. The kinematic distribution of electron and muon

2.2. Designing LSTM model

The network architecture is designed as having two dropouts and two hidden layers with 64 neurons and 32 neurons respectively with RELU activation. Dropout layers follow the hidden layers. The structure of the network is given in Figure 9.

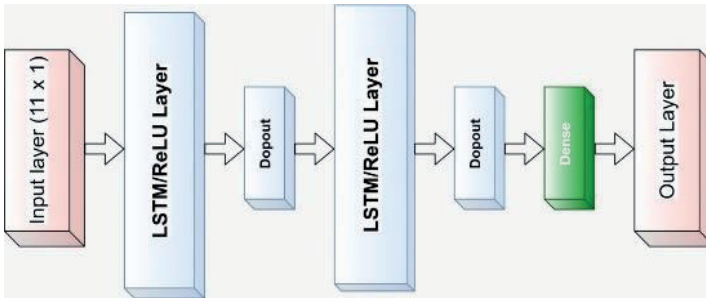


Figure 9. The structure of network architecture

In this model, the time step known as a sliding window is a hyperparameter that shows how many prior events are considered when predicting the next event.

3. Evaluation results

The primary objective of this study is to evaluate the predictions of Z Mass values of a many-to-one type of LSTM network at certain time steps. For example, if the time step is adapted to 5 for the generated Z events located in the saved csv file, the following figure is obtained.

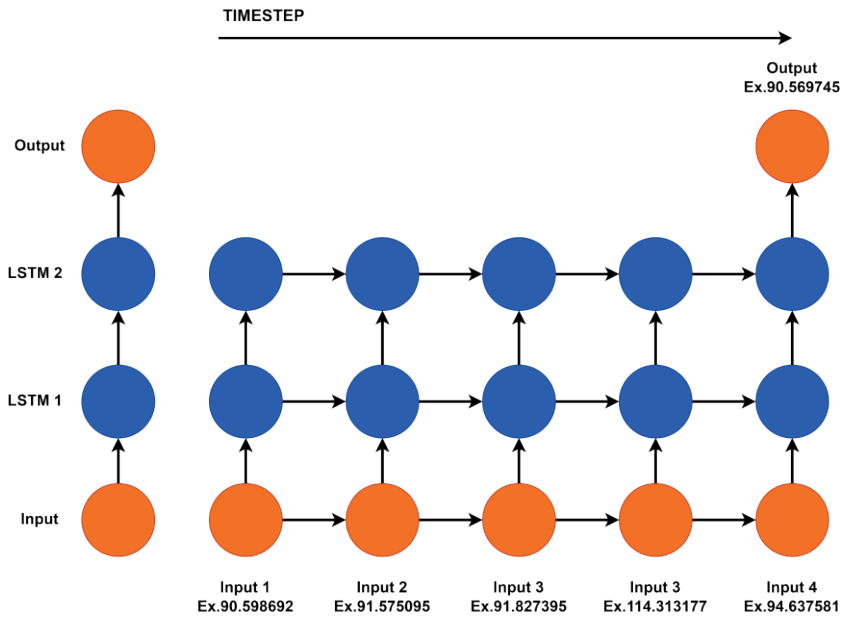
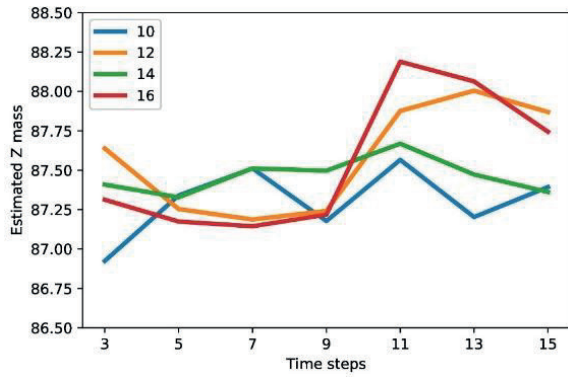


Figure 10. Timestep representation.

Here, the time step is set to 3, 5, 7, 9, 11, 13, and 15 steps when batch size is chosen as 10, 12, 14, and 16 to see if they affect the performance of the LSTM. Besides, the dropout probability is chosen as 0.2. Afterward, the model is trained 100 times with the same dropout for each time step and each batch size, and this leads us to create a file with 100 columns. The column with the highest mean value is selected from the file and the following Figure.11 is obtained.

Figure 11. The mass distribution versus time step for different batch size.



As shown in Fig 11, according to predicted Z mass values the optimal values of time step and batch size are equal to 11 and 16, respectively. In this case the mass distribution of the Z boson is obtained as seen in Figure.12. Upper part of the figure corresponds to the predicted mass distribution of the Z boson while the bottom one represents the mass distribution of a real Z boson.

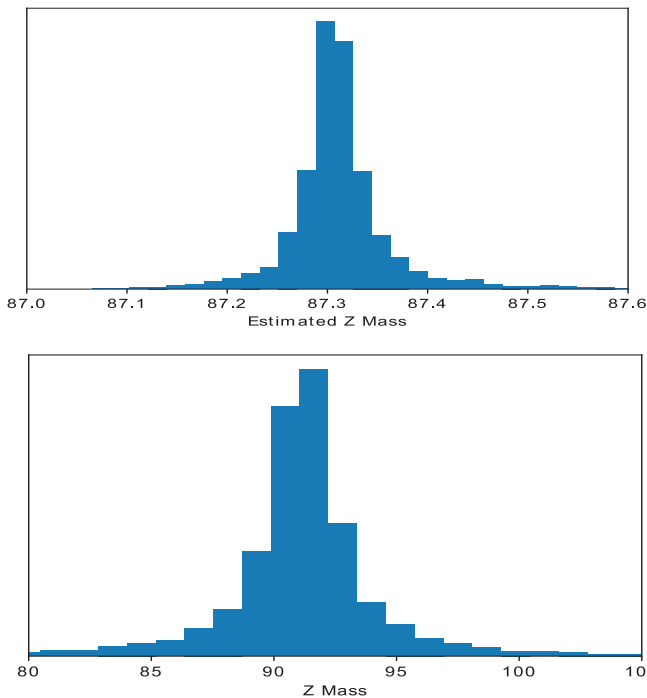


Figure 12. Upper figure corresponds to the predicted mass distribution of the Z boson while the bottom one represents the mass distribution of a real Z boson.

The mean value of the mass distribution of Z bosons is approximately around 88.18 GeV from Fig 12. While this value is compared with real Z mass, the error percentage is calculated between the Z mass and the predicted Z mass. This percentage is an acceptable (Tanabashi, 2018) level that equals approximately 3.1.

4. Conclusions

According to the Standard Model (SM), all particles in the universe are either bosons or fermions. While fermions are matter particles, bosons are the force carriers like the Z0 boson. The reason that the Z Boson behavior modeling involves temporal dependencies is that long Short-Term Memory (LSTM) networks are capable of array processing and gated repetitive units (GRU). The LSTM method is used for modeling of voltage time series of the Large Hadron Collider (LHC). This work has been completed in two stages. In the first stage, by adjusting some Monte Carlo parameters in the MadGraph, the Z boson events were simulated by decaying into two electrons or two muons. The parton-level events having standard LHC identification criteria are generated with MadGraph and automatically written in the LHE file. Then, the events with two opposite charged muons or electrons from this file are collected, and the invariant mass of the Z boson is with the help of Eq. 3. After that, it is saved into a CSV file and a histogram with respect to it is generated. In the second stage, the architecture of LSTM with many-to-one mode was designed and then the Z boson mass was calculated with the help of the LSTM. The Z boson mass with a three percent error by using the LSTM technique on the csv file is predicted.

Finally, some ideas related to the comparison were given. Approximately 10000 events at a center-of-mass energy of 13 TeV were obtained from proton-proton collisions and each event generally includes two opposite-sign isolated electrons or two opposite-sign isolated muons that satisfy both transverse momentum $PT > 10\text{GeV}$ and pseudo rapidity $|\eta| < 2.5$ requirement. While the error percentage is calculated between the Z mass and the estimated Z mass an acceptable level that equals approximately 3.1 is found. Therefore, it can be concluded that many-to-one mode LSTM technique can be successfully applied for this kind of analysis in complex problems.

REFERENCES

- Alwall, J. et al. (2021). MadGraph 5: Going Beyond, arXiv preprint arXiv:1106.0522
- Bora S.L. and Scholar, R. (2019). Z boson mass estimation using Machine Learning, IJEDR, vol. 7
- Brooks, H., and Preuss, C. T. (2021). Efficient multi-jet merging with the Vincia sector shower. *Computer Physics Communications*, 264, 107985
- Dixon, M. (2018). Sequence classification of the limit order book using recurrent neural networks, *Journal of computational science*, 24, pp. 277-286
- Egan, S. et al. (2017). Long Short-Term Memory (LSTM) networks with jet constituents for boosted top tagging at the LHC, arXiv preprint arXiv:1711.09059
- Fontes, D., and Romão, J. C. (2020). FeynMaster: a plethora of Feynman tools. *Computer Physics Communications*, 256, 107311
- Hibat-Allah, M., Ganahl, M., Hayward, L.E., Melko, R.G. and Carrasquilla, J. (2020). Recurrent neural network wave functions, *Physical Review Research*, vol. 2
- Komisike, P.T., Metodiev, E. M. and Thaler, J. (2019). Energy flow networks: deep sets for particle jets, *Journal of High Energy Physics*, vol. 1
- Luo, Y. (2017). Recurrent neural networks for classifying relations in clinical notes, *Journal of Biomedical Informatics*, vol. 72, pp. 85-95
- Mullainathan S. and Spiess, J. (2017). Machine Learning: An Applied Econometric Approach, *J. Econ. Perspect.*, vol. 31, pp. 87-106
- Salam, A. (1968). Weak and Electromagnetic Interactions, Proc 8-th Nobel Symped N Svartholm, pp. 367-377
- Shupe, M.A. (1979). A composite model of leptons and quarks, *Physics Letters B*, vol. 86, pp. 87-92
- Taga, P.M. and Peak, J.E. (1996). Machine learning of maritime fog forecast rules, *J. Appl. Meteorol.*, vol. 35, pp. 714-724
- Tanabashi, M. (2018). Review of Particle Physics, *Phys. Rev. D*, vol. 98.
- Tilaver H. et al. (2021). Deep learning approach to Hubble parameter, *Computer Physics Communications*, vol. 261.
- Wang, Q, et al. (2020). Personalized stride-length estimation based on active online learning, *IEEE Internet of Things Journal*, vol. 7, 4885-4897
- Wielgosz, M., Skoczyn, A. and Mertik, M. (2017). Using LSTM recurrent neural networks for monitoring the LHC superconducting magnets, *Nuclear Instruments and Methods in Physics Research Section A: Accelerators, Spectrometers, Detectors and Associated Equipment*, vol. 867, pp. 40-50
- Zacharakı, E.I. et al. (2009). Classification of brain tumor type and grade using MRI texture and shape in a machine learning scheme, *Magn. Reson. Med.*, vol. 62
- Zaremba W. and Sutskever, I. (2015). Reinforcement Learning Neural Turing Machines-Revised, e-Print: 1505.00521
- Zhao, J., Mao, X. and Chen, L. (2019). Speech emotion recognition using deep 1D & 2D CNN LSTM networks, *Biomedical Signal Processing and Control*, vol. 47, pp. 312-323

Chapter 5

TIME COMPLEXITY OF MACHINE LEARNING METHODS: A REVIEW

Celalettin ARSLAN¹

Volkan KAYA²

1 (M.Sc. Student), Erzincan Binali Yıldırım University, Graduate School of Natural and Applied Sciences, Department of Artificial Intelligence and Robotics, Master's Student, Erzincan, Türkiye, E-mail: celalettinarslan25@gmail.com, ORCID: 0000-0003-1993-0550

2 (Asst. Prof. Dr.), Erzincan Binali Yıldırım University, Faculty of Engineering and Architecture, Department of Computer Engineering, Erzincan, Türkiye, E-mail: vkaya@erzincan.edu.tr, ORCID: 0000-0001-6940-3260

1. Introduction

Machine learning, which has a great impact on artificial intelligence and data analytics, has become an important field of study today (Şengül et al., 2022). Machine learning, which emerged with the aim of developing computer systems with human intelligence capabilities, focuses on algorithms and methods that enable computers to analyze data and make decisions. Machine learning, which offers a different approach from traditional programming, allows the computer to learn automatically and extract information from the data (Akay, 2018).

Although machine learning is at the forefront of its success today, its foundation is based on a very long history. Machine learning, whose first steps were taken with the formation of basic concepts in computer science, gained momentum with Turing's studies and artificial intelligence research in the 1950s. Turing asked, "Can computers think?" This question formed the basis of machine learning research (Dore, 2012). In the 1960s, Arthur Samuel introduced the concept of machine learning and developed a checkers program that allows computers to compete against humans in games. This program has created an artificial intelligence model that learns by improving itself in the game of checkers (Nacar and Erdebilli, 2021). In parallel with these developments, great advances were not made in machine learning applications in the 1980s and 1990s. In these years, due to the limited processing power and data collection methods of computers, machine learning models could not have an effect on large data sets. (Kizrak and Bolat, 2018).

Since the beginning of the 2000s, with the increase in the processing power of computers and the spread of the internet, it has become easy to obtain and store large amounts of data (Şekerli, 2019). With these developments, there has been a revival and rapid progress in the field of machine learning. However, innovative approaches such as artificial neural networks, big data analytics and deep learning have expanded the boundaries of machine learning and increased its application areas in recent years. Today,

machine learning methods are widely used in many fields such as automotive, health, finance, retail, media, and industry (Bozyiğit and Tarhan, 2020; Veranyurt et al., 2020; Calayır and Kabak, 2021; Ustaalı et al., 2021; Koruyan and Ekeryılmaz, 2022; Yürek et al., 2022, Akgül, 2023).

2. Related Works

In this section, recent studies in the field of machine learning methods and time complexity are examined in detail.

Rolnick et al. investigated how to combat climate change using machine learning. In the research, the opinions of experts in many different fields were taken to examine in which areas it would be more beneficial to use machine learning methods. As a result of the research, the interpretation of climate models using machine learning methods in the fight against climate change, solar forecasting for energy companies, ways to optimize supply chains to reduce waste, techniques to automatically evaluate the energy consumption of buildings in cities, tools to improve disaster management, accelerate fusion science, tool Many priority areas have been identified, such as increasing productivity, and it has been suggested that researchers focus on such areas (Rolnick et al., 2022).

Gambhir et al., in their study in India, discussed machine learning methods to examine the spread of the COVID-19 epidemic. As the data set, 154-day COVID-19 case numbers given by the Ministry of Health of India were used. The available data includes the results between January 22, 2020, and June 24, 2020, and it is aimed to estimate the number of cases to be seen in July and August. In this study, the case increase to be experienced by using Support Vector Machine and Polynomial Regression models, which are machine learning methods, was estimated with a success rate of approximately 93% (Gambhir et al., 2020). Yao et al., in their study, examined the importance of machine learning and renewable energy sources. In this study, they examined the machine learning methods used for the collection, storage, conversion, and management of renewable energy and explained the

difficulties that may be encountered in the future or how the existing systems can be improved with machine learning (Yao et al., 2023). Machhale et al. In their study, they used machine learning methods to detect brain tumors. In this study, SVM, KNN, and SVM-KNN hybrid models from machine learning methods were used by using 112 brain MRI images. By using these methods, success rates of 92.86%, 69.57%, and 93.75% were obtained, respectively (Machhale et al., 2015). Aphiwongsophon and Chongstitvatana used machine learning methods to detect fake news in their study. In the study, 9725 real news and 12249 fake news were used as datasets. After these data were trained using machine learning methods, they achieved 99.90% fake news detection success as a result of the test. (Aphiwongsophon and Chongstitvatana, 2018). Erdi et al. In their work, they used machine learning methods to detect fake accounts. In their study, they worked on 100 Twitter user accounts they prepared 238.925 tweet messages and 2102 features obtained from other user information. With the machine learning methods used, they obtained results up to 93.93%. (Erdi et al., 2021).

Aylak et al., in their study, examine machine learning methods used in many areas such as order picking, warehousing, demand forecasting, and supply chain quality control in the logistics industry. They state that development and competition in the logistics sector depend on construction-artificial intelligence cooperation (Aylak et al., 2021). Sani et al., in their study, made an examination on the time complexes of C4.5 and CART, which is one of the machine learning methods and one of the sub-branches of decision trees. In their studies, they aimed to increase the efficiency of learning algorithms on large datasets. In the study, the running times of C4.5 and CART decision tree algorithms in the Python programming language library were examined theoretically and experimentally. In addition, the time complexity of the algorithm was examined by examining different results using different problem settings and positive results were obtained (Sani et al., 2018). Ali et al. used a genetic algorithm, ant bee colony algorithm, particle swarm optimization, and whale optimization techniques for hyperparameter detection in order to reduce the time complexity of support vector machines,

which is one of the machine learning methods. These optimization techniques were analyzed to determine which strategies were most effective in determining hyperparameters, and then the genetic algorithm was found to be the most effective optimization technique (Ali et al., 2023).

In this study, information is given on the point of machine learning methods, future potential, and time complexity. The remainder of the study is structured as follows. In Section 2, current studies on machine learning are examined. In Section 3, detailed information about machine learning methods is given. Section 4 provides information about the time complexity of machine learning methods. In Section 5, the results and suggestions about machine learning are given.

3. Machine Learning Methods

Machine learning is algorithms and techniques developed to bring data analysis and pattern recognition capabilities to computer systems. These methods create models by learning from data-based examples and help solve problems such as prediction, classification, grouping, and pattern recognition. Machine learning is constantly evolving with the emergence of new algorithms and techniques, and solutions can be produced using different methods depending on the problem and the dataset. In this section, some commonly used machine learning methods are given.

3.1. Linear Regression

The linear regression method aims to create a mathematical model that can make an estimation or estimation of the value of the dependent Y variable to be determined by these variables by using the independent X variables (Kılıç, 2013; Roopa and Asha, 2019). Linear regression uses the linear equation structure to express the relationship between the independent variable and the dependent variables. This equation calculates the predicted value of the dependent variable using the weights of the independent variables and a constant term. If there is only one dependent variable for the estimation of the

independent variable in the situation to be examined, it is called "simple linear regression", and if a dependent variable estimation model is to be created using two or more independent variables, this model is called "multiple linear regression" (Maulud and Abdulazeez, 2020).

3.1.1 Simple Linear Regression

In this model, a dependent variable is dependent on an independent variable. The general mathematical expression of the simple linear regression model is given in equation 1.

$$Y_i = \beta_0 + \beta_1 X_i + \varepsilon_i \quad i = 1, 2, 3, \dots, n \quad (1)$$

In this equation, Y is the dependent variable, X is the independent variable, and ε_i is the predicted error term, and Y_i is the difference between the actual value of the dependent variable and its predicted value. β_0 represents the cutoff point and β_1 represents the slope value (Toka et al., 2011). If the β_1 value to be obtained as a result of the calculations is positive, the relationship is evaluated as directly proportional, if it is negative, it is evaluated as inversely proportional.

3.1.2 Multiple Linear Regression

Thanks to the multiple linear regression analysis, the effect of each dependent variable on the value of the independent variable is determined. In the multiple linear regression model, the number of independent variables is j , and the mathematical expression of the model is given in equation 2.

$$Y_i = \beta_0 + \beta_1 X_{i1} + \beta_2 X_{i2} + \dots + \beta_j X_{ij} + \varepsilon_i \quad i = 1, 2, 3, \dots, n \quad j = 1, 2, 3, \dots, n \quad (2)$$

In this equation, Y is the dependent variable, X is the independent variable, ε_i is the predicted error term, and Y_i is the difference between the actual value of the dependent variable and its predicted value. β_0 represents the cutoff point and β_1 represents the slope value. If each β value to be obtained as a result of the calculations is positive, the variable with a coefficient

is directly proportional to the dependent variable, and if it is negative, the variable with a negative coefficient is evaluated as inversely proportional to the dependent variable (Arı and Önder, 2013).

3.2. Logistic Regression

This method is a method that makes the relationship between independent and dependent variables that do not have a linear relationship between them logarithmically linear. The logistic regression method works on the assumption that there is a logit (representing the probabilities or logarithmic ratios of the dependent variable) relationship between the independent and dependent variables. Due to this assumption, nonlinear models are obtained if the relationship is not logit (Baydemir, 2014). This method is classified in three different ways "Binary Logistic Regression Model", "Multi-Category Logistic Regression Model" and "Ranked Logistic Regression Model" according to the status of the dependent variable (Şenel and Alatli, 2014).

3.2.1. Binary Logistic Regression Model

In this model, the independent variable can take two different values categorically. In this model, the occurrence of the investigated event is considered to be 1, and the non-occurrence of the investigated event is considered to be 0 (Öztürk, 2012). This allows us to model the relationship between multiple independent variables and a binomial dependent variable (Harrell, 2001).

3.2.2. Multinomial Logistic Regression Model

In this model, dependent variables containing three or more categorical values are used. In addition, the classification of values is obtained with scales. This model is a generalized version of the binary logistic regression model. Its distinguishing aspect from other model structures is that it examines the differences between different choices of individuals (Zortuk et al., 2014).

The assumptions of this model can be listed as follows (Yamantaş, 2019):

- Values of the dependent variable are independent between them.
- Independent variables do not contain linear connections between them.
- A basic group can be determined and comparisons can be made between other groups.

3.2.3. Ordinal Logistic Regression Model

In simple and multi-category regression models, the variable takes numerical values, in this model the variable takes categorical and ordinal values (Yavuz and Çilengiroğlu, 2020). In this method, the ranking is controlled by taking the average of the independent variable for each level of the dependent variable. If there is no consistent ordering between the levels of the independent variable, some levels need to be combined (Harrell, 2001). In order to apply an ordinal logistic regression model to a structure, that structure must comply with the parallel curves assumption. The assumption of parallel curves means that the coefficients determined in the regression are equal in all categories of the ordinal categorical variable (Altaş and Yilmazer, 2021).

3.3. Decision Trees

Decision trees are a machine learning method used in pattern recognition and classification. This method performs decision-making by dividing complex classification problems into sub-stages (Kavzoğlu and Çölkesen, 2010). Decision trees are composed of roots, leaves, and branches. In this structure, each node represents a different attribute. The first node of the tree contains all the data and is called the root node. As the sub-nodes of the tree are descended, the existing data is divided into sub-data groups.. The structures between the nodes obtained are called branches, and the structure formed at the ends of the branches as a result of similar steps is called a leaf.

Each leaf represents a class. The data reaches the new node through one of the sub-branches, depending on the condition of the node it reaches. Thus, if the node it reaches fulfills the condition specified, it will reach the class in which it will be placed by ending the branching in that section (Demirel and Yakut, 2019). Decision tree models are frequently used in different variations and applications. Figure 1 shows the general model structure of the decision tree.

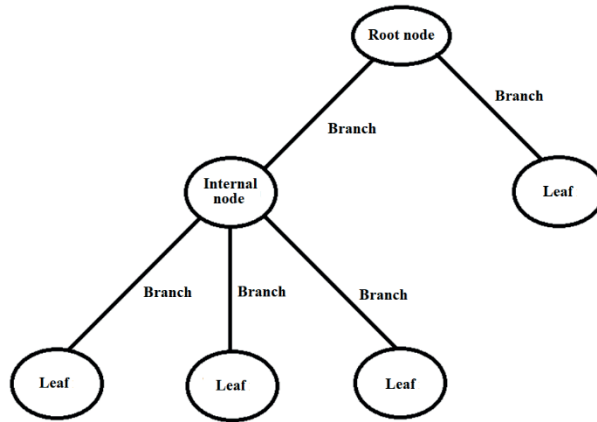


Figure 1. General model structure of the decision tree

3.3.1. Binary Decision Tree

This decision tree method has a structure with at most two children. When this method is applied, a test line is drawn between the starting point and the target point to search for the nearest threat area, and the right and left children are determined. The steps are repeated until all these roads are completed, and at the end, the minimum turning point or the shortest distance on the appropriate roads is selected (Shi et al., 2019).

3.3.2. ID3

ID3 (Iterative Dichotomiser 3) uses information gain and entropy calculations for root property and subsequent partitioning decisions in the tree structure. Entropy is known as the complexity measurement of data, and high entropy refers to complex data with low patterns. Information gain is a

value based on entropy. This ID3 algorithm calculates the information gain value of each feature and selects the feature with the highest information gain as the root. In the construction process of the tree, the next steps are processed according to the same information gain values. Therefore, the ID3 algorithm is called an entropy-based decision tree algorithm (Güldal, 2018).

3.3.3. C4.5

C4.5 is a popular decision tree algorithm that is a more advanced version of the ID3 algorithm (Quinlan, 2014). C4.5 selects the best attribute using the information gain ratio and avoids ID3's bias towards attributes with a large number of values. In addition, C4.5 proposes different tests for each attribute value type to handle continuous attributes (Cherfi et al., 2018). This C4.5 decision tree method uses a "divide and conquer" approach in the training phase (Liu and Gegov, 2016). C4.5 uses the knowledge acquisition rate to map the training set and select splitting attributes. In this method, the tree structure is formed by starting from the root node and progressing towards the leaf nodes. Each instance path provides a decision rule to determine the new instance class to be created (Dai and Ji, 2014). The root node contains the entire training set, taking into account the unknown attribute values (Quinlan, 2014). In this case, if all the training data in the current wedding are in the same class, the algorithm terminates. If the training data belongs to more than one class, the knowledge acquisition rate is calculated for each feature. For dividing the node, the attribute with the highest information gain rate is selected (Ibarguren et al., 2015). The information gain rate for discrete features is calculated by dividing the training data in the node by each value. Continuous features are divided by a threshold value (Pandya and Pandya, 2015).

3.3.4. CART

CART (Classification and Regression Trees) algorithm is a decision tree algorithm used in both classification and regression problems. CART creates the tree by splitting the dataset using Gini impurity or other metrics. It makes

numerical predictions in regression problems while predicting classes in classification problems. The root structure of the algorithm, which starts as the main node, is split into two groups and binary splits continue until the tree structure reaches the maximum level. When cleavage is complete, terminal nodes are formed and are named according to the group that is more concentrated in them. The heterogeneity value of each node is called a measure of impurity (Akşehirli et al., 2014).

CART analysis consists of four basic steps and the first step is the creation of the tree structure. At this stage, a tree is created by recursively dividing the nodes. Each acquired node is assigned a class that is estimated based on the distribution of classes in the learning dataset and the decision cost matrix in that node. The predicted class is assigned regardless of whether the node is subsequently split into child nodes. In the second step, the tree structure creation process is stopped. At this point, a "maximal" tree has been produced, but with possibly overfitting the learning will capture the information in the dataset. The third step is tree "pruning", where more and more important nodes are cut and simple trees are created. The fourth step is the selection of the most suitable tree for optimal tree selection. In this step, the pruned tree is selected from among the tree sequences created during the pruning phase, which fits the information in the learning dataset and does not capture the information with excessive fit (Lewis, 2000).

3.4. K-Nearest Neighbors

K-Nearest Neighbors (KNN) is the most widely used method among machine learning algorithms (Kılınç et al., 2016). In this method, the class of the data is determined by looking at the distance between the new data and the data used for the training data. The data used in the KNN model are specified with n-dimensional numerical quantities and are kept as points in the n-dimensional space. The data to be examined is classified in this n-dimensional space by looking at the distance between the previously trained data (Taşçı and Onan, 2016).

In order to determine the class to which the data examined in the classification phase belongs, the data class with the highest frequency among the k nearest training data is used (Sun and Chen, 2021). The number of k (neighbor) to be used is usually expressed in odd numbers such as 3 or 5. The classification process consists of two stages in the KNN model. In the first stage, the nearest neighbors as much as the specified number of k are determined, and in the second stage, the class to which the analyzed data belongs is determined by majority voting among these neighbors (Cunningham and Delany, 2021). Figure 2 shows the general structure of the KNN model.

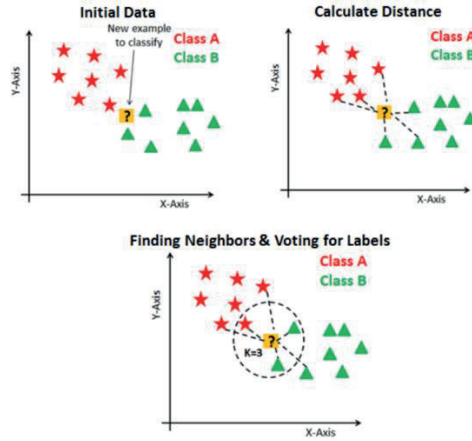


Figure 2. KNN model structure (Github, 2021)

3.5. Support Vector Machine

The support vector machine (SVM), first used in 1992, is still a widely used machine learning method today (Boser et al., 1992; Bottou and Lin, 2007). SVM aims to draw a hyperplane that separates the data points of the classes after placing the data belonging to different data classes in a two or higher-dimensional feature space (Luts et al., 2010). Figure 3 shows the general structure of the SVM model.

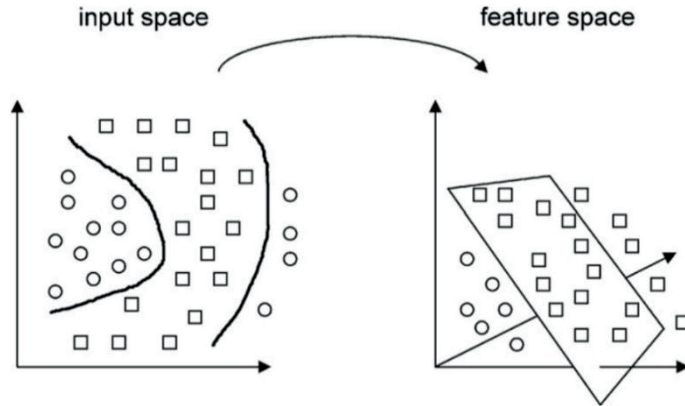


Figure 3. General structure of the SVM model (Luts et al., 2010)

Although support vector machine was originally developed for binary classification (Binary SVM), it is also used to solve classification problems involving more than one class. Multi-Class SVM (Multi-Class SVM) is obtained by combining dual classification SVMs for multi-class classification operations (Ekici et al., 2009).

3.6. Random Forests

Random forests are a combination of tree estimators in which each tree depends on the values of a random vector with the same distribution as all other trees. The increase in the number of trees in the forest converges the generalization error of the forest to a certain limit. The generalization error depends on the correlation and strength of individual trees in the forest (Breiman, 2001). In the random forests method, each tree works independently while making its own estimation in order to obtain a common estimation by combining the estimations of all trees. Each tree is usually trained on random sampling subsets of the dataset. This allows different samples to affect each tree differently, increasing the diversity and generalizability of random forests.

Random forests are a method that gives effective results in classification and regression problems (Gislason et al., 2004; Palimkar et al., 2022). It can also be used in information extraction tasks such as feature selection and feature importance ranking (Şahin, 2017; Eyüpoğlu, 2020). Therefore, random forests are considered a popular machine-learning method and are widely used in various application areas.

4. Time Complexities of Machine Learning Methods

The amount of resources an algorithm uses while running is called computational complexity. Computational complexity is examined under two subheadings time and area complexity. This section analyzes the time complexity of machine learning methods in both training and testing phases.

Time complexity is defined as the determination of the running time of an algorithm. In the time complexity analysis, only the working time is examined, ignoring the resources of the computer used (operating system, processor speed, memory, programming language used, etc.).

There are 3 different approaches to complexity analysis:

1- Big Omega or $\Omega(n)$: This is the notation used in best-case analysis. This notation determines the lower limit of the algorithm's running time.

2- Big Theta or $\Theta(n)$: It is the notation used in the analysis of the mean situation. This notation determines the average running time of the algorithm.

3- Big O or $O(n)$: It is the notation used in worst-case analysis. This notation determines the upper limit of the algorithm's running time.

Big-O notation is used in time complexity analysis with a focus on the worst case. For this reason, Big-O notation was used to calculate the time complexity of the machine learning methods discussed in the study.

4.1. Linear Regression Time Complexity

This method aims to create a linear function that explains the relationship between independent (X_i) and dependent (Y_i) variables in the model (Quinlan, 1987).

$$Y_i = \beta_0 + \beta_1 X_{i1} + \beta_2 X_{i2} + \dots + \beta_j X_{ij} + \varepsilon_i \quad i = 1, 2, 3, \dots, n \quad j = 1, 2, 3, \dots, n \quad (3)$$

In the given linear regression model (equation 3), Y_i denotes the target variable, $X_{i1}, X_{i2}, \dots, X_{ij}$ independent variables, $\beta_0, \beta_1, \beta_2, \dots, \beta_j$ coefficients, and ε_i the error term.

The time complexity of this model can be determined by estimating the coefficients using the least squares method (Yan and Su, 2009). First, the data needs to be arranged as n -dimensional (n number of data) and j -dimensional (m number of independent variables) matrices. The resulting data matrix is arranged so that the dimension of X is $n \times j$ and the size of the target variable Y is $n \times 1$.

The least squares method uses the sum of squared Errors (SSE) as the target function. SSE expresses the sum of the squares of the differences between the observed values (Y_i) and the predicted values (\hat{Y}_i) (equation 4).

$$SSE = \sum_{i=1}^M (Y_i - \hat{Y}_i)^2 = \sum_{i=1}^M (Y_i - (\beta_0 + \sum_{j=1}^N \beta_j X_{ij}))^2 \quad (4)$$

In order to estimate the coefficients for the time complexity analysis, values that will minimize the SSE must be found. For this, coefficients can be estimated with matrix calculations. A column is added to the data matrix X to estimate the coefficients with matrix calculations. This column is arranged to have a fixed value (usually 1) for each data point. Equation 5 is used to calculate the β matrix representing the coefficients.

$$\beta = (X^T * X)^{-1} * X^T * Y \quad (5)$$

In Equation 5, X^T denotes matrix X transpose, $*$ denotes matrix multiplication, (-1) prime denotes inverse matrix (Yan and Su, 2009).

The matrix products $X^T * X$ and $X^T * Y$ in Equation 5 have a time complexity of $O(m^2 * n)$. Finding the inverse matrix in the expression $(X^T * X)^{-1}$ has a time complexity of $O(m^3)$. Considering these situations, the time complexity of the model in the training phase is $O(m^2 * n + m^3)$.

In the test phase, the estimation of the dependent variable is realized by applying new data to the model. The coefficients in the model are multiplied for each independent variable, and the time complexity depends on the number of independent variables. As a result, the test phase time complexity of the model is found as $O(m)$.

4.2. Logistic Regression Time Complexity

The logistic regression model basically works with the logit transformation process. This operation allows to convert the probability values of the dependent variable into a limited range. In this model, the probability values of the dependent variable must be between 0 and 1. However, directly used dependent variables sometimes do not meet this criterion. Logit transform is used to correct this situation. The logit transform expresses the probability values as log ratios. That is, the logit transform for probability $p(x)$ is given in equation 6 (Hilbe, 2009):

$$Y_i = \beta_0 + \beta_1 X_{i1} + \beta_2 X_{i2} + \dots + \beta_j X_{ij} + \varepsilon_i \quad i = 1, 2, 3, \dots, n \quad j = 1, 2, 3, \dots, n \quad (6)$$

$$\text{logit}(p(x)) = \frac{1}{(1+e^{-Y_i})} \quad (7)$$

Equation 7 is used during the training phase of the logistic regression model. The training phase of the logistic regression model is time complexity $O(m * n)$, the number of data to be used in the training phase is M and the number of features is N . The estimation phase of this model is used to calculate the probability value of a given input sample. Since this process will be

repeated as many times as the number of data used, the time complexity of the estimation phase is obtained as $O(m)$.

4.3. Decision Trees Time Complexity

The decision tree method seeks the division that provides the highest information gained during the training phase. Information gain is a measure of the effect of a feature in decision trees to split a dataset (Kaneda, 1995). The decision tree algorithm uses information gain to determine the best-split point or decision node using the features in the dataset. Information gain is expressed in a term called entropy (Quinlan, 1987) and is calculated as the ratio of the entropy drop obtained when a feature is used to the overall entropy before the feature. The calculation of the information gain is made according to equation 8.

$$\text{Information Gain}(S, A) = \text{Entropy}(S) - \sum_{v \in \text{Değerler}(A)} \frac{|S_v|}{|S|} * \text{Entropy}(S_v) \quad (8)$$

Here:

- *Information Gain*(S, A), S represents the information gain of attribute A in the dataset.
- *Entropy*(S), represents the entropy value of the dataset S .
- *Values*(A), it represents the set of values that attribute A can take.
- $|S_v|$, the value of attribute A represents the number of instances that have v .
- $|S|$, represents the total number of samples in the S dataset.
- *Entropy*(S_v), the value of property A expresses the entropy value of the subset of samples with v .

Entropy in this equation is a term that measures the amount of uncertainty in a dataset. A lower entropy value indicates less uncertainty and a more homogeneous dataset. Entropy is calculated as stated in equation 9.

$$Entropy(S) = -\sum_{i=1}^n p_i \log_2 p_i \quad (9)$$

Here:

- $Entropy(S)$, S represents the entropy value in the dataset.
- n represents the number of classes in the dataset.
- p_i , i . represents the ratio of the class to the samples in the dataset.

Considering the mathematical equations in the entropy and information gain equations, $O(n \log n)$ time complexity occurs for each feature, n being the number of training data. When the number of data is m , the time complexity of the training phase is generally found as $O(m * n \log n)$.

Classifying or estimating a data point in the test phase in decision trees means routing the tree to the appropriate decision nodes starting from the root node. This process is directly proportional to the depth of the tree and tree depth refers to the longest path from the deepest node to the root node, depending on the properties of the data set, the size and structure of the tree. Since trees generally have a balanced structure, they have a logarithmic processing time. The time complexity in the test phase is expressed as $O(\log n)$, with the depth of the tree being d .

4.4. K-Nearest Neighbors Time Complexity

During the training phase in the KNN method, the entire dataset is kept in memory. Since the process of keeping the data in memory is done only once for each data, no further action is required. In this case, the number of transactions will be directly proportional to the number of data. Therefore, the time complexity of the training phase is $O(1)$. (Yong et al., 2009).

It includes the steps of finding the nearest neighbors and performing classification/regression for each test sample during the testing phase in the KNN method. To determine the nearest neighbors, the distances between the

test data and all the training data need to be calculated. Calculation of distances is usually done using Euclidean distance or Manhattan distance.

Euclidean distance is calculated as the square root of the sum of the squares of the difference of the coordinates of the two points by measuring the linear distance between the two points. The Euclidean distance between $d(x, y)$, x , and y is expressed as in equation 10. Here, x_1, x_2, \dots, x_n expressions denote the coordinates of the x point, and y_1, y_2, \dots, y_n expressions denote the coordinates of the y point. (Kuang and Zhao, 2009).

$$d(x, y) = \sqrt{(x_1 - y_1)^2 + (x_2 - y_2)^2 + \dots + (x_n - y_n)^2} \quad (10)$$

Manhattan distance is a metric calculated by adding up the vertical and horizontal distances between two points. This metric got its name considering the distance a person moving through city blocks would have to travel. It is used to calculate the "block" distance between two points and is calculated as the sum of the absolute values of the difference between the coordinates of the two points. Manhattan distance can be expressed as in equation 11, $d(x, y)$, Manhattan distance between x and y , x_1, x_2, \dots, x_n expressions being the coordinates of x point and y_1, y_2, \dots, y_n expressions being the coordinates of y point (Kuang and Zhao, 2009).

$$d(x, y) = |x_1 - y_1| + |x_2 - y_2| + \dots + |x_n - y_n| \quad (11)$$

Considering the above metrics used in the testing phase, when the number of data is n and the data size is m , the time complexity becomes $O(m * n)$. If the number of neighbors is $k > 1$, since these calculations will be repeated for each neighbor data, the time complexity of the test phase of the KNN method is generally $O(k * m * n)$.

4.5. Support Vector Machine Time Complexity

In the training phase, the time complexity of SVM mostly relies on calculations to determine support vectors. SVM performs various inner

product and optimization operations between data points. During the training phase of the SVM, it is important to calculate the inner products between the data points. This inner product is the sum of the product of two vectors and is used in decision function and optimization processes in SVM.

When using linear kernel in SVM, the inner product is directly the product of feature vectors (equation 12).

$$K(x_i, x_j) = x_i^* x_j \quad (12)$$

In the training phase of the SVM, an optimization process is performed to determine the decision boundary and support vectors. This optimization process is usually performed using Lagrangian multipliers and solution equations. Lagrangian multipliers are the values of support vectors multiplied by their class labels. Lagrange multipliers are calculated as in equation 13, with n the number of data points, Lagrange multiplier α_i of data point i ., and class label y_i of data point i . (Mangasarian and Musicant, 2001).

$$\sum_{i=1}^n \alpha_i * y_i = 0, 0 \leq \alpha_i \leq C \quad (13)$$

In this equation, C is the cost parameter, a hyperparameter used in the training phase of the SVM, and is used to control the balance between tolerating marginal errors and flexibility of the decision boundary.

SVM aims to separate classes from each other in the best way to find decision boundaries. This decision limit is expressed as a hyperplane and is optimized using support vectors and Lagrangian multipliers. The decision limit is usually expressed in equation 14.

$$w * x + b = 0 \quad (14)$$

In this equation, Lagrangian multipliers are used to optimize the decision boundary. In this case, the vector form of the decision boundary is expressed as in equation 15 with Lagrangian multiplier α_i , class label y_i and support vectors x_i (Bottou and Lin, 2007).

$$w = \sum_{i=1}^n \alpha_i * y_i * x_i = 0 \quad (15)$$

While doing the optimization, the processes of finding Lagrangian multipliers and determining the decision limits are performed. These operations are performed using matrix calculations and nested loops. Therefore, the time complexity of the training phase of the SVM is expressed as $O(n^3)$.

In the testing phase, the classification of new data takes place using the trained SVM model. This classification process requires the calculation of the decision function for each data in the test dataset. While calculating the decision function, it is necessary to do the inner product with support vectors and other calculations. Thus, there is a linear relationship between the number of transactions and the number of data. Because of this situation, the time complexity in the testing phase of SVM can be expressed as $O(n)$.

4.6. Random Forests Time Complexity

The random forests method is an ensemble method in which multiple decision trees are brought together (Liaw and Wiener, 2002). In the training phase, each decision tree is created separately. Therefore, the time complexity is the sum of the time complexity of the creation process of each tree. Each decision tree is created with a subset of the training dataset during the training phase. The subset is selected from the original dataset by random sampling method. Feature selection is usually done randomly or by selecting a certain number of features from the subset. Therefore, a separate decision tree is created for each tree.

After the decision trees are created, the predictions of each tree are obtained at the end of the training phase. In classification problems, tree estimates are combined by consensus or mean method. In regression problems, the trees combine the estimations with the mean method (Liaw and Wiener, 2002). The time complexity of decision trees is $O(m * n \log n)$. The random forests method consists of bringing together k decision trees.

Therefore, the time complexity of the training phase of random forests is the sum of the time complexity of constructing the decision tree k . In this case, the time complexity of the training phase of random forests is usually expressed as $O(k * m * n \log n)$. In the testing phase of the random forests method, the class or predictive value is calculated by passing the data points through all trees and combining the obtained predictions. This operation has a time complexity of $O(\log n)$ for each tree. Since more than one tree is generally used in the random forests method, the process of traversing all trees, including k , has a time complexity of $O(k * \log n)$. In addition, since the operations performed on each data point are independent, the test phase time complexity of the random forests method in the final case is $O(k * m * \log n)$, with the number of features being m .

According to the findings, in Table 1, the time complexity of both the training and testing stages of the linear regression, logistic regression, decision trees, KNN, SVM, and random forests machine learning methods discussed in the study are given comparatively.

Table 1. Time complexity of machine learning methods

Machine Learning Method	Time Complexity	
	Training Stage	Testing Stage
Linear Regression	$O(m^2 * n + m^3)$	$O(m)$
Logistic Regression	$O(m * n)$	$O(m)$
Decision Trees	$O(m * n \log n)$	$O(\log n)$
K-Nearest Neighbors	$O(1)$	$O(k * m * n)$
Support Vector Machines	$O(n^3)$	$O(n)$
Random Forests	$O(k * m * n \log n)$	$O(k * m * \log n)$

When the results given in Table 1 are examined in detail, it is seen that the time complexity of the machine learning methods in the training and testing stages is different.

The first part of the expression for the training time complexity of the linear regression method corresponds to the term $m^2 * n$. This expression grows with the square of the data size and the product of the number of data. Therefore, the increase in data size and number of data means that the training time will increase. The second part has the term m^3 and grows in proportion to the cube of the data size. This shows that the training time increases even more with larger data sizes. The test shows that in time complexity, the data size grows in direct proportion to m . In this case, the test time increases linearly with increasing data size.

The $m * n$ expression is included in the time complexity of the training phase of the logistic regression method. This expression indicates that the training phase time complexity is linearly dependent on the product of the data size and the number of data. Therefore, as the data size and number of data increases, the training time will increase linearly. That is, an increase in data size or an increase in the number of data will increase the training time at the same rate. The testing phase shows that the data size grows in direct proportion to m in time complexity. In this case, the test time increases linearly as the data size increases.

The time complexity of the training phase of the decision tree method includes the expression $m * n \log n$. This expression shows that the data size multiplied by the number of data grows linearly with the logarithm. Therefore, as the data size and number of data increases, the training time will increase but will be limited by a logarithmic factor. The logarithm of the number of data slows down the training time and reduces the ramping rate on larger datasets. The time complexity of the testing phase is expressed as $\log n$. This expression indicates that the number of data will increase depending on the

logarithm. As the number of data increases, the test time also increases logarithmically.

The training phase time complexity of the K-nearest neighbors method is found to be $O(1)$, that is, it has a constant time complexity. The KNN algorithm does not create a model by saving the data directly to the memory during the training phase. Therefore, the training time does not change in relation to the data size, the number of data, or the number of neighbors. In the time complexity of the test phase, the expression $k * m * n$ takes place. This expression shows that there is a linear relationship between the product of the number of neighbors and the size of the data and the number of data. Testing time increases linearly as the number of neighbors increases and the data size and number of data increases.

The time complexity of the training phase of the SVM method includes the expression n^3 . This expression shows that complexity grows linearly with the cube of the number of data. Therefore, as a result of the increase in the number of data, the training period increases rapidly. This shows that the training time will be high in large datasets. In the time complexity of the test phase, the expression n takes place. Since this expression shows that it is linearly dependent on the number of data, the test time will increase linearly as the number of data increases. Test duration is independent of data size and depends only on the number of data.

The time complexity of the training phase of the random forests method includes the expression $k * m * n \log n$. This expression shows that the number of decision trees increases linearly with the data size and the logarithm of the data number. Therefore, as the number of decision trees, data size and number of data increases, the training time increases linearly. However, thanks to the logarithmic factor, as the number of data increases, the rate of increase in the training time is reduced. In the time complexity of the test phase, the expression $k * m * \log n$ is included. According to this expression, the number of decision trees increases linearly with the data size and the

logarithm of the data number. Increasing the data size and number of data during the test also increases the number of decision trees linearly. However, the logarithmic factor decreases the rate of increase of the test time with the increase in the number of data.

5. Conclusions

In this study, the time complexity of linear regression, logistic regression, decision trees, k-nearest neighbors, support vector machines and random forests methods, which are among the machine learning methods and frequently used in the literature, were examined in detail. The training and testing time complexity of each method was analyzed separately. The results show that the time complexity of different machine learning methods is different. In some methods, such as decision trees and KNN, the training time complexity increases linearly with data size and number of data, while in other methods, such as logistic regression and SVM, the training time has a lower complexity. Test time complexity generally has a linear relationship with data size.

This study provides a basis for analyzing and comparing the time complexity of machine learning methods. This information can be helpful in decision-making when selecting machine learning algorithms and working on large datasets. In particular, it is important to consider time complexity for scalability when working with large datasets. In studies to be conducted in this area, the time complexity of more machine learning methods can be analyzed and the performance of these methods can be evaluated on larger datasets.

In conclusion, time complexity analysis is an important tool for evaluating the effectiveness and scalability of machine learning methods. This study aims to help researchers who want to work in the field of machine learning to understand which machine learning method has better time complexity.

REFERENCES

- Akay, E. Ç. (2018). Ekonometride yeni bir ufuk: Büyük veri ve makine öğrenmesi. *Sosyal Bilimler Araştırma Dergisi*, 7(2), 41-53.
- Akgül, İ. (2023). A novel deep learning method for detecting defects in mobile phone screen surface based on machine vision. *Sakarya Univ. J. Sci.* 27 (2), 442-451.
- Akşehirli, Ö., Ankaralı, H., Cangür, Ş., & Sungur, M. A. (2014). Breiman Algoritması Kullanılarak Homojen Alt Grupların Belirlenmesi: Bir Uygulama. *Bilişim Teknolojileri Dergisi*, 7(1), 19-24.
- Ali, Y. A., Awwad, E. M., Al-Razgan, M., & Maarouf, A. (2023). Hyperparameter search for machine learning algorithms for optimizing the computational complexity. *Processes*, 11(2), 349.
- Altaş, D., & Yılmaz, A. (2021). Yaşam Memnuniyeti ve Yaşam Memnuniyetini Etkileyen Faktörlerin Sıralı Lojistik Regresyon Analiziyle İncelenmesi. *Balkan ve Yakın Doğu Sosyal Bilimler Dergisi*, 7(02), 67-76.
- Aphiwongsophon, S., & Chongstitvatana, P. (2018). Detecting fake news with machine learning method. In 2018 15th international conference on electrical engineering/electronics, computer, telecommunications and information technology (ECTI-CON), Chiang Rai, Thailand, 18-21 July 2018, 528-531.
- Arı, A., & Önder, H. (2013). Farklı veri yapılarında kullanılacak regresyon yöntemleri. *Anadolu Tarım Bilimleri Dergisi*, 28(3), 168-174.
- Aylak, B. L., Okan, O., & YAZICI, K. (2021). Yapay zeka ve makine öğrenmesi tekniklerinin lojistik sektöründe kullanımı. *El-Cezeri*, 8(1), 74-93.
- Baydemir, M. B. (2014). Lojistik regresyon analizi üzerine bir inceleme. *Sosyal Bilimler Enstitüsü, İnönü Üniversitesi*.
- Boser, B. E., Guyon, I. M., & Vapnik, V. N. (1992). A training algorithm for optimal margin classifiers. In *Proceedings of the fifth annual workshop on Computational learning theory*, Pittsburgh, Pennsylvania, USA, 27 - 29 July, 144-152.
- Bottou, L., & Lin, C.-J. (2007). Support vector machine solvers. *Large scale kernel machines*, 3(1), 301-320.
- Bozyiğit, B. Ş., & Tarhan, Ç. (2020). Makine öğrenmesi yöntemleri kullanılarak sosyal medyada marka itibar analizi. *Yönetim Bilişim Sistemleri Dergisi*, 6(2), 57-76.

- Breiman, L. (2001). Random forests. *Machine learning*, 45, 5-32.
- Calayır, G. N., & Kabak, M. (2021). Bakım için makine öğrenme tekniklerinin analizi ve bir uygulama. *Journal of Turkish Operations Management*, 5(1), 662-675.
- Cherfi, A., Nouira, K., & Ferchichi, A. (2018). Very fast C4. 5 decision tree algorithm. *Applied Artificial Intelligence*, 32(2), 119-137.
- Cunningham, P., & Delany, S. J. (2021). k-Nearest neighbour classifiers-A Tutorial. *ACM Computing Surveys (CSUR)*, 54(6), 1-25.
- Dai, W., & Ji, W. (2014). A mapreduce implementation of C4. 5 decision tree algorithm. *International journal of database theory and application*, 7(1), 49-60.
- Demirel, Ş., & Yakut, S. G. (2019). Karar ağacı algoritmaları ve çocuk işçiliği üzerine bir uygulama. *Sosyal Bilimler Araştırma Dergisi*, 8(4), 52-65.
- Dore, F. (2012). Güçlü yapay zekaya karşı çin odası argümanı. *Afyon Kocatepe University Journal of Social Sciences*, 14(1).
- Ekici, S., Yıldırım, S., & Poyraz, M. (2009). Mesafe koruma için bir örüntü tanıma uygulaması. *Gazi Üniversitesi Mühendislik Mimarlık Fakültesi Dergisi*, 24(1), 51-61.
- Erdi, B., Şahin, E. A., Toydemir, M. S., & Dökeroğlu, T. (2021). Makine öğrenmesi algoritmaları ile trol hesapların tespiti. *Düzce Üniversitesi Bilim ve Teknoloji Dergisi*, 9(1), 430-442.
- Eyüpoğlu, C. (2020). Korelasyon Temelli Özellik Seçimi, Genetik Arama ve Rastgele Ormanlar Tekniklerine Dayanan Yeni Bir Rahim Ağzı Kanseri Teşhis Yöntemi. *Avrupa Bilim ve Teknoloji Dergisi*, (19), 263-271.
- Gambhir, E., Jain, R., Gupta, A., & Tomer, U. (2020). Regression analysis of COVID-19 using machine learning algorithms. In *2020 International conference on smart electronics and communication (ICOSEC)*, Trichy, India, 10-12 September 2020, 65-71.
- Gislason, P. O., Benediktsson, J. A., & Sveinsson, J. R. (2004). Random forest classification of multisource remote sensing and geographic data. In *IGARSS 2004. 2004 IEEE International Geoscience and Remote Sensing Symposium*, Anchorage, AK, USA, 20-24 September 2004, 1049-1052.
- Github, (2021). 100-Days-of-Machine-learning. Retrieved from <https://github.com/charvibannur/100-Days-of-Machine-learning>
- Güldal, H. (2018). Karar ağacı algoritmalarının eğitsel veriler üzerindeki performanslarının incelenmesi. In *13th International Balkan Education and Science Congress*, Edirne, 6-8 September 2018, 6-10.

- Harrell, F. E. (2001). Regression modeling strategies: with applications to linear models, logistic regression, and survival analysis. Springer, New York.
- Hilbe, J. M. (2009). Logistic regression models: CRC press.
- Ibarguren, I., Pérez, J. M., & Muguerza, J. (2015). CTCHAID: extending the application of the consolidation methodology. In Progress in Artificial Intelligence: 17th Portuguese Conference on Artificial Intelligence, Coimbra, Portugal, 8-11 September 2015, 572-577.
- Kaneda, J. (1995). Quinlan, JR: C4. 5 Programs for Machine Learning, Morgan Kaufmann, San Mateo, California (1992). Artificial Intelligence, 10(3), 475-476.
- Kavzođlu, T., & Çölkesen, İ. (2010). Karar ağaçları ile uydu görüntülerinin sınıflandırılması. Harita Teknolojileri Elektronik Dergisi, 2(1), 36-45.
- Kılıç, S. (2013). Doğrusal regresyon analizi. Journal of Mood Disorders, 3(2), 90-92.
- Kılınç, D., Borandađ, E., Yücalar, F., Tunalı, V., Şimşek, M., & Özçift, A. (2016). KNN algoritması ve r dili ile metin madenciliđi kullanılarak bilimsel makale tasnifi. Marmara Fen Bilimleri Dergisi, 28(3), 89-94.
- Kizrak, M. A., & Bolat, B. (2018). Derin öğrenme ile kalabalık analizi üzerine detaylı bir araştırma. Bilişim Teknolojileri Dergisi, 11(3), 263-286.
- Koruyan, K., & Ekeryılmaz, A. (2022). Makine Öğrenmesi ile Müşteri Şikayetlerinin Sınıflandırılması. AJIT-e: Academic Journal of Information Technology, 13(50), 168-183.
- Kuang, Q., & Zhao, L. (2009). A practical GPU based kNN algorithm. The 2009 International Symposium on Computer Science and Computational Technology (ISCSCI 2009), Huangshan, P. R. China, 26-28, December 2009, 151-155.
- Lewis, R. J. (2000). An introduction to classification and regression tree (CART) analysis. In Annual meeting of the society for academic emergency medicine in San Francisco, California, 1-14.
- Liaw, A., & Wiener, M. (2002). Classification and regression by randomForest. R news, 2(3), 18-22.
- Liu, H., & Gegov, A. (2016). Induction of modular classification rules by information entropy based rule generation. In Innovative Issues in Intelligent Systems, 217-230.
- Luts, J., Ojeda, F., Van de Plas, R., De Moor, B., Van Huffel, S., & Suykens, J. A. (2010). A tutorial on support vector machine-based methods for classification problems in chemometrics. Analytica chimica acta, 665(2), 129-145.

- Machhale, K., Nandpuru, H. B., Kapur, V., & Kosta, L. (2015). MRI brain cancer classification using hybrid classifier (SVM-KNN). In 2015 International Conference on Industrial Instrumentation and Control (ICIC), Pune, India, 28-30 May 2015, 60-65.
- Mangasarian, O. L., & Musicant, D. R. (2001). Lagrangian support vector machines. *Journal of Machine Learning Research*, 1, 161-177.
- Maulud, D., & Abdulazeez, A. M. (2020). A review on linear regression comprehensive in machine learning. *Journal of Applied Science and Technology Trends*, 1(4), 140-147.
- Nacar, E. N., & Erdebilli, B. (2021). Makine öğrenmesi algoritmaları ile satış tahmini. *Endüstri Mühendisliği Dergisi*, 32(2), 307-320.
- Öztürk, S. (2012). Yeni doğan bebeklerde düşük doğum ağırlığının ikili lojistik regresyonla en çok olabilirlik ve mars yaklaşımına dayalı modellenmesi. *Fen Bilimleri Enstitüsü, Muğla Sıtkı Kocaman Üniversitesi*.
- Palimkar, P., Shaw, R. N., & Ghosh, A. (2022). Machine learning technique to prognosis diabetes disease: Random forest classifier approach. In *Advanced Computing and Intelligent Technologies: Proceedings of ICACIT 2021*, 219-244.
- Pandya, R., & Pandya, J. (2015). C5.0 algorithm to improved decision tree with feature selection and reduced error pruning. *International Journal of Computer Applications*, 117(16), 18-21.
- Quinlan, J. R. (1987). Simplifying decision trees. *International journal of man-machine studies*, 27(3), 221-234.
- Quinlan, J. R. (2014). *C4.5: programs for machine learning*. Elsevier.
- Rolnick, D., Donti, P. L., Kaack, L. H., Kochanski, K., Lacoste, A., Sankaran, K., Ross, A. S., Milojevic-Dupont, N., Jaques, N., Waldman-Brown, A., Luccioni, A. S., Maharaj, T., Sherwin, E. D., Mukkavilli, S. K., Kording, K. P., Gomes, C. P., Ng, A. Y., Hassabis, D., Platt, J. C., Creutzig, F., Chayes, J., & Bengio, Y. (2022). Tackling climate change with machine learning. *ACM Computing Surveys (CSUR)*, 55(2), 1-96.
- Roopa, H., & Asha, T. (2019). A linear model based on principal component analysis for disease prediction. *IEEE Access*, 7, 105314-105318.
- Sani, H. M., Lei, C., & Neagu, D. (2018). Computational complexity analysis of decision tree algorithms. *Artificial Intelligence XXXV: 38th SGAI International Conference on Artificial Intelligence*, Cambridge, UK, December 11–13, 2018, 191-197.

- Shi, Y., Zhang, L., & Dong, S. (2019). Path Planning of Anti ship Missile based on Voronoi Diagram and Binary Tree Algorithm. *Defence Science Journal*, 69(4), 369-377.
- Sun, B., & Chen, H. (2021). A survey of k nearest neighbor algorithms for solving the class imbalanced problem. *Wireless Communications and Mobile Computing*, 2021, 1-12.
- Şahin, E. K. (2017). Özellik seçimi algoritmaları kullanılarak heyelanda etkili faktörlerin belirlenmesi ve heyelan duyarlılık haritalarının üretilmesi. *Fen Bilimleri Enstitüsü, İstanbul Teknik Üniversitesi*.
- Şekerli, E. B. (2019). Ticari havayolu taşımacılığı sektöründe makine öğrenmesi uygulamalarının incelenmesi. *Selçuk Üniversitesi Sosyal Bilimler Meslek Yüksekokulu Dergisi*, 22(2), 405-419.
- Şenel, S., & Alatli, B. (2014). Lojistik regresyon analizinin kullanıldığı makaleler üzerine bir inceleme. *Journal of Measurement and Evaluation in Education and Psychology*, 5(1), 35-52.
- Şengül, M. K., Tarhan, Ç., & Tecim, V. (2022). Toplu taşıma işletmelerinde akıllı ulaşım sistem verilerinin büyük veri teknolojileri ile desteklenmiş iş zekâsı mimarisinde uygulanması: Bir literatür incelemesi. *Kahramanmaraş Sütçü İmam Üniversitesi İktisadi ve İdari Bilimler Fakültesi Dergisi*, 12(1), 89-105.
- Taşcı, E., & Onan, A. (2016). K-en yakın komşu algoritması parametrelerinin sınıflandırma performansı üzerine etkisinin incelenmesi. *Akademik Bilişim*, 1(1), 4-18.
- Toka, O., Çetin, M., & Altunay, S. A. (2011). Basit Doğrusal Regresyonda Sağlam ve Theil Kestiricilerinin Karşılaştırılması. *İstatistik Araştırma Dergisi*, 8(3), 45-53.
- Ustalı, N. K., Tosun, N., & Tosun, Ö. (2021). Makine öğrenmesi teknikleri ile hisse senedi fiyat tahmini. *Eskişehir Osmangazi Üniversitesi İktisadi ve İdari Bilimler Dergisi*, 16(1), 1-16.
- Veranyurt, Ü., Devenci, A., Esen, M. F., & Veranyurt, O. (2020). Makine öğrenmesi teknikleriyle hastalık sınıflandırması: random forest, k-nearest neighbour ve adaboost algoritmaları uygulaması. *Uluslararası Sağlık Yönetimi ve Stratejileri Araştırma Dergisi*, 6(2), 275-286.
- Yamantaş, Ö. (2019). Türkiye sağlık araştırması verilerinin yapay sinir ağları ve çok kategorili lojistik regresyon yöntemiyle incelenmesi. *Fen Bilimleri Enstitüsü, Gazi Üniversitesi*.

- Yan, X., & Su, X. (2009). Linear regression analysis: theory and computing. world scientific.
- Yao, Z., Lum, Y., Johnston, A., Mejia-Mendoza, L. M., Zhou, X., Wen, Y., Aspuru-Guzik, A., Sargent, E. H., Seh, Z. W. (2023). Machine learning for a sustainable energy future. *Nature Reviews Materials*, 8(3), 202-215.
- Yavuz, A., & Çilengirođlu, Ö. V. (2020). Lojistik regresyon ve CART yöntemlerinin tahmin edici performanslarının yaşam memnuniyeti verileri için karşılaştırılması. *Avrupa Bilim ve Teknoloji Dergisi*, (18), 719-727.
- Yong, Z., Youwen, L., & Shixiong, X. (2009). An improved KNN text classification algorithm based on clustering. *Journal of computers*, 4(3), 230-237.
- Yürek, E. E., Yağmahan, B., Akyüz, B. C., Samast, E. S., & Çetrez, N. D. (2022). Parça ıskartalarının makine öğrenmesi kullanılarak azaltılması: Otomotiv sektöründe bir uygulama. *Uludağ Üniversitesi Mühendislik Fakültesi Dergisi*, 27(1), 291-308.
- Zortuk, M., Eylem, K., & Bayrak, S. (2014). Hanehalkları satın alma kriterlerinin analizi: multinominal lojistik regresyon yaklaşımı. *Dumlupınar Üniversitesi Sosyal Bilimler Dergisi*, 163-176.

Chapter 6

MASS TRANSPORT AND UARBAN RAILWAYS IN THE CONTEXT OF SUSTAINABILITY

Mehmet Çaęrı KIZILTAŞ¹

Vail KARAKALE²

1 mckiziltas@ticaret.edu.tr, Istanbul Ticaret University

2 Prof.Dr., vail.karakale@medeniyet.edu.tr, Istanbul Medeniyet University

Transportation has had an important position in all periods of history in the context of the social, economical and cultural relationships of societies each other. At industrial revolution and access to modern period, the improvement of technical possibilities have had a high importance and transportation as one of these possibilities has become driving power. Transportation has an effective position both passenger and good transports on the scale of intraurban, inter urban, local, regional and national. Transportation abilities have enhanced on the parallel of technological improvements that has emerged new opportunities and threats. The development of transportation has been affecting to economy positively in all historical periods. The usage of transportation system effective and efficient on today's world is related to the minimization of existing problems and adaptation of innovations to the system.

Although railway transportation mode has become favourite mode since the earliest of 20th century, highway transportation mode has gained a big significance by the parallel of wide currency of automobile. But since 1980s, it has understood that the existing consumption-environmental balance is not sustainable by international parts notably westerner countries. And on this context, the sustainability notion which has been confessed is contained three main issue which are social, economical and environmental. Railway transportation mode has been emerging a sustainable transportation with the properties of less fuel consumption, occupying less road section and the usage with high passenger capacity. High speed railways (HSR) transportation mode provides the level of service parameters as operation speed, comfort, safety and punctuality on the highest levels beside the mentioned properties. Providing of intermodal integration and balanced modal distribution in transportation system is either a necessity or the result of development.

Evaluation Of The Transportation System In Turkey and Europe

The developments in 21st century and last quarter of 20th century have revived different modal searches and environmental approaches. Railways of Turkey has remained incapable to meet the potential freight and passenger demands in terms of current cost, service quality and safety. Inadequate infrastructure is one of the reasons of blocking the railways to reach the expected point level of service and the low level of demand. Also the issues like the lack of academy-sector integration and financing source can be stated in the unphysical reasons of railway transportation mode stability. The way of directing the increasing transportation demand to railways truly contains doing investments that improve current network and enhance railway infrastructure, realizing the academical and constitutive reforms which aim restructuring of railway investment and financement system, forming railway infrastructure and operation in seperately establishments.

Providing the balanced modal distribution is one of the key issues of sustainable transportation. One of the main reasons of usage of private cars in European wide is ensuring the possibility of transporting door to door although traffic congestion and parking problems. On the other hand, the usage of private car enhances the traffic incident rates and results problems as energy dependence, travel time losses and environmental changes. One of the effective way to decrease these affects is providing intermodal integration and intermodal access which are based to origin-destination variety. Because of these, planning of balanced modal distribution gives significant contributions to coordinated usage of different energy sources and transforming the transportation system totally more sustainable. Today in Europe, the main axis is high speed railway transportation mode at the intermodal network. High speed railway constitutes the most important part of intermodal integration planning although physical and environmental limits as slope and railway traffic.

Liberalization and investments of railways that has been faced since 1990s and 2000s are part of privatization on global scales. As in other infrastructure sectors, it is aimed to enhance the competitiveness resistance of all modes by exceeding the one mode transportation system problem at the reforms of railway sector too. Because of can not reach the competitiveness on railway sector has forced the companies which have the ability of interoperability to the single train operations. This case bring the issue of necessity of accepting infrastructure and operation as different management topics into the forefront at constituting a more competitive railway system. The transformation that has been realizing on railway system states that the plans can vary according to different environmental and economical conditions of each country. By year of 2000, when the total freight transport capacity of European Union (EU) is 3.068.000 million tonnesXkm, only the railway freight transport capacity of United States Of America (USA) is 2.468.206 million tonnesXkm that is a 38% share on freight transport modal distribution. This value corresponds to 58,82% share in total land transport in USA which this rate is only 15,11% for EU. As it has seen from this table too, EU has realized total freight transport only less than half of the total freight transport USA that are the share of marinerway is 41,40% and the total share of other modes (inland waterways, pipelines and airway) is 48,24% for EU freight transport. Railway has a vital role for the industrial and economical developments of countries which the railway freight transport of EU has faced a decrease at the alarming rate especially at carriage in last periods. Approximately 21% of carriage has been realized by railways in European countries in 1970s. This share has decreased to 8,1% in 2000s. At the same period, this ratio has increased from 30,8% to 43,8% for highway freight transport for EU. While only railway freight transportation modal share has faced a decrease, all other freight

transport modes have realized an increase in the period of 1970-2000 years. Also a considerable decrease has been recorded for railway passenger transport modal share from 10,2% to 6,3% at same years. The most important reason of this case is not being as competitive as highway transportation mode of railway transportation mode. Beside all of these, railway transportation mode has some specific advantages too. Railways is an environmentalist and safe transportation sector, a train can transport 60 trucks freight and railway infrastructure is suitable for improving.

European Community Commission has agreed on the issue that constituting common policy about foreign trade, agriculture and transportation by Rome Alliance. The 74th-84th articles of Rome Alliance are about transportation.

Principles and objective related transportation in memorandum which was prepared by European Community Commission in 1961 are:

- Constituting free competition environment
- Providing infrastructure organization
- Establishing of payment system

TINA Report and European Union Transport Policies

TINA Report is an opening work for providing free movement of persons, goods and services and giving possibility to sustainable mobility of extension period of multi modal transportation network of European Union (TEN-T, Trans European Network for Transport) on the paralel of candidacy of Turkey to the union. This report contains all over the Turkey and its all transportation modes (highway, railway, marineway and airway etc.), investments that are on planning, constructing and bidding phases. One of the special objective of TINA Report is specifying the necessities of transportation infrastructure investments for next 15 years that will integrate Turkey to the union. For reducing the transportation sourced negative effects as hazardous chemical emissions, a policy that increase the railway freight transport demand and making railway preferable to another modes which has to be pursued.

Various implementations exist for transferring traffic from other modes to railway transportation mode. Cost reduce is an important method for providing traffic access between different modes. The factors that affect to population increase in a corridor are work and cultural relations on high levels between different cities and high population density. Travel cost and punctuality have to be on a feasible level beside reliability, safety and security for competitiveness of railway with other transportation modes. Especially in critical corridors that have high loaded traffic between intercity travels in existing transportation modes, high speed railways attract the customers more

than others. The potential of network affects is an important factor for access level of traffic to railways. When railway line is established on locations that contain many origin and transfer points, more passenger will be transferred to railways. It has been estimated to transport of future traffic volumes from highway and railway by Marmaray as a new alternative.

Because of all of these reasons, prevention of external affects on unacceptable levels as a necessity of increasing safety and smart policies beside an expensive transportation which is the main objective of European Union is establishing a transportation system that is sustainable and well balanced and has a robust financial structure.

European Union Transportation Policies that have constituted on direction of these objectives can be summarized as follows:

- Integration of transportation markets and supporting to cancel of monopolies
- Easing of boarder crossings, producing effective logistics and work possibilities, supporting the transport of persons, goods and services and so enhancing the transportation effectiveness on European wide.
- Usage of all transportation systems in an integration, giving priority to railway, inner waterway, short distanced marineway and combined transport in freight transport and giving priority to mass transport in passenger transport
- Providing a transportation environment that is safety and acceptable in terms of society and environment, enhancing the transportation safety and security, stating targets for this objective, reducing the differences on current regulations in Europe
- Enhancing construction and operation of transportation system (infrastructure, vehicle, equipment and process)

The necessary precautions for reaching these objectives are:

- Adaptation of the regulation
- Liberalization
- Developing of multi modal transportation
- Improvement of mass transport in passenger transport
- Enhancing of infrastructure
- Development of intelligent transportation systems
- Cooperation at research and development
- Implementations of interiorising of external costs

- Easing of transit accesses by bettering of the process in border crossings
- Reducing of crime and fraud on international transports

In this sense, European Union policies meet new challenges on the parallel of inclining of social life to more mobility. Current highway and airway traffic have a share of approximately 1% in GNP (Gross National Product) while European Union citizens has been expecting higher level of service parameters day by day. On the parallel of all of these, 40% increase has been estimated till 2030 and 80% increase has been estimated from 2005 to 2050 on high speed railway freight transport. The ratios for the same year periods are for 34% and 51% respectively for high speed railway passenger transport. At this point, it is aimed to break the fuel oil dependency while 96% of transportation energy needs have been met still by fuel oil that is a decreasing energy source on worldwide which is estimated to increase of the cost of fuel oil to double of today in 2050. Also for limiting the global warming, USA has to cut the national fuel oil consumption on 60% levels until 2050s.

The most leading of the disadvantages of European Union railway policies is seen that giving too more significance to passenger transport than freight transport which is the share of railways in interurban passenger transport is 6,25% in European Union while this share is only 0,32% in United States Of America.

Railway routes are limited that improving these for passenger transport has many possibilities and studies which is the case for freight transport is different. For improving European Union railway freight transport, there are the technical possibilities of multi disciplinary operation and cooperation of locomotive driver trainings. Two important topics at this point are financment sources and coordination. Another critical phase is demand balance between freight and passenger transports that has been provided which is existing significant limitations for providing this issue especially on intraurban freight transport in European Union. The possibilities of directly increasing the railway freight transport modal share are enhancing the line capacity, improving the signalization, bettering the infrastructure quality.

Any other important issues are promoting the railway freight transport and increasing the sectoral competitiveness. Shorter freight transport distances and longer coastal strips are the structural characteristics of European Union as compared with United States Of America that the production variety in mentioned two geographies are another indicative. At this point, the main factor is developing policies of European Union on the concept of railway freight transport which is seen the most important advantage of the union. Mid term reflections of these policies are on the direction of the ability of an increase acceleration of 65% on railway freight transportation. One of

the main objective of White Paper that is constituted in 2001 by European Commission. But, inside of all of these changings and projections, it is not seen possible to reach of European Union's railway freight transport modal share to United States of America's related modal share that is 38%.

The Development Trends In Urbanization and Transportation In Turkey

Turkey is a country that has urbanized on high levels which is the 72% of the population lives on the urban areas. This rate has increased 10% on last decade and approximated to European Union values. The increase on urbanization results high traffic volumes because of the plenty of origin and destination points in urbans. The number of car ownership has doubled in ten years that the current rates are stil under the related values on the union but tghe increase acceleration in Turkey is continuing. Problems have emerged in terms of the sustainability of urban transportation system because of the hihg increase on traffic congestion values. Mainly, the traffic congesiton on city centers is related to the increase on car ownership, population density and business acitivities. Unbalanced share of highway on freight and passenger transports results permenant congesitons, bottlenecks and high road loads. When the increasing trend on car ownership continues, existing case will be worse.

The conclusive objective of national strategy of Turkey on transportation sector is establishing a efficient, effective, safe, environment friendly, smart, sustainable, intermodal integrated and accessible transportation system that is planned to have a strong network with Europe and the rest of the world. For reaching to these objectives, Turkey 2023 vision involves transportation and communication strategy, higher mobility, less traffic congestion, less emission, estabilishing a more suitable transportation system which is more safe with reducing the traffic incidents and mortalities, more cost effective with improving mass transport, smart city planning, smart charging implementation. Mass transport is very important on the solution of the problems which are based on energy, economy and environment and supports to enhance of life quality. The incline of usage mass transport increases on the parallel of population increase. The benefits of mass transport has given as below:

- Increases the personal alternatives
- Provides fuel saving
- Reduces the traffic congestion
- Presents economical opportunities, provides social development and recovery
- Provides cost saving
- Reduces fuel oil consumption

- Decreases carbon footprint

Population of Istanbul has increased geometrically since 1970s and quadruplicated. On the same period the increase on car ownership is more than the increase on the population and carownership has enhanced approximately 30 times from 1970s to 2000s. The increase difference between car ownership and population can be expressed with the increase on GDP (Gross Domestic Product), the radical change on consumption culture and the high modal share of highway transportation mode on both transportation system and mass transport. Vehicle number per person is 0,017 in 1970s, 0,042 in 1980s and 0,140 in 2000s. This means approximately 10 times increase in last 30 years that has reached on higher levels in today's. Istanbul has been only single centered around the historical peninsula before the republic period which has developed on Beşiktaş-Ortaköy-Taksim line in European side and Üsküdar-Kadıköy line in Asian side subsequently. Multi centered development has accelerated since 1990s that the centroid of the city which is arisen by the high populated and employment areas of the city has started to move from coast lines and bosphorus. Developing the new urbanization areas far away from the bosphorus has become easier by starting to operate of bosphorus bridges and completing the access roads. In general, the high share of highway transportation mode in all periods in Istanbul has attracted the attention.

It has been understood that operating of bosphorus bridges supports the increase on private car usage than the increase on highway modal share. Because of this, it can not be said that constructing of new bosphorus bridge will occur negative effect to the balanced modal distribution in Istanbul categorically. On this context, existing of railway lines (probably high speed railway) on 3rd bosphorus bridge has to be considered additionally. But it is a clear point that the necessity of right directing of private car usage. Carownership ratio is 19,30% in start to operation year of 1st bosphorus bridge and this ratio has become 19,20% in start to operation year of 2nd bosphorus bridge that has become 26,34% in 2006.

At the same period, the share of taxi-dolmuş in modal distribution has decreased clearly that the service vehicle share which is used for work and school trips has recorded a serious increase from 10,40% to 21,48%. After 1996 period has an important effect at this increase. On this context, the increase of private car usage can be evaluated parallel to the increase on service vehicle usage. But it can be said too that the possibilities of integration of service vehicles to the seways are more than the possibilities of integration of private cars to the seaway.

Here another significant point is that can be said that the mass transport fleets have been realized the necessary and sufficient increase on the parallel of the increase on population and Gross National Product (GNP) since 1987.

From this point it can be seen that the urgent necessity of mass transport is integration more than the fleet enhance. For the same period, the share of minibus has been 19,00% in 1987 to 16,71% in 2006. The rational based partial decrease on minibuses can be read by the increase in GNP and the enhance on mass transport service infrastructure. But it can be understood that the existing of an amountly based increase on minibus lines because of urbanization and increase of transportation networks. It is a necessity too that is the standardization of minibus lines in terms of level of services parameters especially as comfort, safety, security, travel time etc. of vehicle, line and operation. The modal share of city buses (IETT + private city buses) has decreased by 35,20% in 1987 to 24,12% in 2006 that after 1996 period is a milestone in this decrease. This decrease has been sourced especially in private city buses that the main reason of this is intra urban railway system investments.

When the accesses from Asia to Europa is investigated, it is seen that the 81% of accesses is realized by the bosphorus bridges and 19% of accesses is realized by marinelines. Also it has seen that the 82% of bosphorus bridge accesses is realized by private cars. In spite of that, only 24% of bosphorus bridges passenger transport is realized by private cars. As it has been mentioned before, as a result of increase of carownership rates and existing only 1-2 passenger in each private car, private cars which are the most important factor of traffic congestion on bosphorus bridges meet only the 24% part of the passenger transport on bosphorus bridges. From this point, it is concluded that is provided the vehicle accesses than the passenger accesses by bosphorus bridges.

Intraurban railway notably subway invesments have increased rapidly in last decade but it is not only sufficient for providing balanced modal distribution and reducing of carownership ratios. This case states a wide area that is from management of consumption culture to urbanization and transportation master plan and integration of all of these.

Results

Tending to mass transport in all transportation modes and presenting a service with more integrated, comfortable, safe and punctual provide considerable fedbacks on short terms. A punctual, comfortable, safe and cost effective continuous mass transport service possibility along South axis of Istanbul is going to emerge with starting to operate of full line of Marmaray. On this context, Gebze-Halkali travel time will be 105 minutes, Bostanci-Bakirkoy travel time will be 37 minutes.

Below on Table 1 is illustrated the urban railway system investments that are planned starting to operate till 2019. Marmaray is on a key point because of affecting on the traffic congestion problem of Istanbul, position on interurban freight transport and its functions on regional and international scale freight transport.

Marmaray is going to enable a very significant function on the South axis of the city also that has a considerable affect area on the coastal lane of bosphorus and Marmara Sea with completing the related sectios and extentions, start to operate with full capacity and providing relevant integrations of Marmaray.

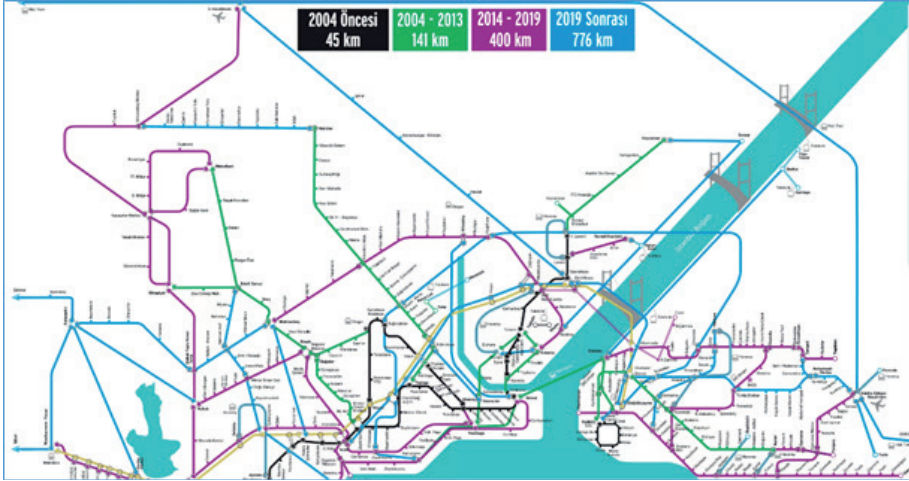


Figure 1. Urban Railway Lines Plans Of Istanbul For The Year Of 2019

The basic mentality of service is the ability of improvement an approach which is human focused. As a result of the periods related to economical, cultural, political and technical aspects, state investments or private sector initiatives can come to the fore cyclicly. But at this point, only statist or only liberalist approaches are not functional. Collimator to the approaches and a system improvement ability is the human focused mentality. On the parallel of this understanding, public private partnership approaches can be developed.

The objectives that have been specified for urban railway systems line km in 2023 can be realized by sufficient coordination and distribution of work between local authority (Istanbul Grand Municipaity) and government (Ministry Of Transportation, Maritime Affairs and Communications).

At this point, the right understanding of satisfaction and expectations of Istanbulites from mass transport is very important. Istanbulites use BRT (metrobüs) too often but are not satisfied from the level of service parameters as comfort and safety. But on the other hand, the route of BRT is one of the main axis of Istanbul. Istanbulites are satisfied from the subway investments and demand continuing as increasingly of this. But it must not hope that decrease on the usage of private car of Istanbulites without additional precautions and sufficient integration. Istanbulites use minibus lines as only an obligation that is not satisfied the level of service parameters. Because of these, the rapid entrance to the period of urban railway investments can present the

possibility of re evaluation about the connection between main axis and para-transit (feeder) lines. In modal distribution of Istanbul, it has seen that the modal share of railways can reach to 30% by subway line investments and the necessity modal share of the seaways is 20% in urban transportation of Istanbul. It is considered that the negative effects of formations and decisions which support consumption culture to balanced modal distribution of Istanbul and the modal distribution plans has to be done in this context. In this regard, cableway investments have been prioritized that is attracted the attention which the lines have been planned with the consideration of urban developments of the specific regions that are Çamlıca-Altunizade-Zincirlikuyu-Mecidiyeköy cableway and short-long distanced cableways that are paralel to Bosphorus coast. Aslo, the transfer centers that connect many different transportation modes will affect the development of the related region radically.

The railed system and especially the metro investments have a vital prospect when the traffic congestion in Istanbul is drawn to the affordable levels. And also; As in Istanbul, in the middle of the sea and in the type distribution of a city that surrounds the sea, the sea route is well below the expected level and is around 1-2%. Whereas; In Istanbul this rate can be 20-25%. More ahead; In the Bosphorus, parallel to the shore line application, transportation practices between the settlements on the same side have been tried but the desired efficiency has not been obtained. Here; Among the nearby distances, the existing city line ferry is big enough and prevents the right direction of the demand line. Because of the frequent lines parallel to such a shore, more frequent flights have to be made by approaching the quays with shorter ferry lines and ensuring filling and separation. In Istanbul, the City Lines operate with a 10% capacity and the use of the capacitor even at 40-50% will reduce the blockage of the throat bridge significantly.

A rapidly and effective establishment period has been realized on high speed railway (HSR) transportation modes, intraurban-inter urban and interregional projects railway system projects particularly Marmaray have been realized, the load on the highway transportation mode has been transferred to railway and airway transportation modes comparatively by existing transportation investments. On this context, human focused approach, considering the environmental factors and improving a sustainable understanding will be very signicifant on the investment period.

According to 2023 Strategy Action Plan, the target of being one of the biggest ten economy of the world which was specified by Turkish Republic Government can be realized by establishing a transportation system that functional, efficient, powered by smart investment perspective, focused to supporting of social justice, canalized the consumption culture and habits on the right way, accessed on highly level of safety, education, health and basic socio-economic instruments.

REFERENCES

- [1] Kızıldaş, M, Ç, (2015). Traffic Safety and Railway Applications, Transportation World Newspaper
- [2] Ilıcalı, M., Çatbaşı, N., Öngel, A., Kızıldaş, M. Ç., 2013, 'Multimodal Transportation Issues in Istanbul: A Case Study for Traffic Redistribution Due to Long Span Bridge Rehabilitation', Hong Kong
- [3] TR 10. Government Plan Transportation and Traffic Safety Ö.İ.K. Report, Ankara (2012).
- [4] Kızıldaş, M, Ç, 2018. Uluslararası Çerçeve de Kentleşme ve Ulaştırma Örnekleri, Transist 2018, İstanbul Ulaşım Kongresi ve Fuarı, İstanbul, 8-10 Kasım
- [5] Kızıldaş, M, Ç, Tekin, A, Ç, 2017. İstanbul'da Raylı Sistem Hatlarının Hat ve Sefer Entegrasyonlarının İncelenmesi, Transist 2017, İstanbul Ulaşım Kongresi ve Fuarı, İstanbul, 2-4 Kasım
- [6] Wang, F.Z., Google released the product of smart home: Google Home. Available from <http://tech.163.com/16/0519/01/BND3AHMH000915BD.html> (in Chinese) (2016)
- [7] Sak, H., Senior, A., Beaufays, F., (2014) Long short-term memory recurrent neural network architectures for large scale acoustic modeling. INTERSPEECH, p.338-342.
- [8] Langford, B., Cherry, C., Yoon, T., Worley, S., Smith, D., (2013) North America's first ebike share: a year of experience. Transport. Res. Record: J. Transport. Res. Board (In Press)
- [9] Takatsu T, (2007) "The history and future of high-speed railways in Japan". *Japan Railway & Transport Review*, 48, 6-21
- [10] TÜİK nüfus verileri, 2015
- [11] Golobič, M., & Marot, N., (2011) Territorial impact assessment: Integrating territorial aspects in sectoral policies. Evaluation and program planning, 34(3), 163–173. doi:10.1016/j.evalprogplan.2011.02.009
- [12] Kızıldaş, M.Ç., Altan, M.F., (2018) A Review In Term Of Service Parameters On The Modal Choice sand Mass Transport, İzmir
- [13] Saatçioğlu, C., Çelikok, K., (2017) Avrupa Birliği Ortak Ulaştırma Politikası Çerçevesinde Türkiye'de Uygulanan Ulaştırma Politikalarının Değerlendirilmesi
- [14] Simonyan, K., Zisserman, A., (2014) Very deep convolutional networks for large-scale image recognition. arXiv:1409.1556.
- [15] Kızıldaş, M.Ç., Altan, M.F., (2017) Evaluation of Intermodal Integration on the Context of Marmaray and Bosphorus Bridges, IRF Regional Congress, Dubai.
- [16] Altan, M.F., Kızıldaş, M.Ç., (2018) Toplu Taşımada Çok Amaçlı Karar Verme

ve Metropolitan Bir Alanda Ev-İş Ulaşım Hizmeti Modellemesi, Karaelmas Fen ve Mühendislik Dergisi, ULAKBİM

- [17] Altan M.F., Kızıldaş M.Ç., (2020) Yüksek Hızlı Demiryolları, Yolcu Ve Yük Taşımacılığı Karşılaştırmaları Bağlamında Küresel Ölçekli Bir Derleme Çalışması, Dicle Üniversitesi Mühendislik Fakültesi Dergisi, ULAKBİM (yayın aşamasında)
- [18] Dill, J., Rose, G., (2012) E-Bikes and transportation policy: insights from early adopters. In: Transportation Research Board 91st Annual Meeting, Washington DC.
- [19] García-Palomares, J.C., Gutiérrez, J., Latorre, M., (2012) Optimizing the location of stations in bike-sharing programs: a GIS approach. *Appl. Geogr.* 35, 235e246.
- [20] Theurel, J., Theurel, A., Lepers, R., (2012) Physiological and cognitive responses when riding an electrically assisted bicycle versus a classical bicycle. *Ergonomics* 55, 773e781.
- [21] Kızıldaş, M, Ç, 2018. Küresel Örnekleri ile Toplu Ulaştırma, Transist 2018, İstanbul Ulaşım Kongresi ve Fuarı, İstanbul, 8-10 Kasım
- [22] Dianov V.N., Gevondian T.A., (2014) Parking system of high reliability innovation technologies. Vol. 2. pp 531-535.
- [23] Granado, F.J., Coady, D. and Gillingham, R., (2012) The Unequal Benefits of Fuel Subsidies: A Review of Evidence for Developing Countries, *World Development* Vol. 40, No. 11.
- [24] Veneri, P., & Burgalassi, D., (2012) Questioning polycentric development and its effects. Issues of definition and measurement for the Italian NUTS-2 regions. *European Planning Studies*, 20(6), 1017–1037. doi:10.1080/09654313.2012.673566
- [25] Kızıldaş M.Ç., ‘Ulaştırma Yatırımları ve Marmaray-1’, <http://www.ulastirmadunyasi.com/index.php/2013/12/ulastirma-yatirimlari-ve-marmaray-1/> (25.05.2014)
- [26] J. Fujie, “An advanced arrangement of the combined propulsion, levitation and guidance system of superconducting Maglev,” *IEEE Trans. Magn.*, vol. 35, no. 5, pp. 4049–4051, Sep. 1999.
- [27] P. Burke, R. Turton, and G Slemon, “The calculation of eddy losses in guideway conductors and structural members of high-speed vehicles,” *IEEE Trans. Magn.*, vol. MAG-10, no. 3, pp. 462–465, Sep. 1974.
- [28] B.-T. Ooi, “Electromechanical dynamics in superconducting levitation systems,” *IEEE Trans. Magn.*, vol. MAG-11, no. 5, pp. 1495–1497, Sep. 1975.
- [29] G. Bohn, “Calculation of frequency responses of electro-magnetic levitation magnets,” *IEEE Trans. Magn.*, vol. MAG-13, no. 5, pp. 1412–1414, Sep. 1977.
- [30] Amendo, C., Hamm, P., Kelly, J., Maerz, L., Brunette, K., Scudato, M., Finley, G. & Greene, L., 2016. Autonomous Vehicles-Considerations for Personal and

Commercial Lines Insurers. Munich Re.

- [31] Dixit, V.V., Chand, S., Nair, D.J., 2016. Autonomous vehicles: disengagements, accidents and reaction times. PLoS One 11, e0168054.
- [32] Faisal, A., Kamruzzaman, M., Yiğitcanlar, T., Currie, G., 2019. Understanding Autonomous Vehicles: A Systematic Literature Review On Capability, Impact, Planning and Policy, 45–72.
- [33] Meulen, R.V.D., Gartner, J.R., 2015. Gartner Says By 2020, a Quarter Billion Connected Vehicles Will Enable New In-Vehicle Services and Automated Driving Capabilities. Gartner, STAMFORD, Conn.
- [34] Schwarting, W., Mora, J., Rus, D., 2018. Annual Review Of Control, Robotics and Autonomous Systems, Vol. 1:187-210.
- [35] Kızıldaş, M.Ç., Altan, M.F., 2017, Evaluation of Intermodal Integration on the Context of Marmaray and Bosphorus Bridges, IRF Regional Congress, Dubai.
- [36] Altan, M.F., Kızıldaş, M.Ç., 2018, Toplu Taşımada Çok Amaçlı Karar Verme ve Metropolitan Bir Alanda Ev-İş Ulaşım Hizmeti Modellemesi, Karaelmas Fen ve Mühendislik Dergisi, ULAKBİM
- [37] Kızıldaş, M, Ç, 2018, Küresel Örnekleri ile Toplu Ulaştırma, Transist 2018, İstanbul Ulaşım Kongresi ve Fuarı, İstanbul.
- [38] Duarte, F., Ratti, C., 2018. The Impact Of Autonomous Vehicles on Cities: A Review. Journal Of Urban Techology. 3-18.
- [39] Harrison, A. J. (1974) Economics of Transport Appraised. London: Croom and Helm. Opinion Research Centre, (1971) "Report on London Commuters" ORC No. 950, London.
- [40] Fagnant, D., Kockelman, K., 2015, Preparing A Nation For Autonomous Vehicles: Opportunities, Barriers and Policy Recommendations, Transportation Research Part A.
- [41] Chana, J., Ishak, R., Shiftan, Y., 2017, User Preferences Regarding Autonomous Vehicles, Transportation Research Part C: Emerging Technologies. Vol. 78, 37,49.
- Litman, T., (2012). Parking Management: Strategies, Evaluation and Planning. Victoria Transport Policy Institute http://www.vtpi.org/park_man.pdf
- Ptuhina I., Spiridonova T., Musorina T. (2015) Performance evaluation of high-rise complex construction depending on building site placement. Applied Mechanics and Materials. Vol. 725-726. Pp. 153-159.
- Altan M.F., Kızıldaş M.Ç., 2019, Yüksek Hızlı Demiryolları, Yolcu ve Yük Taşımacılığı Karşılaştırmaları Bağlamında Küresel Ölçekli Bir Derleme Çalışması, Dicle Üniversitesi Mühendislik Fakültesi Dergisi, ULAKBİM (yayın aşamasında)
- Diaz, M., Soriguera, F., Autonomous Vehicles: Theoretical and Practical Challenges, 2018, Transportation Research Procedia, Vol. 33, 275,282.
- Rueda, D., Nieuwenhuijsen, M., Khreis, H., Frumkin, H. Autonomous Vehicles and

Public Health, 2019, Annual Review Of Public Health.

- Nurumbayeva L.M., Badanin A.N. (2014) Justification for determination of the depth of an active zone based on the ii group of limiting states Applied Mechanics and Materials. Vol. 580-583.Pp. 98-104.
- Dianov V.N., Gevondian T.A. (2014) Parking system of high reliability innovation technologies. Vol. 2. pp 531-535.
- A. Vaibhav, D. Shukla, S. Das, S. Sahana, P. Johri, Security challenges, authentication, application and trust models for vehicular Ad Hoc network-a survey, Int. J. Wirel. Microw. Technol. 3 (2017) 36–48, doi:10.5815/ijwmt.2017.03.04.
- [42] Altan M., Kızıldaş M., Ayözen Y. 2020. High Speed Railways, Current Status and Development Trends at International Scale and Turkey, İstanbul Aydın Üniversitesi, IJEMME Dergisi (yayın aşamasında)
- [43] Xia C., Xia H., Roeck G. 2014. “Dynamic response of a train-bridge system under collision loads and running safety evaluation of high-speedtrains, Computers and Structures, vol. 140, pp.23–38.
- [44] Zhou H., Ni Y., Ko J. 2010. “Constructing input to neural Networks for modeling temperature-caused modal variability: mean temperatures, effective temperatures, and principal components of temperatures,” Engineering Structures, vol. 32, no.6, pp.1747–1759.
- [45] Levin, M.W., Boyles, S.D., 2016 A multiclass cell transmission model for shared human and autonomous vehicle roads. Transp. Res. Part C: Emerging Technol. 62, 103–116.
- [46] Altan M., Kızıldaş M., Ayözen Y. 2020. Comparative Evaluation of the Development, Current Situation and Investment Plans of High Speed Railways on National, Regional and International Basis, İstanbul Aydın Üniversitesi, IJEMME Dergisi (yayın aşamasında)
- [47] M. Zhu, H. Chen, A model predictive speed tracking control approach for autonomous ground vehicles, MSSP 87, Part B (2017) 138–152.
- [48] Amendo C., Hamm P., Kelly J., Maerz L., Brunette K., Scudato M., Finley G., Greene L. 2016. Autonomous Vehicles-Considerations for Personal and Commercial Lines Insurers. Munich Re.
- [49] Kızıldaş M. 2015. Traffic Safety and Railway Applications, Transportation World Newspaper.
- [50] Nijkamp P. 2009. Regional development as self-organized converging growth, In: Kochendörfer-Lucius, G., Pleskovic, B. (Eds.), Spatial Disparities and Development. The World Bank, Washington DC, pp. 265–281.
- [51] Geurs K., vanWee B. 2004. Accessibility evaluation of land-useand transport strategies review and research directions, Journal of Transport Geography 12, 127– 140.

Chapter 7

CLAY MINERALS IN NANOTECHNOLOGY: IMPORTANCE AND APPLICATIONS IN ENGINEERING

Dilek ŐENOL ARSLAN¹

¹ Dr. Dilek ŐENOL ARSLAN

Abdullah Gul University, Nanotechnology Engineering Department

ORCID: 0000-0001-9639-2843

1. Introduction

Clay is a material with a layered structure that is naturally formed from fine-grained (approximately < 0.002 mm.) minerals containing aluminum (Al_2O_3) and silica (SiO_2), which are very common in nature (Bergaya & Lagaly, 2006; Borden, Ping, McCarthy, & Naidu, 2010). The SiO_2 and Al_2O_3 crystal structures (tetragons and octahedrons) combine in various ways to build layers and thus form clay minerals with different properties (Brown, 1982; Yahaya, Jikan, Badarulzaman, & Adamu, 2017).

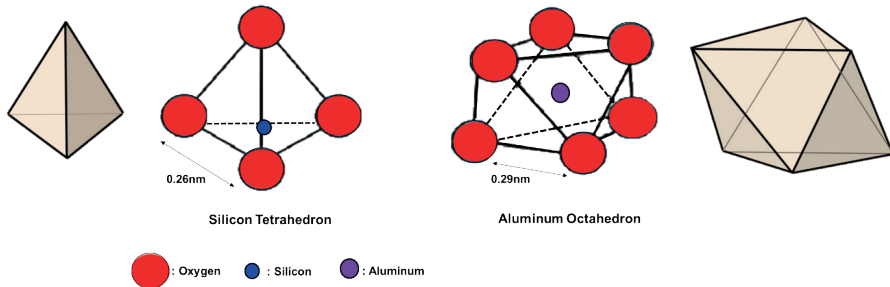


Figure 1. Basic units of clay minerals.

As can be seen from Figure 1, the Si-Tetrahedron unit comprises a central silicon Ion (Si^{4+}) surrounded by four Oxygen atoms positioned at the corners of a regular tetrahedron. When these units come together, Si-Tetrahedral layer is formed. The Al-Octahedron unit is formed in such a way that +3 valence Aluminum atom is located in the center of 6 Oxygen atoms. These units come together to form the Al-Octahedral layer (Alemayehu & Teshome, 2021; F. Uddin, 2018).

All clays consist of layered silica tetrahedral (T) and alumina octahedral (O) layers. The ratio between T and O layers changes for each clay. Common cations coordinating with octahedral sheets are Al, Mg, Fe^{3+} , and Fe^{2+} , with occasional substitution in considerable amounts by Li, V, Cr, Mn, Ni, Cu, and Zn. (Kumari & Mohan, 2021).

An important characteristic of clay minerals is how they bond to each other. The tetrahedra and octahedra are strongly bonded to each other within the layers, but the layers are only weakly bonded to each other. The layers that make up a clay mineral grain have a tendency to slide in relation to each other and, as a result, clay mineral masses tend to be soft and plastic and not very strong (Weaver & Pollard, 2011).

The major grouping of clay minerals is principally based on the configuration of their layers and their chemical affinities (de Farias, Spaltonzi, da Silva, da Silva, & Vieira, 2022). The main classes of clay minerals are summarized in Figure 2, together with examples of their species.

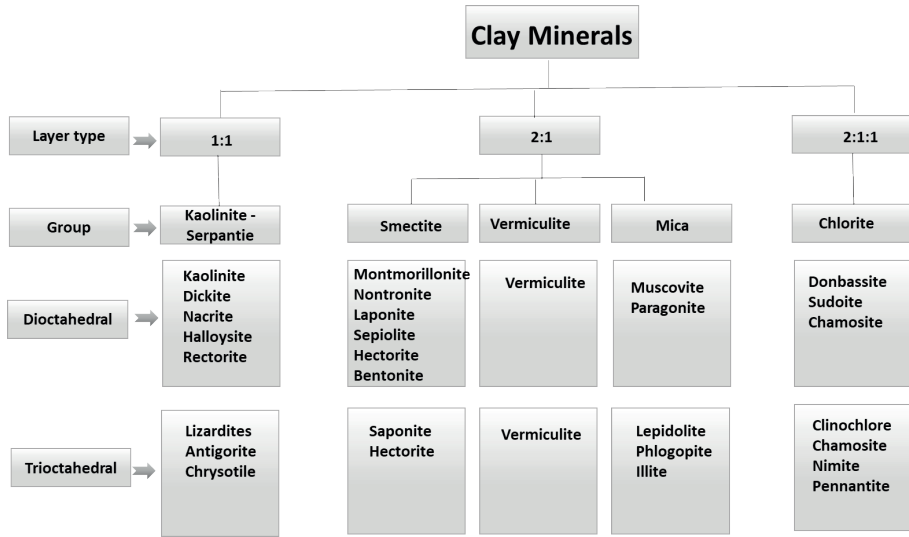


Figure 2. The main classes of clay minerals with examples of their species.

In nature, clay contains mostly limestone, silica, mica, iron oxide minerals (Carroll & Hathaway, 1953; Torrent & Cabedo, 1986). Clay minerals have usually found in white, reddish, green, yellowish colors and various shades of brown (Carroll, 1958; Košarová, Hradil, Němec, Bezdička, & Kanický, 2013). The color of the clay gives an idea about the substances contained in it. For example, if limonite is present in the clay, the color is brown, if iron peroxide is present, the color is red, if manganese dioxide is present, the color is black and if organic substances are present, the color is violet (He, Yang, Hu, Zhang, & Li, 2023)

Clay minerals are typically characterized by several specific properties, including;

1. The thickness of a 1:1 (TO) layer is approximately 0.7 nm, and a 2:1 (TOT) layer is approximately 1 nm.
2. There is anisotropy evident in the layers or particles.
3. The presence of different surface types is evident, including external basal (planar) and edge surfaces, as well as internal (interlayer) surfaces.
4. The versatility of modifying the exterior and frequently the interior surfaces through techniques such as adsorption, grafting, and ion Exchange.
5. Plasticity properties
6. Presence of hardening during drying or firing. This condition is common to most (but not all) clay minerals.

(Bergaya & Lagaly, 2006).

2. The Significance of Clay Minerals in Nanotechnology

Clay minerals have attracted great interest in nanotechnology due to their unique properties and potential applications.

The main important properties of clay minerals in nanotechnology are listed below:

The largeness of the surface area: Clay minerals have a large surface area due to their layered structure. Thanks to their unique properties, they provide a large surface area-to-volume ratio that allows for greater interaction with other nanoparticles or molecules (Kumari & Mohan, 2021). Thus, clay minerals can act as excellent nanocarriers or nanoscaffolds and enhance the performance of various nanomaterials in different disciplines (Singh, Dubey, Pradhan, & Singh, 2013).

Adsorption and absorption characteristics: The adsorption properties of clay minerals are often associated with their structural features. The first is the large specific surface area and the permanent negative layer charge, which provide large cation exchange capacities; the second is the presence of reactive hydroxyl groups on their edge surfaces, which can specifically bind a number of chemical species (Orucoglu et al., 2022; M. K. Uddin, 2017). This property is used in a number of applications, including water treatment, cosmetics, drug delivery systems, mineral processing, and environmental cleanup (Budash, Plavan, Tarasenko, Ishchenko, & Koliada, 2023; Nguyen et al., 2023; H. Zhang et al., 2023). The reason for this preference is that clay minerals are good adsorbents for pollutants and impurities due to their high surface area and strong electrostatic interactions. In addition to their many advantages, its low prices and availability allow it to be preferred in many different areas (B. Ghosh & Chakraborty, 2023).

Compatibility assessment with other nanomaterials: Clay minerals can be modified and functionalized to increase their compatibility with many other nanomaterials, such as polymers, metals, and organic materials (Barakan & Aghazadeh, 2021). Thanks to the synergistic effect of clay minerals, when added to nanocomposites, they enable the different materials to develop new functional materials with improved performance (Ordonez, Valencia, Chang, & Wanielista, 2020).

Controlled release systems: Clay minerals are widely used due to their high adsorption capacity. This has generated interest in their biological application to stabilize drugs and pharmaceutical products. They are capable of regulating the release of encapsulated compounds, including drugs, herbicides, or pesticides (Silva et al., 2019). Their laminated structure allows active chemicals to permeate between the layers, enabling controlled release. This makes clay nanoparticles ideal for use in drug delivery systems, where

controlled release of therapeutic agents is necessary (Edussuriya, Keerthanan, Rajapaksha, & Vithanage, 2023; Rezanejad Gatabi, Heshmati, Mirhoseini, & Dabbaghianamiri, 2023; Rodríguez-Mejías et al., 2023).

Mechanical reinforcement: Nano-sized clay minerals are used as fillers and reinforcements in composites to enhance the thermal and mechanical stability of nanomaterials (Tan & Thomas, 2017). Moreover, Nano-clay doped plastics have nanokil uygulayan mühendislik alanlarından bazılarıhigher tensile strength, improved barrier and abrasion properties, reduced flammability, low thermal expansion, superior surface qualities (Fu & Yang, 2017; Kumar, Singh, & Thakur, 2020; Rangavar, Taghiyari, Oromiehie, Gholipour, & Safarpour, 2017).

Catalytic properties: Certain clay minerals, including montmorillonite and kaolinite, exhibit natural catalytic properties and can be used as catalysts or catalyst supports for various chemical reactions such as hydrogenation, oxidation and acid-base reactions (She, Qiu, Li, Liu, & Zhou, 2023; X. Zhang et al., 2023). The adaptable surface properties and abundance of active sites of clay minerals suggest their potential as catalysts for environmentally friendly and sustainable chemical processes (Fidchenko, Alekhina, Beznosyuk, Varnavskaya, & Mishchenko, 2023).

Biocompatibility: Clay minerals, particularly natural ones, are widely viewed as biocompatible and non-toxic, therefore they are suitable for varied biomedical applications. These minerals can be employed in several areas such as drug delivery systems (Saadat, Rawtani, & Parikh, 2022), tissue engineering (García-Villén et al., 2021), wound healing (Ghadiri, Chrzanowski, & Rohanizadeh, 2014), and biosensors (An, Zhou, Zhuang, Tong, & Yu, 2015). Modification of the clay mineral surface facilitates interaction with biological molecules, leading to efficient and targeted delivery of therapeutic agents.

Porosity: Clay minerals have a nanoporous structure with interlayer spaces and channels that allow molecules to be trapped within their structure (Aringhieri, 2004). This feature makes them appropriate for various applications such as gas separation (Ismail et al., 2019), water filtration (Mota, Silva, Queiroz, Laborde, & Rodrigues, 2011), and controlled drug release (de Sousa Rodrigues et al., 2013).

Ion exchange capacity: Clay minerals have a high ion exchange capacity, enabling them to exchange ions with others in their surrounding medium (Patzkó & Dékány, 1993). This makes them valuable for environmental remediation (Otunola & Ololade, 2020), wastewater treatment (Chang, Li, Jiang, & Sarkar, 2019), and soil conditioning purposes (Ye, Wang, Yang, Sheng, & Xiao, 2017).

Self-assembly: Clay minerals can self-assemble into ordered structures thanks to their layered structure and electrostatic interactions. This property

has allowed the development of techniques for producing nanoscale devices, sensors and controlled release systems (Dadwal, Prasher, Sengupta, & Kumar, 2023; Feng et al., 2023).

Optical Properties: Certain types of clay minerals demonstrate fascinating optical properties, including luminescence and photoluminescence, which could prove advantageous in optoelectronics, imaging, and sensor applications (Ambid, Teysse, Mary, Laurent, & Montanari, 2006; D. Ghosh et al., 2021; Tetsuka, Ebina, & Mizukami, 2008).

Swelling capacity: The ability of clay minerals to adsorb water causes swelling or expansion of interlayer spaces. This expansion is due to hydration energy forces. Swollen clays exhibit significant volume changes with changes in their water content. The swelling capacity of clay minerals depends on their layer charge density, the type of interlayer cations (monovalent or divalent), the concentration of ions in solution, the amount of water in the interlayer space, and the composition of the clay mineral (Kumari & Mohan, 2021).

2. Engineering applications of Nano-clays

Nano-clay is a form of clay found within the category of nanomaterials, and is regarded as a sub-sector of nanotechnology. It performs a crucial function across multiple domains within the engineering sciences presented in Figure 3.



Figure 3. List of some engineering fields using Nano-clay.

Nano-clays have very important application areas in different sectors. Some of the important ones among these are mentioned below:

The application of nano-clay in food packaging effectively inhibits the growth of microorganisms, consequently enhancing food safety while also mitigating the risk of contamination on food surfaces (Maisanaba, Ortuño,

Jordá-Beneyto, Aucejo, & Jos, 2017).

In water treatment systems, the use of nano-clay serves as an effective neutralizer of hazardous bacteria and viruses, resulting in safer water usage (Lazaratou, Vayenas, & Papoulis, 2020).

The use of nano-clay in textile products prevents the growth of microorganisms, resulting in the production of hygienic and odour-free textiles (de Oliveira, Batistella, Lourenço, Ulson, & de Souza, 2021).

Also, nano-clay can be utilized to provide antibacterial properties in surface coatings. This strategy prevents the transmission of microorganisms on surfaces in hospitals, public transportation, and other public places (Zhuang & Yu, 2002).

Nano-clay can be used to prevent the growth of microorganisms on the surface of biomaterials. It can be used in hospital equipment, implants and other medical devices. Nano-clay reinforced biomaterials offer a promising new avenue in advanced healthcare materials, with potential to revolutionize the treatment of musculoskeletal defects. (Yu, Lv, Wu, & Chen, 2023). Natural tissues display various significant chemical, mechanical, biological, and physical properties that manufactured biomaterials must imitate to attain maximum tissue integration and regeneration. The ease of chemical functionalization of nano-clays significantly strengthens mechanical performance and can provide bioactive properties (Nazari, Naeimi, Rafienia, & Monajjemi, 2023). Therefore, nano-clays have the potential to become a key component of future orthopedic biomaterials.

Concerning agriculture and its products, nano-clay can control diseases and pests while enhancing the nutrient uptake and yields of plants (Manjaiah et al., 2019).

Additionally, nano-clay can be applied in energy storage (Lan et al., 2021). It has been found effective in increasing energy storage device efficiency. Specifically, it can serve as a cathode material in lithium-ion batteries (Balkanloo, Marjani, Zانبلي, & Mahmoudian, 2022).

Nano-clay is a technology used in many different application areas. Here are some of them presented in Figure 4.

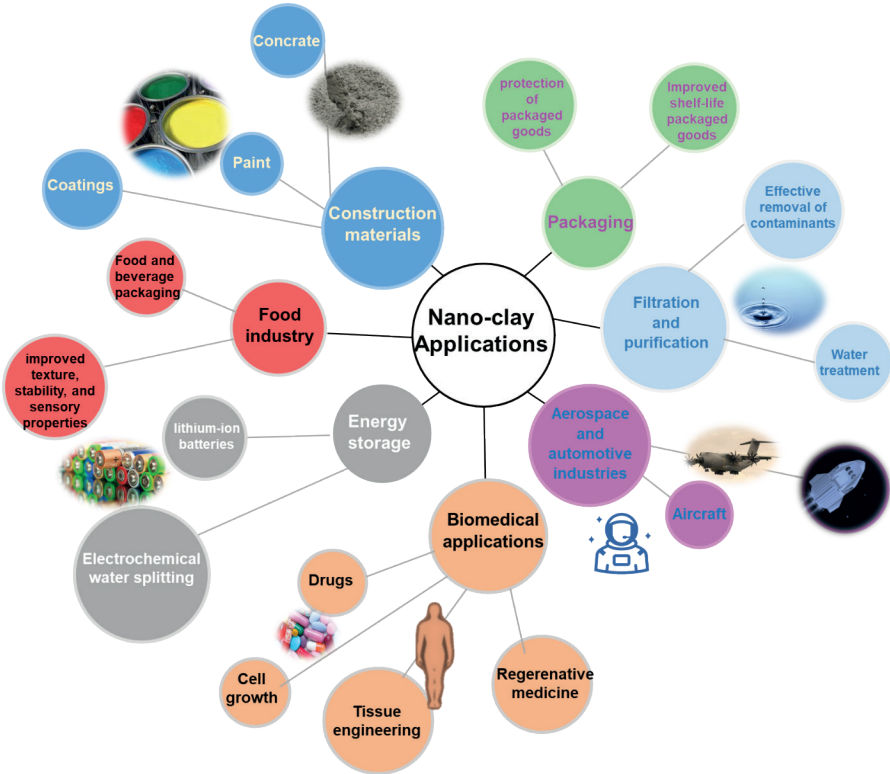


Figure 4. Schematic representation of Nano-clay applications.

3. Conclusion

In conclusion, the significance of clay minerals in nanotechnology rests upon their distinctive properties and adaptable applications in engineering. Their layer structure, coupled with the ease of modification, allows the development of nanostructured materials with enhanced performance. Clay minerals possess extensive applications in a range of engineering fields, and as such have the potential to be a game-changer for the engineering industry, contributing to the development of nanotechnology.

REFERENCES

- Alemayehu, B., & Teshome, H. (2021). Soil colloids, types and their properties: A review. *Open Journal of Bioinformatics and Biostatistics*, 5(1), 008-013.
- Ambid, M., Teyssedre, G., Mary, D., Laurent, C., & Montanari, G. C. (2006). Optical properties and luminescence behaviour of PP/clay nanocomposites. *IEEE Transactions on Fundamentals and Materials*, 126(11), 1097-1104.
- An, N., Zhou, C. H., Zhuang, X. Y., Tong, D. S., & Yu, W. H. (2015). Immobilization of enzymes on clay minerals for biocatalysts and biosensors. *Applied Clay Science*, 114, 283-296.
- Aringhieri, R. (2004). Nanoporosity characteristics of some natural clay minerals and soils. *Clays and clay minerals*, 52(6), 700-704.
- Balkanloo, P. G., Marjani, A. P., Zambili, F., & Mahmoudian, M. (2022). Clay mineral/polymer composite: characteristics, synthesis, and application in Li-ion batteries: A review. *Applied Clay Science*, 228, 106632.
- Barakan, S., & Aghazadeh, V. (2021). The advantages of clay mineral modification methods for enhancing adsorption efficiency in wastewater treatment: a review. *Environmental Science and Pollution Research*, 28, 2572-2599.
- Bergaya, F., & Lagaly, G. (2006). General introduction: clays, clay minerals, and clay science. *Developments in clay science*, 1, 1-18.
- Borden, P. W., Ping, C.-L., McCarthy, P. J., & Naidu, S. (2010). Clay mineralogy in arctic tundra Gelisols, northern Alaska. *Soil Science Society of America Journal*, 74(2), 580-592.
- Brown, G. (1982). *Crystal structures of clay minerals and their X-ray identification* (Vol. 5): The mineralogical society of Great Britain and Ireland.
- Budash, Y., Plavan, V., Tarasenko, N., Ishchenko, O., & Koliada, M. (2023). Effect of Acid Modification on Porous Structure and Adsorption Properties of Different Type Ukrainian Clays for Water Purification Technologies. *Journal of Ecological Engineering*, 24(5).
- Carroll, D. (1958). Role of clay minerals in the transportation of iron. *Geochimica et Cosmochimica Acta*, 14(1-2), 1-28.
- Carroll, D., & Hathaway, J. C. (1953). Clay minerals in a limestone soil profile. *Clays and clay minerals*, 2, 171-182.
- Chang, P.-H., Li, Z., Jiang, W.-T., & Sarkar, B. (2019). Clay minerals for pharmaceutical wastewater treatment. *Modified Clay and Zeolite Nanocomposite Materials*, 167-196.
- Dadwal, A., Prasher, M., Sengupta, P., & Kumar, N. (2023). Quantifying nematic order in evaporation-driven self-assembly of Halloysite nanotubes: Nematic islands and critical aspect ratio. *arXiv preprint arXiv:2309.11323*.

- de Farias, M. B., Spaolonzi, M. P., da Silva, T. L., da Silva, M. G. C., & Vieira, M. G. A. (2022). Natural and synthetic clay-based materials applied for the removal of emerging pollutants from aqueous medium *Advanced materials for sustainable environmental remediation* (pp. 359-392): Elsevier.
- de Oliveira, C. R. S., Batistella, M. A., Lourenço, L. A., Ulson, S. M. d. A. G., & de Souza, A. A. U. (2021). Cotton fabric finishing based on phosphate/clay mineral by direct-coating technique and its influence on the thermal stability of the fibers. *Progress in Organic Coatings*, 150, 105949.
- de Sousa Rodrigues, L. A., Figueiras, A., Veiga, F., de Freitas, R. M., Nunes, L. C. C., da Silva Filho, E. C., & da Silva Leite, C. M. (2013). The systems containing clays and clay minerals from modified drug release: A review. *Colloids and Surfaces B: Biointerfaces*, 103, 642-651.
- Edussuriya, R., Keerthanan, S., Rajapaksha, A. U., & Vithanage, M. (2023). Slow Release-Formulations for Weed and Pest Control by Clay Composites *Clay Composites: Environmental Applications* (pp. 511-527): Springer.
- Feng, Y., He, Y., Lin, X., Xie, M., Liu, M., & Lvov, Y. (2023). Assembly of Clay Nanotubes on Cotton Fibers Mediated by Biopolymer for Robust and High-Performance Hemostatic Dressing. *Advanced Healthcare Materials*, 12(1), 2202265.
- Fidchenko, M., Alekhina, M., Beznosyuk, A., Varnavskaya, A., & Mishchenko, E. (2023). Development and Study of a Carbon–Mineral Catalyst Based on Natural Clay and Tire Crumb for the Oxidative Decomposition of Nonionic Surfactants with Hydrogen Peroxide in Wastewater. *Kinetics and Catalysis*, 64(3), 260-269.
- Fu, L., & Yang, H. (2017). Structure and electronic properties of transition metal doped kaolinite nanoclay. *Nanoscale Research Letters*, 12, 1-7.
- García-Villén, F., Ruiz-Alonso, S., Lafuente-Merchan, M., Gallego, I., Sainz-Ramos, M., Saenz-del-Burgo, L., & Pedraz, J. L. (2021). Clay minerals as bioink ingredients for 3D printing and 3D bioprinting: Application in tissue engineering and regenerative medicine. *Pharmaceutics*, 13(11), 1806.
- Ghadiri, M., Chrzanowski, W., & Rohanizadeh, R. (2014). Antibiotic eluting clay mineral (Laponite®) for wound healing application: an in vitro study. *Journal of Materials Science: Materials in Medicine*, 25, 2513-2526.
- Ghosh, B., & Chakraborty, D. (2023). The Present and the Future: Advantages, Drawbacks, and Future Prospects of Clays for Protection of Human Health. *Clay Minerals: Their Antimicrobial and Antitoxic Applications*, 123-145.
- Ghosh, D., Ganayee, M. A., Som, A., Srikrishnarka, P., Murali, N., Bose, S., . . . Pradeep, T. (2021). Hierarchical assembly of atomically precise metal clusters as a luminescent strain sensor. *ACS applied materials & interfaces*, 13(5), 6496-6504.
- He, W., Yang, Z., Hu, J., Zhang, K., & Li, H. (2023). Color Origin of Red Beds within the Danxia Basin, Southern China. *Minerals*, 13(8), 1054.
- Ismail, N., Ismail, A., Mustafa, A., Zulhairun, A., Aziz, F., Bolong, N., & Razali, A.

- (2019). Polymer clay nanocomposites for gas separation: A review. *Environ. Contam. Rev*, 2, 01-05.
- Košařová, V., Hradil, D., Němec, I., Bezdička, P., & Kanický, V. (2013). Microanalysis of clay-based pigments in painted artworks by the means of Raman spectroscopy. *Journal of Raman Spectroscopy*, 44(11), 1570-1577.
- Kumar, K., Singh, K., & Thakur, R. (2020). *Analysis on milling of nanoclay-doped epoxy/carbon laminates using taguchi approach*. Paper presented at the Proceedings of International Conference in Mechanical and Energy Technology: ICMET 2019, India.
- Kumari, N., & Mohan, C. (2021). Basics of clay minerals and their characteristic properties. *Clay Clay Miner*, 24, 1-29.
- Lan, Y., Liu, Y., Li, J., Chen, D., He, G., & Parkin, I. P. (2021). Natural clay-based materials for energy storage and conversion applications. *Advanced Science*, 8(11), 2004036.
- Lazaratou, C., Vayenas, D., & Papoulis, D. (2020). The role of clays, clay minerals and clay-based materials for nitrate removal from water systems: A review. *Applied Clay Science*, 185, 105377.
- Maisanaba, S., Ortuño, N., Jordá-Beneyto, M., Aucejo, S., & Jos, Á. (2017). Development, characterization and cytotoxicity of novel silane-modified clay minerals and nanocomposites intended for food packaging. *Applied Clay Science*, 138, 40-47.
- Manjaiah, K. M., Mukhopadhyay, R., Paul, R., Datta, S. C., Kumararaja, P., & Sarkar, B. (2019). Clay minerals and zeolites for environmentally sustainable agriculture *Modified Clay and Zeolite Nanocomposite Materials* (pp. 309-329): Elsevier.
- Mota, M., Silva, J., Queiroz, M., Laborde, H., & Rodrigues, M. (2011). Organophilic clay for oil/water separation process by finite bath tests. *Brazilian Journal of Petroleum and Gas*, 5(2).
- Nazari, S., Naeimi, M., Rafienia, M., & Monajjemi, M. (2023). Fabrication and Characterization of 3D Nanostructured Polycaprolactone-Gelatin/Nanohydroxyapatite-Nanoclay Scaffolds for Bone Tissue Regeneration. *Journal of Polymers and the Environment*, 1-17.
- Nguyen, D. T., Nguyen, M. T., Le, T. Q., Duong, L. H., Nguyen, A. Q., Pham, A. T., . . . Nguyen, M. N. (2023). Sorption of cosmetic and personal care polymer ingredients to iron oxides, clay minerals and soil clays: An environmental perspective. *Science of The Total Environment*, 861, 160606.
- Ordonez, D., Valencia, A., Chang, N.-B., & Wanielista, M. P. (2020). Synergistic effects of aluminum/iron oxides and clay minerals on nutrient removal and recovery in water filtration media. *Journal of Cleaner Production*, 275, 122728.
- Orucoglu, E., Grangeon, S., Gloter, A., Robinet, J.-C., Madé, B., & Tournassat, C. (2022). Competitive adsorption processes at clay mineral surfaces: a coupled experimental and modeling approach. *ACS Earth and Space Chemistry*, 6(1), 144-159.

- Otunola, B. O., & Ololade, O. O. (2020). A review on the application of clay minerals as heavy metal adsorbents for remediation purposes. *Environmental Technology & Innovation*, 18, 100692.
- Patzkó, Á., & Dékány, I. (1993). Ion exchange and molecular adsorption of a cationic surfactant on clay minerals. *Colloids and Surfaces A: Physicochemical and Engineering Aspects*, 71(3), 299-307.
- Rangavar, H., Taghiyari, H. R., Oromiehie, A., Gholipour, T., & Safarpour, A. (2017). Effects of nanoclay on physical and mechanical properties of wood-plastic composites. *Wood Material Science & Engineering*, 12(4), 211-219.
- Rezanejad Gatabi, Z., Heshmati, N., Mirhoseini, M., & Dabbaghianamiri, M. (2023). The Application of Clay-Based Nanocomposite Hydrogels in Wound Healing. *Arabian Journal for Science and Engineering*, 48(7), 8481-8494.
- Rodríguez-Mejías, F. J., Scavo, A., Chinchilla, N., Molinillo, J. M., Schwaiger, S., Ma-uromicale, G., & Macías, F. A. (2023). Perspectives and Advances in Organic Formulations for Agriculture: Encapsulation of Herbicides for Weed Control. *Agronomy*, 13(7), 1898.
- Saadat, S., Rawtani, D., & Parikh, G. (2022). Clay minerals-based drug delivery systems for anti-tuberculosis drugs. *Journal of Drug Delivery Science and Technology*, 103755.
- Sagadevan, S., Schirhagl, R., Rahman, M. Z., Ismail, M. F. B., Lett, J. A., Fatimah, I., . . . Oh, W.-C. (2023). Recent advancements in polymer matrix nanocomposites for bone tissue engineering applications. *Journal of Drug Delivery Science and Technology*, 104313.
- She, Q., Qiu, M., Li, K., Liu, J., & Zhou, C. (2023). Acidic and basic sites on the surface of sodium montmorillonite active for catalytic transesterification of glycerol to glycerol carbonate. *Applied Clay Science*, 238, 106916.
- Silva, F. C., Lima, L. C., Viseras, C., Osajima, J. A., da Silva Júnior, J. M., Oliveira, R. L., . . . Silva-Filho, E. C. (2019). Understanding urea encapsulation in different clay minerals as a possible system for ruminant nutrition. *Molecules*, 24(19), 3525.
- Singh, D., Dubey, P., Pradhan, M., & Singh, M. R. (2013). Ceramic nanocarriers: versatile nanosystem for protein and peptide delivery. *Expert opinion on drug delivery*, 10(2), 241-259.
- Tan, B., & Thomas, N. L. (2017). Tortuosity model to predict the combined effects of crystallinity and nano-sized clay mineral on the water vapour barrier properties of polylactic acid. *Applied Clay Science*, 141, 46-54.
- Tetsuka, H., Ebina, T., & Mizukami, F. (2008). Highly luminescent flexible quantum dot–clay films. *Advanced Materials*, 20(16), 3039-3043.
- Torrent, J., & Cabedo, A. (1986). Sources of iron oxides in reddish brown soil profiles from calcarenites in Southern Spain. *Geoderma*, 37(1), 57-66.
- Uddin, F. (2018). *Montmorillonite: An introduction to properties and utilization* (Vol. 817): IntechOpen London, UK.

- Uddin, M. K. (2017). A review on the adsorption of heavy metals by clay minerals, with special focus on the past decade. *Chemical Engineering Journal*, 308, 438-462.
- Weaver, C. E., & Pollard, L. D. (2011). *The chemistry of clay minerals*: Elsevier.
- Yahaya, S., Jikan, S. S., Badarulzaman, N. A., & Adamu, A. D. (2017). Chemical composition and particle size analysis of kaolin. *Traektoriâ Nauki= Path of Science*, 3(10), 1001-1004.
- Ye, X., Wang, S., Yang, J., Sheng, D., & Xiao, C. (2017). Soil conditioning for EPB shield tunneling in argillaceous siltstone with high content of clay minerals: case study. *International Journal of Geomechanics*, 17(4), 05016002.
- Yu, Y., Lv, B., Wu, J., & Chen, W. (2023). Mussel-based biomimetic strategies in musculoskeletal disorder treatment: From synthesis principles to diverse applications. *International Journal of Nanomedicine*, 455-472.
- Zhang, H., Larson, S., Ballard, J., Nie, J., Zhang, Q., Kazery, J. A., . . . Olafuyi, O. M. (2023). Interaction of exopolysaccharide with clay minerals and their effects on U (VI) adsorption. *Journal of Soils and Sediments*, 1-15.
- Zhang, X., Wang, J., Wang, L., Li, Z., Hu, W., Dai, Y., . . . Zhang, W. (2023). Catalytic capacity evolution of montmorillonite in in-situ combustion of heavy oil. *Fuel*, 333, 126621.
- Zhuang, J., & Yu, G.-R. (2002). Effects of surface coatings on electrochemical properties and contaminant sorption of clay minerals. *Chemosphere*, 49(6), 619-628.



Chapter 3

CURRENT APPROACHES ON THE USE OF BIODIESEL AS AN ALTERNATIVE FUEL IN INTERNAL COMBUSTION ENGINES

*Hicri YAVUZ*¹

¹ Hicri YAVUZ, Assist. Prof. Dr. Afyon Kocatepe University, Vocational School of Afyon, Department of Engine Vehicles and Transportation Technology, ORCID ID: 0000-0001-8427-5164

INTRODUCTION

Studies on the search for alternative fuels in internal combustion engines date back to ancient times. One of the most important reasons for the search for alternative fuels is due to supply crises related to petroleum-based fuels, countries' desire to reduce foreign dependency, efforts to reduce emission rates, or limited oil reserves. Today, vehicles using internal combustion engines have high thermal efficiency, high torque values, etc. Diesel engines are preferred for reasons such as. These engines also have disadvantages due to their emission values. Today, the fact that electric vehicles are trying to replace internal combustion engines in passenger vehicles also creates a disadvantage. Although electric vehicles have become more common in vehicles instead of internal combustion engines, there are various concerns about electric vehicles. While the most important of these concerns is the range distance, other factors can be summarized as stranded as a result of the battery running out while the vehicle is traveling, how long the battery life will be, how these batteries will be disposed of when the battery life is over, waiting time at charging stations and creating the necessary energy lines for charging stations. In addition to these questions, using electric motors instead of internal combustion engines in a short time is impossible because turning millions of vehicles into scrap may cause undesirable consequences for the country's economy.

Although the use of diesel engines has decreased in various European countries, diesel fuels must continue to be used to meet the high torque requirement in machines and vehicles such as generators, tanks, and ships, which are used extensively in areas where there are no power lines or in cases of power outages. It is essential that biodiesel fuel is used in high torque internal combustion engines without any modifications to the engine, and also contributes to the reduction of exhaust emissions (Erdoğan, Balki, Aydın, & Sayın, 2020; Seraç, Aydın, & Sayın, 2020). In our age, energy is essential for the continuation of life. Due to the increase in population, the need and demand for energy is increasing daily. The inadequacy of existing energy resources to meet the demand has led to the emergence of alternative energy resources. In this regard, various incentives were created in the first place for the efficient use of energy and then for the search for alternative energy sources. Biomass and waste are used as energy sources in various fields. Research is being conducted on using biodiesel as an alternative fuel in internal combustion engines running on diesel fuel (Söyler, Balki, & Sayın, 2023). Traditionally, fossil fuels have been used mainly in the transportation and energy sectors. Biodiesel fuels, which can be an alternative to fossil fuels due to their reserve life, are on the agenda. With the increase in population and the resulting industrialization, alternative energy sources will have a significant potential. The key benefits of biodiesel, an alternative fuel, include its ability to be

utilized in internal combustion engines without requiring much modification and being renewable, sustainable, ecologically benign, and biodegradable. Biodiesel also provides advantages in reducing exhaust emissions compared to diesel fuel (Haşimo lu et. al., 2008; Tosun, Özcanli, & Akar, 2022). The widespread use of electric vehicles will also lead to increased electricity consumption. Indirectly, this effect increases fossil fuel consumption rates and environmental pollution. For these reasons, researchers are focusing on alternative fuels to petroleum (Uysal, Uslu, & Aydin, 2022).

Diesel internal combustion engines are used not only in light vehicles but also in cargo vehicles, agricultural vehicles, generators, etc., fixed devices such as minimum tanks etc. It is widely preferred and used in vehicles and maritime transportation. For all these reasons, the search for alternative fuels instead of diesel fuel in internal combustion engines has continued until today. An essential issue in the search for alternative fuels is that the desired power, torque, and specific fuel consumption values from diesel engines must be satisfactory in addition to having low emission values. In studies conducted by scientists on alternative fuels, fuels defined as biodiesel obtained from many different vegetable and animal oils by esterification or transesterification method, which is another name, have attracted much attention. This new fuel type can be used in internal combustion engines by mixing it with 100% or different proportions of diesel fuel without requiring additional by-products such as systems, units, or parts. Governments may provide incentives for alternative energy sources instead of petroleum-based fuels or obligations to use them in a particular proportion of diesel fuel.

Within the scope of this study, the use of some biodiesel fuels, which are alternative fuel options used in internal combustion engines running on diesel fuel in recent years, and their performance and emission values are discussed.

BIODIESEL FUEL PRODUCTION METHODS

Using biodiesel fuels directly in internal combustion engines may cause various problems in the fuel system and storage. For this reason, instead of using various oils directly in internal combustion engines, chemical processes are carried out in these oils, and the fuels are made ready for use.

The fuel known as biodiesel is created by reacting goods with alcohol in the presence of a catalyst, such as soybean oil, animal fat, or waste oil. This fuel obtained in internal combustion engines can be used 100%, or it can be used by mixing it with diesel fuel in different proportions to solve the solidification problem in cold operating conditions. As a production method, the methods listed in the diagram below can be used in biodiesel production (Sayın, Erdoğan, & Baki, 2019).

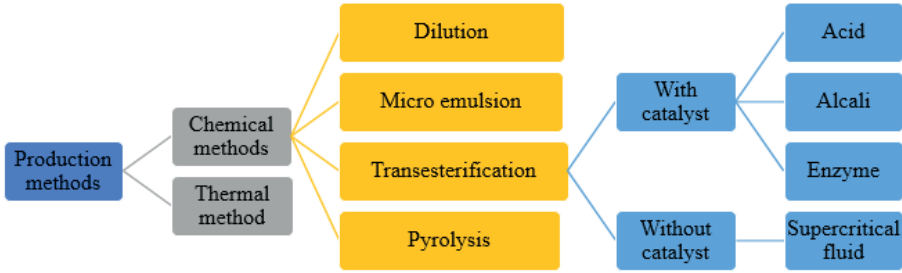


Figure 1. Methods of obtaining biodiesel from oils (Sayın et. al., 2019)

DETERMINATION OF BIODIESEL FUEL PROPERTIES

Chemical and physical properties of biodiesel fuels, combustion parameters, etc. Scientists seek various features to determine it. These features are required not only to comment on the combustion process of fuel in internal combustion engines but also in processes such as mathematical combustion modeling. Table 1 (Can et. al., 2016) shows the properties of fuels, which are generally given as a result of experiments and tests carried out in studies.

Table 1. Physical and chemical properties determined for biodiesel fuels

Property	Unit
Density @ 15 °C	g/cm ³
Lower heating value	MJ/kg
Cetane number	-
Kinematic viscosity @ 40	mm ² /s
Flash point	°C
Cold filter plugging point	°C
Distillation	°C
Initial boiling point (IBP)	-
Final boiling point (FBP)	-
Sulfur content	ppm

PERFORMANCE EVALUATIONS of INTERNAL COMBUSTION ENGINES USING BIODIESEL

Internal combustion engines’ most advantageous operating states are maximum power, maximum torque, and minimum specific fuel consumption. The power produced by the engine is consumed in unstable situations such as vehicle speed, road condition, load, and acceleration. Operating conditions may only sometimes be stable due to variable loads on the engine. Engine torque is increased by sending more fuel to the engine. For all these reasons, the analysis of operation in internal combustion engines should include a few operating situations and different operating situations. The power and

economy of internal combustion engines during operation are evaluated with engine characteristic performance curves. According to the engine speed, the torque, power, and specific fuel consumption values in these characteristics demonstrate the changes in diesel internal combustion engines when the fuel pump lever is in a particular position, and the temperatures of the lubricating oil and cooling water are stable (Çetinkaya, 2015).

Using sustainable and environmentally friendly fuels in internal combustion engines instead of petroleum-based fuels attracts much attention today. These fuels, called biodiesel, have emerged as a biodegradable fuel that is non-toxic and reduces harmful emissions when used in diesel internal combustion engines (Kumar et. al., 2023). For these reasons, in addition to evaluating engine performance, it is essential to determine emission rates in internal combustion engines. In studies on biodiesel, carbon monoxide, carbon dioxide, azotoxide, and soot emission values are generally determined (Karabektaş, Ergen, Hasimoglu, & Murcak, 2016; Uyumaz et. al., 2020). Figure 2 provides a schematic illustration of the biodiesel fuel testing procedures for internal combustion engines.

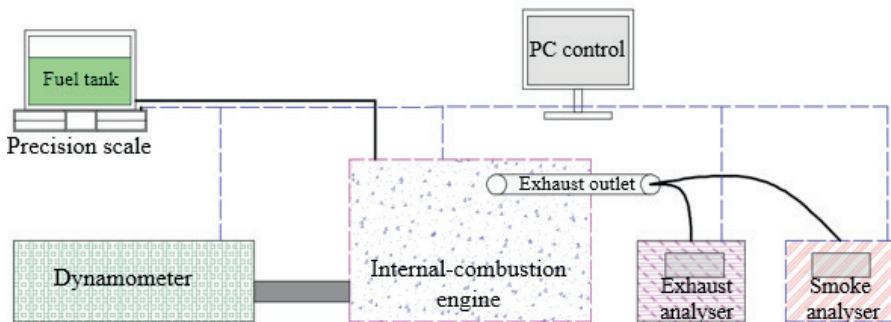


Figure 2. Schematic picture of biodiesel fuel internal combustion engine testing equipment

CURRENT STUDIES ON BIODIESEL USE

Studies on green, sustainable, bio-based alternative fuels in internal combustion engines have been conducted intensively for decades. Today, studies are being carried out to improve fuel properties by using different production methods, working in different atmospheric conditions, using oils with different characteristics specific to the region, and using different additives. As previously described, various vegetable or animal oils manufacture fuels. After the chemical and physical characteristics of the fuel are established, engine performance testing and emission tests are conducted in test rigs known as dynamometers. Biodiesel fuels can be used 100% or mixed with diesel fuel in different proportions and used in internal combustion engines.

Some of the current studies carried out by researchers in this section are given below.

Reşitoğlu & Keskin; They carried out a study to use biodiesel, which they produced from waste oil, as an alternative fuel in an internal combustion engine running on diesel fuel. They used the biodiesel they produced by mixing it with diesel fuel in different volumetric proportions. As a result, blended fuels gave similar performance values to diesel fuel. Nitrogen oxide emissions increased while there was a decrease in hydrocarbon, smoke opacity, and carbon monoxide rates in the biodiesel blend compared to diesel fuel. It has been stated that using biodiesel produced by esterification with waste oil taken from a cafeteria increases the specific fuel ratio and reduces engine power and torque compared to some diesel fuel. They stated that biodiesel fuel blends improve emission rates, can be used in diesel internal combustion engines, and positively contribute to ecology and economy (Reşitoğlu & Keskin, 2018).

Ulusoy et.al.; Stating that biodiesel is a popular fuel, they performed technical operations on improving the viscosity and calorific value of waste frying oil methyl ester. They conducted the experiments by mixing biodiesel with diesel fuel in different proportions in an internal combustion engine running on four-stroke direct injection diesel fuel. While we observed decreased carbon monoxide and hydrocarbon rates, slightly more smoke and nitrogen oxide emissions were obtained. They stated that although waste frying oil has a different structure and lower quality than other biodiesel fuels, it gives a good performance value. It is stated that the best mixing ratio is 10% (Ulusoy et. al., 2018).

Aksoy et al; In the study, waste olive oil was converted into biodiesel using transesterification. Internal combustion engine experiments were conducted using diesel fuel and the obtained biodiesel (30%). According to the study, biodiesel has a thermal efficiency between 1% and 5% lower than diesel fuel. Compared to diesel fuel, it emits fewer carbon monoxide, more carbon dioxide, more nitrogen oxide, and fewer soot particles. It was consequently claimed that biodiesel made from wasted olive oil might be utilized by blending it with diesel fuel (Aksoy et. al., 2019).

Erdoğan et. al.; In his research, he looked at how two distinct kinds of biodiesel and blends of these biodiesels affected a diesel-powered generator's performance, exhaust emissions, and combustion. Animal fat biodiesel from bovine bone marrow, vegetable oil biodiesel from a safflower/canola oil blend, and ultra-low sulfur diesel were all used in the experiments. Additionally, the blend of animal fat biodiesel with ultra-low sulfur diesel and vegetable fat biodiesel with ultra-low sulfur diesel were examined. They concluded that the cylinder gas pressure and net heat release rate rose when animal fat biodiesel and its blends were employed in a diesel generator. The average gas temperature


and exhaust gas temperature values increased using animal fat biodiesel, whereas thermal efficiency, carbon monoxide, and overall hydrocarbon emissions dropped. Carbon dioxide emissions were higher than low-sulfur diesel but lower than vegetable oil biodiesel. Nitrogen oxide emissions showed a similar change in all fuel types. In this study, the usability of alternative fuel biodiesel was investigated to improve diesel generators' performance and emissions (Erdoğan et. al., 2020).


✚Seraç et. al.; They stated that the importance of biofuels and renewable energy sources has increased due to increased environmental pollution and the rise in the prices of petroleum-derived fuels. It is stated that the production of soybean oil-based biodiesel can significantly contribute to the economy and employment of countries. In this context, research was conducted to test the usability of soy fuel in a generator set running on internal combustion diesel fuel. The study examined how various fuel blends affected a diesel engine's efficiency, emissions, and combustion style. The results showed that biodiesel blends exhibited similar combustion behaviors to diesel fuel. However, it has been stated that carbondioxide emissions increase as engine load increases. It has also been stated that biodiesel blends reduce volatile hydrocarbon emissions and reduce smoke opacity. It has been stated that the energy density of these biofuels is lower. They can be utilized in diesel engine generating sets without issues because of their low specific fuel consumption values. Finally, the researchers suggested that future studies address issues such as increasing the amount of air and testing additives that would improve biodiesel fuel properties (Seraç et. al., 2020).


✚Aydın & Çalışkan; By transesterifying tea seed oil, they created tea oil methyl ester. To create test fuels, this biodiesel was combined in various ratios with diesel fuel, and its varied qualities were assessed. These characteristics include tests for copper rod corrosion, density, kinematic viscosity, cetane number, pH amount, turbidity, pour and freezing points, calorific value, and color determination. The results showed that methyl ester blends can serve as a diesel fuel alternative and be used in diesel engines without altering the engine. However, it has been stated that using entirely biodiesel fuel is unsuitable for cold flow properties. Considering all the evaluations, it has been stated that the fuel mixture using 20% biodiesel gives the best results, and tea oil methyl ester can be used as fuel (Aydın & Çalışkan, 2021a).

✚Aydın; In his study, he emphasized the importance of energy production from waste and focused on how biodiesel is produced using waste sunflower oil and the benefits of this biodiesel. The research draws attention to the future importance of energy production from waste and states that countries' ability to produce their energy will provide an advantage over other countries. Biodiesel was produced by converting waste sunflower oil into methyl ester by transesterification. By blending ternary biodiesel, ethanol, and euro diesel

fuel, this was put to the test. The experiments revealed that adopting the most suitable ternary mixture as an environmentally friendly fuel mixture would result in energy conversion from waste. As an advantage of the triple fuel mixture, it has been stated that biodiesel eliminates the deficiency of low-sulfur euro diesel fuel, reduces viscosity, reduces ethanol emissions, increases energy efficiency, and increases combustion efficiency since it is an oxygenated fuel (Aydın, 2021).

 Aydın & Çalışkan; They studied biodiesel fuel to increase engine performance, reduce environmental pollution, and use alternative fuels. This study also tested biodiesel fuel internal combustion engines in a laboratory environment. Biodiesel was produced using *Camelina sativa* oil. Experiments were carried out on the chassis dynamometer by mixing biodiesel fuel with Eurodiesel in different proportions. These tests measured vehicle performance and exhaust emissions at different speeds. The findings showed that particular fuel usage rose as the biodiesel ratio rose. It has been stated that the biodiesel mixture has an effect on exhaust emissions, and it has been stated that it reduces carbon monoxide, carbon dioxide, and hydrocarbon values but increases nitrogen oxide values (Aydın & Çalışkan, 2021b).

 Ardebili et al; Statistical techniques were used to analyze the impact of fuel mixes by combining JP-8 military aviation fuel with sunflower oil as biodiesel in various ratios on the internal combustion engine's performance and ideal operating conditions. The tests used conventional JP-8 fuel, pure biodiesel fuel, and a combination of these fuels. As a result, they discovered that fuel usage decreases as engine load increases. Increases in exhaust temperature, nitrogen oxide emissions, and carbon monoxide emissions occur as the biodiesel ratio rises (Ardebili, Kocakulak, Aytav, & Calam, 2022).

 Ögüt et. al.; He tested the outcomes of converting horse fat into biodiesel using the transesterification process and this biodiesel in an experimental mixture with diesel fuel. The created biodiesel and diesel fuel mixture yielded two distinct mixtures, D100 and D95B5. Engine performance, energy analysis, and noise emissions were evaluated concerning these fuels' characteristics. Gasoline D95 B5 generated 4.06% more power and 0.68% more torque than gasoline D100. According to the minimal particular fuel consumption criterion, D100 fuel used 4.70% less than D95 B5 fuel. The maximum torque speed, lowest specific fuel consumption rate, and highest power rate for experimental fuels were established using the energy analysis results. As engine speed increased, fuel energy flow increased. When D95 B5 fuel was used in the engine, there was 0.56% less noise than D100 fuel. It has been stated that D95 B5 fuel produces less noise due to its higher cetane value. It has been reported that blending biodiesel made from horse fat with diesel fuel improves engine efficiency and reduces noise pollution. It has been said that using this fuel type in diesel engines does not require any adjustments.

New biodiesel raw materials such as horse oil are a potential way to popularize biodiesel and make it competitive. Studies can be carried out on increasing the blending ratios in the future (Öğüt, Oğuz, & Aydın, 2022).

Öztürk & Can; They looked at the utilization of biodiesel fuels from canola oil in diesel engines. The study concentrated on nitrogen oxide emissions from biodiesel fuels, which are higher than those from diesel fuels, and various management strategies were examined to address this issue. The study looked at three control strategies: ethanol addition, injection delay, and exhaust gas recirculation. Comparative experiments on a %10 biodiesel blend have shown that exhaust gas recirculation is an effective method to improve combustion parameters, and the best performance and emission results are achieved with a 2° delayed injection timing. Research has shown that adding 2% ethanol to the B10 biodiesel blend does not positively affect performance and negatively affects the emissions of this blend. However, it was concluded that all methods examined in the study have the potential to reduce nitrogen oxide emissions. It was stated that the composition of the canola oil used in this study, which produced canola oil biodiesel, consisted of oleic and linoleic acid. The necessary conditions for conversion to methyl esters are also specified. This study has demonstrated that optimal performance and emission outcomes can be achieved by slightly delaying fuel injection timing. It has been stated that using EGR (exhaust gas recirculation) can help achieve similar combustion parameters with diesel fuel but may negatively affect performance parameters. It was concluded that the addition of ethanol only had a positive effect on emissions (Öztürk & Can, 2022).


Uyaroğlu et. al.; Crambe Orientalis conducted an experimental study to see how organic manganese addition in biodiesel affected emissions, performance, and combustion in diesel engines. The performance and emissions of diesel engines were studied concerning Crambe orientalis biodiesel with organic manganese addition. The MATLAB/Simulink environment was used to process data related to in-cylinder pressure. These facts allowed for calculating the fuel combustion process, heat release rate, ignition delay, average adequate pressure, thermal efficiency, and maximum pressure increase rate. It was determined that biodiesel fuel mixtures caused a 1.96% and 1.82% increase in the specified thermal efficiency compared to pure diesel fuel. However, it has been noted that these mixes increase the use of a particular fuel. It has been reported that using biodiesel mixes reduces emissions of hydrocarbons, smoke, and carbon monoxide. The average in-cylinder pressure, maximum in-cylinder pressure increase, combustion onset, combustion duration, brake-specific fuel consumption, and carbon monoxide and hydrocarbon emissions are all reportedly affected by organic manganese. Although it has been underlined that increasing biodiesel density impacts particular fuel consumption values and combustion start, diesel engines


can still use it without any modifications. This study showed that *Crambe orientalis* oil is an excellent complementary fuel for diesel fuel and that organic manganese additive can improve the performance of biodiesel by affecting the combustion process. The results also show that organic manganese is a suitable additive that can overcome the weak properties of biodiesel to reduce exhaust emissions (Uyaroğlu, Gürü, Uyumaz, & Kocakulak, 2022).


✚ Söyler et. al.; He examined biodiesel production from oil containing high-free fatty acids from waste olives. The study concentrated on an optimization method for acid esterification that uses the least amount of alcohol and catalysts. The manufacturing of biodiesel using ultrasound assistance resulted in time and energy savings. The study's originality lies in converting oil containing high-free fatty acids from waste olive fruit into an alternative fuel. In addition, essential findings such as determining the optimum parameters of sulfuric acid use have been achieved. The results show that waste olives can be transformed into an economically valuable product and that efficient biodiesel production is possible from oils containing high free fatty acids. Using the ultrasound-assisted transesterification method for this purpose can potentially reduce costs and improve biofuel production. This study adopted a unique approach in which the amount of catalyst was calculated according to the weight of free fatty acids in the oil. It has been stated that this situation can help prevent reaction disruptions and increases in sulfur content, that biodiesel complies with EN 14.214 standards, and that the esterification process is carried out effectively (Söyler et. al., 2023).

✚ Çalık et.al.; They claimed in their analysis that internal combustion engine use of alternative fuels was the main focus of attempts to lessen reliance on fossil fuels. The research addresses a compression ignition engine's performance and emission characteristics by examining the combined effects of nanoparticle additives and hydrogen fuel. Combinations of biodiesel, titanium dioxide nanoparticles, and hydrogen have been used. Nanoparticles compensated for the decrease in engine performance caused by biodiesel and further improvements were observed by adding hydrogen. According to the emission results, carbon dioxide emissions decreased using biodiesel, nanoparticle additives, and hydrogen. Because these increased the combustion quality and prevented incomplete combustion. However, due to increased cylinder temperature, nitrogen oxide emissions increased with the use of biodiesel, nanoparticles, and hydrogen. In terms of torque and power, biodiesel decreased compared to diesel fuel, but the addition of nanoparticles compensated for this decrease. The use of hydrogen further increased performance with the use of biodiesel, carbon monoxide decreased, nanoparticles reduced carbon monoxide, and hydrogen minimized carbon monoxide emissions. The use of biodiesel, nanoparticles, and hydrogen has caused an increase in nitrogen oxide emissions compared to diesel fuel. These


increases were explained by the biodiesel's oxygen content, the nanoparticles' catalytic effect, and the hydrogen's faster combustion (Çalık, Tosun, Akar, & Özcanlı, 2023).


 Pawar et. al.; It has been stated that the decrease in fossil fuel resources, the increase in prices, and the disruption of natural balances by harmful environmental emissions increase the need for alternative fuels. They claimed that biodiesel could be a crucial alternative fuel for diesel engines. This study compared the effects of Karanja oil biodiesel with Cacklebur seed oil biodiesel on emissions and thermal performance. In the research, experiments were conducted with mixtures of Cacklebur seed oil biodiesel (20%) and Karanja oil biodiesel (80%) by adjusting different engine variables to determine the optimum conditions in the diesel engine. These experiments were carried out using an orthogonal array (Taguchi Design L9) with maximum thermal efficiency, minimum fuel consumption, and minimum levels of pollutants such as nitrogen oxide, carbon monoxide, hydrocarbons, and smoke. The results show that when 20% Cacklebur biodiesel is mixed with Karanja biodiesel, the maximum thermal efficiency increases by 0.98%. It has been stated that using a mixture of Cacklebur biodiesel and Karanja oil biodiesel as fuel increases thermal performance and affects some emissions (Pawar, Hole, Bankar, Channapattana, & Srinidhi, 2023).

 Ashfaque et. al.; In their study, they emphasized that the need for alternative fuels has increased due to the increase in fossil fuel prices, environmental impacts, and the need for sustainable development, and therefore the research and development of alternative fuels has gained importance. It has been stated that alternative fuels based on renewable energy sources offer solutions to the problems of fuel depletion, unavailability, and environmental pollution. It has been stated that biofuels have the potential to develop green energy in particular and are produced from biomass such as agricultural waste. It has been explained that the commonly used method for biodiesel production is Transesterification and that this process is three-stage and cost-effective. Additionally, it has been stated that biodiesel properties may differ depending on the geographical location of the raw material. Therefore, it is stated that these features should be taken into account before biodiesel production, and the rise of a science and engineering approach focusing on sustainable energy solutions is explained by emphasizing the importance of alternative fuels and the properties of biofuels (Ashfaque et. al., 2023).

 Bhonsle et. al.; The potential of inedible plants such as Cannabis Sativa and Sapium sebiferum for industrial biodiesel production has been examined. Using a new solvent, fatty acid methyl ester obtained from these plants was synthesized, and 98.7% and 97.8% fatty acid methyl ester yield was obtained. Three possible mechanisms and technical innovations of the new solvent are also described. The produced biodiesel and its blends met the physicochemical

properties following ASTM/BIS specifications. The study also compared biodiesel production from *Sapium sebiferum* and *Cannabis sativa* plants. Biodiesel obtained from both plants was produced with a shorter reaction time at ambient temperature. The ASTM/BIS procedures were used to analyze the fuel qualities of the created biodiesel and biodiesel-diesel mixes, and it was discovered that the flash point and pour point of the generated B-20 mixtures complied with the specifications by favorably altering the mixture concentration. According to this study, non-edible plants might be a source of biodiesel (Bhonsle et. al., 2023).

 Liu et.al.; They examined the use of ultrasound-assisted methods in biodiesel production and optimized the processes of producing biodiesel by extracting oil from field pennycres seeds. They stated that the biodiesel obtained by ultrasound-assisted transesterification has a quality under biodiesel standards. It has been stated that the production methods studied significantly reduce energy consumption compared to traditional methods. The effects of different extraction methods are demonstrated through microstructure observations. It has been stated that it contributes to developing new, efficient, and environmentally friendly processes in producing biodiesel from field pennycres seeds. Future research should focus on the design and application stages for industrial production, such as optimizing ultrasonic reactors and pilot-scale tests. A new pathway for biodiesel production has been opened, highlighting its commercial production potential (Liu et. al., 2023).


 Krishnamoorthi et. al.; They carried out a study on the significance and impacts of using biodiesel made from *Delonix regia* seed. *Delonix Regia* seed biodiesel has the potential to displace conventional fuels due to its ability to lower the emission of toxic exhaust fumes, according to specific reports. They coated the pistons and cylinder liners with their mixtures, claiming that the engine efficiency was not the same as that of standard diesel fuels. According to reports, these coatings will act as a thermal barrier. The study concentrated on using a compression-ignition engine using a blend of 80% *Delonix Regia* biodiesel. *Delonix Regia* biodiesel has reportedly undergone little scientific research because of its characteristics, such as high viscosity and low calorific value. However, it has been claimed that using it in thermal barrier-coated internal combustion engines improves engine performance and lowers emissions. During testing, it was discovered that 80% biodiesel increased specific fuel consumption, improved brake thermal efficiency, and decreased carbon monoxide and unburned hydrocarbon emissions. According to a study, nitrogen oxide emissions are increasing while smoke opacity is decreasing. The benefits of cetane number and oxygen concentration in *Delonix regia* seed biodiesel helped lower carbon monoxide emissions and unburned hydrocarbons (Krishnamoorthi, Sudalaimuthu, Dillikannan, & Jayabal, 2023).


✚ Anwar et. al.; This research examined biodiesel production using karanja (*Pongamia pinnata*) seed oil. Karanja seed oil has been used for biodiesel synthesis by base-catalyzed transesterification reaction. With the help of sulphuric acid and the esterification reaction, the oil's free fatty acid content was decreased. To create methyl esters of karanja oil, the esterified oil was transesterified with methanol and a potassium hydroxide catalyst. The usability of biodiesel was supported by the discovery that its fuel qualities are by ASTM requirements. The study highlights the potential of Karanja seed oil for quality biodiesel production as a non-food oil source. It has been stated that in countries experiencing an energy crisis, such as Pakistan, using locally available and underutilized resources in biodiesel production can offer a solution to reduce energy dependency. With this study, researchers stated that Karanja seed oil is a suitable alternative for biodiesel production and has the potential to meet the demand for renewable energy resources and that they aim to contribute to the more effective use of agricultural waste in countries such as Pakistan (Anwar, Tariq, Nisar, Ali, & Kanwal, 2023).

✚ Meng et. al.; According to researchers, using biodiesel made from used cooking oil as diesel fuel is one of the crucial steps to ensuring global energy transformation and sustainable growth. They investigated how a diesel engine with a common-rail fuel injection system would respond to a fuel combination made of biodiesel and used cooking oil. Under various operating situations, they experimentally investigated the impact of four different fuel mixture ratios (0%, 10%, 20%, and 30%) on engine combustion and emission characteristics. According to study findings, adding biodiesel from used cooking oil lengthened the combustion time. For combustion under medium and high load conditions (50% and 75%), favorable results were attained. The emission concentration decreased when the load was low as the mixture ratio increased. Nitrogen oxide and Acetaldehyde emissions increased, and soot emissions did not change with mixture ratio changes. Emission concentration decreased as the mixing ratio increased under medium and high load conditions. However, nitrogen oxide emissions have increased slightly. According to the study, adding biodiesel from used cooking oil enhanced the common-rail diesel engine's combustion and emission characteristics at 50% and 70% load levels (Meng et. al., 2023).


✚ El yaakouby et. al.; They emphasized the significance of looking into alternative energy sources as energy demand rises due to the depletion of fossil fuels and their adverse impacts on the environment. They created a new catalyst to improve biodiesel synthesis generated from palm oil. A high-temperature thermal shock and sulfonation process synthesized this catalyst. Under optimal conditions, with this catalyst, they could convert up to 96.75%, which is a high rate for conversion from palm oil to biodiesel. Additionally, in tests on the reusability of the catalyst, they determined that it maintained its


effectiveness throughout three consecutive reaction cycles. They determined that the produced biodiesel has properties that comply with international standards. This study indicates that a catalyst derived from sardine scales is an effective alternative for biodiesel production and can reduce dependence on fossil fuels (El yaakouby, Rhrissi, Abouliatim, Hlaibi, & Kamil, 2023).

 Jit Sarma et. al.; As a result of the increasing need for alternative fuel sources, a study was conducted to examine the use of nano-based biodiesel blends to improve the performance of biodiesel. It has been stated that the demand for alternative fuel sources increases as air quality decreases and fossil fuel reserves begin to be depleted. It has been stated that biodiesel is seen as an alternative fuel obtained from plant or animal sources. However, it has certain drawbacks, including poor atomization, low calorific value, high molecular mass, and low thermal efficiency. Researchers used titanium oxide nanoparticles as additions to biodiesel made from mahua oil to enhance its performance. Experiments were carried out using various test fuels, and the results were compared. It has shown that nano-based biodiesel blends reduce carbon monoxide emissions by 37.42% to 46.54%, hydrocarbon emissions by 22.54% to 28.4%, and nitrogen oxide emissions by 2.3% to 4%. As a result of these results, researchers stated that nano-based biodiesel blends give hope that they can replace fossil fuels and reduce environmental impacts. They stated that further optimization studies and performance enhancement are required and that this study represents a promising step towards developing alternative fuel sources using the combination of biodiesel and nanotechnology (Jit Sarma et. al., 2023).

 Malyadri et. al.; It has been stated that economic and environmental factors related to biodiesel production should be addressed, focusing on the importance of alternative fuels and the potential of biodiesel to reduce fossil fuel consumption. It has been accepted that alternative fuels are fuels that can be used in various applications, from automobiles to aircraft, maritime to energy production, and that it is essential to improve the properties of these fuels so that they can be used in the future. For this reason, researchers have emphasized that alternative fuel sources such as biodiesel are essential in reducing fossil fuel consumption and greenhouse gas emissions. They examined alternative fuel sources' long-term sustainability, economic advantages, and environmental impacts. The properties of the mixture obtained by mixing *Madhuca longifolia* biodiesel and diesel fuel were examined. The properties of the mixture were compared with pure diesel and pure *Madhuca longifolia* biodiesel. The results show the usability of *Madhuca longifolia* biodiesel and diesel mixture as engine fuel. In particular, it was determined that the MLB10 mixture developed by the researchers had a better flash and combustion point and less density than diesel fuel. The calorific value and viscosity of the MLB10 mixture are closer to diesel. This study focused on increasing the usability of


Madhuca longifolia biodiesel blends in internal combustion engines. Using the 10% mixture as an alternate fuel for diesel engines has been proposed (Malyadri et. al., 2023).


 Rex et. al.; Researchers have figured out how waste cooking oil impacts engine performance and pollutants when put in various volumes in the engine. However, the use of biofuel generated from frying oil has led to an increase in nitrogen oxide emissions. Additionally, it was noted that, while using biodiesel made from used cooking oil, specific fuel consumption increased somewhat but tolerably, considering the drop in exhaust pollutants. More nitrogen oxide emissions are seen during combustion engines powered by biodiesel, while carbon monoxide, hydrocarbon, and particulate matter emissions can be reduced. According to what has been said, it is generally accepted that biodiesel's higher oxygen content causes more complete combustion and less emissions. Higher oxygen content also causes a fall in calorific values, increasing fuel use and power losses. Due to higher density, viscosity, inadequate filtration, and decreased volatility, it is physically impossible to directly use purified biodiesel or methyl ester as a diesel fuel substitute in traditional diesel engines. Using used cooking oil is an appealing method for making biofuel at a reasonable price. The high free fatty acid content is the only drawback, however. Utilizing biodiesel in the industry is difficult due to its high cost. It has been claimed that employing a less expensive feedstock, like used cooking oil, will raise the price of biofuel to parity with that of crude oil. This study had a 4–12% reduction in carbon monoxide emissions. Emissions of nitrogen oxide increased by 15%. There was a 6% to 9% loss of electricity. The study claimed that leftover cooking oil can be converted into renewable fuel (Rex, Rex, Shiny, & Annrose, 2023).

 Rajpoot et. al.; The study examined the energy-exergy emissions of a single-cylinder, water-cooled, 4-stroke diesel engine and the sustainability analysis of spirulina microalgae biodiesel. The following four fuel samples were used: 100% diesel, 0% spirulina biodiesel, 20% spirulina biodiesel, 80% spirulina biodiesel, and 100% spirulina biodiesel. They looked at engine performance at various loads and compression ratios. According to the study, about one-third of the energy is employed for actual work, while the other two-thirds is lost as energy. By using Spirulina biodiesel, emissions are reduced by 28.09%. It has been stated that Spirulina biodiesel has potential in terms of sustainability and can replace traditional fuels. However, researchers stated that engine modifications and operating conditions should be optimized to reduce energy losses. It has been stated that the disadvantages of using Spirulina biodiesel include raw material supply, energy inputs, and technological limitations (Rajpoot, Choudhary, Chelladurai, Nath, & Pugazhendhi, 2023).

 Leo et. al.; This study evaluates the performance, combustion, and

emissions of biodiesel blends generated from cerium dioxide nanoparticles, acetylene injection, and cashew nut shell oil in diesel engines used for agricultural purposes. The thermal efficiency of engine brakes fell by 1.38% when biodiesel was used. However, the yield was significantly boosted by adding acetylene and cerium dioxide nanoparticles. Because of acetylene injection's higher combustion efficiency, peak pressure increased by 10.42% and engine brake thermal efficiency by 3.18%. Acetylene injection fuel exhibited lower nitrogen oxide emissions than the other test fuels. Using cerium dioxide nanoparticles reduced the hydrocarbon and carbon monoxide emissions of biodiesel generated from cashew nut shell oil by 5.92% and 3.3%, respectively. The improved results showed that the engine performance was highest when cerium dioxide and cashew shell nut oil were combined. The potential of cerium dioxide nanoparticles and acetylene injection was evaluated to enhance the usability and performance of cashew nut oil biodiesel blends, which support the resolution of energy and environmental concerns in using energy resources in agricultural diesel engines (Leo et. al., 2023).

 Jain et. al.; A study was done to examine if biodiesel made from Mesua Ferrea seed oil may enhance the performance of a diesel engine. This research was carried out using energy, exergy, and emission analysis. Experiments were carried out with different injection timings and load settings. The results showed that 20° injection timing increased fuel conversion efficiency. With the use of Mesua Ferrea seed oil biodiesel, energy consumption has decreased, and emissions have also decreased. It has also been stated that using tire pyrolysis oil increases energy and exergy efficiency in the fuel mixture. In addition, peanut oil biodiesel and carbon nanotube nanoparticles were used in a diesel engine, and the results were stated to be similar to diesel fuel in terms of energy and exergy analysis. The first study examined the effect of diesel engines running on Mesua Ferrea seed oil biodiesel on injection timing and load adjustment. It is aimed to increase the performance of diesel engines with this type of biodiesel that can be used for energy production in rural areas. The key finding was that 20° injection timing improves fuel conversion efficiency while lowering carbon monoxide, carbon dioxide, hydrocarbons, and nitrogen oxide emissions (Jain et. al., 2023).

 Rajpoot et. al.; This investigation focused on fuel mixtures and added 100 ppm graphene nanoparticles to the second-generation Jatropha biodiesel to assess the performance of a single-cylinder internal combustion engine. Pure Jatropha biodiesel (JB100), a blend of 20% biodiesel and 80% diesel (JB20), pure Jatropha biodiesel plus fuel with 100 ppm graphene nanoparticles added (JB100Gn100), and a combination of 20% biodiesel and 80% diesel plus fuel with 100 ppm graphene nanoparticles (JB20Gn100) The following gasoline blends were identified: (JB20Gn100). The study analyzed engine behavior parameters such as heat produced in the cylinder, engine efficiency, fuel

consumption, smoke opacity, and PM emissions. Different fuel mixtures were compared. The results show that adding graphene nanoparticles increases the engine's thermal efficiency by 0.57% to 1.54%, reduces fuel consumption by 0.36% to 1.33%, reduces smoke opacity by 0.45% to 4.12%, and reduces PM emissions. It showed that it decreased between 1.68% and 9.62%. This research has shown that biodiesel blends containing graphene nanoparticles can improve engine performance. It was concluded that by adding graphene nanoparticles to *Jatropha* biodiesel, its physicochemical properties were improved, and thus, better combustion was achieved. The addition of graphene nanoparticles to JB20 and JB100 fuels increased engine performance. With graphene oxide nanoparticles, fuel consumption decreased, and smoke opacity and PM emissions decreased. As a result, it has been determined that biodiesel fuels containing graphene nanoparticles can increase the efficiency of engines and reduce emissions. Future research should focus on the stability and sustainability of such blended biodiesel blends (Rajpoot, Choudhary, Chelladurai, & Patel, 2023).

Ch et. al.; The usage of Kusum biodiesel blends as an alternative fuel for diesel engines was looked into. A single-cylinder diesel engine was used to test mixes with various biofuel percentages. Kusum biofuel was used to make fuel blends of 10% Kusum and 90% diesel (K-10 D-90), 20% Kusum and 80% diesel (K-20 D-80), 30% Kusum and 70% diesel (K-30 D-70), and 40% Sesame biofuel and 60% diesel (K-40 D-60). Performance and emission parameters of internal combustion engines were evaluated. According to the researchers, the 20% biofuel and 80% diesel blend (K-20 D-80) performed the best. This combination uses the most minor gasoline specifically for brakes while providing the best thermal efficiency. It has been reported that kusum biodiesel blends perform effectively as an alternative fuel for diesel engines. Although the thermal efficiency of the brakes is reduced and the amount of fuel precisely needed for the brakes is increased when the kusum biofuel ratio is raised. Hydrocarbon and carbon monoxide emissions have decreased, but nitrogen oxide emissions have grown. According to research, the K-20 D-80 is the best combination for increasing engine performance and lowering emissions (Ch, S, Mahesh, & Boni, 2023).

Opuz et. al.; The transesterification method created biodiesel from canola oil biodiesel, and 20% pure diesel fuel (B20) was added to this biodiesel. Later, many studies were conducted using B20 fuel and carbon nanoparticles (carbon quantum dots) at 50, 100, and 150 ppm concentrations. The study's findings show that as engine load grew, the difference in cylinder pressure between diesel and blended fuels decreased. The addition of metallic fuel shortens ignition delay. It was determined that specific fuel consumption decreased with the addition of carbon nanoparticles, and thermal efficiency increased. Higher in-cylinder pressure values were obtained at low engine

loads compared to pure diesel fuels. However, this difference decreased with increasing engine load. In addition, since the addition of carbon nanoparticles improves the cetane number and calorific value of the fuel, improvements in fuel economy have been observed. However, adding carbon nanoparticles extended the flame duration and increased the burning time. It was determined that carbon monoxide and nitrogen oxide emissions increased with the addition of carbon nanoparticles, while hydrocarbon emissions decreased. As a result, it has been stated that adding carbon nanoparticles to biodiesel blended fuels improves the properties of the fuel and reduces emissions (Opuz et. al., 2023).

RESULTS

Vegetable oils were used to invent internal combustion engines running on diesel fuel. Afterward, oil-derived fuels gained importance due to the search for oil, finding suitable reserves and species, and the reserve life of these species being satisfactory in those years. In the last 30 years, the search for alternative engines or fuels has accelerated due to concerns about oil reserves, the lack of oil mines in all countries, and the emissions they emit to the environment. Biodiesel fuel has been the subject of research by researchers in internal combustion engines for many years, and the research has continued unabated until today. In current studies conducted by researchers, it has been determined that in addition to intensive studies on plant and animal products in every country, biodiesel studies are also carried out on waste products. As shown schematically in Figure 3, the physical and chemical properties of these fuels developed after the biodiesel production process are first determined. Then performance and emission tests are carried out in internal combustion engines.

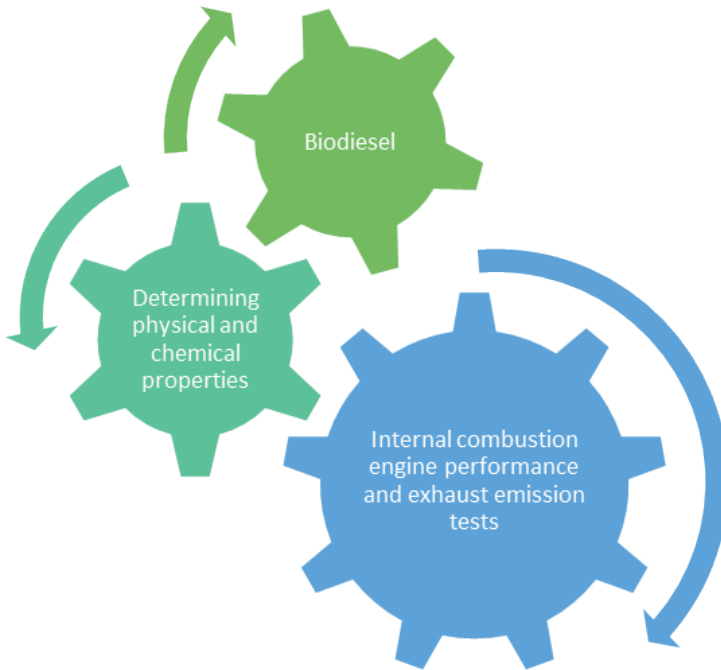


Figure 3. *Experimental processes of developed biodiesels*

Researchers have used various additives to eliminate the disadvantages that may arise in using biodiesel fuel in internal combustion engines, and it has been determined that using biodiesel fuel gives satisfactory results. It has been discovered that biodiesel fuels can be used as renewable fuels in diesel engines as an alternative fuel because they have nearly the same fuel consumption and torque power values as diesel fuel while reducing carbon monoxide, carbon dioxide, and smoke darkness emission rates somewhat. The reason why biodiesel fuels cannot be widely used and are not available in the market may be that the control and standardization that may arise regarding this fuel is not fully formed, it may be produced under inappropriate and uncontrolled conditions, and the fuel system in new generation internal combustion diesel engines consists of susceptible parts. In order to solve these problems, countries can work on various legal regulations and standardization, and after these studies, they can supply suitable fuel for final consumer use. Using this fuel will positively contribute to the country's economy and lead to more effective use of existing resources. Biodiesel can be considered an alternative energy source in internal combustion engines in popularizing electric vehicles' battery, range, and charging stations, which are widely researched today.

REFERENCES

- Aksoy, F., Akay, F., Ayhan Baydır, Ş., Solmaz, H., Yılmaz, E., Uyumaz, A., ... Calam, A. (2019). An Experimental Investigation on The Effects of Waste Olive Oil Biodiesel on Combustion, Engine Performance and Exhaust Emissions. *International Journal of Automotive Engineering and Technologies*, 8(3), 103-116. Geliş tarihi gönderen <https://dergipark.org.tr/en/pub/ijaet>
- Anwar, F., Tariq, M., Nisar, J., Ali, G., & Kanwal, H. (2023). Optimization of biodiesel yield from non-food karanja seed oil: Characterization and assessment of fuel properties. *Sustainable Chemistry for the Environment*, 3(100035), 1-7. <https://doi.org/10.1016/j.scenv.2023.100035>
- Ardebili, S. M. S., Kocakulak, T., Aytav, E., & Calam, A. (2022). Investigation of the effect of JP-8 fuel and biodiesel fuel mixture on engine performance and emissions by experimental and statistical methods. *Energy*, 254. <https://doi.org/10.1016/j.energy.2022.124155>
- Ashfaq, A., Ramana Murty Naidu, S. C. V., Kumar, M., Kumar Yadav, R., Kaur Sohal, J., Hidayatulla Shariff, S., ... Sharma, A. (2023). Impact of biodiesel on engine performance and emission. *Materials Today: Proceedings*. <https://doi.org/10.1016/j.matpr.2023.07.275>
- Aydın, F. (2021). The investigation of fuel properties of mixtures obtained by adding waste sunflower biodiesel and ethanol to euro diesel fuel. *International Journal of Automotive Engineering and Technologies*, 10(2), 91-99. <https://doi.org/10.18245/ijaet.874772>
- Aydın, F., & Çalışkan, S. (2021a). Investigation of Fuel Properties of Tea Seed Oil Biodiesel and Diesel Fuel Mixture. *International Journal of Automotive Science and Technology*, 5(4), 339-344. <https://doi.org/10.30939/ijastech..973072>
- Aydın, F., & Çalışkan, S. (2021b). Investigation of Fuel Properties of Tea Seed Oil Biodiesel and Diesel Fuel Mixture. *International Journal of Automotive Science and Technology*, 5(4), 339-344. <https://doi.org/10.30939/ijastech..973072>
- Bhonsle, A. K., Rawat, N., Trivedi, J., Singh, R., Singh, J., & Atray, N. (2023). Biodiesel production using novel solvent from agricultural crop Cannabis sativa L. and Sapium sebiferum L. and their fuel properties characterisation using blends. *Bioresource Technology Reports*, 23(101155), 1-9. <https://doi.org/10.1016/j.bi-teb.2023.101555>
- Can, Ö., Öztürk, E., Solmaz, H., Aksoy, F., Çinar, C., & Yücesu, H. S. (2016). Combined effects of soybean biodiesel fuel addition and EGR application on the combustion and exhaust emissions in a diesel engine. *Applied Thermal Engineering*, 95, 115-124. <https://doi.org/10.1016/j.applthermaleng.2015.11.056>
- Ch, N. K., S, V. S. S., Mahesh, G., & Boni, M. (2023). Suitability of kusum biodiesel blends as an alternate fuel for a single cylinder diesel engine. *Materials Today: Proceedings*, Article in press, 1-4. <https://doi.org/10.1016/j.matpr.2023.06.136>

- Çalık, A., Tosun, E., Akar, M. A., & Özcanlı, M. (2023). Combined effects of hydrogen and TiO₂nanoparticle additive on terebinth oil biodiesel operated diesel engine. *Science and Technology for Energy Transition*, 78(9), 1-6. <https://doi.org/10.2516/stet/2023007>
- Çetinkaya, S. (2015). *Taşıt mekaniği* (C. 7).
- El yaakouby, I., Rhrissi, I., Abouliatim, Y., Hlaibi, M., & Kamil, N. (2023). Moroccan sardine scales as a novel and renewable source of heterogeneous catalyst for biodiesel production using palm fatty acid distillate. *Renewable Energy*, 217, 1-15. <https://doi.org/10.1016/j.renene.2023.119223>
- Erdoğan, S., Balki, M. K., Aydın, S., & Sayın, C. (2020). Performance, emission and combustion characteristic assessment of biodiesels derived from beef bone marrow in a diesel generator. *Energy*, 207(118300), 1-11. <https://doi.org/10.1016/j.energy.2020.118300>
- Haşimoğlu, C., Ciniviz, M., Özsert, I., İçingür, Y., Parlak, A., & Salman, M. S. (2008). Performance characteristics of a low heat rejection diesel engine operating with biodiesel. *Renewable Energy*, 33, 1709-1715. <https://doi.org/10.1016/j.renene.2007.08.002>
- Jain, A., Bora, B. J., Kumar, R., Sharma, P., Medhi, B. J., Rambabu, G. V., & Deepanraj, B. (2023). Energy, exergy and emission [3E] analysis of Mesua Ferrea seed oil biodiesel fueled diesel engine at variable injection timings. *Fuel*, 353(129115), 1-17. <https://doi.org/10.1016/j.fuel.2023.129115>
- Jit Sarma, C., Sharma, P., Bora, B. J., Bora, D. K., Senthilkumar, N., Balakrishnan, D., & Ayesha, A. I. (2023). Improving the combustion and emission performance of a diesel engine powered with mahua biodiesel and TiO₂ nanoparticles additive. *Alexandria Engineering Journal*, 72, 387-398. <https://doi.org/10.1016/j.aej.2023.03.070>
- Karabektaş, M., Ergen, G., Hasimoglu, C., & Murcak, A. (2016). Performance and Emission Characteristics of a Diesel Engine Fuelled with Emulsified Biodiesel-Diesel Fuel Blends. *International Journal of Automotive Engineering and Technologies*, 5(4), 176-185. Geliş tarihi gönderen www.academicpaper.org
- Krishnamoorthi, T., Sudalaimuthu, G., Dillikannan, D., & Jayabal, R. (2023). Influence of thermal barrier coating on performance and emission characteristics of a compression ignition engine fueled with delonix regia seed biodiesel. *Journal of Cleaner Production*, 420(138413), 1-8. <https://doi.org/10.1016/j.jclepro.2023.138413>
- Kumar, S., Singh, P., Shrivastava, V., Kaur Sohal, J., Sharma, A., Kumar, M., ... Singh Yadav, A. (2023). Potential non-edible oil seeds for biodiesel production: An Indian context. *Materials Today: Proceedings*. <https://doi.org/10.1016/j.matpr.2023.05.419>
- Leo, G. M. L., Murugapoopathi, S., Thodda, G., Baligheid, S. M., Jayabal, R., Nedunchezhiyan, M., & Devarajan, Y. (2023). Optimisation and environmental analysis of waste cashew nut shell oil biodiesel/cerium oxide nanoparticles blends

- and acetylene fumigation in agricultural diesel engine. *Sustainable Energy Technologies and Assessments*, 58(103375), 1-9. <https://doi.org/10.1016/j.seta.2023.103375>
- Liu, J., Zhang, Z., Tang, S., Yu, Z., Zhang, Y., & Zheng, B. (2023). Ultrasound-assisted production of biodiesel from field pennycress (*Thlaspi arvense* L.) seeds: Process optimization and quality evaluation. *Industrial Crops and Products*, 203(117224), 1-15. <https://doi.org/10.1016/j.indcrop.2023.117224>
- Malyadri, T., Saravanan, R., Pothula, N., Swetha, S., Anbucheziyan, G., & Reddy, M. M. (2023). Synthesis of blending in *Madhuca longifolia* biodiesel for properties enhancement for the usage of engine fuel. *Materials Today: Proceedings, Article in press*. <https://doi.org/10.1016/j.matpr.2023.06.249>
- Meng, J., Xu, W., Meng, F., Wang, B., Zhao, P., Wang, Z., ... Yang, Y. (2023). Effects of waste cooking oil biodiesel addition on combustion, regulated and unregulated emission characteristics of common-rail diesel engine. *Process Safety and Environmental Protection*, 178, 1094-1106. <https://doi.org/10.1016/j.psep.2023.08.065>
- Opuz, M., Uyumaz, A., Babagiray, M., Solmaz, H., Calam, A., & Aksoy, F. (2023). The effects of metallic fuel addition into canola oil biodiesel on combustion, engine performance and exhaust emissions. *Journal of the Energy Institute*, 111(101390), 1-9. <https://doi.org/10.1016/j.joei.2023.101390>
- Öğüt, H., Oğuz, H., & Aydın, F. (2022). Experimental analysis of energy, performance and noise emissions for biodiesel fuel obtained from animal waste fat. *Environmental Progress and Sustainable Energy*, 41(5), 1-10. <https://doi.org/10.1002/ep.13847>
- Öztürk, E., & Can, Ö. (2022). Effects of EGR, injection retardation and ethanol addition on combustion, performance and emissions of a DI diesel engine fueled with canola biodiesel/diesel fuel blend. *Energy*, 244, 1-13. <https://doi.org/10.1016/j.energy.2022.123129>
- Pawar, S., Hole, J., Bankar, M., Channapattana, S., & Srinidhi, C. (2023). Use of Taguchi method for optimizing engine parameters of Variable Compression Ratio Diesel Engine using Cacklebur seed oil biodiesel blended with Karanja oil biodiesel. *Materials Today: Proceedings, Article in press*. <https://doi.org/10.1016/j.matpr.2023.08.129>
- Rajpoot, A. S., Choudhary, T., Chelladurai, H., Nath, T. V., & Pugazhendhi, A. (2023). Sustainability analysis of spirulina biodiesel and their bends on a diesel engine with energy, exergy and emission (3E's) parameters. *Fuel*, 349(128637), 1-15. <https://doi.org/10.1016/j.fuel.2023.128637>
- Rajpoot, A. S., Choudhary, T., Chelladurai, H., & Patel, N. K. (2023). Effect of graphene nanoparticles on the behavior of a CI engine fueled with *Jatropha* biodiesel. *Materials Today: Proceedings, Article in press*, 1-5. <https://doi.org/10.1016/j.matpr.2023.03.785>
- Reşitoğlu, İ. A., & Keskin, A. (2018). The Effect of Biodiesel Derived from Waste Oil on

Engine Performance and Emission Characteristics. *Journal of Environmental Science Studies*, 1(1), 55-62. <https://doi.org/10.20849/jess.v1i1.432>

- Rex, C. R. B. S., Rex, C. R. E. S., Shiny, S., & Annrose, J. (2023). Power performance and emissions analysis of outboard diesel engines by use of waste cooking oil biodiesel. *Materials Today: Proceedings, Article in press*, 1-5. <https://doi.org/10.1016/j.matpr.2023.09.005>
- Sayın, C., Erdoğan, S., & Baki, M. K. (2019). *Alternatif Yakıtlar: Çevresel atıkların içten yanmalı motor yakıtı olarak değerlendirilmesi* (C. 1).
- Seraç, M. R., Aydın, S., & Sayın, C. (2020). Comprehensive evaluation of performance, combustion, and emissions of soybean biodiesel blends and diesel fuel in a power generator diesel engine. *Energy Sources, Part A: Recovery, Utilization and Environmental Effects*, 42(18), 2316-2331. <https://doi.org/10.1080/15567036.2020.1748144>
- Söyler, H., Balki, M. K., & Sayın, C. (2023). Determination of optimum parameters for esterification in high free fatty acid olive oil and ultrasound-assisted biodiesel production. *Biomass Conversion and Biorefinery*, 13, 12043-12056. <https://doi.org/10.1007/s13399-021-01976-y>
- Tosun, E., Özcanlı, M., & Akar, M. A. (2022). A Review on Biodiesel: From Feedstock to Utilization in Internal Combustion Engines. *OKU Journal of The Institute of Science and Technology*, 5(1), 417-428. Geliş tarihi gönderen <https://orcid.org/0000-0002-0192-0605>
- Ulusoy, Y., Arslan, R., Tekin, Y., Sürmen, A., Bolat, A., & Şahin, R. (2018). Investigation of performance and emission characteristics of waste cooking oil as biodiesel in a diesel engine. *Petroleum Science*, 15(2), 396-404. <https://doi.org/10.1007/s12182-018-0225-2>
- Uyaroğlu, A., Gürü, M., Uyumaz, A., & Kocakulak, T. (2022). Experimental research of the effects of organic manganese-added biodiesel produced from crambe orientalis oil on engine performance, combustion, and emissions. *Environmental Progress and Sustainable Energy*, 41(5), 1-10. <https://doi.org/10.1002/ep.13848>
- Uysal, C., Uslu, S., & Aydın, M. (2022). Exergetic and exergoeconomic analyses of a diesel engine fueled with binary and ternary blends of diesel–palm oil biodiesel–diethyl ether for various injection timings. *Journal of Thermal Analysis and Calorimetry*, 147, 12641-12659. <https://doi.org/10.1007/s10973-022-11500-7>
- Uyumaz, A., Aydoğan, B., Yılmaz, E., Solmaz, H., Aksoy, F., Mutlu, İ., ... Calam, A. (2020). Experimental investigation on the combustion, performance and exhaust emission characteristics of poppy oil biodiesel-diesel dual fuel combustion in a CI engine. *Fuel*, 280. <https://doi.org/10.1016/j.fuel.2020.118588>

Chapter 9

ALTERNATIVE FUELS IN THE FUTURE OF THE MARITIME INDUSTRY

Ayfer ERGİN¹

M. Fatih ERGİN²

1 Assistant Prof. Dr., İstanbul University-Cerrahpaşa, Faculty of Engineering, Maritime Transport Management Engineering Department, Avcılar Campus, İstanbul, Türkiye
ayfersan@iuc.edu.tr

ORCID ID: 0000-0002-6276-4001

2 Dr., İstanbul University-Cerrahpaşa, Faculty of Engineering, Chemical Engineering, Avcılar Campus, İstanbul, Türkiye

mfergin@iuc.edu.tr

ORCID ID: 0000-0003-4158-368X

1. Introduction

Maritime transport is one of the lifelines of global trade and makes significant contributions to the growth of the world economy. Accounting for approximately 80-90% of global trade, maritime transportation forms the backbone of international commerce (Ergin & Ergin, 2021; Shi & Li, 2017). Over the last three decades, the volume of cargo transported by sea has almost tripled as countries' populations have increased and their economies have grown (Ergin & Sandal, 2023; UNCTAD, 2021). This rapid growth in the economy has led to an increase in fuel consumption, as expected, and it has been stated that a significant portion of fuel consumption originates from national and international maritime transportation (Deniz & Zincir, 2016). However, the use of high-sulfur-containing fossil fuels, especially heavy fuels, in maritime transportation (Rony et al., 2023) has confronted maritime transportation with environmental problems. Emissions released by ships into the atmosphere include harmful greenhouse gases such as sulfur oxide, nitrogen oxide, and particulate matter. Approximately 70% of these gases accumulate in an area of approximately 400 square kilometers, including terrestrial regions (Endresen et al., 2003; Eyring, Köhler, Lauer, & Lemper, 2005). This poses a serious risk to both the environment and people's health (Ampah, Yusuf, Afrane, Jin, & Liu, 2021; Bengtsson, Andersson, & Fridell, 2011). The presence of these gases causes serious fatal diseases for humans (lung cancer, heart failure, bronchitis, etc.) and negative environmental effects such as global warming (Noor, Noor, & Mamat, 2018).

In a study conducted by the International Maritime Organization (IMO) in 2014, it was determined that ships emit 938 million tons of carbon dioxide (CO₂) into the atmosphere annually. This figure represents approximately 2.6% of human-caused emissions globally. Nowadays, the maritime industry has become more aware of its environmental responsibility as the possible effects of global climate change on people and the environment attract more attention. According to IMO data, exhaust emissions from ships constitute a significant part of total transportation emissions worldwide. Specifically, ships are responsible for 60% of sulfur oxide (SO_x) emissions, 40% of nitrogen oxide (NO_x) emissions, and 15% of CO₂ emissions. These exhaust emission percentages reflect the growth in maritime transportation over the past 30 years (Hwang et al., 2020).

In this context, IMO has made important commitments to reduce the carbon footprint of the maritime industry. It is planned to reduce CO₂ emissions from shipping by 40% by 2030 and 70% by 2050. In addition, it is aimed to reduce greenhouse gas emission values by 50% by 2050 (compared to 2008 levels). These studies reflect the long-term goals of the maritime industry towards the ultimate goal of completely eliminating these emissions by 2100 (Balcombe et al., 2019; IMO, 2018; Joung, Kang, Lee, & Ahn, 2020).

Moreover, these commitments represent important steps taken by the maritime industry to ensure environmental sustainability and play a vital role in combating global climate change. Therefore, the shipping industry needs additional innovative approaches to increase environmental sustainability and reduce carbon footprint. As fossil fuels are rapidly depleted and therefore expensive, renewable energy is becoming much more attractive. At the same time, since the production of petroleum-based fuel resources is limited to certain countries (Ali, Mamat, & Faizal, 2013), the search for new alternative fuels is also increasing (Noor et al., 2018). As a result of this need in recent years, alternative ship fuels and advanced technologies have initiated a major transformation in the maritime industry. Diesel has begun to be replaced by clean energy sources such as liquefied natural gas (LNG), hydrogen fuels, electricity and biofuels. By choosing these alternative fuels, carbon emissions can be reduced, air quality can be improved and energy efficiency can be increased. Alternative ship fuels play an important role in reducing negative impacts on the environment and making maritime transportation more environmentally friendly.

This study examines various alternative types of marine fuel and focuses on their characteristics, advantages and disadvantages. In addition, the applicability and future potential of these fuels in maritime transportation are also evaluated. Alternative ship fuels can help the shipping industry move towards a cleaner, more sustainable future. Therefore, the research and application of these fuels is of great importance for both maritime professionals and environmental advocates. Additionally, another aim of this study is to understand this critical issue in detail and provide a road map to reduce the environmental impacts of maritime transportation.

2. Alternative Ship Fuels

2.1.Liquefied Natural Gas (LNG)

LNG (Liquefied Natural Gas) is a fuel obtained by turning methane gas into liquid at low temperatures. This liquefaction process reduces the volume of natural gas, making it easier to transport and store, while also providing clean burning properties. In recent years, LNG has gained popularity as a marine fuel. When liquefied into liquid form, it occupies only approximately 1/600 of the volume of the gaseous product, making it ideal for use on ships (S. Wang & Notteboom, 2014). It is a particularly popular choice for cruise ships, container ships, and Ro-Ro ships (S. Wang & Notteboom, 2014). Xu and Yang found that the use of LNG gives the best results for ship types that make shorter stops and have appropriate ship sizes (Xu & Yang, 2020). Additionally, the inland waterway transportation segment offers a potential market for LNG bunkering (S. Wang & Notteboom, 2014).

2.1.1. Emission Levels of LNG

LNG offers one of the highest levels of energy density compared to other hydrocarbon fuels and also has one of the lowest levels of carbon emissions (Balcombe et al., 2021). Choosing LNG as a fuel instead of traditional marine fuels results in a significant reduction in sulfur oxide (SO_x), nitrogen oxide (NO_x), and particulate matter (PM) emissions. While NO_x emissions are reduced by 85-90%, SO_x and PM emissions are almost completely eliminated. Additionally, CO₂ emissions are reduced by 15-20% (Bengtsson et al., 2011). Greenhouse gas emissions such as water vapor, nitrogen oxide and carbon dioxide produced during the combustion of LPG are also lower (Xu & Yang, 2020). LNG therefore improves air quality and reduces the shipping industry's negative impact on the environment and people.

2.1.2. Performance and Efficiency of LNG

When ship engines run on LNG, they produce more energy, allowing ships to travel or cover longer distances with fewer emissions (Balcombe et al., 2021). This is especially important for ships engaged in long-distance transportation. When LNG is burned, clean combustion occurs, resulting in reduced combustion residues. Additionally, nitrogen oxide (NO_x) emissions during LNG consumption are significantly lower than carbon dioxide (CO₂) emissions. This helps the maritime industry comply with environmental regulations and improve air quality. Higher energy efficiency leads to reduced fuel costs. The cost of LNG can be competitive or lower than traditional shipping fuels, helping shipping companies reduce operating costs. LNG-powered ships may require less maintenance. Clean combustion helps reduce engine wear and extend the life of components, potentially reducing maintenance costs.

2.1.3. Storage and Transportation Challenges of LNG

Storage and transportation of LNG require special requirements. To remain in liquid form, LNG must be kept at approximately -162°C (-260°F). This low temperature requires the use of special storage tanks. These tanks are lined using high-quality materials and are completely leak-proof. Additionally, LNG tanks are kept under vacuum to minimize temperature loss. LNG storage tanks are usually located underground or under the bottom of ships. This is done to better control the temperature and increase safety (Kim, Koo, & Joung, 2020). Storage and transportation of LNG are complex processes that require special requirements and high safety standards. However, this process allows LNG to contribute to maritime transportation as a clean and environmentally friendly fuel.

2.1.4. Global Growth

The maritime transportation sector is compelled to comply with environmental regulations. The need to reduce environmental impacts

and control emissions steers shipowners toward cleaner fuel sources. LNG, with its low emissions and environmentally friendly characteristics, supports the industry's compliance with these regulations. The use of LNG in maritime transportation has led to the development of new technologies and infrastructure improvements. The construction of LNG terminals and stations requires advanced infrastructure for the supply and storage of LNG. This infrastructure development triggers economic growth.

2.1.5. The Future Role of LNG

LNG continues to play a significant role in the sustainability, energy security, and economic growth of the maritime transportation sector. However, for LNG to sustain this role, technological advancements, infrastructure development, and compliance with environmental regulations are necessary. As a clean and efficient fuel that meets future energy needs, LNG is expected to remain a key player in the transformation of maritime transportation. Cengiz and Zincir compared the environmental and economic performance of alternative fuel types, including Methanol, Ethanol, Liquefied Methane, and Hydrogen, using the AHP method and found that LNG is the best alternative (Deniz & Zincir, 2016).

2.2. Hydrogen Fuels

Hydrogen fuels are garnering increasing attention within the maritime transportation industry as an environmentally friendly and sustainable alternative. Hydrogen is a clean energy source that emits no pollutants except water vapor when burned. Consequently, it has been adopted to reduce the carbon footprint and mitigate environmental impacts in maritime operations (Jain, 2009; Y. Wang, Chen, Mishler, Cho, & Adroher, 2011).

However, storing and transporting hydrogen pose challenges that require infrastructure development. The primary challenges include establishing a new refueling infrastructure and ensuring the safe operation of these hydrogen carriers on ships (Gong et al., 2022).

2.2.1. Hydrogen Fuel Production

Hydrogen is typically produced through methods like water electrolysis or hydrocarbon reforming. Water electrolysis involves splitting water into hydrogen and oxygen gases using electrical energy. This method supports clean hydrogen production when environmentally friendly energy sources are used. Hydrogen is one of the lightest elements (Gopinath & Marimuthu, 2022), and is considered an environmentally friendly energy source (McKinlay, Turnock, & Hudson, 2021). Hydrogen fuels are utilized for energy generation through hydrogen combustion or chemical reactions.

2.2.2. Emission Levels of Hydrogen Fuel

Hydrogen fuels only yield water vapor during combustion, resulting in zero carbon emissions (Gong et al., 2022). Consequently, when employed in maritime transportation, it enhances air quality and diminishes greenhouse gas emissions (McKinlay et al., 2021).

2.2.3. Efficient Energy Production

Hydrogen boasts a high energy density and delivers efficient energy production when burned. This enables ships to cover greater distances at faster speeds (Shih, Zhang, Li, & Bai, 2018).

2.2.4. Storage and Transportation Challenges of Hydrogen Fuel

Hydrogen exists in gaseous form at ambient temperatures with a critical temperature of 33 K (-240°C) (Züttel, 2003). Hydrogen has an extremely low density in its gaseous state and requires special conditions for storage. Compressing or liquefying hydrogen allows for denser storage, but these processes can increase energy demand by up to 30% (Mazloomi & Gomes, 2012). Hydrogen has a wide flammability range in air, spanning from 4% to 77%, indicating potential explosiveness (Goldmann et al., 2018). While this risk can be mitigated, it may necessitate additional regulatory frameworks and safety protocols, potentially resulting in heightened expenditures and size prerequisites. Moreover, hydrogen's lack of odor, non-toxic nature, and invisibility pose challenges in detecting leaks (Mazloomi & Gomes, 2012).

2.2.5. Hydrogen Fuel Infrastructure

In order to use hydrogen fuels, it requires the establishment of appropriate infrastructure. Special facilities are required for storage, transportation, and refueling. Developing and disseminating this infrastructure may take time. Additionally, it will be essential to provide specific support for the construction of high-capacity storage tanks, pipelines, and hydrogen exchange and distribution. (Shih et al., 2018).

2.2.6. Future Role of Hydrogen Fuel

Hydrogen fuels hold significant potential in supporting sustainability initiatives within the maritime transportation industry. The increased utilization of eco-friendly energy sources and the advancement of hydrogen technologies can propel the maritime sector towards a more sustainable future.

In conclusion, hydrogen fuels are emerging as a potential solution to reduce the environmental impact of maritime transportation and advance towards a sustainable future. However, infrastructure development and cost reduction are imperative for the widespread adoption of this technology.

2.3. Ammonia

Ammonia is a colorless chemical gas consisting of 3 hydrogen and 1 nitrogen, containing no carbon, and known for its distinctive pungent odor. It is widely used in various sectors, especially fertilizer production (Wolny, Tuśnio, & Mikołajczyk, 2022).

2.3.1. Emission Levels of Ammonia

Since ammonia does not contain carbon, it does not produce carbon emissions during its combustion, and the resulting emissions can also contribute to reducing carbon emissions. Consequently, ammonia (NH_3) is gaining increasing interest as one of the alternative ship fuels in maritime transportation (Zamfirescu & Dincer, 2008). However, it does lead to NO_x emissions during combustion, signifying that the process is not entirely emission-free. These emissions are known to have the potential to contribute to acid rain, smog formation, ozone layer depletion, and adverse health effects (Crutzen, 2016).

2.3.2. Storage and Transportation Challenges of Ammonia

Ammonia has a high energy density that allows it to be transported in small quantities to meet the energy requirements of ships, thus requiring less storage space and potentially extending the range of the ship (Al-Aboosi, El-Halwagi, Moore, & Nielsen, 2021). Ammonia is non-flammable in the air (Klerke, Christensen, Nørskov, & Vegge, 2008), minimizing explosion or fire risks. However, secondary ignition fuel, such as natural gas or hydrogen, is required for combustion. In maritime transportation, ammonia can be used as fuel for ship engines (McKinlay et al., 2021). Ammonia is one of several hydrogen carriers that can be used as fuel in internal combustion engines. Additionally, compressed or liquefied forms of ammonia can be stored and transported to adequately meet ships' energy needs. Nonetheless, a major concern regarding ammonia pertains to its high toxicity, capable of inducing loss of consciousness even at relatively low levels of exposure (Klerke et al., 2008; Little, Smith III, & Hamann, 2015). Thus, preventing direct contact with humans is crucial when large quantities of ammonia are stored, both onshore and offshore. In this case, security standards need to be improved, which may result in higher capital costs and storage space requirements (such as an extra layer of containment). Ammonia is extremely corrosive, so storage options need to be carefully considered to prevent material degradation.

2.4. Methanol

Methanol is an industrial compound also known as methyl alcohol or wood alcohol. It has the chemical formula CH_3OH (Figure 1) and is a colorless, flammable liquid. In maritime transportation, methanol is typically produced from biomass or natural gas sources (Xing, Stuart, Spence, & Chen, 2021). Methanol is a low-flashpoint, sulfur-free, and easily storable liquid fuel.

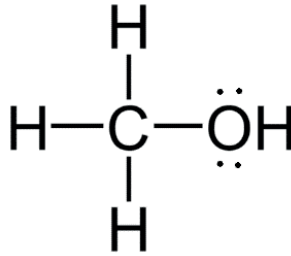


Figure 1. Methanol structure.

2.4.1. Emission Levels of Methanol

Compared to traditional marine fuels, methanol generates fewer emissions and has a smaller carbon footprint (Rony et al., 2023). Additionally, since methanol contains no nitrogen or sulfur content, SO_x emissions are negligible (Gilbert et al., 2018). Although NO_x can still be formed owing to the air's nitrogen concentration, it is believed to be substantially less than ammonia levels and around 60% less than HFO (DnV, 2016). Stena Germanica, the first marine vehicle powered by methanol, reduced carbon dioxide emissions by 25%, nitrogen oxide emissions by 60%, sulfur oxide emissions by 99%, and particle emissions by 95% (Rony et al., 2023).

2.4.2. Storage and Transportation Challenges of Methanol

Methanol has a larger explosion range than LNG, HFO, or ammonia due to its low flashpoint of 12°C. Even yet, hydrogen has a flashpoint of -231°C, making it less explosive (Mazloomi & Gomes, 2012). However, the serious toxicity of methanol to humans (Class 2) is of greatest concern (Kavet & Nauss, 1990; Pharmacopeia, 2016). As a result, the IMO contends that storage of methanol will need a more thorough monitoring system than that of existing fuels. The engineering difficulties and financial hazards related to methanol may rise as a result of these safety factors. The bulk of the technology needed for the secure handling and use of methanol on ships is, however, recognized as being in a mature state (DnV, 2016).

2.5. Biofuels

Biofuels are renewable energy sources obtained from biological resources and offered as an alternative to traditional fossil fuels (Noor et al., 2018) (Figure 2). These fuels can reduce the carbon footprint by replacing traditional diesel fuels. These fuels can reduce the carbon footprint by replacing traditional diesel fuels. There are several alternative fuels suitable for the marine industry, these range from straight vegetable oil (SVO) for low-speed engines, biodiesel for low- and medium-speed engines, and bio-LNG for gas engines. Biodiesel attracts attention due to its environmental friendliness, non-toxicity, and

similarity to diesel fuels (Dharma et al., 2016; Johari et al., 2015; Lin, 2013). Biodiesel can be preferred because it can be used in diesel engines without any modifications and it also offers better emission results compared to fossil fuels (Ghazali, Mamat, Masjuki, & Najafi, 2015).



Figure 2. Biofuels processes obtained from biological materials.

2.5.1. Types of Biofuels

First-generation and second-generation biofuels are divided into two categories (Figure 3). While first-generation biofuels are mostly produced from agricultural products such as grains and oilseeds, second-generation biofuels are produced from lignocellulosic materials such as forest waste. Second-generation biofuels have overcome the problems created by first-generation biofuels, despite financial and technical difficulties (Carriquiry, Du, & Timilsina, 2011; Havlík et al., 2011). These issues include competition with food production, limited production potential, and environmental concerns (Sims, Taylor, Saddler, & Mabee, 2008).

First- and second-generation technology can be used to create biodiesel and biogas, respectively. Vegetable oils can be transformed into biodiesel by gasification, followed by Fischer-Tropsch synthesis (a second-generation biofuel), or transesterification (Fatty Acid Methyl Esters, a first-generation biofuel). Anaerobic digestion of biomass can produce biogas, a first-generation biofuel, whereas gasification and subsequent methanation of biomass can produce biomethane, a second-generation biofuel.

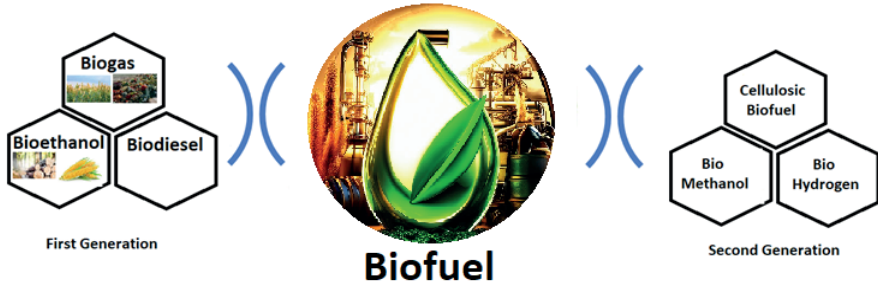


Figure 3. Classification of biofuels.

2.5.2. Emission Levels of Biofuels

One significant advantage of biofuels over fossil fuels is their lower carbon emissions. Plant-based biofuels absorb carbon from the atmosphere through photosynthesis, resulting in a net reduction in carbon emissions. Biofuels also contain minimal sulfur or aromatics. Some studies suggest that biodiesel use can reduce greenhouse gas emissions by up to 78% (Firoz, 2017).

2.5.3. Renewable and Sustainable Sources

Biofuels can be continuously produced from renewable sources, enhancing energy security and reducing dependence on finite fossil fuel resources.

2.5.4. Resources for Biofuel Production

Various resources can be used for biofuel production, providing diversity. Commonly used resources include vegetable oils. Pure vegetable oils may also be utilized if they are acceptable to the engine’s specs. Because it is a liquid fuel, biodiesel may use the same infrastructure as HFO and marine gas oil (MGO). Additionally, biodiesel serves as a natural lubricant. Mixing biodiesel with petroleum diesel increases lubrication, reduces engine wear, and extends engine life (Noor et al., 2018). Rapeseed and soybean oils are frequently used to make biodiesel in Europe and the United States, whereas palm oil is utilized to make biodiesel in tropical nations like Indonesia, Malaysia, Thailand, and Colombia. However, the production of biofuels requires agricultural land and soil resources, potentially competing with food production and causing environmental issues if not managed properly.

2.6. Wind and Solar Energy

Zero-carbon fuels generated from renewable sources, such as wind, or solar, are considered promising options by the EU to achieve desired greenhouse gas reductions (Lindstad, Lagemann, Riiland, Gamlem, & Valland, 2021). Incorporating wind turbines and solar panels into ship design can partially fulfill energy needs from renewable sources (Figure 4).



Figure 4. Ship designed with sails and solar panels.

2.6.1. Wind Energy

The process of producing electricity from the kinetic energy of the wind is known as wind energy. In maritime transportation, wind energy can be utilized in the following ways:

Sails: Some modern ships use sails as an alternative to traditional fuel-powered engines (*Figure 5*). These sails capture wind energy to propel the ship. This technology is used, especially in large cargo ships and dedicated sailing vessels designed for maritime transportation. Rutkowski noted that about 200 years ago, sailing vessels traveling the oceans achieved speeds of 16 knots or more without using a drop of oil while transporting goods worldwide without emissions (Rutkowski, 2016).



Figure 5. A modern ship using sails as alternative fuel.

Wind Turbines: Platforms or ships at sea can be equipped with wind turbines that generate electricity using wind power. This electricity can be used to meet the ship's needs or stored for later use.

Ship Design: Some ships are designed to have different aerodynamic features, consume less energy, and use the wind more efficiently. By 2035, a number of technologies that are now under testing should be economically feasible. The German business SkySails has added auxiliary towing kites to two multifunction ships and one bulk carrier. Rotors have been tested on various cargo ships traveling between Rotterdam and Teesport, UK, by the shipping company Bore (Li, Zhang, Li, Zhang, & Guo, 2021).

Wind energy can help reduce the use of fossil fuels and minimize environmental impacts in maritime transportation. According to Chou et al., the use of Wind-assisted Ship Propulsion (WASP) technology has the potential to reduce emissions by more than 20% (Chou, Kosmas, Acciaro, & Renken, 2021). Furthermore, these energy sources offer the potential to reduce energy costs for ship operators and provide energy independence.

2.6.2. Solar Energy

Solar energy includes using photovoltaic, or PV, panels or thermal collection devices to convert sunlight into electricity or heat. Solar energy can be used in maritime transportation in several ways:

On-Deck PV Panels: Some ships are equipped with solar energy panels. These panels convert sunlight into electrical energy, which can meet the ship's energy requirements. Depending on the type of sails being used, solar panels can be positioned either horizontally or vertically on the deck. To increase the area where solar energy is collected, this method can be paired with mast-like structures used for wind technology (Rony et al., 2023).

Solar Collectors: Thermal solar collectors are used to convert sunlight into heat energy. This heat energy can be utilized to meet the ship's heating or hot water needs (Sandal, 2006).

Energy Storage: Solar energy can be stored using batteries or other energy storage systems, making it available for use during the night or when sunlight is weak.

Solar energy is a clean and sustainable energy source for maritime transportation. Integrating solar panels onto ship decks can improve energy efficiency and reduce environmental impacts. Smith et al. assumed a reduction in auxiliary motor fuel consumption between 0.1% and 3% when using solar energy (Smith et al., 2016). Bouman et al. reported potential carbon dioxide reductions ranging from 0.2% to 12% in various studies (Bouman, Lindstad, Riialand, & Strømman, 2017).

Both energy sources play a vital role in a greener future for maritime transportation. These renewable energy sources have the potential to make the industry more sustainable and reduce its carbon footprint. Wind, waves, and solar energy systems can be installed on a wide range of ships, from large vessels like car carriers, bulk cargo ships, passenger ferries, and oil tankers to smaller vessels like commuter ferries, riverboats, and pleasure craft (Rutkowski, 2016).

Conclusion

One of the most important problems facing the world is environmental problems, and the maritime industry plays a big role in these problems. The shipping industry has a major obligation to significantly reduce greenhouse gas emissions to keep global temperature increases under control. The shipping industry's emissions reduction targets become more challenging with the increasing need for national and international maritime commercial activities.

The International Maritime Organization (IMO) has taken significant steps to encourage and help the industry significantly reduce greenhouse gas emissions. He emphasized how important it is to make maritime services independent of fossil fuels and continues to work on this issue. However, despite the commercial use of alternative fuels, a permanent transformation has not yet occurred.

Bouman and others noted in their study that rapidly adopting multiple measures to reduce emissions and using these measures together could achieve an emissions reduction of over 75%. In other words, greenhouse gas emissions can be reduced by 4-6 times for each unit of cargo transported with current technologies by 2050. In this regard, significant amounts of fuel and greenhouse gas savings can be achieved through measures such as

slow steaming, changes in ship design, use of renewable resources, and their combined application.

Safety/risk assessments are important in using alternative fuels in maritime transportation. These evaluations evaluate the safety of alternative fuels, focusing on cargo transportation, storage and crew health (Zincir & Deniz, 2018). Accordingly, depending on the type of alternative fuel to be used, improvements may be needed in components such as fuel tanks, fuel preparation rooms and fuel supply systems in ship engine systems, which may lead to additional costs. However, it is also critical to develop port infrastructures, adapt to new technologies, and increase investments and research to encourage and disseminate alternative fuels.

In this study, the potential of the maritime sector to reduce emissions and the use of alternative energy sources to achieve this goal were examined. While the shipping industry can implement a variety of technological and operational measures to reduce greenhouse gas emissions, it is clear that no single measure is insufficient to achieve significant sector-wide reductions.

REFERENCES

- Al-Aboosi, F. Y., El-Halwagi, M. M., Moore, M., & Nielsen, R. B. (2021). Renewable ammonia as an alternative fuel for the shipping industry. *Current Opinion in Chemical Engineering*, 31, 100670.
- Ali, O. M., Mamat, R., & Faizal, C. K. M. (2013). Review of the effects of additives on biodiesel properties, performance, and emission features. *Journal of renewable and sustainable energy*, 5(1).
- Ampah, J. D., Yusuf, A. A., Afrane, S., Jin, C., & Liu, H. (2021). Reviewing two decades of cleaner alternative marine fuels: Towards IMO's decarbonization of the maritime transport sector. *Journal of Cleaner Production*, 320, 128871.
- Balcombe, P., Brierley, J., Lewis, C., Skatvedt, L., Speirs, J., Hawkes, A., & Staffell, I. (2019). How to decarbonise international shipping: Options for fuels, technologies and policies. *Energy conversion and management*, 182, 72-88.
- Balcombe, P., Staffell, I., Kerdan, I. G., Speirs, J. F., Brandon, N. P., & Hawkes, A. D. (2021). How can LNG-fuelled ships meet decarbonisation targets? An environmental and economic analysis. *Energy*, 227, 120462.
- Bengtsson, S., Andersson, K., & Fridell, E. (2011). A comparative life cycle assessment of marine fuels: liquefied natural gas and three other fossil fuels. *Proceedings of the Institution of Mechanical Engineers, Part M: Journal of Engineering for the Maritime Environment*, 225(2), 97-110.
- Bouman, E. A., Lindstad, E., Rialland, A. I., & Strømman, A. H. (2017). State-of-the-art technologies, measures, and potential for reducing GHG emissions from shipping—A review. *Transportation Research Part D: Transport and Environment*, 52, 408-421.
- Carriquiry, M. A., Du, X., & Timilsina, G. R. (2011). Second generation biofuels: Economics and policies. *Energy Policy*, 39(7), 4222-4234.
- Chou, T., Kosmas, V., Acciaro, M., & Renken, K. (2021). A comeback of wind power in shipping: An economic and operational review on the wind-assisted ship propulsion technology. *Sustainability*, 13(4), 1880.
- Crutzen, P. J. (2016). The influence of nitrogen oxides on atmospheric ozone content. *Paul J. Crutzen: A Pioneer on Atmospheric Chemistry and Climate Change in the Anthropocene*, 108-116.
- Deniz, C., & Zincir, B. (2016). Environmental and economical assessment of alternative marine fuels. *Journal of Cleaner Production*, 113, 438-449.
- Dharma, S., Masjuki, H., Ong, H. C., Sebayang, A., Silitonga, A., Kusumo, F., & Mahlia, T. (2016). Optimization of biodiesel production process for mixed *Jatropha curcas*–*Ceiba pentandra* biodiesel using response surface methodology. *Energy conversion and management*, 115, 178-190.
- DnV, G. (2016). Methanol as marine fuel: Environmental benefits, technology readi-

- ness, and economic feasibility. <http://www.imo.org/fr/OurWork/Environment/PollutionPrevention/AirPollution/Documents/ReportMethanol>, 21, 2016.
- Endresen, Ø., Sørgård, E., Sundet, J. K., Dalsøren, S. B., Isaksen, I. S., Berglen, T. F., & Gravir, G. (2003). Emission from international sea transportation and environmental impact. *Journal of Geophysical Research: Atmospheres*, 108(D17).
- Ergin, A., & Ergin, M. F. (2021). THE ROLE OF ANTIFOULING COATING IN THE MARINE INDUSTRY. *Research & Reviews in Engineering*, 53.
- Ergin, A., & Sandal, B. (2023). Mobbing among seafarers: Scale development and application of an interval type-2 fuzzy logic system. *Ocean Engineering*, 286, 115595.
- Eyring, V., Köhler, H., Lauer, A., & Lemper, B. (2005). Emissions from international shipping: 2. Impact of future technologies on scenarios until 2050. *Journal of Geophysical Research: Atmospheres*, 110(D17).
- Firoz, S. (2017). A review: advantages and disadvantages of biodiesel. *International Research Journal of Engineering and Technology*, 4(11), 530-533.
- Ghazali, W. N. M. W., Mamat, R., Masjuki, H. H., & Najafi, G. (2015). Effects of biodiesel from different feedstocks on engine performance and emissions: A review. *Renewable and Sustainable Energy Reviews*, 51, 585-602.
- Gilbert, P., Walsh, C., Traut, M., Kesime, U., Pazouki, K., & Murphy, A. (2018). Assessment of full life-cycle air emissions of alternative shipping fuels. *Journal of Cleaner Production*, 172, 855-866.
- Goldmann, A., Sauter, W., Oettinger, M., Kluge, T., Schröder, U., Seume, J. R., . . . Dinkelacker, F. (2018). A study on electrofuels in aviation. *Energies*, 11(2), 392.
- Gong, Y., Yao, J., Wang, P., Li, Z., Zhou, H., & Xu, C. (2022). Perspective of hydrogen energy and recent progress in electrocatalytic water splitting. *Chinese Journal of Chemical Engineering*, 43, 282-296.
- Gopinath, M., & Marimuthu, R. (2022). A review on solar energy-based indirect water-splitting methods for hydrogen generation. *International Journal of Hydrogen Energy*, 47(89), 37742-37759.
- Havlík, P., Schneider, U. A., Schmid, E., Böttcher, H., Fritz, S., Skalský, R., . . . Kraxner, F. (2011). Global land-use implications of first and second generation biofuel targets. *Energy Policy*, 39(10), 5690-5702.
- Hwang, S. S., Gil, S. J., Lee, G. N., Lee, J. W., Park, H., Jung, K. H., & Suh, S. B. (2020). Life cycle assessment of alternative ship fuels for coastal ferry operating in Republic of Korea. *Journal of Marine Science and Engineering*, 8(9), 660.
- IMO, D. (2018). Adoption of the initial IMO strategy on reduction of GHG emissions from ships and existing IMO activity related to reducing GHG emissions in the shipping sector. In: International Maritime Organization (IMO) London.
- Jain, I. (2009). Hydrogen the fuel for 21st century. *International Journal of Hydrogen Energy*, 34(17), 7368-7378.

- Johari, A., Nyakuma, B. B., Nor, S. H. M., Mat, R., Hashim, H., Ahmad, A., . . . Abdullah, T. A. T. (2015). The challenges and prospects of palm oil based biodiesel in Malaysia. *Energy*, 81, 255-261.
- Joung, T.-H., Kang, S.-G., Lee, J.-K., & Ahn, J. (2020). The IMO initial strategy for reducing Greenhouse Gas (GHG) emissions, and its follow-up actions towards 2050. *Journal of International Maritime Safety, Environmental Affairs, and Shipping*, 4(1), 1-7.
- Kavet, R., & Nauss, K. M. (1990). The toxicity of inhaled methanol vapors. *Critical reviews in toxicology*, 21(1), 21-50.
- Kim, H., Koo, K. Y., & Joung, T.-H. (2020). A study on the necessity of integrated evaluation of alternative marine fuels. *Journal of International Maritime Safety, Environmental Affairs, and Shipping*, 4(2), 26-31.
- Klerke, A., Christensen, C. H., Nørskov, J. K., & Vegge, T. (2008). Ammonia for hydrogen storage: challenges and opportunities. *Journal of Materials Chemistry*, 18(20), 2304-2310.
- Li, B., Zhang, R., Li, Y., Zhang, B., & Guo, C. (2021). Study of a new type of Flettner rotor in merchant ships. *Polish Maritime Research*.
- Lin, C.-Y. (2013). Strategies for promoting biodiesel use in marine vessels. *Marine Policy*, 40, 84-90.
- Lindstad, E., Lagemann, B., Riialand, A., Gamlem, G. M., & Valland, A. (2021). Reduction of maritime GHG emissions and the potential role of E-fuels. *Transportation Research Part D: Transport and Environment*, 101, 103075.
- Little, D. J., Smith III, M. R., & Hamann, T. W. (2015). Electrolysis of liquid ammonia for hydrogen generation. *Energy & Environmental Science*, 8(9), 2775-2781.
- Mazloomi, K., & Gomes, C. (2012). Hydrogen as an energy carrier: Prospects and challenges. *Renewable and Sustainable Energy Reviews*, 16(5), 3024-3033.
- McKinlay, C. J., Turnock, S. R., & Hudson, D. A. (2021). Route to zero emission shipping: Hydrogen, ammonia or methanol? *International Journal of Hydrogen Energy*, 46(55), 28282-28297.
- Noor, C. M., Noor, M., & Mamat, R. (2018). Biodiesel as alternative fuel for marine diesel engine applications: A review. *Renewable and Sustainable Energy Reviews*, 94, 127-142.
- Pharmacopeia, U. (2016). USP 39-NF34. *The United States Pharmacopeial*.
- Rony, Z. I., Mofijur, M., Hasan, M., Rasul, M., Jahirul, M., Ahmed, S. F., . . . Show, P. L. (2023). Alternative fuels to reduce greenhouse gas emissions from marine transport and promote UN sustainable development goals. *Fuel*, 338, 127220.
- Rutkowski, G. (2016). Study of Green Shipping Technologies-Harnessing Wind, Waves and Solar Power in New Generation Marine Propulsion Systems. *International Journal on Marine Navigation and safety of sea transportation*, 10(4).
- Sandal, B. (2006). *Güneş Enerjili Konut Isıtma Sistemlerinin F-Grafik Yöntem İle Op-*

- timum Boyutlandırılması*. Yüksek Lisans Tezi, İstanbul Üniversitesi, İstanbul,
- Shi, W., & Li, K. X. (2017). Themes and tools of maritime transport research during 2000-2014. *Maritime Policy & Management*, 44(2), 151-169.
- Shih, C. F., Zhang, T., Li, J., & Bai, C. (2018). Powering the future with liquid sunshine. *Joule*, 2(10), 1925-1949.
- Sims, R., Taylor, M., Saddler, J., & Mabee, W. (2008). From 1st-to 2nd-generation biofuel technologies. *Paris: International Energy Agency (IEA) and Organisation for Economic Co-Operation and Development*, 16-20.
- Smith, T., Raucci, C., Hosseinloo, S. H., Rojon, I., Calleya, J., De La Fuente, S. S., . . . Palmer, K. (2016). CO2 emissions from international shipping: Possible reduction targets and their associated pathways. *UMAS: London, UK*.
- UNCTAD. (2021). *United Nations Conference on Trade and Development, 2021 Review of Maritime Transport 2021*. Retrieved from
- Wang, S., & Notteboom, T. (2014). The adoption of liquefied natural gas as a ship fuel: A systematic review of perspectives and challenges. *Transport Reviews*, 34(6), 749-774.
- Wang, Y., Chen, K. S., Mishler, J., Cho, S. C., & Adroher, X. C. (2011). A review of polymer electrolyte membrane fuel cells: Technology, applications, and needs on fundamental research. *Applied energy*, 88(4), 981-1007.
- Wolny, P., Tuśnio, N., & Mikołajczyk, F. (2022). Explosion Risks during Firefighting Operations in Storage Rooms and the Transport of Ammonium Nitrate-Based Fertilizers. *Sustainability*, 14(14), 8565.
- Xing, H., Stuart, C., Spence, S., & Chen, H. (2021). Alternative fuel options for low carbon maritime transportation: Pathways to 2050. *Journal of Cleaner Production*, 297, 126651.
- Xu, H., & Yang, D. (2020). LNG-fuelled container ship sailing on the Arctic Sea: Economic and emission assessment. *Transportation Research Part D: Transport and Environment*, 87, 102556.
- Zamfirescu, C., & Dincer, I. (2008). Using ammonia as a sustainable fuel. *Journal of Power Sources*, 185(1), 459-465.
- Zincir, B., & Deniz, C. (2018). Assessment of alternative fuels from the aspect of ship-board safety. *Journal of ETA Maritime Science*, 6(3), 199-214.
- Züttel, A. (2003). Materials for hydrogen storage. *Materials today*, 6(9), 24-33.

Chapter 10

EFFECTS OF EARTHQUAKES ON GROUNDWATER: THE CASE OF KAHRAMANMARAŞ

Göknur KAYATAŞ ONGUN¹

Arda YALÇUK²

1 Dr. Göknur Kayataş Ongun, Bolu Abant İzzet Baysal Üniversitesi, goknurezgi.kayatas@gmail.com

2 Prof.Dr. Arda Yalçuk, Bolu Abant İzzet Baysal Üniversitesi, ayalcuk@gmail.com

INTRODUCTION

Nowadays, although scientific and public awareness studies and preparations for pollution disaster types are sufficient, especially in developed countries, sometimes natural (earthquake, landslide, tsunami, volcanism, flood, etc.) and artificial disasters (power plant/hazardous material facility explosions, oil/radioactive substance leaks, chemical fires, etc.) that exceed these limits occur despite all knowledge, attention, and precautions. Effects of disasters sometimes occur due to anthropogenic (human-induced) reasons, such as the failure to comply with regulations in practice or the failure to update existing regulations in a timely manner according to changing conditions. Hence the structural damage that occurs after these events and the pollutants that are brought or carried by water, mud, gas clouds or rain, flood and wind may be the main reasons for various types of environmental disasters by affect large-medium-small scale areas with environmental impacts and risks.

The relationship between groundwater level changes and earthquakes is established on a scientific and project basis in many countries of the world. In Turkey, which is important in terms of earthquake and groundwater potential, revealing the effects of earthquakes on aquifers at an academic level becomes important after these developments. To determine the groundwater potential throughout Turkey and monitor changes that may occur in aquifers, groundwater level measurements are performed with limnigraphs in suitable boreholes (Özel, 2020).

Water quality can also be impacted by earthquakes when the earthquake is at least strong enough to be felt. Well, water can become cloudy, especially since the shaking movement brings out loose sediment from pores and cracks in rocks supplying water to the well. This is a temporary condition, and its effects disappear within hours or days. However, severe earthquakes can also damage sewer lines, gas lines, or any infrastructure containing hazardous materials, causing more specific pollutants to enter the water and resulting in more significant effects on water quality. Therefore, sampling and analyzing spring and well water before and after earthquakes is extremely important to detect such changes and take precautions. Apart from these, earthquakes can increase subsurface permeability and connect aquifers containing water with different chemical structures. However, since the effect of such events on water quality is quite low, they are difficult to detect and are unlikely to pose a danger to public health (Kırmızıtaş & Kaya, 2000).

GROUNDWATER

All water that is stationary or in motion underground is called groundwater (Law on Groundwater No. 167 dated 16/12/1960, Official Gazette Number: 10688). The fact that groundwater is the largest freshwater resource in the world after glaciers (Uluatam, 1998) shows how important

this freshwater resource is. In this regard, studies on groundwater, which is a hidden resource, gain importance.

Formation of Groundwater

Some of the precipitation that falls to the ground flows into rivers and lakes. Some of this precipitation is also used by vegetation. Another part of this precipitation evaporates and returns to the atmosphere. The remaining part of the precipitation infiltrates into the soil. Water leaking from the soil surface to the unsaturated zone reaches the saturated water surface. The water below the saturated zone is called groundwater. This is how groundwater is formed in summary. Once groundwater reaches the aquifer, it will not remain stationary and will continue to move until it discharges into another aquifer, lake, river, or ocean. The zone called aquifer is the name given to the permeable place where groundwater is located. At the same time, groundwater is charged by melting snow and water flowing under some lakes and rivers. Excessive crop irrigation can also recharge groundwater (Yılmaz, 2021; IGRAC, 2018).

Contrary to popular belief, groundwater does not exist in the form of underground veins or rivers. It fills the gaps and cracks of rocks under the surface, just like water fills the gaps of a sponge. Precipitation is the source of all groundwater. Precipitation falling to the surface wets the ground and moves downward through the unsaturated zone under the influence of gravity. It reaches the upper limit of the saturated zone, called the water level, and feeds the groundwater stored in water-bearing layers called aquifers.

Importance of Groundwater

When we exclude glaciers, it can be seen that groundwater is the largest freshwater resource in the world. In addition to being used as drinking water, groundwater is also an important resource used in industry and agriculture. Groundwater is a crucial resource that must be protected not only because of these features but also because of its environmental value. Groundwater contributes to the flow of many rivers, and it can contribute to more than 90% of the flow even during less regular flow periods in the summer months. Hence a negative situation that may occur in groundwater may also cause adverse effects on other waters. Groundwater is important because it is usually located in regions where surface water resources are limited, its water quality is good and does not change throughout the year, it meets the needs during summer months and drought periods, it does not require large infrastructure costs like surface water, and it does not require costly storage areas for water storage (Yılmaz, 2021).

Groundwater Pollution

Groundwater pollution occurs when pollutants reach groundwater. These pollutants can vary in different types, from solid to liquid waste.

Unlike surface water pollution, groundwater pollution is difficult to detect and control because groundwater is a hidden resource. Therefore, it is of vital importance to take the necessary precautions before groundwater pollution. It is easy to take precautions to prevent groundwater pollution, but cleaning after pollution will be difficult.

EARTHQUAKE

Earthquakes occur as a result of the movement of fractures known as fault lines in the uppermost layer of the earth's crust. The fault line is formed as a result of the rocks on the earth's crust fracturing under high-pressure conditions such as tension and compression.

Turkey is a country where natural disasters frequently occur due to its geological and topographic structure and climate characteristics. If we are to list the natural disasters experienced in Turkey with respect to their effects in percentage terms, earthquakes constitute 64%, floods 15%, landslides 16%, fires 4%, and avalanches and others constitute 1% (Erkoç, 2004). Compression and expansion forces in the earth's crust play the most crucial role in the formation of faults. Such forces move rock masses along fractures. However, in some parts where rock masses cannot be moved along fractures, it causes intense energy accumulation. The energy accumulated deep in the ground must eventually be discharged in some way, and earth tremors (earthquakes) occur during the discharge of this energy. In short, an earthquake is a phenomenon that develops as a result of the sudden release of energy accumulated on fractures, which are defined as fault planes in the ground. When rocks fracture, an energy release or earthquake occurs. Most earthquakes occur within the elastic part of the earth's crust at a depth of 20-35 km. However, in places where the oceanic crust breaks and dives into the ground, earthquake focuses can also occur at depths of up to 350-400 km. Since the temperature at deeper levels is above 400 °C, the displacement movement can occur in the form of slow plastic deformation without an earthquake (Atabey, 2000).

EARTHQUAKE WAVES

During the release of the energy accumulated along a fracture, seismic waves are emitted to the environment. These seismic waves, which are described as earthquake waves, are first felt as slight shaking and noises resembling gunshots coming from within the ground. Then the tremors suddenly begin to intensify and reach their highest level after a while. After creating the most severe tremor, the earthquake slows down again and continues in the form of mild earthquakes (aftershocks) on the same fracture within the day-year period. There are two types of earthquake waves. These are body and surface waves.

Three types of deformation are observed in underground structures, depending on the characteristics of the earthquake movements that occur and whether these movements are in the same direction as the axis of the structure or perpendicular to the axis of the structure. We can list these deformations as follows:

- Axial stretching and compression
- Longitudinal bending (twisting)
- Ovalization (fracture)

Axial deformations in underground structures are caused by stresses resulting from movements produced by earthquake waves parallel to the axis of the structure (Owen & Scholl, 1981).

WAVE MOVEMENTS CREATED BY EARTHQUAKES

The tremors that occur during an earthquake are caused by wave movements that occur as a result of the stresses and movements at the focus of the earthquake. In other words, the potential energy at the focus of the earthquake turns into kinetic energy with these waves released. We can divide earthquake waves into three types. These are longitudinal, transverse, and surface waves (St. John & Zahrah, 1987).

Longitudinal Waves

Longitudinal waves are called P waves and are the earthquake waves that propagate the fastest and are, therefore, the first recorded on seismographs. Their destruction effect is low, and the vibration movement is in the direction of propagation (Figure 1).

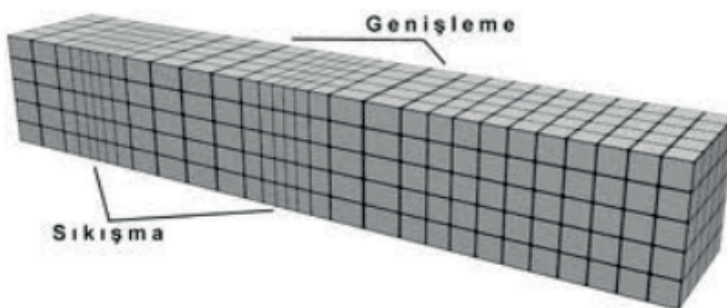


Figure 1. P Wave

Transverse Waves

Transverse waves are slower than longitudinal waves and are called S waves. They are waves recorded secondarily on seismographs. Unlike P waves,

the vibrational movement is perpendicular to the direction of propagation 14. Their propagation speed is low, but they are waves that cause destruction in structures (Figure 2).

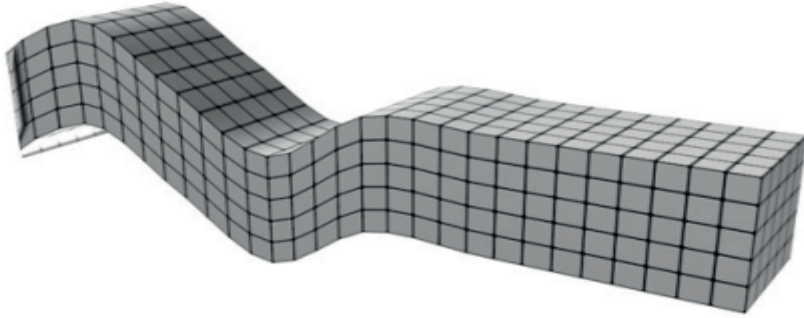


Figure 2. S Wave

Surface Waves

Surface waves are the slowest propagating waves. Their amplitudes are larger than P and S waves. Surface waves are divided into Love (C) and Rayleigh (D) waves. While the Love wave propagates faster, the amplitude of the Rayleigh wave is larger (Figures 3a and 3b).

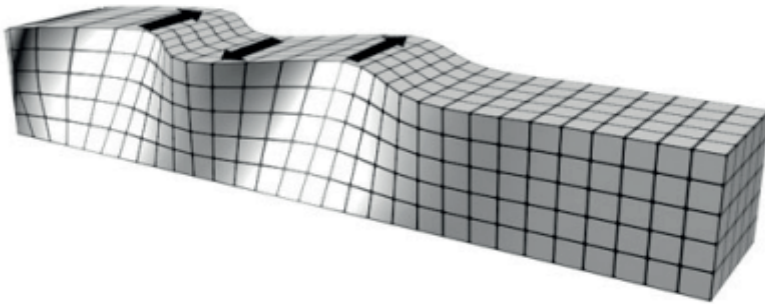


Figure 3a: Love Wave

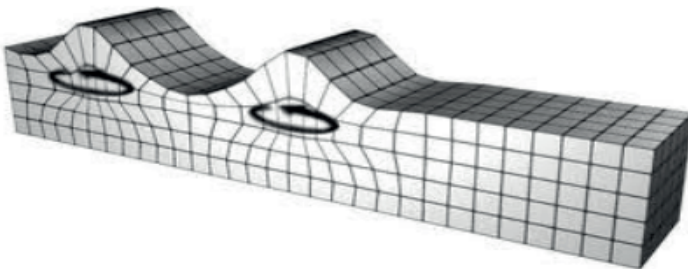


Figure 3b: Rayleigh Wave

Love waves occur in the lower layers, in stratified soils, where the speed of S waves is low, and their speed has a value between the propagation speeds of the S wave on the surface and in the lower layers. The propagation speed of Rayleigh waves is almost close to that of S waves. While S and P waves are subject to refraction and reflection depending on different ground types in which they propagate, local displacement amplitude may increase or decrease. Changes in the topography of the surface on which waves propagate and discontinuities in the lower layers are factors that considerably impact refraction and reflection events. Surface topography is another element influencing surface waves (St. John & Zahrah, 1987).

Aquifer Types

An unconfined aquifer is a layer of water-bearing formations or rocks that does not have a confining bed at the top of the groundwater, called the groundwater table, where the pressure becomes equivalent to atmospheric pressure. The change in groundwater levels varies and depends on pumping from wells, permeability, recharge and discharge area, and actually affects the increasing or decreasing water rates in wells extracted from aquifers. The water table is free to rise or fall, often called the free or water surface. Contour plots and water table profiles of water-using wells can be prepared from well elevations to determine available water quantities as well as water distribution and movement. Accumulated water resources are a case of unconfined aquifers, and their high susceptibility to pollution is a major problem with unconfined aquifers. If something is spilled on the surface, it infiltrates vertically and goes down to the groundwater reservoir.

Confined Aquifer

A confined aquifer is defined as a formation in which groundwater is isolated from the atmosphere by impermeable geological formations at the point of discharge, and confined groundwater is usually subject to pressure higher than atmospheric pressure. It is also known as artesian or pressured aquifers and is mostly formed just above the base of confined rock masses or layers, composed primarily of clay, that can protect it from surface pollution. Wells drilled from artesian aquifers are more prone to fluctuation with water depths due to changes in pressure rather than the amount of water stored. When such an aquifer is well penetrated, as in flowing and artesian wells, the water level should rise above the bottom of the confined layer (Ekinici & Orakoğlu, 2012). Water reaches a confined aquifer in a zone where the confining layer reaches the surface (Figure 4).

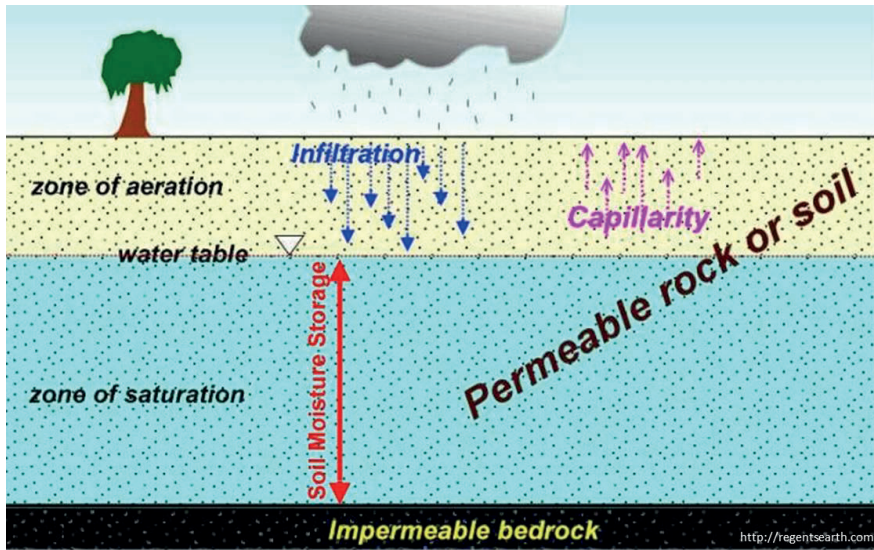


Figure 4. Groundwater and Aquifers

The system of groundwater flow into aquifers, either vertically or horizontally, is frequently affected by gravity and geological formations in such areas. A zone that supplies water to a restricted area is considered a recharge area, and water can even leak into a confined bed. The ups and downs of water in confined aquifers penetrating wells are primarily caused by pressure changes rather than storage volume changes. Confined aquifers, therefore, show only limited variation in storage and are predominantly used as conduits to transport water from recharge areas to natural or artificial discharges.

Leaky Aquifer

Completely unconfined or confined aquifers are less common than leaky or semi-confined aquifers. This is common under plains, alluvial valleys, a semi-permeable aquitard, a semi-confining bed or in old lake basins covered by a permeable layer. Pumping water from a well into a leaky aquifer removes water in two directions, including vertical flow from the aquitard to the aquifer and horizontal flow within the aquifer.

Fractured Aquifer

Fractured rock aquifers differ from groundwater systems stored in geological formations. Sedimentary aquifers retain and move significant amounts of water through the pore spaces between certain sedimentary granules. Therefore, fractured rock aquifers have hydraulic properties (in common with terms defined as drilling yield) that differ from those in

sedimentary aquifers with accessible water. It is typically defined by the nature (opening, size, and extent) and the degree of connectivity in the rock mass between discontinuities. In fractured rock aquifers, the long-term yield from a well depends on the location of the discontinuity degree and the relationship of discontinuities in the total rock mass rather than on the permeability of geological materials near the extraction stage. Moreover, aquifers in fractured rock typically depend on precipitation, which results in surface water runoff that is significantly greater than in flat areas (Ekinici & Orakoğlu, 2012).

Features of the Aquifer

There are various features contributing to the identification and characterization of the aquifer. These features of the aquifer are as follows:

Porosity

Porosity (n) is an intrinsic property of a substance and refers to the amount of voids or empty spaces in any material. Porosity (voids) is defined by the ratio between the volume of empty space and the volume of rocks/soil when formed between the soil or rock fragments.

Hydraulic conductivity and permeability

Permeability is defined as the ability of water to move through rock or soil, which is directly related to porosity and applies to interconnected pore spaces in the rock or soil. Considering the relationship between repulsive and resisting forces on a microscopic scale during flow into a porous medium, the permeability K defined is a function only of the area where hydraulic conductivity occurs (Figure 5).

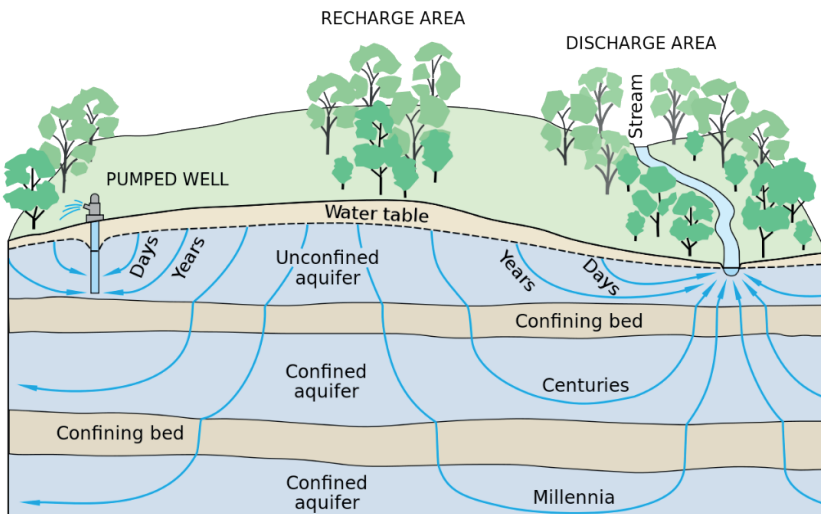


Figure 5. Schematic of an aquifer showing confined zones, groundwater travel times, a spring and a well

Hydraulic conductivity (K) is a physical property that calculates the capacity of a material in the context of an applied hydraulic gradient to transport water through rock/soil pore spaces and fractures. Porosity depends on various physical variables, including the structure of the soil matrix, grain size distribution, type of soil fluid, particle arrangement, water content, void ratio, and other factors.

DISASTER AND POLLUTION

Pollution and Environmental Problems After Disasters

Despite today's knowledge and precautions, material and moral losses and serious environmental problems still occur after natural and artificial disasters or as a result of industry and human activities, which are a necessity of urban life. As is known, pollution is an important environmental problem, regardless of its source and type, and nowadays, it is still an increasing problem despite all kinds of legal measures, warnings, and scientific and technological developments related to the elimination of pollution. Therefore, whether on a global or a regional and local scale, a secondary disaster occurs after natural events such as earthquakes, volcanism, tsunamis, and floods, or due to industry, urban life, and construction areas. This disaster is pollution and can also be a source of new secondary pollution. This secondary disaster situation can also impact an area suddenly and on a large scale. On the other hand, even if the area that it affects is small in the beginning, it can create a wider area of impact with a rapid spread from the interference areas in a very short time. This type of secondary disaster may be an air, water, soil, odor, and visual pollution event that occurs suddenly at the first stage. However, pollution disasters that emerge after natural events can also occur by artificial means. These may be caused by power plant explosions, oil/radioactive substance leaks, chemical fires (oil-chemical production facility fire, mining accidents, etc.), and problems during periods of social conflict and turmoil. Although precautions are initially taken for all these known problems, tsunami disasters occur after major earthquakes in countries with ocean or sea coasts on active earthquake zones (Özel, 2020). Volcanoes become active from time to time in countries with active volcanism (for example, Iceland and Pacific island countries), and depending on the character of the volcano, bad weather conditions with intense smoke, fragmented rock and ash showers from the explosion, or mud volcano disasters in the form of flows (such as in Hawaiian volcanoes), or nuclear power plant explosions, oil and chemical fire events lead to disasters. However, if a classification is to be made, these disasters can be divided into three groups. The first group of disasters: These are the pollution and environmental problems caused by natural events such as earthquakes, landslides, tsunamis, volcanism, storms, and floods. Natural events are the most common events, and their impact area can sometimes be very large, depending on the type of disaster. They can impact cities, countries,

and sometimes even life and living spaces in a large part of a continent (e.g., the Sumatra (Indonesia) earthquake and tsunami, the great Marmara (Turkey) earthquake). The second group of disasters: These are disasters resulting from artificially caused power plant explosions, chemical fires and leakage-related nuclear, oil and similar chemical events and the pollution and environmental problems arising from them. These problems are among the most important reasons for the disruption of nutrient, water, and species cycles due to soil and water pollution. Examples include the Chernobyl-Ukraine and Fukushima-Japan power plant explosions, the Gulf of Mexico oil spill and fires. The third group of disasters: These are pollution and environmental problems arising from the disruption of waste disposal in cities, its obstruction, and temporary inability to perform it due to problems experienced in waste disposal in local governments, industries, and across the country/countries, particularly during periods of civil wars, terrorism, economic crisis, and mismanagement, or the lack of adequate treatment facilities, and wastes abandoned to nature without solid-liquid-gas treatment in industries. Examples of these are gaseous and solid chemical wastes originating from various war materials used in the wars that lasted for many years in the Middle East, the Balkans, and Africa.

After natural and artificial disasters or human-induced leakage pollution in the soil, groundwater/surface water, and mining processing waste pools and pollution disasters in thermal waters can also be a source of secondary pollution disasters. Pollution is a secondary disaster that occurs with various natural events such as earthquakes, volcanism, tsunamis, tornadoes, storms, floods, and climate change. In the pollution caused by these events, the pollution source(s) will be different depending on the type of natural event. Especially as a result of these natural events, various artificial wastes are formed in urban environments or different construction areas (roads, bridges, dams, facilities), all of which create soil, air, water, odor, and visual and noise pollution. For example, soil, groundwater, and surface water pollution with gasses and liquids leaking from damaged infrastructure systems and industrial facilities after the great Marmara earthquake, sea pollution along the seashore with solid-liquid-gas pollutants originating from urban settlements, and thermal pollution near geothermal resources are observed (Özel, 2020).

ABOUT KAHRAMANMARAŞ

Kahramanmaraş province, located in the Eastern Mediterranean, is Turkey's 11th largest city with a surface area of 14.327 km² and 18th most populous city with 1,177,436 inhabitants according to the population data for 2022. It is located between 37-38 northern parallels and 36-37 eastern meridians. Kahramanmaraş province, which has 11 districts, gained the status of metropolitan in 2013. (Figure 6). The northern parts of the province, which has an altitude of 568 m above sea level, are quite mountainous. Approximately 59.7% of its territory is covered with mountains, 0.3% with

plains, and 24% with plateaus and highlands. In Kahramanmaraş province where three different geographical regions (Eastern Anatolia, Mediterranean, and Southeastern Anatolia regions) approach each other, landforms mostly consist of mountains that are extensions of the Southeastern Taurus Mountains and depression areas between them. While the higher parts of mountains mostly consist of bare rocks, the lower belts are covered with forests (URL 1, 2023). The center of Kahramanmaraş is located at the foot of Mountain Ahır. Therefore, the city center is rough. Although some areas outside the city center are flat, it generally has a rough structure. Due to its geographical location and other factors, it has a climate characteristic closer to the “Degraded Mediterranean Climate” among the three different climate types. There is Mediterranean climate in the south of the province, and continental climate in the north. Summer months are hot, while winter months are cold. Moreover, the fact that the territory of the province is located in the transition area of the Mediterranean and Southeastern Anatolia regions has caused the climatic conditions in the province to be different (URL 2, 2023). Kahramanmaraş ranks first in Turkey and third in the world in terms of water resources per kilometer. Furthermore, the Ceyhan River, one of the most important water basins of our country, continues its journey in the Mediterranean through this province. Kahramanmaraş, which currently has 24 rivers, 8 dams, 6 of which are active and 2 of which are under construction, 10 irrigation ponds, 3 natural lakes and 1 wetland, constitutes one of the important water resources of Turkey. Kahramanmaraş, which contains important water resources of our country, also attracts attention with its dams. Sır, Menzelet, Kılavuzlu, Ayvalı, and Kartalkaya dams, which are among the most important dams in Turkey, are located within the provincial borders (Tercan, 2023).

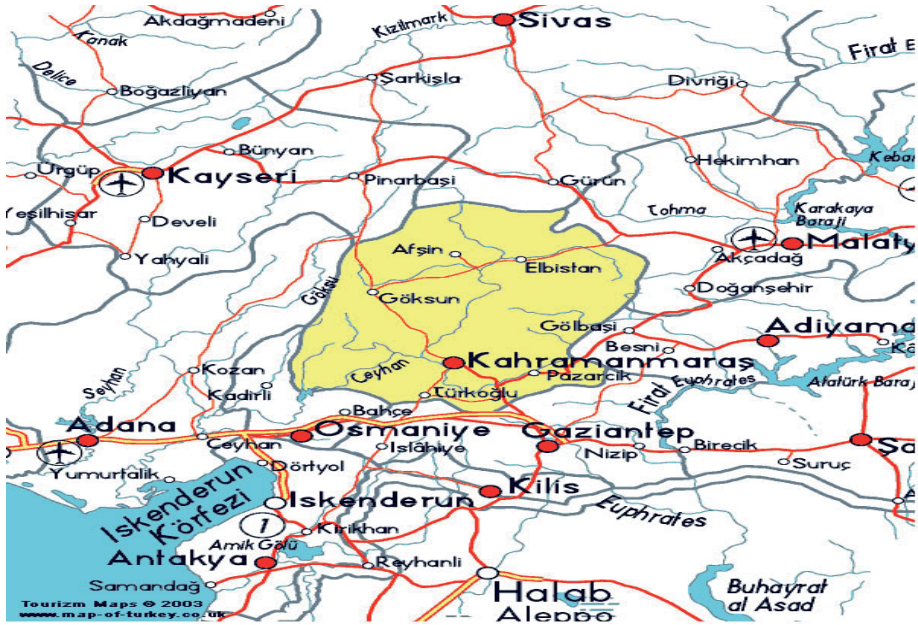


Figure 6. Map of Kahramanmaraş

Kahramanmaraş province is located on the Eastern Anatolian Fault Zone and the Dead Sea Fault Zone. The Eastern Anatolian Fault Zone (EAFZ), formed by the convergence and collision of the Arabian and Eurasian plates, is located in the Alpine-Himalayan orogenic belt. The EAFZ, a NE-trending left-lateral strike-slip fault zone extending for approximately 600 km between the Arabian and Anatolian plates in the east of Turkey, is one of the two most active fault zones in the country. The EAFZ, which extends between Karlıova in the northeast and Hatay in the southwest, plays an important role in terms of the region's geodynamic evolution and earthquake risk. The Dead Sea Fault Zone (DSFZ), which forms the border between the African and Arabian plates, is one of the most important active fault zones in the world. The left-lateral strike-slip EDFZ, extending from the Red Sea in the south to the Eastern Anatolian Fault Zone (EAFZ) in the north, serves as a transform boundary between the Arabian and African plates and forms a tectonic belt about 1000 km in length. The arm that borders the west of the Ghab Basin in the south of Turkey enters the borders of our country from the southeast of Antakya. Proceeding along the Asi River in approximately N-S direction, the DSFZ extends toward the Amik Plain in the north and continues to the north, merging with the EAFZ in the Narlı region (İmamoğlu & Çetin, 2007).

EFFECT OF EARTHQUAKES ON GROUNDWATER QUALITY

Spring and well waters can usually display minor chemical changes before and after earthquakes, which suggests that earthquake shaking can increase permeability below the surface and bring together aquifers with nearby formations containing water with different chemical properties. These changes are very small and are unlikely to pose a danger to human health.

Groundwater levels in wells can oscillate up and down when seismic waves pass through. Water levels may remain high or low for a while after the end of seismic waves, but sometimes long-term changes may occur in groundwater levels following an earthquake. The measurements of the US Geological Research Center determined that the largest earthquake-induced water oscillation recorded in a well varied between 1-1.5 m. It was found that groundwater quality could be affected by earthquakes, typically in locations where shaking is at least strong enough to be felt. The water of the well may become cloudy since the resulting shaking brings out loose sediment from the pores and cracks in rocks that supply water to the well. However, this condition is usually temporary. Large and severe earthquakes can cause more serious effects on groundwater quality by damaging sewer lines, natural gas lines, or infrastructure carrying hazardous materials. Very large earthquakes can even cause water level fluctuations in some wells thousands of kilometers away, depending on the local geological conditions around the well (Rahmani, 2016).

Groundwater level responses to earthquakes have been studied for decades in places near and far from earthquake epicenters. The most common groundwater level response is water level oscillation. This occurs often but is usually not recorded because measurements are not performed frequently to capture it. These level changes may be large enough to provide additional flow into a well, or they may also cause a well near an earthquake to dry out. However, water level changes are 50-60 cm or less. Return to pre-earthquake water level may occur immediately, it may take days or months, or it may not occur at all (Yılmaz, Korkmaz & Korur, 2011).



Figure 7. Groundwater

The oscillation in the groundwater level mostly occurs when the earthquake's seismic wave train arrives but can also be observed after the wave train has passed. Nevertheless, scientists also study changes in groundwater levels before an earthquake (preseismic) (Figure 7).

Changes in groundwater levels mostly occur in the 'near area' of the epicenter of an earthquake. Because earthquakes expose the earth's crust, including aquifer systems, to stress and deformation forces. This deformation process causes fluid pressure in aquifer systems to change and, as a result, can create water levels different from each other. Since the stress and force effects on the system are variable, water level changes can be upward or downward. The compaction of overlying sediments in shallow wells can raise groundwater levels. Alternatively, in a fractured rock aquifer, the cracks supplying water to the well may be widened, occluded, or closed by the wave train of an earthquake. Even new water-bearing fractures can be formed. As a result, water levels in these systems may increase or decrease permanently (Yilmaz, Korkmaz & Korur, 2011).

It is thought that conducting more detailed research to determine the effects of earthquakes on changes in groundwater level, quality, and temperature in Turkey, which is an earthquake country, would be useful for revealing the effects of earthquakes. Earthquakes can cause two important changes in groundwater. (Boulding, 1996). There may be changes in groundwater level and chemistry. While some wells smell like rotten eggs, methane gas, carbon dioxide, and sulfur gases may be mixed in some wells. For example, during the Düzce earthquake in 2022, methane gas inflows were determined in some wells. The temperature increase generally occurs due to geothermal water mixing with groundwater. Water with rising temperatures

should be definitely analyzed before being used for drinking and agricultural irrigation and should be used after obtaining expert opinions. In general, geothermal waters contain heavy metals (sulfur, iron, sulfate, chloride, magnesium, boron, etc.).

The shaking caused by earthquakes will bring out loose sediments from pores and cracks in rocks supplying water to the well, so the water of the well may become cloudy. For example, the water in the wells in Köprübaşı district of Manisa province, which is approximately 1100 km away from the earthquake center, flowed cloudy after the earthquake. Water wells used for agricultural irrigation in the Amik Plain in Hatay and Samandağ district were also impacted and damaged by earthquakes. It is estimated that there are approximately 2,500 wells in the plain and approximately 2,000 of them were damaged by the earthquake. Pipes in deep wells were crushed, fragmented, and bent like the letter 'S.'

Usually, shortly before earthquakes, subtle changes occur in groundwater levels and spring water temperature, hardness, electrical conductivity, and pH. If these changes can be detected before an earthquake, it can give an idea about when an earthquake will occur. However, this method alone is insufficient to predict earthquakes beforehand. However, it is beneficial to use this method because it is easy to observe continuously and has a low cost. It is of great importance that geologists, seismologists, and agriculturalists collaborate and develop these methods (Ekinci & Orakoğlu, 2012).

Turkey has long been known as an “earthquake country” due to its location and geographical structure. Destructive earthquakes have occurred on active fault lines since the Ottoman Empire. The major earthquakes that occurred in our Turkey during the Republic period are the 1930 Hakkari, 1939 Erzincan, 1941 Van-Erciş, 1946 Varto, 1967 Adapazarı, 1971 Bingöl, 1976 Denizli, 1992 Erzincan, 1995 Dinar, 1998 Ceyhan and 1999 Marmara and Düzce, 2003 Bingöl, 2011 Van, 2020 Elazığ, and 2021 İzmir earthquakes. Among these, the 1930 Hakkari, 1939 Erzincan, and 1999 Kocaeli earthquakes had magnitudes greater than 7 Mw (moment magnitude). It is possible to say that earthquakes have caused damage mostly in city centers in recent years in relation to the rate of urbanization and, therefore, the increase in urban population.

The Kahramanmaraş-centered earthquake that hit Turkey on February 6, 2023, is one of the most severe earthquakes of recent years. The earthquakes that occurred on the same day in Pazarcık District of Kahramanmaraş (7.8 Mw) and Elbistan District of Kahramanmaraş (7.7 Mw) caused great damage in eleven provinces, including Adana, Adıyaman, Diyarbakır, Gaziantep, Hatay, Kahramanmaraş, Kilis, Malatya, Osmaniye, Şanlıurfa, and later Elazığ. These earthquakes were recorded as the second and third largest earthquakes in Turkey (İTÜ, 2023; Özer, 2023), (Figure 8). According to the findings of

the Disaster and Emergency Management Presidency and the Ministry of Environment, Urbanization and Climate Change dated March 13, 2023, nearly 17,000 aftershocks occurred, and to date, nearly 301,000 residences and workplaces were destroyed or received moderate to severe damage, more than 50,000 lives were lost, and the cost of these earthquakes is estimated to be approximately 104 billion dollars. According to analyses performed by various institutions, including ITU and METU, the main determining factors in building destruction are the severity of ground movement, the low bearing capacity of the ground on which the foundations of buildings are laid, deficiencies in the building quality in terms of design and structure, the age of buildings, the non-compliance of building construction with the legislation, and the lack of maintenance (TERRA, 2023). Natural disasters and earthquakes can have many causes and consequences.



Figure 8. The moment of February 6, 2023 Kahramanmaraş earthquake.

It is essential to solve the sanitation problem in the aforesaid provinces after the earthquake and provide people with a clean water source. Groundwater, which is a strategic resource, becomes important after such natural disasters. Methane, sulfur, and carbon dioxide gases from sulfide mineralization areas and organic-containing sediments may mix with groundwater or groundwater-supplying wells due to the earthquake effect. Because of ground displacements, the lines carrying drinking water and the lines carrying sewage may break, and therefore, the drinking water may contain pathogens and organic pollution. There is also uncertainty in terms of other water quality parameters, especially pathogenic bacterial content in groundwater and surface water. Additionally, the efficiency of drinking water treatment plants is lost or weakened due to earthquake damage. Furthermore, waste storage areas may interact with surface water and groundwater due to

reasons such as sliding/collapse and polluting these resources. In some cases, new geothermal waters emerge as springs along fault zones, and existing hot waters can mix with cold groundwater that has the potential to be used as drinking water (Keskin, 2014).

Significant changes were observed in the color and taste of natural water resources due to the effect of the earthquake in the region. These changes may have caused the mixing of volatile components under the effect of long and deep fractures during the earthquake, the mixing of rock and mineral particles fractured at depth due to fractures into the water, and especially the interaction of mineral rocks (such as pyrite, chalcopyrite, galena, hematite, limonite) with water, causing the pollution of groundwater. The main elements causing pollution may be mobile elements (such as As, B, U, and Th). The above-mentioned elements are extremely harmful to human health due to their high solubility and high potential to pass into solution. Hence in the region where the earthquake occurred, ophiolitic rocks superimposed on the geologically basic metamorphic rocks and intrusive (Göksun granite) and volcanic rocks intersecting them have a high potential in terms of such mobile element content (Yıldız, 2019).

Samples will be taken from natural water resources in Kahramanmaraş and its surroundings, the brown colored turbidities in these waters will be precipitated, and their mineralogical and geochemical properties will be revealed. It is predicted that the turbidity in the water may be caused by lithologies as a result of particles fracturing and crumbling during the earthquake and/or the ground collapsing toward the bottom. The mineralogical compositions of particles will be revealed, and the same particles will be analyzed geochemically and compared with the mineral and chemical compositions of the surrounding rocks. Moreover, approaches will be shown regarding the possible chemical contamination and pollution source that appeared in water resources immediately after the earthquake. In addition to the color changes of the natural water resources of Kahramanmaraş, according to the images from the press of Şanlıurfa Balıklıgöl, which has a similar feature, the transparent Balıklıgöl gained a completely brown-colored blurry appearance after the earthquake.



Figure 9. Effect of earthquake on groundwater

When earthquake shock waves occur, the groundwater level rises and returns to its previous state over time (Figure 9). Since this happens underground, we cannot see it on the surface. However, it is possible to determine it in observation wells. In some earthquake areas, if there is a water source, it may dry up, or a new source may form. For example, in the city of Santa Rosa, the center of Sonoma County in the US state of California, a dried stream became active again after the earthquake.

WATER AND HYGIENE MANAGEMENT IN THE EARTHQUAKE ZONE

It is possible to provide the most effective solution to the water and hygiene needs that will arise after an earthquake by identifying this risk beforehand and carrying out the necessary work to reduce it to the lowest level, i.e., to a more manageable level. To this end, prefabricated houses, portable toilets and shower cabins, and emergency water wells had to be kept ready in temporary settlement areas. However, unfortunately, it seems that preparation in this regard was not good enough in earthquake regions. In this case, the needs that arise after the earthquake cannot be met, and difficulties in managing the crisis situation occur. Emergency water management is a matter of taking inventory and planning before and after the disaster. What we call planning, in a way, means creating alternatives. Considering the water system of a city, we see surface and underground water resources, water treatment facilities, transmission elements such as distribution lines, water pipes, pumps and valves, and storage and end-use systems as a whole (Buğdaycı, 1999). The process of supplying water to the city consists of various stages, from source to treatment, storage, and distribution. We have to plan solutions for access

to drinking water at the local and neighborhood scale against water cuts that may occur as a result of the collapse or disruption of any of the central systems due to a disaster. It is very important to do this on a neighborhood basis because each neighborhood has different physical characteristics, such as social structure, water infrastructure, and urbanization (Gençoğlu, Özmen & Güler, 1996).

In developed countries, local solutions are produced in emergency disaster plans against major damage to urban infrastructure facilities, such as sewage and clean water lines, and management plans are created to ensure post-disaster water supply. This article examined the possible effects of possible regional water supply and sewage system damage caused by the earthquake in our country and post-damage emergency water management plans. Water and sewage infrastructure facilities are also severely damaged in the earthquake. This situation is one of the issues that should be considered to perform the necessary interventions quickly, both immediately after the earthquake and during the post-earthquake emergency aid period (Kınacı, 2000).

The water network consists of transmission pipelines, tanks, and pumping stations. These units are weak enough to cause serious interruptions in water lines during an earthquake. Drinking water is vital for extinguishing fires, meeting water needs, and cleaning after an earthquake. Experiences gained in past earthquakes have shown that the probability of severe damage to the drinking water network due to ground shaking, liquefaction, landslides, and faulting is very high. The behavior of pipes depends entirely on the damage to the ground in which they are buried or supported. Damage very rarely results from inertial forces.

In the 2022 Provincial Disaster Risk Reduction Plan published by AFAD of Hatay province, one of the centers heavily damaged in the February 6 earthquake, it was shown that the area between Hatay and Kahramanmaraş graben had a high risk of ground amplification, liquefaction, and sinking during a possible earthquake. Most of the residential areas were classified as the Weakest and Weak soil. In the Disaster Risk Reduction Plan of Kahramanmaraş province, it was stated that the Pazarcık region had suitable soil for liquefaction.

It is observed that damage occurs to underground pipes in areas with weak soil properties in Sewage and Drinking Water Supply systems after the earthquake. Kayseri Water and Sewerage Administration was assigned for Kahramanmaraş, which was the epicenter, whereas Antalya Water and Sewerage Administration was assigned for Hatay, and infrastructure works, pipe damage repairs, leak detection with an acoustic ground microphone, and chimney cleaning with combined vehicles are currently carried out.

It is essential to provide water tanks to cities damaged by earthquakes and experiencing problems in water supply and activate the infrastructure systems for the established container cities.

In regions with soft alluvial soil and loose soil, the fact that groundwater levels are close to the surface causes soil amplification by increasing earthquake amplitudes of earthquake waves in case of a possible earthquake (Korkmaz, 2006). Considering the potential for liquefaction in areas with high groundwater levels during earthquakes and similar disasters, damages in the form of overturning, sinking, and bending were observed in buildings during the Kocaeli earthquake of August 17, 1999. The study conducted on buildings and foundation systems due to these damages showed that the design had been made independently of the soil properties and general criteria had not been taken into consideration at all (Gündüz & Arman, 2005).

CONCLUSIONS

Earthquakes create changes in groundwater levels, quality, and temperature. These changes vary depending on some factors, such as the magnitude of the earthquake, the characteristics of the groundwater table, and geological formations. In this regard, studies are conducted in many countries to determine changes in the level and chemical properties of groundwater before, during, and after the earthquake.

Since Turkey is situated in an earthquake zone, losses of life and property due to earthquakes are quite high. The loss of life and property during the Adapazarı earthquake of August 17, 1999 confirmed this fact. When the damages to buildings were carefully examined, it was revealed that many of them were not designed and constructed in accordance with the soil behavior. It emphasizes the fact that the soil factor should be examined in detail for the concept of earthquake-resistant construction and foundation design, and the importance of choosing the foundation system of structures to be built in regions with problematic soils. The simplest explanation of foundation engineering, which is another subject of geotechnical studies, is the selection and sizing of the foundation system using the soil parameters found through research. As a result, geotechnical engineering evaluates the soil on which the structure will be constructed, the type of foundation of the structure to be constructed on the soil, and other factors affecting the foundation as a whole.

It is crucial to allocate funds from aid and state resources to repair irrigation wells, irrigation tools, and machines damaged during the earthquake and bring them into working order.

REFERANCES

1. Özel, S. (2020). Afetlerden Sonra Kirlilik ve İkincil Kirliliği Afet Olarak Değerlendirmek İçin Bir Tartışma. İleri Mühendislik Çalışmaları Ve Teknoloji Dergileri, 1(1), 39-48.
2. Kırmızıtaş, H., Kaya, N. (2000). Depremlerin Yeraltısuyu Seviyelerinde Meydana Getirdiği Değişiklikler Üzerine Bir Araştırma. DSI Teknik Bülteni, Sayı: 96.
3. Yeraltı Suları Hakkında Kanun, Kanun Numarası: 167 Kabul Tarihi: 16/12/1960 Yayımlandığı R. Gazete: Tarih: 23/12/1960 Sayı: 10688 Yayımlandığı Düstur: Tertip: 4 Cilt: 1 Sayfa: 814 (<https://www.mevzuat.gov.tr/mevzuatmetin/1.4.167.pdf>).
4. Uluatam, Ö. (1998). Makro İktisat, Ankara. s.127-128.
5. Yılmaz, M. (2021). Türkiye’de Yeraltı Suları Yönetiminin Yasal ve Kurumsal Açısından İncelenmesi. Dicle Üniversitesi Sosyal Bilimler Enstitü Dergisi, ISSN: 1308 – 6219, Haziran-2021, Sayı:27.
6. <https://www.unigrac.org/sites/default/files/resources/files/20191018%20Report%202018%20-%20print.pdf>.
7. Erkoç, T. (2004). İl ve ilçe Acil Yardım Teşkilatları. İçişleri Bakanlığı Eğitim Dairesi başkanlığı, 88. Dönem Kaymakamlık Kursu Ders Notları. Ankara.
8. Atabey, E. (2000). Deprem. Maden Tetkik ve Arama Genel Müdürlüğü Yayınları Eğitim Serisi No. 34, Ankara.
9. Owen, G. Scholl, R. (1981). Earthquake Engineering of Large Underground Structures. Federal Highway, Administration, and National Science Foundation.
10. St. John, C. M. Zahrah, T. F. (1987). Aseismic Design of Underground Structures. Tunneling and Underground Space Technology, 2, pp. 165-197.
11. URL 1: <https://kahramanmaras.bel.tr/kesfedin/kahramanmarasin-cografyasi/> (2023).
12. URL 2: <https://kahramanmaras.ktb.gov.tr/TR-142132/genel-bilgiler.html> (2023).
13. Tercan, B. (2023). Yüzyılın Afeti: 06 Şubat 2023 Kahramanmaraş Depremleri Üzerine Bir Değerlendirme. Küreselleşen Dünyada Sosyal Bilimler, Duvar Kitapevi, (pp.655).
14. İmamoğlu, M. Ş. Çetin, E. (2007). Güneydoğu Anadolu bölgesi ve yakın yöresinin depremselliği. Dicle Üniversitesi Ziya Gökalp Eğitim Fakültesi Dergisi, (9), 93- 103.
15. Rahmani, G. Y. (2016). Yeraltı Su Seviyesi Yüksek Zeminlerde İksa Sitemlerinin Analizi. Yüksek Lisans Tezi, Çukurova Üniversitesi, Fen Bilimleri Enstitüsü, Adana.
16. Yılmaz, A. Korkmaz, S.Z. Korur, S. (2011). Depremler Ve Sonrasında Karşılaşılan Çevre Sorunları. ISSN:1306-3111, e-Journal of New World Sciences Academy 2011, Volume: 6, Number: 4.
17. Ekinci, C.E. Orakoğlu M.E. (2012). Zeminlerinin Mühendislik Özelliklerinin Be-

- lirlenmesi Üzerine Bir Çalışma. İleri Teknoloji Bilimleri Dergisi, (1), 1-6.
18. Boulding J.R. (1996). "EPA Environmental engineering sourcebook", Ann Arbor Press, Inc., Chelsea, MI, USA, 404 p.
 19. İstanbul Teknik Üniversitesi-İTÜ (2023). 6 Şubat 2023: 04.17 Mw 7,8 Kahramanmaraş ve 13.24 Mw 7,7 Kahramanmaraş Depremleri: Ön İnceleme Raporu, İstanbul Teknik Üniversitesi.
 20. Özer, M. (2023). Education Policy Actions by the Ministry of National Education after the Historical Earthquake Disaster on February 6, 2023 in Türkiye. Bartın University Journal of Faculty of Education, 12(2), 1-14.
 21. Türkiye Earthquakes Recovery And Reconstruction Assessment (TERRA). Presidency Of The Republic Of Turkey Presidency Of Strategy And Budget (2023).
 22. Keskin, C. B. (2014). Deprem Etkisindeki Yeraltı Yapılarının Zaman Tanım Alanında Doğrusal ve Doğrusal Olmayan Çözümlemesi. İstanbul Teknik Üniversitesi, Fen Bilimleri Enstitüsü, Deprem Mühendisliği Programı, Yüksek Lisans Tezi, Mayıs 2014.
 23. Yıldız, D. (2019). Deprem ve Su Raporu.
 24. Buğdaycı, İ. (1999). Depremin Dili. Sismoloji: TÜBİTAK, Bilim ve Teknik, Sayı 382, 26-29.
 25. Gençoğlu, S. Özmen, B. Güler, H. (1996). Yerleşim birimleri ve deprem. Türkiye Deprem Vakfı (TDV).
 26. Kınacı, C. (2000). Deprem ve Çevre. Su Kirlenmesi Kontrol Dergisi, Cilt 10 Sayı:1 sh. 5-8.
 27. Korkmaz, H. (2006). Antakya'da Zemin Özellikleri ve Deprem Etkisi Arasındaki İlişki. Coğrafi Bilimler Dergisi, 49-66.
 28. Gündüz Z. ve Arman H. (2005). Zemin Davranışına Uygun Yapı Tasarımı İlkele-ri ve Uygulanabilirliği. Kocaeli Deprem Sempozyumu, 1237-1243.

A decorative graphic for the chapter title. It features a large, stylized number '11' in a bold, black, serif font. The '11' is set against a green semi-circular background. This is all contained within a white circular area that has a subtle radial gradient. The white circle is surrounded by a thick, light green border that curves around it, creating a sense of depth and movement.

Chapter 11

HEATERS USED FOR ENGINEERING SYSTEMS

Hatice Aylin KARAHAN TOPRAKÇI¹

Sertan TURAN²

Varol KORKMAZ³

1 Yalova University, Department of Polymer Materials Engineering, 77200 Yalova, Turkey, Assoc. Prof. Dr. Hatice Aylin Karahan Toprakci aylin.toprakci@yalova.edu.tr
ORCID ID: 0000-0001-7078-9690

2 Martur Automotive Seating Systems, Bursa, Turkey, Sertan Turan sertan.turan@marturfompak.com, ORCID ID: 0000-0002-3586-8649

3 Martur Automotive Seating Systems, Bursa, Turkey, Varol Korkmaz varol.korkmaz@marturfompak.com, ORCID ID: 0000-0003-0705-694X

1. Introduction

Energy is essential for the sustainability of life. It can be in different forms such as electrical energy, thermal energy, mechanical energy, solar energy, wind energy, nuclear energy, and so on. Since it has various forms, it should be converted into the required form for special applications. Heaters are systems used to generate heat by converting chemical, and electrical energy into heat. They can function by using various sources including gas, oil, hot water, electrical, and so on. Since their basic functions are heat generation and heat transfer; their structural, physical, and morphological properties should be considered before the designing step. In this review definitions, functions, and types of heaters are given. Additionally, mechanisms of heat transfer and factors affecting the performance of a heater are given with common materials used for heaters and basic applications.

A heater is a device or system used to generate and emit heat by different mechanisms for increasing the temperature of a liquid, gas form, or solid body. Heaters have become indispensable parts of our lives since they provide heat for our vital activities and comfort. Additionally, they are essential components of various industrial activities. Parallel with these, they are mostly used for warming up rooms, buildings, designated areas, outdoors, vehicles, and so on. Also, they are used to facilitate industrial processes from drying to chemical synthesis, welding to melt mixing. They can be portable, built-in systems, or both (hybrid).

The basic functions of a heater can be summarized as:

- to generate heat,
- to emit, transfer, circulate, and/or distribute heat,
- to regulate the temperature,
- to protect from cold environments,
- to prevent frost and freeze,
- to provide and maintain consistent comfort and well-being,
- to sustain industrial processes (to dry, to heat, to melt, and so on).

2. Types of Heaters

There are various types of heaters based on source of the energy used for heat generation in the system. In all cases additional components might be required for heat transfer and distribution. The basic conventional types can be given as:

- **Gas Heaters:** Gas heaters are systems that generate heat because of burning of a fuel including natural gas, propane and so on. The mechanism is

based on conversion of chemical energy to heat. The burning takes place by a burner or in a combustion chamber.

- **Oil Heaters:** Oil heaters are used to convert chemical energy to heat. Burner is also a part of the system to start burning of the fuel oil.
- **Solar Heaters:** Solar energy is used to any fluid including air, water, oil.
- **Geothermal Heaters:** Geothermal water is used for heating buildings.
- **Electric Heaters:** An electric heater is a system that functions based on the conversion of electric energy to heat. The most important component of the system is the electric heater known as an electrical resistor. The principle is referred to as Joule heating that describes the heat generation during the current flow from a resistor. Electric heaters can have different components. In one mode heat is generated inside the system and directly transferred to the environment. In another mode, the resistor is used to generate heat, and heat is transferred to increase the temperature of a fluid (oil) then heated oil is used to regulate the temperature. Infrared (IR) heaters, oil/water-filled radiators, and ceramic heaters generate heat by resistive wires. While IR heaters transfer heat by radiation; the others work based on convection which is explained in the next section.

Based on the recent developments and adaptation of heaters to various surfaces, equipment and, clothes led to the development of new heaters. They can be classified as:

- **Wearable Heaters:** Wearable heaters are used for personal thermal management, and healthcare generally by using resistive electric heaters. They can be mounted on textiles or skin (An et al., 2016; He et al., 2022; Wang et al., 2022).
- **Flexible Heaters:** Flexible heaters are made from polymeric materials. They have many advantages including such as lightness and bendability. They can be mounted on various surfaces and equipment (Park et al., 2022).
- **Stretchable Heaters:** Stretchable heaters are the state of the art in polymer-based heaters and can function even under stretched conditions (An et al., 2016).

3. Mechanism of Heaters

The basic reason for heat transfer is the temperature difference between a heater and an object or environment. Since the foremost important function is the heat transfer, the working principle of a heater is critical in terms of performance, cost, and life of the system. There are three mechanisms for the heat transfer (Hegbom, 2017; Levenspiel, 1984):

Conduction: Heat transfer is performed by direct contact from one atom or molecule to the other as shown in Figure 1. Since molecular-level contact is required, it mostly occurs in solid or liquids states based on the fact that gas molecules are not closely packed (Hegbom, 2017; Levenspiel, 1984).

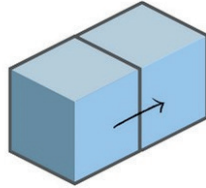


Figure 1. Heat transfer by conduction

Convection: Heat transfer is performed by bulk movement of molecules within fluids such as gases and liquids. In the first place heat is transferred by conduction at the molecular level between the object and the fluid then fluid starts to move, and transfer is carried out by the movement of the fluid as shown in Figure 2. Conduction and convection cannot take place simultaneously. Convection can be evaluated as natural convection and forced convection based on the system components. While natural convection does not require additional external effects for fluid movement, forced convection is controlled by externally controlled circulation and/or distribution through the use of mechanical systems such as fans, mixers, or compressors. Convection heaters generally function by forced hot air circulation(Hegbom, 2017; Levenspiel, 1984).

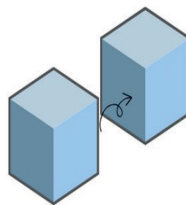


Figure 2. Heat transfer by convection

Radiation: Heat transfer is performed by electromagnetic waves known as radiant heat that is emitted from the heater/hot body as given in Figure 3. The formation of electromagnetic waves is mainly caused by thermally excited electrons.

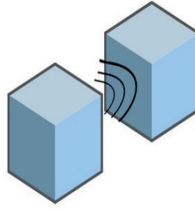


Figure 3. Heat transfer by radiation

As given in Figure 4, the electromagnetic waves in the thermal radiation zone have various energy levels and wavelength ranges (0.1-100 μm) such as ultraviolet (near UV), visible light (entire), and infrared (entire IR) and they are absorbed reflected or transmitted through the body that has a lower temperature. The wavelength and energy of the radiation depend on the bulk, surface properties, and temperature of the system. Thermal radiation is a consequence of oscillations or transitions of the electrons that occur and are sustained by the internal energy/temperature of the system, and it is emitted from anybody that has a temperature above absolute zero. It can emit from solid, liquid, or gas phases. Another important point is it does not require a material-based medium for heat transfer (Fig. 3). Radiant heaters are the common systems that work based on this mechanism. They emit IR radiation and IR radiation directly heats up the bodies without heating the surrounding air, so it is very practical and efficient for outdoor, and indoor heating (Hegbom, 2017; Levenspiel, 1984; Meseguer et al., 2012).

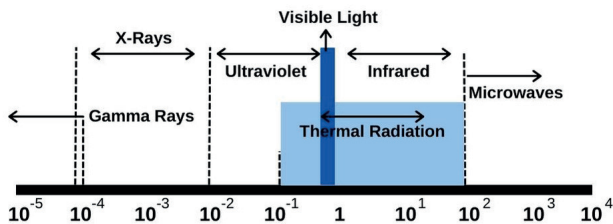


Figure 4. Electromagnetic spectrum and thermal radiation zone

4. Factors Affecting Performance of the Heating Elements

The performance of the heaters can be affected by various factors that can be related to the system, interface properties, heating element properties, and so on. In all the most significant ones are classified as given in Figure 5 based on the heating element properties including electrical, thermal, radiative, and physical properties. Additionally, failures and environmental properties are included.

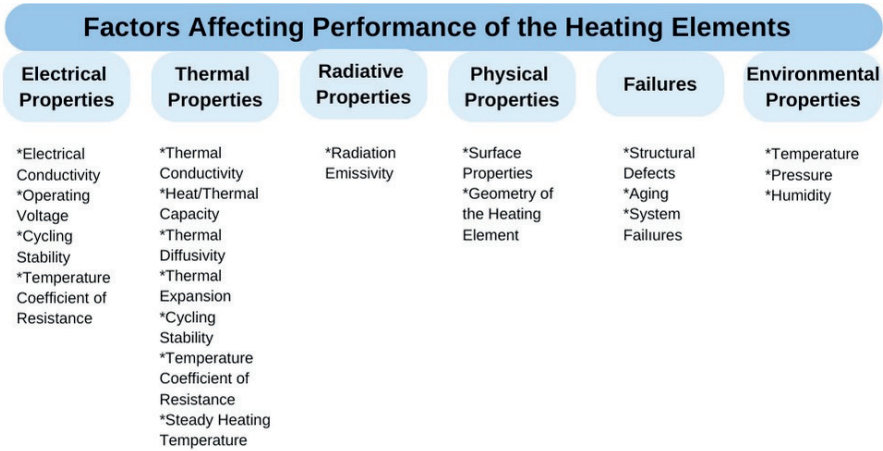


Figure 5. Classification of factors that affect the performance of the heating elements

Electrical Conductivity: Electrical conductivity is a property that shows the level of current (I) flow through a material. It is the reciprocal of resistivity and it has a vital importance for resistive heaters. In the case of lower conductivity/higher resistivity, current flow becomes difficult and level of heat generation is higher. Depending on the form of the heater two common electrical properties are used for evaluation of heating performance. Sheet resistance (ohms per square, Ω/\square) gives us the resistance value of a given surface between the electrodes and calculated from surface resistivity by considering geometry/size of the sample. If the material has very thin film-like, fiber or 3D form, generally sheet resistance is used as performance indicator by using a 4-probe system for other materials conductivity/resistivity (S m-1/ohm m) can be used. The power generated by a heater is expressed as $P=I^2R$ ($P=IV$) and higher the resistance and current, higher the output. By considering this fact, materials with higher resistivity are preferred for resistive heating elements. However, it should be taken into account that, higher resistivity requires higher voltage and heating materials should have enough resistance not to fail under given voltage and temperature conditions. In other words, every material has limits such as maximum current density, maximum service temperature and maximum applied voltage and resistance changes depending on the temperature. Likewise materials very high electrical conductivity is not desired since current easily flows through the material and generation of heat can not reach the levels of a heater. To conclude, the resistivity, sheet resistance of a material should be determined carefully based on the application and targeted life cycle of a heater. General range of a sheet resistance was given as 0–100 Ω/sq in the literature. While 10 Ω of resistance can be enough for a small heater, this value can be several 10s ohms of more for bigger heating systems (Ghorbani & Taherian, 2019; Hegbom, 2017; Hu

et al., 2021).

Operating Voltage: Operating voltage (V), is another factor that effects the generated heat from a heater. As previously mentioned applied voltage has a direct relationship with the “Joule Effect”. In the case of higher applied voltage, higher thermal energy is obtained. However, material properties including electrical conductivity, thermal conductivity, thermal capacity, thermal diffusivity, thermal cyclic behaviour have effect on efficiency and steady functioning conditions. In addition to these, operation voltage of a heater depends on the application, size of the heater and targeted heating volume (Hegbom, 2017; Hu et al., 2021).

Temperature Coefficient of Resistance: Temperature coefficient of resistance (TCR) is another important factor for heating elements. TCR can basically be calculated from the following formula: $(\Delta R/R_0)/\Delta T$ $1/^\circ\text{C}$. The resistance of a heating element changes with temperature. TCR can be positive (PCR) and negative (NCR) based on increase or decrease in resistance. If scattering of the thermally induced charge carrier takes place resistance will increase (PTCR) on the other hand, decrease (NTCR) in resistance is observed in the case of thermally enhanced charge transport. Although high TCR is very useful for temperature sensors, heating elements show very low TCR in terms of obtaining stable heating performance (Cui et al., 2019; Hegbom, 2017).

Thermal Conductivity: Thermal conductivity is a property of a material that is used to understand its ability to conduct heat in the molecular level. It is the reciprocal of thermal resistivity and this value is important for heating elements. Heat is transferred by electrons, phonons, electromagnetic waves, spin waves. In the case of conductors such as metals electrons are responsible heat transfer. On the other hand, for insulators phonons are dominantly responsible for the transfer. The level of thermal conductivity of materials changes due to some structural properties basically but not limited to crystal type, crystal size, grain size, imperfections, homogeneity, density. In the case of lower thermal conductivity/higher thermal resistivity, conduction and dissipation of heat becomes difficult and level of heat transfer becomes lower. So, rate of heat transfer is closely related to thermal conductivity. It is denoted as k and the unit of k is $\text{W/m}\cdot\text{K}$ (Watts per meter Kelvin) (Hegbom, 2017; Yang, 2004).

Thermal Expansion/The Coefficient of Thermal Expansion: Thermal expansion defines the change in dimensions such as length, width, area, volume, shape as a result of increase in temperature. During heating the kinetic energy of the molecules increases and that leads to increase vibration and average separation between molecules increases. This is known as expansion of a substance. In order to determine the degree of expansion, coefficient of thermal expansion is calculated. Linear, one dimensional, thermal expansion

is calculated from $(\Delta L/L_0)/\Delta T$ ($1/^\circ\text{C}$). This value can change under different temperature ranges and based on that the contraction behaviour might be different under different circumstances. The expansion speed can be significant for some applications, quick response to heat might lead to some mechanical failures that is related to components and purity of the heating element. In the case of alloys, composites or hybrid structures thermal expansion coefficient of each component should be taken into consideration (Bajpai, 2018; Hegbom, 2017)

Heat/Thermal Capacity: Heat capacity (C) is another thermal property that is used to determine the amount of heat to change the temperature of a material 1 K. The unit of C is (J/K). In order to determine the heat capacity for a given mass specific capacity (c) is used that is basically calculated by dividing C to the mass and expressed as J/K kg. Higher heat capacity indicates higher heat storage performance in the case of same temperature change (ΔT) and heat gain or loss take longer time compared to lower heat capacity that can affect the heating/cooling rate. For the heating systems heat capacity is of significance in terms of stability of the heat transfer. Higher heat capacity leads to higher stability and less temperature fluctuations during heat transfer and that is critical for providing a stable, controllable thermal management (Hegbom, 2017; Hu et al., 2021; Krastev, 2010) .

Thermal Diffusivity: Thermal diffusivity (D) is another criteria used for diffusion/heat transfer rate in a medium. $D = k/(\rho C_p)$, k: thermal conductivity, ρ : density, C_p : specific heat at constant pressure. Higher thermal diffusivity is an indication of higher speed of heat dissipation through the material and heating temperature might be lower. Thermal diffusivity is of importance in terms of thermal management. It should also be underlined that, it is affected by the temperature and at higher temperatures, thermal diffusivity decreases (Hegbom, 2017; Hu et al., 2021; Larciprete et al., 2022).

Steady Heating Temperature: Steady heating temperature ($\text{K}/^\circ\text{C}$) of a heater defines the temperature value(s) at which heating performance is optimum. This is related to thermal conductivity, thermal capacity and thermal diffusivity. Wider steady heating temperature range results in better thermal management (Hegbom, 2017; Hu et al., 2021).

Cycling Stability/Hysteresis: Any type of heater is used for hours for years. The most important expectancy from a consumer is the life and performance of a heater both of which are directly related to the cycling stability/hysteresis. Although cycling stability looks like one behaviour, for heaters it should be investigated under three titles such as thermal, electrical and mechanical behaviour of the heating element under repeated usage. Thermal cycling behaviour basically indicates the fluctuations from the

optimum temperature range. Minimum deviation under given conditions gives good cycling stability and less hysteresis. Since heat generation is directly related with the electrical properties of the heating element, electrical conductivity/resistivity should show stable cycling behaviour under working conditions. Any structural change might lead to change in electrical properties and that might lead to change in thermal cyclic behaviour. Mechanical cycling behaviour is related with the dimensional stability of the heater. As known solid materials tend to expand/contract under heating/cooling. During this cyclic heating process, if the temperature exceeds the dimensional stability limits of the heating element, micro/macro-structural defects occur that can result in the deterioration of the mechanical properties, and some failures including deformation, bending, and cracking can be observed. Also alloys, composites or hybrid structures consist of at least two phases and the response of each phase to heat energy can be different and that might cause some mechanical defects and failure. The cyclic stability of a heater can be given as a cycle (heating-cooling) number (Hegbom, 2017; Hu et al., 2021).

Radiation Emissivity: All materials emit thermal radiation above absolute zero temperature. However total thermal radiation is determined by the emissivity of the object. Radiation emission of a heating element is caused by thermally excited electrons and can be in a wavelength range from 0.1 to 100 μm in the form of ultraviolet, visible and infrared light. Level of emissivity, known as emissivity coefficient (ϵ) gives the radiation level of heat from a body in comparison to an ideal black body ($\epsilon = 1$) under same conditions (wavelength, temperature etc.). The total emissivity is directly related to spectra and in some cases, spectral emission can be determined at particular wavelength. The emissivity of a surface is not only related to bulk properties, temperature but also surface properties including cleanliness, roughness etc. and can be between 0-1 (Hegbom, 2017; Jackson & Yen, 1994).

Physical, Surface Properties and Geometry of the Heating Element: Although bulk properties are critical for the heating performance, physical, surface properties, tolerances and geometry of the heating element affect the output of the heater. As known conductance, resistance are related to geometry (ribbon, wire etc.) of the heating element. Melting point, density, cleanliness, surface finish, surface smoothness, hardness are also important for obtaining stable heating performance (Hegbom, 2017).

Failures: Even if best materials are chosen for heating elements, various failures can take place including oxidation, corrosion, mechanical defects and they might lead to failures. Oxidation can take place at higher temperatures and layer on the surface of the heating element can flake off. This not only effects the surface morphology but also structural properties including electrical and thermal properties. In the long-range use oxidization can take place from outer to inner layers. The layers can flake off because of the

differences in thermal expansion coefficient between heating element and oxidized surface layers. Based on morphological changes, hot-spots can also form during heating that can be observed as the shiny points that are the points with the highest temperature. Another common reason for the failures is the corrosion that is caused by direct contact of heating element by water or chemicals (Hegbom, 2017).

Environmental Conditions: In addition to structural, physical, surface properties, geometry and cyclic behaviour of the heating element, environmental conditions are significant in terms of heating performance of conduction, convection heaters. Although some conditions are controlled during the heating process, some of them can not be controlled due to weather or systematic problems. In order to obtain the highest efficiency, acclimation of the environment can be a quick solution. In this case, relative humidity, minimum and maximum temperature range, air flow, heat transfer rate, insulation and so on can be controlled. Also, environmental conditions might triggered reactions such as oxidation and corrosion (Hegbom, 2017).

5. Materials used for Heating Elements

Heaters can be used for various applications from building heating to personal (body) heating. Based on the requirements of the system and temperature range, different heating elements can be fabricated by using metals, alloys, carbon-based materials, ceramics, conductive polymers, conductive metal oxides, nanocomposites, hybrid conductive materials, IR emitting materials. As mentioned previously heat is transferred by conduction throughout the heating element and transfer of heat to the environment can be by conduction or radiation. In all cases heating element should have some properties including high purity (minimum amount of trace elements), high melting point, high resistivity, low-temperature coefficient of resistance, high thermal dimensional stability, high strength, high resistance to oxidation and corrosion etc. Metals such as aluminium, copper, gold, iron, nickel, platinum, silver, tungsten, stainless steel can be used as heating elements such for special applications below 600 °C. Metals with high conductivity, low resistivity are generally used under low voltage range for long heating elements. The most common alloys can be classified as iron based (Iron-Chrome-Aluminium (FeCrAl) and nickel based (Nickel-Chromium (NiCr), Copper Nickel (CuNi) alloys. Also, silicon and porous carbon can be used for some applications (Hegbom, 2017). As known, in addition to high capacity industrial heating systems; personal (relatively micro) heating systems have been developed recently. In these systems metal/metal alloy wires (Bahadır & Sahin, 2018), metal coated fibers (Petru et al., 2023), carbon containing polymer composites (Tarfaoui et al., 2019), conductive polymers (Zhou et al., 2017) can be used in various scales from nano to mm.

6. Applications of Heaters

Heaters are indispensable parts of our lives. They are used in various electrical appliances for domestic and industrial applications. Domestic applications can be given as: Space heating, water heating, cooking, personal care, caring of clothes, personal comfort, vehicle heating (Hegbom, 2017).

- Radiators, convection heaters, air conditioners, fan heaters, floor heaters, can be given as space heaters.
- Dishwasher, washing machine, coffee/tea maker, kettles can be given some examples of water heaters.
- Baking ovens, rice cookers, cooking plates, hot plates, toasters, grills, egg/vegetable boilers can be given some cooking applications of heaters.
- Hair dryers, hair crimpers, heated hairbrush can be given as heaters used for personal care.
- Tumble dryers, iron, hot presses can be given as the common applications for caring of clothes.
- Saunas, heated massage seats, waterbed, wearable heaters, electrical blankets can be given as heaters used for personal comfort.
- Cigarette lighters, car seat heaters, ceiling heaters, windshield heaters, interior heaters, car lock heaters can be given as the heaters used in vehicles.

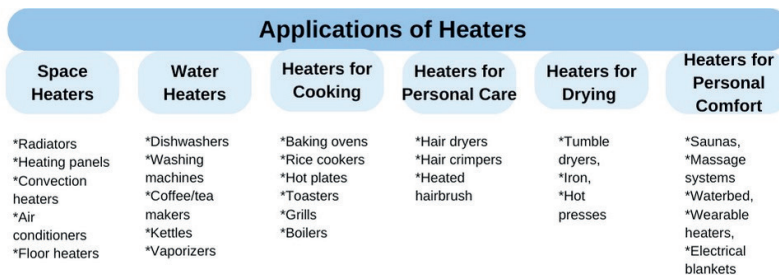


Figure 6. Basic applications of heaters

Conclusions

Energy is the common source for industrial and domestic applications and systems. Any process that needs increase in temperature requires thermal energy. Conversion of chemical/electrical energy into heat requires a special equipment known as heaters. Heating element is the heart of the heaters, and its structural, physical, geometrical and morphological properties are of vital importance and they should be carefully investigated before designing a

heating system.

Acknowledgement

The present study was supported by Martur with the project name: FIR heating system integrated in car interior.

LITERATURE

- An, B. W., Gwak, E. J., Kim, K., Kim, Y. C., Jang, J., Kim, J. Y., & Park, J. U. (2016). Stretchable, Transparent Electrodes as Wearable Heaters Using Nanotrough Networks of Metallic Glasses with Superior Mechanical Properties and Thermal Stability. *Nano Letters*, 16(1). <https://doi.org/10.1021/acs.nanolett.5b04134>
- Bahadir, S. K., & Sahin, U. K. (2018). A Wearable Heating System with a Controllable e-Textile- Based Thermal Panel. In *Wearable Technologies*. <https://doi.org/10.5772/intechopen.76192>
- Bajpai, P. (2018). Properties of Wood. In *Biermann's Handbook of Pulp and Paper*. <https://doi.org/10.1016/b978-0-12-814240-0.00007-0>
- Cui, Z., Poblete, F. R., & Zhu, Y. (2019). Tailoring the Temperature Coefficient of Resistance of Silver Nanowire Nanocomposites and their Application as Stretchable Temperature Sensors. *ACS Applied Materials and Interfaces*, 11(19). <https://doi.org/10.1021/acsami.9b04045>
- Ghorbani, M. M., & Taherian, R. (2019). Methods of measuring electrical properties of material. In R. Taherian & A. Kausar (Eds.), *Electrical Conductivity in Polymer-Based Composites* (pp. 365–394). William Andrew Publishing.
- He, G., Wang, L., Bao, X., Lei, Z., Ning, F., Li, M., Zhang, X., & Qu, L. (2022). Synergistic flame retardant weft-knitted alginate/viscose fabrics with MXene coating for multifunctional wearable heaters. *Composites Part B: Engineering*, 232. <https://doi.org/10.1016/j.compositesb.2022.109618>
- Hegbom, T. (2017). Integrating electrical heating elements in product design. In *Integrating Electrical Heating Elements in Product Design*. <https://doi.org/10.1201/9781315214436>
- Hu, Z., Zhou, J., & Fu, Q. (2021). Design and Construction of Deformable Heaters: Materials, Structure, and Applications. In *Advanced Electronic Materials* (Vol. 7, Issue 11). <https://doi.org/10.1002/aelm.202100459>
- Jackson, J. D., & Yen, C.-C. (1994). MEASUREMENTS OF TOTAL AND SPECTRAL EMISSIVITIES OF SOME CERAMIC FIBRE INSULATION MATERIALS. In *The Institute of Energy's Second International Conference on Ceramics in Energy Applications*. <https://doi.org/10.1016/b978-0-08-042133-9.50016-2>
- Krastev, R. K. (2010). Measuring of heat capacity. *International Journal of Heat and Mass Transfer*, 53(19–20). <https://doi.org/10.1016/j.ijheatmasstransfer.2010.05.001>
- Larciprete, M., Orazi, N., Gloy, Y. S., Paoloni, S., Sibilia, C., & Li Voti, R. (2022). In-Plane Thermal Diffusivity Measurements of Polyethersulfone Woven Textiles by Infrared Thermography. *Sensors*, 22(3). <https://doi.org/10.3390/s22030940>
- Levenspiel, O. (1984). The Three Mechanisms of Heat Transfer: Conduction, Convection, and Radiation. In O. Levenspiel (Ed.), *Engineering Flow and Heat Exchange* (pp. 161–188). Springer US. https://doi.org/10.1007/978-1-4615-6907-7_9

- Meseguer, J., Pérez-Grande, I., & Sanz-Andrés, A. (2012). Thermal radiation heat transfer. In *Spacecraft Thermal Control*. <https://doi.org/10.1533/9780857096081.73>
- Park, H., Kim, H., Kim, S. H., Cho, E., Kim, H. K., & Lee, S. J. (2022). Transparent and flexible heaters using plasma polymer fluorocarbon/silver bilayer thin films. *Thin Solid Films*, 753. <https://doi.org/10.1016/j.tsf.2022.139294>
- Petru, M., Ali, A., Khan, A. S., Srb, P., Kucera, L., & Militky, J. (2023). Flexible Coated Conductive Textiles as Ohmic Heaters in Car Seats. *Applied Sciences*, 13(12). <https://doi.org/10.3390/app13126874>
- Tarfaoui, M., El Moumen, A., Boehle, M., Shah, O., & Lafdi, K. (2019). Self-heating and deicing epoxy/glass fiber based carbon nanotubes buckypaper composite. *Journal of Materials Science*, 54(2). <https://doi.org/10.1007/s10853-018-2917-9>
- Wang, X., Lei, Z., Ma, X., He, G., Xu, T., Tan, J., Wang, L., Zhang, X., Qu, L., & Zhang, X. (2022). A lightweight MXene-Coated nonwoven fabric with excellent flame Retardancy, EMI Shielding, and Electrothermal/Photothermal conversion for wearable heater. *Chemical Engineering Journal*, 430. <https://doi.org/10.1016/j.cej.2021.132605>
- Yang, J. (2004). Theory of Thermal Conductivity. In T. M. Tritt (Ed.), *Thermal Conductivity: Theory, Properties, and Applications*. Kluwer.
- Zhou, R., Li, P., Fan, Z., Du, D., & Ouyang, J. (2017). Stretchable heaters with composites of an intrinsically conductive polymer, reduced graphene oxide and an elastomer for wearable thermotherapy. *Journal of Materials Chemistry C*, 5(6). <https://doi.org/10.1039/c6tc04849h>

Chapter 12

GENETIC PROGRAMMING MODEL FOR PREDICTION OF WEAR BY MEANS OF HARDNESS VALUES OF STEEL MATERIAL

*Yenal ARSLAN*¹

¹ Dr. Öğr. Üyesi, Ankara Yıldırım Beyazıt Üniversitesi Mühendislik ve Doğa Bilimleri Fakültesi, Yazılım Mühendisliği Bölümü, Ankara, Orcid Id: 0000- 0002-1776-6091, yenalarslan@aybu.edu.tr

1. INTRODUCTION

Generally, wear is undesired surface changes that are caused due to pieces breaking off because of mechanic loading that occurs during the operation of objects that are contacting each other and moving together (İzciler, 1997). Wear is much more destructive than just loss of material because it ruins the form of machine components and diminishes or terminates their capacity to work (Karaoğlu, 2006). For this reason, it is very important to predict in advance the extent of wear, as wear can lead to high costs and loss of time. Even though many parameters affect wear, the parameters that affect wear the most are both the hardness of the wear and the causes of corrosion (Güven et al., 2005). The hardness of the material is a condition with many random, unknown forms, such as the structure of the component and the crystal structure.

Evolutionary calculations have successfully been used in the solution of such complicated problems. Evolutionary algorithms are known by different names according to their presentation and formulization. According to this, Evolutionary Algorithms can be divided into four groups, which are Genetic Algorithms, Evolutionary Programming, Evolution Strategies, and Genetic Programming (Holland, 1975).

Evolutionary algorithms separate from traditional solution methods in creating a solution candidate population. How close the candidate is to the solution is determined with a fitness function. In every one of these, the algorithm calculates how strong each candidate is and then calculates, according to this, the parents of the next generation or the individuals that are to cease existing. After this, to create a new, logical generation it applies the genetic searching processors (reproduction, crossover, and mutation). This cycle is repeated continuously, creating stronger individuals each time. Genetic algorithms, which are the most used sub-branch of evolutionary algorithms, were developed for the first time by John Holland and his colleagues at the University of Michigan (Koza, 1992). Holland conducted his research based on natural selection and genetic evolution to search and find the optimum. Throughout the process, he selected, as an example, those individuals who could harmonize with the environment they were located in, to reach optimum levels. Computer programs were also developed to search for this optimum level and to discover mechanical problems (Boun, 2001). However, Genetic Algorithms were not appropriate for formulizing complicated problems and modeling (Goldberg, 1989) so, instead of this, the Genetic Programming approach was suggested by John Koza (Koza, 1992). Besides this, one of the differences between Genetic Programming and Genetic Algorithm is the presentation of the individuals. While Genetic Programming uses hierarchical tree structures, a pre-determined length of a string character series is used in Genetic Algorithm (Koza, 1994). Genetic Programming is an

Evolutionary Algorithm technique that targets the probable primitive solution types that are formed by the building blocks of the problem (Grosman et al., 2004). In addition to GP solving a problem whose solution space is rather large and difficult, such as modeling the hardness of materials, Artificial Neural Network (ANN) approaches have also become popular. Every technique has an advantage and a disadvantage. The technique regarding ANN's is effective when applied to situations where the relations of variables that are affected, and that are directly dependent, are non-linear and very loud (Giles et al., 2001). What ANNs are fundamentally lacking is a formula provided for the benefit of understanding the process; and because it is a closed book, clearly stated rules regarding the problem are not offered. This is why users are quite limited while working with ANNs (Faris et al., 2020). On the other hand, the previously mentioned problems do not arise while working with GPs. GP also has extra advantages compared to neural networks which are the capabilities of giving an insight into the underlying system by producing compact and being easy to evaluate mathematical models. GP is then reliable and logical in modeling various engineering applications under uncertain environments (Faris et al., 2020).

Barclay et al. developed a GP program to generate tool paths for 2D milling and changes were observed in the product shape without Problems. Garg et al. used GP for the formulation of geometry optimization function of the direct absorption solar collector (DASC) system in the fields of renewable energy. Compared with ANN methods, they saw that GP can generate the model with better fitting performance (Garg et al., 2020). A new approach is presented by Ranansigle et al based on GP for the predictions of the efficacy of Rolling dynamic compaction RDC (used with the help of a tractor and it has been found to be useful to improve problematic soils and widely used globally), which is considered to be an alternative to conventional soil compaction technology. And the GP model has a better predictive performance than the existing ANN model developed earlier by the authors (Ranansigle et al., 2019).

In the literature, artificial intelligence technologies are used a lot in terms of wear. Silva et al. observed cutting tool wear using signal processing, artificial neural networks and expert system approach (Silva et al., 1998). Yan et al. examined the particles in the oils used to reduce wear in their studies and wanted to make wear inferences from the particles in question. For this purpose, they established an intelligent analysis system by developing an expert system using object-based information presentation method (Yan et al., 2005). Iqbal et al. studied the side edge wear of cutting tools, which is important for the quality and economy of the milling process. When the flank wear of the cutting tools reaches a certain level, they must be replaced for the efficiency of the process, but it is impossible to measure the wear during the process. This wear can only be predicted. For this purpose, researchers developed a

fuzzy expert system to predict wear online and offline and compared these methods with each other (Iqbal et al., 2007). Kor et al. developed a fuzzy-based expert system to predict and reduce the wear of high chromium alloys during phosphate grinding and compared them with traditional statistical methods (Kor et al., 2010). Although artificial intelligence technologies are used a lot in the literature, there is not much research on hardness, which is the main factor affecting wear. Low, medium, and high intensity carbon steel was used in this study because this material has been used widely in the industry. In this study, it was tried to formulate the basic inputs that affect the hardness of steels by using the genetic programming method for the first time in the literature. It is thought that the experimental study will find industrial use in more specific steel groups.

2. GENETIC PROGRAMMING

2.1 The Genetic Programming Approach

Before initiating a genetic program, the terminals, functions, fitness function, control parameters and terminating criteria need to be selected (Tay et al., 2008). In order to create GP individuals, terminals and functions are used. Carefully selecting the terminal and functions for solving the problem is rather important (Chen et al., 2008). Terminals are variables or constants that are directly effective in establishing and diagnosing a problem. Functions are objects that enable the terminals to be integrated according to specific process logic. The smallest building blocks, namely individuals, which enable a solution, are created as a result of integrating the functions and terminals in order to form a purposeful structure within a hierarchic understanding (Göloğlu and Arslan, 2009).

The individuals provide a mathematical or functional result, depending on the type and description of the problem that is being approached. These results are passed through a structure named fitness function and are conducted according to a diagnosed procedure and transformed into a type of numerical quantity that represents the individuals' problem-solving capabilities. They are then arranged in a line according to this quantity (Göloğlu and Arslan, 2009).

Control Parameters are criteria that are applied after GP has been initiated to work. One of the most important parameters is population. The others are generally the probability of the application of the genetic operators, such as the ratio of crossover and the ratio of mutation. The terminating criteria can be specified as the maximum generation that the program creates while operating, or any individual reaching the desired degree of fitness (Wang et al., 2021).

2.2 Working Principles of Genetic Programming

After the above-mentioned five topics are specified, GP is ready to work. The stages of Genetic Programming can be listed as follows (Nguyen et al., 2020):

Creating the pool of individuals (population) at random

Repeating the below series of actions until a condition of stopping is reached:

a) Evaluating the quality of the solution of the problem that is coded by every one of the individuals formed in the pool.

b) Differentiating the pool by applying evolutionary agents (processors) in consideration of this evaluation.

Selection: selecting which individuals from a differentiated pool are to be transferred to the next generation.

Reproduction: selecting individuals to be transferred to the new generation without being differentiated by any other genetic operator (crossover, mutation).

Crossover: paring some of the individuals in the pool and producing new chromosomes named children, and that contain the gene information of the individuals named ancestors. This way, one of the genes of every child shall be the same as one of the ancestor's genes.

Mutation: As in nature, randomly changing some of the gene values of the individuals that have been randomly selected from the pool.

The flow chart of GP is shown in Figure 1 below.

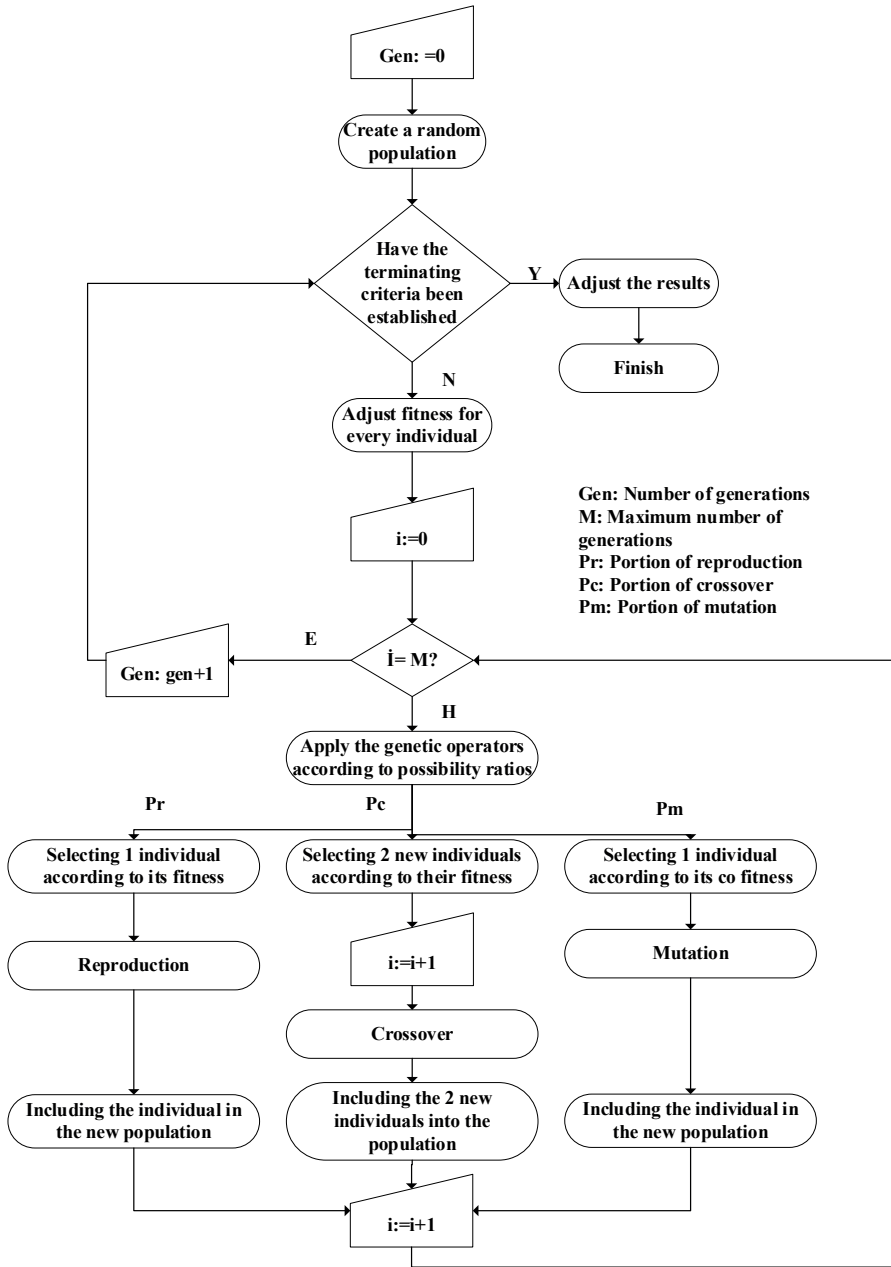


Figure 1. Flow chart of Genetic Programming (Göloğlu and Arslan, 2009)

Within the scope of this work, a program named USYAAP has been designed that utilizes various expert system approaches regarding wear. The USYAAPGEN GP modeler program was designed as a sub module of this main application. It has been created by using Microsoft Visual Studio 2005 VB.Net programming language.

3. MODELING THE HARDNESS OF WEAR BY USING GENETIC PROGRAMMING

In the study low carbon, medium carbon and high carbon steel, each of which complies with international standards, have been used as carbon steel. The corrosion behavior of the steel has been scanned from literature, and experiment sets have been created according to these. The ambient temperature and heat processes have been kept constant while creating the experiment sets and the components of the materials have been used. In the literature, there are very few studies on the estimation of steel material compounds using genetic programming. Kovacic et al 2019, used roll diameter, contact time, carbon equivalent, rolling temperature and quantity of rolled material as input to identify the parameters affecting the working roll wear in the hot rolling process. The prediction of machinability of steel was studied by Brezovnik and his friends, and is dependent on input parameters percentage of calcium, percentage of oxygen, percentage of sulfur (Brezovnik et al., 2006). In this study to estimate the hardness of steel, the percentage of carbon, percentage of manganese, percentage of phosphate, percentage of sulfur were used while keeping other parameters constant.

These experiment sets that have been created were operated by using a USYAAP-GEN program on a Vmware ESX 3.5 update 3 cyber hosts that have the features of 4 AMD Opteron 2500 GHz processors, 16 GB Ram and installed on a Windows 2003 Enterprise Edition sp2 64bit operation system. These conducted works have been repeated many times, changing the genetic parameters of the USYAPP-GEN program.



Figure 2. *Main screen of the USYAAP-GEN program*

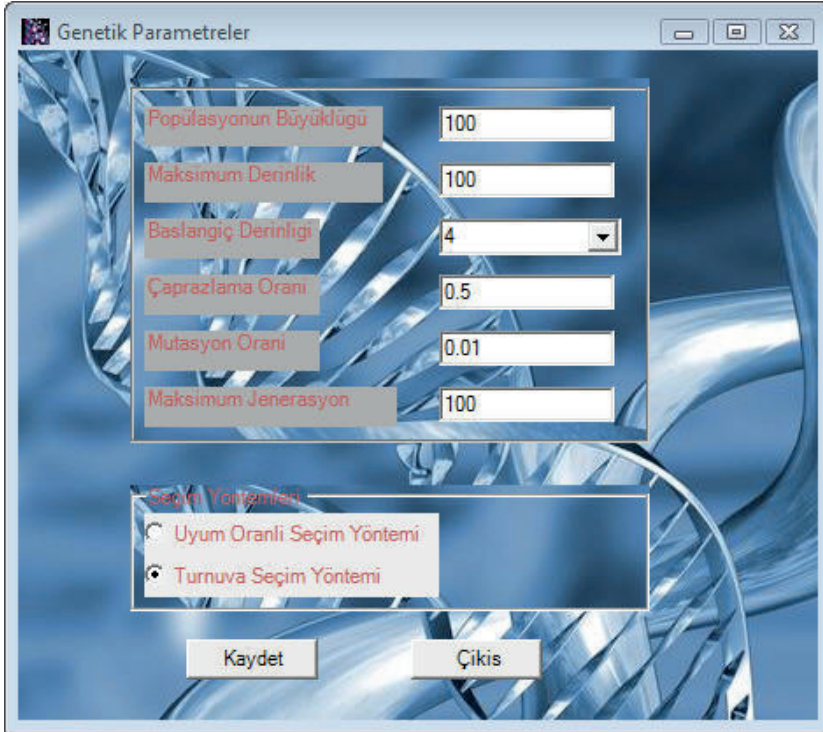


Figure 3. Adjustment of genetic parameters in USYAAP-GEN



Figure 4. Selection of genetic parameters in USYAAP-GEN

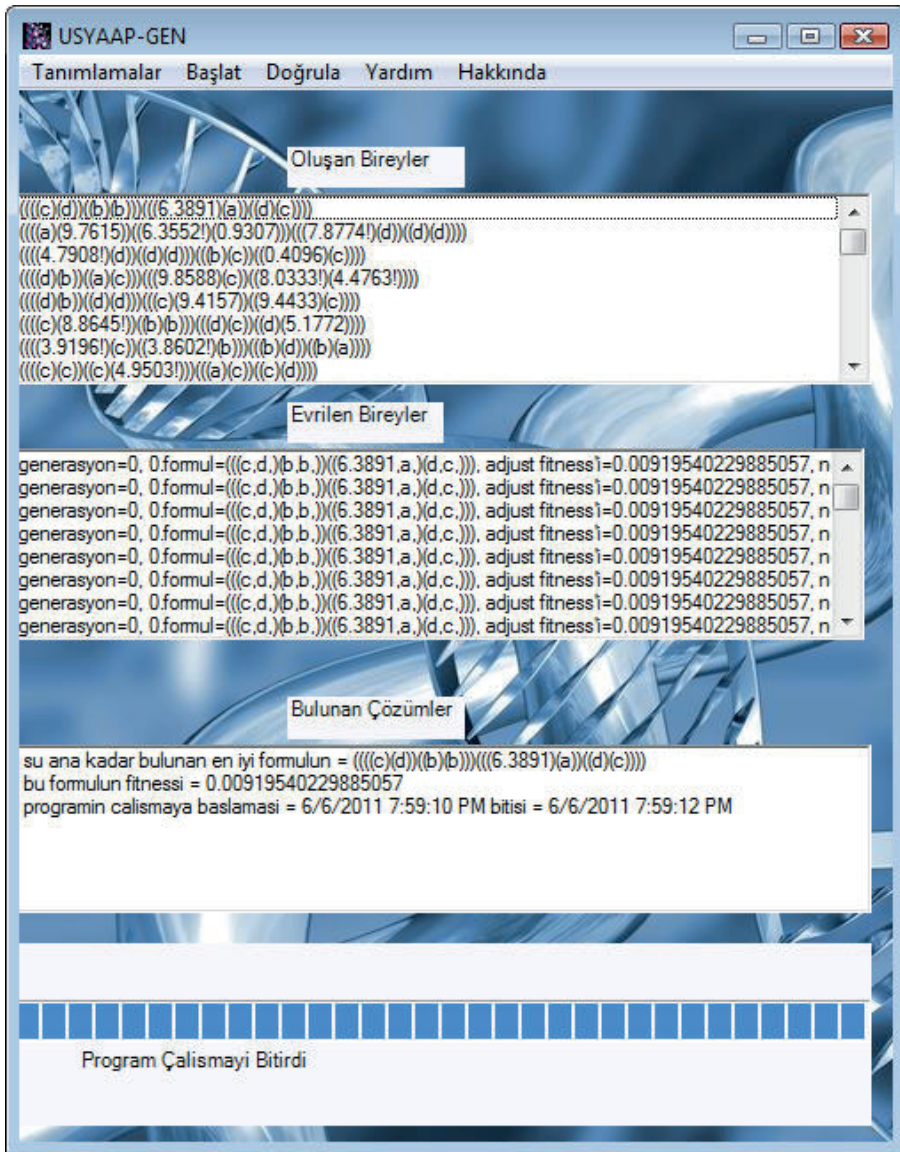


Figure 5. Creation of random starting population in Lisp layout in USYAAP-GEN and demonstration of program start-up

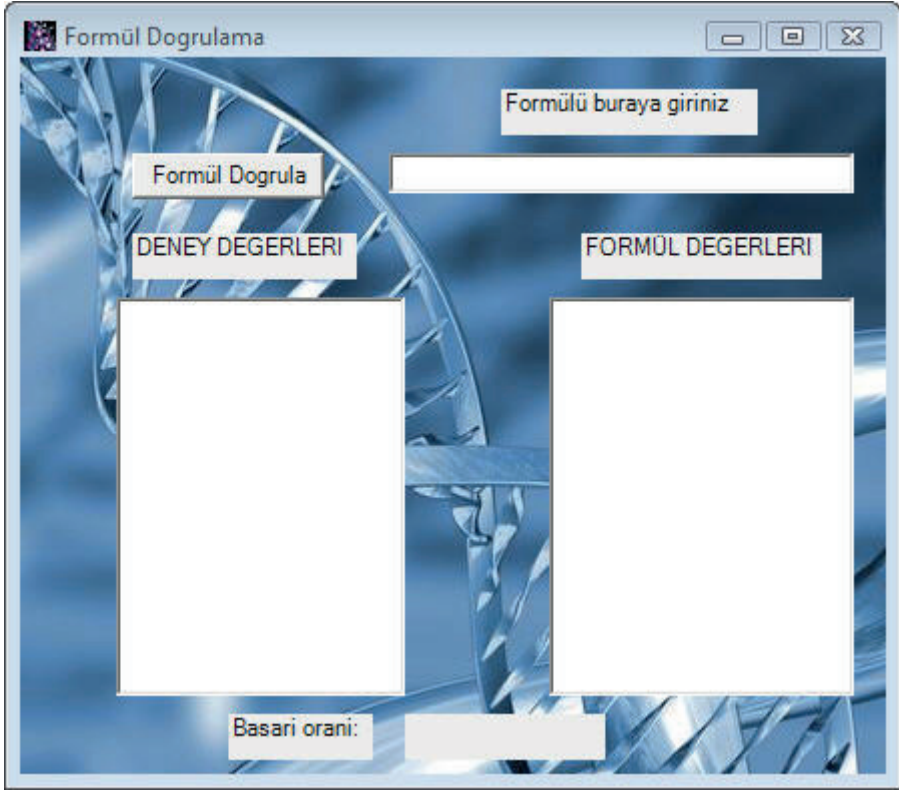


Figure 6. Verification of any formula in USYAAP-GEN

3.1. Low Carbon Steel

Low carbon steel has been used in the conducted experiment.

Table 1. Test data of low carbon steel.

Name of the Material	Carbon (C), %	Manganese(Mn), %	Phosphate(P), %	Sulfur(S), %	Hardness(Hb)
AISI 1006	0.08	0.325	0.040	0.050	86
AISI 1010	0.105	0.45	0.040	0.050	95
AISI 1015	0.155	0.45	0.040	0.050	101
AISI 1018	0.175	0.75	0.040	0.050	116
AISI 1019	0.175	0.85	0.040	0.050	116
AISI 1020	0.205	0.45	0.040	0.050	111
AISI 1023	0.225	0.45	0.040	0.050	111
AISI 1026	0.250	0.75	0.040	0.050	126

Table 2. *Verification data of low carbon steel.*

Name of the Material	Carbon (C), %	Manganese(Mn), %	Phosphate(P), %	Sulfur(S), %	Hardness(Hb)
AISI 1008	0.10	0.40	0.040	0.050	86
AISI 1012	0.125	0.45	0.040	0.050	95
AISI 1016	0.155	0.75	0.040	0.050	111
AISI 1022	0.205	0.85	0.040	0.050	121

Many experiments have been conducted with low carbon steels test data. As a result of these experiments, the best formula found by the USYAAP-GEN genetic programming modeler is below.

LISP notation was used in the formulas (Hicklin, 1986; Fujiki and Dickinson, 1987). In the LISP representation, first the function is written, and then the terminals that this function will operate on are listed as the first and second parameters, respectively. For example, the expression (+ 8 3) means that 8 and 3 are added together. So it means (8 + 3). To give one more example, the expression (- (* 6 3) (+ 4 7)) is equivalent to the expression ((6 * 3) - (4 + 7)). The most important point in LISP representation is the parentheses and parenthesis precedence. In Formulas we use 4 constant terminals [a=C, b=Mn, c=P, d=S and real numbers in the interval between -1 and 1], and 4 functions ["+" is the mathematical operation of addition, "-" is the mathematical operation of subtraction, "*" is the mathematical operation of multiplication, "/" is the mathematical operation of division], "!" in order not to confuse the subtraction with the negativity of the terminal, an exclamation statement is used. In the notation in the formula, the exclamation point refers to the negativity of the terminal.

In order to obtain the best formula from those found in the many experiments that were conducted, the size of the population was computed as 10000, the maximum depth of the population 400, the ratio of reproduction 0.2, the ratio of crossover 0.8, the ratio of mutation 0.2, and the maximum generation was 100; error based fitness function was used as the fitness function, tournament selection as the selection method, 7 as the initial depth and the saturation method was used to create the initial population. As a result, a formula that has a fitness of 92.6% was produced.

Formula:

$$(-(*(-(-/(4.1276,(+/(-(/(1.5126,(+b,(+*(-(-1.5126,b)/(3.5307,d))),1.5126,)(-d,(/8.1096,(+1.5126,(-/(-d,1.5126,),(+2.0792!,(*(-(-8.1096,b)/(d,1.5126,),1.5126,)),a,)),4.1276,)),)),),1.5126,)(+(-d,b),a,)),(+(/(-8.1096,4.1276,)(+(-d,b),a,)),8.1096,)),1.5126,)(+(-d,b),a,)),8.1096,)),(+/(1.5126,(+(/(-8.1096,4.1276,)(+(-d,b),a,)),8.1096,)),1.5126,)(+(-d,b),a,)),3.5307,)),(-d,(/2.0792!,(+(-a,b),(-/(-c,3.5307,),(+2.0792!,(*(-(-8.1096,b)/(c,8.1096,)),8.1096,)),a,)),4.1276,)),),)/(-d,8.1096,)),d,)),a,)(-b,(/(-/3.5307,(+8.1096,(/(-/4.1276,(+(*(-(-c,(/8.1096,(+2.0792!,8.1096,)),)/(-d,8.1096,)),d,)),a,))(-c,(/(-/(-d,b,),(+b,8.1096,)),1.5126,))(+(-a,b),a,))),8.1096,)),1.5126,)(+(-d,b),a,))),1.5126,)(+(-d,b),a,)))(-2.0792!,(+3.5307,b),d,)))$$

The results of the test data obtained from this formula are below.

Table 3. *The results of the test data of low carbon steel.*

Name of the Material	Hardness (Hb)	The hardness estimated by the formula (Hb)
AISI 1006	86	86.3194
AISI 1010	95	95.0144
AISI 1015	101	101.0142
AISI 1018	116	116.0718
AISI 1019	116	115.9446
AISI 1020	111	111.0504
AISI 1023	111	111.0106
AISI 1026	126	126.0993

The results of the validation data obtained from this formula are below.

Table 4. *The results of the validation data of low carbon steel.*

Name of the Material	Hardness (Hb)	The hardness estimated by the formula (Hb)
AISI 1008	86	91.9882
AISI 1012	95	106.0761
AISI 1016	111	111.99
AISI 1022	121	121.233

3.2. Medium Carbon Steel

Medium carbon steel has been used in the conducted experiment.

Table 5. *Test data of medium carbon steel.*

Name of the Material	Carbon (C), %	Manganese(Mn), %	Phosphate(P), %	Sulfur(S), %	Hardness(Hb), %
AISI 1030	0.31	0.75	0.040	0.050	137
AISI 1037	0.35	0.85	0.040	0.050	143
AISI 1039	0.405	0.85	0.040	0.050	156
AISI 1042	0.435	0.75	0.040	0.050	163
AISI 1044	0.465	0.45	0.040	0.050	163
AISI 1046	0.465	0.85	0.040	0.050	170
AISI 1050	0.515	0.75	0.040	0.050	179

Table 6. *Verification data of medium carbon steel.*

Name of the Material	Carbon (C), %	Manganese(Mn), %	Phosphate(P), %	Sulfur(S), %	Hardness(Hb), %
AISI 1038	0.385	0.75	0.040	0.050	149
AISI 1040	0.405	0.75	0.040	0.050	149
AISI 1043	0.435	0.85	0.040	0.050	163
AISI 1045	0.465	0.75	0.040	0.050	163

Many experiments have been conducted with medium carbon steels test data. As a result of these experiments, the best formula found by the USYAAP-GEN genetic programming modeler is below.

In order to obtain the optimum formula from those found in the many experiments that were conducted, the size of the population was computed as 5000, the maximum depth of the population 200, the ratio of reproduction 0.2, the ratio of crossover 0.8, the ratio of mutation 0.2, and the maximum generation was 100; error based fitness function was used as the fitness function, tournament selection as the selection method, 7 as the initial depth and the saturation method was used to create the initial population. As a result, a formula that has a fitness of 96.2% was produced.

Formula:

$$\begin{aligned}
 &(-+(\wedge(-d,(\wedge/b,(\wedge a,c,)),a))(-(*a,c,)(-8.4191,c,)))/(-(/(a,d,)(+d,d,)))(+(*5.2004,6.6513,)) \\
 &(\wedge d,(\wedge(+1.7182!,(+(/c,(-(*d,8.4191,)),b,)))(\wedge(+((+(/c,(-(\wedge c,(/(*((+(/(+(\wedge(- \\
 &b,c,)),5.3479!,)),1.7182!,)(-7.2024,b,)))(\wedge(*a,7.2024,)))/(-(*(+d,c,)(-b,c,)))/(\wedge c,d,)) \\
 &(*2.2896!,a,)))(*(-(*(-c,a,)),a,)),6.6513,)(-/a,a,)(-b,b,)))))))(\wedge(*a,1.7182!,)/(-(*(+d,c,)) \\
 &(-2.2896!,c,)))/(\wedge c,d,)(*4.9831,a,)))(*(-(*(-c,a,)),a,))(\wedge d,(+(\wedge a,c,)),d,)))(-/a,a,)(- \\
 &b,b,)))))))(a,)(+d,b,)),b,)))(\wedge(+d,b,)/a,d,)))(-c,a,)))(\wedge(+d,b,)/a,d,)))(b,)),6.6513,)) \\
 &(*a,5.3479!,)))))((+(*(-b,(-7.8002,(-(+(/c,(-(*d,6.3756,)),b,)))(\wedge(+d,b,)/a,d,)))(c,)))/ \\
 &b,d,)))(*/3.4161,a,)(-0.3785!,a,)))/(\wedge(\wedge d,(\wedge(-(\wedge c,(/(*((+(/(+(\wedge(-b,c,)),5.3479!,),/c,(- \\
 &(\wedge c,(/(*((+(/(+(\wedge(-b,c,)),5.3479!,)),1.7182!,)(-7.2024,b,)))(\wedge(*a,7.2024,)))/(-(*(+d,c,)(- \\
 &b,c,)))/(\wedge c,d,)))(*2.2896!,a,)))(*c,(-/a,a,)(-b,b,)))))))(\wedge(*a,1.7182!,)/(-(*(+d,c,)) \\
 &(-4.9831,c,)))/(\wedge c,d,)(*4.9831,a,)))(*(-(*(-c,a,)),a,))(\wedge d,(+(\wedge a,b,)),d,)))(-/a,a,)(- \\
 &b,b,)))))))(a,)(+d,b,)),b,)))(-7.2024,b,)))(\wedge(*a,7.2024,)))/(-(*(+d,c,)(-b,c,)))/(\wedge c,d,)) \\
 &(*2.2896!,a,)))(*(-(*(-c,a,)),a,)),6.6513,)(-/a,a,)(-b,b,)))))))(\wedge(*a,1.7182!,)/(-(*(+d,c,)) \\
 &(-2.2896!,c,)))/(\wedge c,d,)(*4.9831,a,)))(*(-(*(-c,a,)),a,))(\wedge d,(+(\wedge a,c,)(*d,d,)),)(-/a,a,)(- \\
 &b,b,)))))))(a,)(+d,b,)),b,)),(*1.7182!,(+((+(/c,(-(\wedge(-c,c,)),(*((+((+(\wedge(- \\
 &b,c,)),5.3479!,)),1.7182!,)(-5.3479!,b,)))(\wedge(*a,7.3000,)))/(*d,8.4191,)))(*(-(*(- \\
 &c,a,)),a,)),2.2896!,)/(-(*a,4.9831,)),a,)),a,)))(\wedge(+d,b,)/a,d,)))(-c,a,)))(/d,b,))(- \\
 &\wedge d,c,)(-b,c,))))))
 \end{aligned}$$

The results of the test data obtained from this formula are below.

Table 7. The results of the test data of medium carbon steel.

Name of the Material	Hardness (Hb)	The hardness estimated by the formula (Hb)
AISI 1030	137	136.9162
AISI 1037	143	142.9901
AISI 1039	156	155.9978
AISI 1042	163	162.985
AISI 1044	163	163.1134
AISI 1046	170	169.9925
AISI 1050	179	179.0268

The results of the validation data obtained from this formula are below.

Table 8. The results of the validation data of medium carbon steel.

Name of the Material	Hardness (Hb)	The hardness estimated by the formula (Hb)
AISI 1038	149	152.6248
AISI 1040	149	156.8309
AISI 1043	163	162.2629
AISI 1045	163	169.5737

3.3. High Carbon Steel

High carbon steel has been used in the conducted experiment.

Table 9. *Test data of medium carbon steel.*

Name of the Material	Carbon (C), %	Manganese(Mn), %	Phosphate(P), %	Sulfur(S), %	Hardness(Hb), %
AISI 1055	0.55	0.75	0.040	0.050	192
AISI 1064	0.65	0.65	0.040	0.050	201
AISI 1070	0.70	0.75	0.040	0.050	212
AISI 1078	0.785	0.45	0.040	0.050	207
AISI 1084	0.865	0.75	0.040	0.050	241
AISI 1086	0.865	0.45	0.040	0.050	229
AISI 1095	0.965	0.45	0.040	0.050	248

Table 10. *Verification data of medium carbon steel.*

Name of the Material	Carbon (C), %	Manganese(Mn), %	Phosphate(P), %	Sulfur(S), %	Hardness(Hb), %
AISI 1065	0.65	0.75	0.040	0.050	201
AISI 1074	0.75	0.65	0.040	0.050	217
AISI 1080	0.815	0.75	0.040	0.050	229
AISI 1090	0.915	0.75	0.040	0.050	248

Many experiments have been conducted with high carbon steels test data. As a result of these experiments, the best formula found by the USYAAP-GEN genetic programming modeler is below.

In order to obtain the optimum formula from those found in the many experiments that were conducted, the size of the population was computed as 10000, the maximum depth of the population 400, the ratio of reproduction 0.2, the ratio of crossover 0.8, the ratio of mutation 0.2, and the maximum generation was 100; error based fitness function was used as the fitness function, tournament selection as the selection method, 7 as the initial depth and the saturation method was used to create the initial population. As a result, a formula that has a fitness of 97.8% was produced.

Formula:

$$\begin{aligned}
 &(-(+(/7.8080,c,)(*c,(-/(-c,7.8080),d),(-c,(+(*b,(+(*+b,c),(*a(/b,(+c,(+(*+b,c),(*+ \\
 &+a,(*c,(-c,(-(/b,(+c,(*(+a,(+d,d),)(-(/b,(+c,(*+^b,(+a,(-a,(+(+a,c, \\
 &(*+b,(*(+a,(+d,d),)(*b,(+a,(*b,a,)),)(*b,a,)),a)),)+b,(-(/a,(/(-c,(+8.3384,a,)), \\
 &+a,c,)),a),(+(+a,c,)(*+b,b,a,)),a,)),),+d,d,)),a,)(*b,a,)),)+a,(*+a,c,)(+ \\
 &(*b,(+a,(*b,a,)),c,)),(+(+a,c,)(*+b,b,a,)),a,)))(*+d,d,a,)),a,)(+((+a,c,)(* /(- \\
 &^/b,(+c,(*+a,(+d,d),)(*b,(+a,(*b,a,)),)(*b,a,)),)+(+a,a,)(+d,d,)(*b,(+ \\
 &(*+b,c,)(*a(/b,(+c,(+(*+b,c,)(*+a,(*c,(+c,d,)),)+b,c,)),(*a,a,)),c,)),),c,)))(+ \\
 &(+a,(+a,c,)))(*+b,b,)),a,)),a,)),c,)(*a,a,)),),a,)),),)(*+b,c,)),a,)), \\
 &(*a,a,)),),c,)),),c,)),a,)),))(* /(-(/b,(+c,(*+a,(+d,d),)(*b,(+a,(*b,a,))) \\
 &(*b,a,)),)+(+b,a,)(+d,d,))(-/(-c,(+^b,(+(*b,(+(*+b,c,)(*+a,(*c,(*+a,(*c, \\
 &+d,d,)))(*a,(*+(*c,(+a,(*b,a,)),)+d,d,)))(*+a,(+d,d,)),)+b,c,)(*c,a,))) \\
 &(*a,a,)),)(*a,a,)),)(*a,(*+(*c,(+a,(*b,a,)),)+d,d,)))(*+a,(+d,d,)),)+b,c, \\
 &(*c,a,)))(*a,a,)),)(*a,a,)),(-a,(+((+a,c,)(*+b,b,a,)),a,)),d,)),a,)),(-(/b,(+ \\
 &+a,c,)(* /(-(/b,a,))(+c,(+d,d,)))(*b,(+(*+b,c,)(*+a,(*c,(*+a,(*c, \\
 &+d,d,)))(*+a,(+d,d,)),)+(+a,(*c,(-c,(-(/b,(+c,(*+a,(+d,d,))(-(/b,(+c,(*+a, \\
 &+a,(+d,d,)))(*b,(+a,(*b,a,)),)(*b,a,)),),)+a,b,)))+(+a,c,)(*+b,b,a,)),a,)) \\
 &(*a,a,)),a,)(+((+a,c,)(* /(-(/b,(+c,(*+a,(+d,d,)))(*b,(+a,(*b,a,))) (*b,a,))),)+ \\
 &+a,a,)(+d,d,)))(*b,(+(*+b,c,)(*a(/b,(+c,(+(*+b,c,)(*+a,(*7.8080,(+d,d,))) (*a, \\
 &(*+(*c,(+a,(*b,a,)),)+d,d,)))(*+a,(+d,d,)),)+b,c,)(*c,a,))) (*a,a,)), \\
 &(*a,a,)),),c,)),),c,)),)+(+a,(+a,c,))(*+b,b,a,)),a,)),c,)(*a,a,)),a,)),), \\
 &(*+b,c,a,)),(*c,a,)))(*a,a,)),(*a,a,)),),c,)),),c,)),)+((-(/b,(+c,(*+a,(+a, \\
 &+d,d,)),)(*b,(+a,(*b,a,)),)(*b,a,)),),)+a,a,)))+((+a,c,)(*+b,b,a,)),c,)) \\
 &(*+b,b,a,)),a,)),c,)(*a,a,)),)^/a,(/(-c,(+8.3384,a,)),d,)),a,)),),c,)))+((+a,c, \\
 &(*+b,b,a,)),a,)),b,)))+((+a,c,)(*+b,b,a,)),a,)),c,)(*a,a,))
 \end{aligned}$$

The results of the test data obtained from this formula are below:

Table 11. The results of the test data of high carbon steel.

Name of the Material	Hardness (Hb)	The hardness estimated by the formula (Hb)
AISI 1055	192	191.9905
AISI 1064	201	201.0052
AISI 1070	212	211.9575
AISI 1078	207	206.954
AISI 1084	241	240.9512
AISI 1086	229	228.9946
AISI 1095	248	248.008

The results of the validation data obtained from this formula are below.

Table 12. *The results of the validation data of high carbon steel.*

Name of the Material	Hardness (Hb)	The hardness estimated by the formula (Hb)
AISI 1065	201	204.7759
AISI 1074	217	212.1569
AISI 1080	229	230.9879
AISI 1090	248	250.7439

4. RESULTS

Carbon steel has given a significant positive reaction to the Genetic programming modeler. To achieve generalization capability for the formulations, the experimental data is divided into two sets as training and validation sets. As K ok and Kanca, 2010 stated in their studies, the validation data in the literature were selected at the rate of 20-30% of the test data. Similar rates were used in the study. It has been observed that the formula in the study, whose statistical results are given in Table 13, provides close to 100% compliance with the test data, but does not match the verification data at the same rate. It is thought that increasing the number of experiments and the data set used and using extra parameters as input can be beneficial to overcome this situation. You can see the other chemical, physical and mechanical properties of AISI standard carbon steel from Azom web site (Azom, 2021).

Table 13. *The statistical results of the experiment.*

Steel	Statistical Parameter	Test (Training) Set	Validation Set
Low Carbon	RSquare(R^2)	0.9999	0.9316
Medium Carbon	RSquare(R^2)	0.9999	0.7789
High Carbon	RSquare(R^2)	0.9999	0.9643

It has been observed that the USYAAP-GEN program can be used successfully for the solution for problems such as wear in steel. On the other hand, the overfitting situation seen in the study can be eliminated by working with much larger experimental sets.

In the study, mutation rate was taken as 20% as a genetic parameter. In the literature, similar mutation rates were used in Faris et al. 2020 (15%) and Kolodziejczyk et al. 2008 (25%), studies that worked on genetic programming with carbon steels. Nguyen et al, 2020 (%30) use GP for evolving models for storm surge forecasting. Ranansigle et al. 2019 (%30) used GP for predictions of effectiveness of rolling dynamic compaction. When the mutation rate was used low, it was observed that the population stuck to local minimum

and local maximums. The high mutation rate in similar studies should be considered as a new research topic.

It has also been observed that the USYAAP-GEN program, or genetic programming modelers in general, necessitate a great deal of computer hardware (CPU, RAM, TIME), and long processing periods are required in order to solve these kinds of complicated problems. Thus the study, which is experimentally conducted with limited test and verification data, should be verified with much larger data sets in future studies. In future experiments, new generation servers with GPU base processors can be used.

It has been seen that, out of the harmonic ratio selection method, and the tournament selection method that was placed in the USYAAP-GEN genetic programming modeler, the tournament selection method was more successful in these types of problems.

In the conducted study, hardness that has a rather large solution space and is a complicated problem has been successfully formulized, and this has proved to be successful in achieving the solution for these kinds of problems.

REFERENCES

- Azom, 2021, Online publication for the Materials Science community, <https://www.azom.com>
- Barclay J., Dhokia V., Nassehi A., 2015 “Generating milling tool paths for prismatic parts using genetic programming”, 9th CIRP Conference on Intelligent Computation in Manufacturing Engineering, Procedia CIRP 33, 490 – 495.
- Boun, 2001, Bogazici University, Robot Site, <http://robot.cmpe.boun.edu.tr/593>.
- Brezocnik, M., Kovacic, M., Psenicnik, M., 2006. “Prediction of steel machinability by genetic programming”. *Journal of Achievements in Materials and Manufacturing Engineering*. 16.
- Chen, J. S., Chang, C. L., Hou, J. L., Lin, Y. T., 2008, “Dynamic proportion portfolio insurance using genetic programming with principal component analysis”, *Department of Information Management, National Central University, Expert Systems with Applications* 35, 273–278.
- Faris, R., Almasri, B., Faris, H., AL-Oqla, F. M., Dalalah, D., 2020, “Evolving Genetic Programming Models for Predicting Quantities of Adhesive Wear in Low and Medium Carbon Steel”, doi: 10.1007/978-981-32-9990-0_7.
- Fujiki, C., Dickinson, J., 1987, “Using the genetic algorithm to generate LISP source code to solve the prisoner’s dilemma”, *Genetic Algorithms and Their Applications: Proceedings of the Second International Conference on Genetic Algorithms*, Erlbaum.
- Garg, A., Su, S., Li, F., Gao, L., 2020, “Framework of model selection criteria approximated genetic programming for optimization function for renewable energy systems”, *swarm and evolutionary computation*, 59.
- Giles, C. L., Lawrence, S. and Tsoi, A.C., 2001, “Noisy Time Series Prediction Using A Recurrent Neural Network and Grammatical Interface”, *Machine Learning*, 44, 1-2, 161-183.
- Goldberg, D.E., 1989, “Genetic Algorithms in Search, Optimization, and Machine Learning”, Addison-Wesley Publishing Company, USA.
- Göloğlu, C., Arslan, Y., 2009, “Zigzag machining surface roughness modelling using evolutionary approach.” *J Intell Manuf* 20, 203–210. <https://doi.org/10.1007/s10845-008-0222-1>
- Grosman B., Lewin R. D., 2004, “adaptive genetic programming for steady-state process modeling”, *Computer and Chemical engineering*, Vol 28, Issue 12, Pages 2779-2790, ISSN 0098-1354, doi: 10.1016/j.compchemeng.2004.09.001
- Güven, A., Özcan, T. M., 2005,” Effect of material hardness on abrasive wear of plain carbon steels in mineral environments “, *Engineer and Machine*, 46, 545.
- Hicklin, J., F., *Application of the Genetic Algorithm to Automatic Program Generation*. M. S. thesis, Computer Science Dept., University of Idaho, 1986.

- Hien, N.T., Tran, C.T., Nguyen, X.H., et al., 2020 “Genetic Programming for storm surge forecasting.” *Ocean Engineering*. Vol 215, ISSN 0029-8018, doi:10.1016/j.oceaneng.2020.107812.
- Holland, J. H., 1975, “Adaptation in Natural and Artificial Systems”, The University of Michigan Press, Ann Arbor, MI.
- Iqbal, A., He, N., Dar, N., Li, L., 2007, Comparison of fuzzy expert system based strategies of offline and online estimation of flank wear in hard milling process. *Expert Systems With Applications*, 33. 61-66. 10.1016/j.eswa.2006.04.003.
- İzciler, M., 1997, “The effects of alloy additive rate and heat treatment conditions on the abrasive wear behavior of high chromium alloy cast irons at different temperatures”, PhD Thesis, University of Firat, Institute of Science, Elazığ.
- Karaoğlu, Y., 2006, “Design and Manufacture of a Wear Test Device”, Master Thesis, University of Sakarya, Institute of Science, Sakarya.
- Kolodziejczyk, T., et al., “A methodological approach ball bearing damage prediction under fretting wear conditions.” 2008 4th International IEEE Conference Intelligent Systems, Varna, Bulgaria, 2008, pp. 10-53-10-59, doi: 10.1109/IS.2008.4670497.
- Kor, M., Abkhoshk, E., Tao, D., Chen, G., Modarres H., 2010. Modeling and optimization of high chromium alloy wear in phosphate laboratory grinding mill with fuzzy logic and particle swarm optimization technique. *Minerals Engineering*, 23. 713-719. 10.1016/j.mineng.2010.04.009.
- Kovačič, M., Mihevc, A., Terčelj, M., 2019, “Roll wear modeling using genetic programming – industry case study”. *Materials and Technology*. 53. 319-325. doi:10.17222/mit.2018.104.
- Koza J., 1992,” Genetic programming on the programming of computers by means natural selection”, The MIT Press, USA.
- Koza, J., 1994, “Genetic Programming II: Automatic Discovery of Reusable Programs. MIT Press, Cambridge”, MA, USA.
- Kök, M., and Kanca, E., 2010, “Abrasive wear model for al2o3 particle reinforced mmcs using genetic expression programming,” *Computers, Materials & Continua*, vol. 18, no.3, pp. 213–236.
- Ranansigle, R., Jaksa, M., Nejad, F., Kuo, Y., 2019, “Genetic programming for predictions of effectiveness of rolling dynamic compaction with dynamic cone penetrometer test results”, *Journal of Rock Mechanics and Geotechnical Engineering*, Vol 11, Issue 4, Pages 815-823, ISSN 1674-7755, doi:1016/j.jrmge.2018.10.007.
- R.G. Silva, R.L. Reuben, K.J. Baker, S.J. Wilcox, Tool Wear Monitoring of Turning Operations by Neural Network and Expert System Classification of a Feature Set Generated From Multiple Sensors, *Mechanical Systems and Signal Processing*, Volume 12, Issue 2, 1998, Pages 319-332, ISSN 0888-3270, <https://doi.org/10.1006/mssp.1997.0123>.
- Tay, j. C., Ho B. N., 2008, “Evolving dispatching rules using genetic programming for

solving multi-objective flexible job-shop problems”, *Computers & Industrial Engineering* 54, 453–473.

Wang, H., Dong, G. and Chen, J., 2021, “Application of genetic programming in the identification of tool wear”, *Engineering Computations*, Vol. ahead-of-print No. ahead-of-print. <https://doi.org/10.1108/EC-08-2020-0470>

X.P. Yan, C.H. Zhao, Z.Y. Lu, X.C. Zhou, H.L. Xiao, A study of information technology used in oil monitoring, *Tribology International*, Volume 38, Issue 10, 2005, Pages 879-886, ISSN 0301-679X, <https://doi.org/10.1016/j.triboint.2005.03.012>.

Chapter 13

EVALUATION OF MASS TRANSPORTATION SYSTEMS IN ISTANBUL AND MODAL SELECTION

Mehmet Çaęrı KIZILTAŞ¹

Vail KARAKALE²

1 mckiziltas@ticaret.edu.tr, Istanbul Ticaret University Engineering Faculty, Civil Engineering Department

2 Prof.Dr., vail.karakale@medeniyyet.edu.tr, Istanbul Medeniyyet University Engineering Faculty, Civil Engineering Department

Introduction

Transportation is one of the most important factors affecting the economic development and welfare of a country. Effective transport systems facilitate socio-economic opportunities and benefits by facilitating access to markets, businesses and investments. Transportation is changing rapidly in today's world in parallel with globalization and economic growth. Rapid development of science and technology and population growth; led to high capacity, faster, safer and more comfortable transportation.

Investments in urban oriented systems; has developed rapidly over the last decade, especially on the subway. Investments in subway alone will not be sufficient to achieve balanced distribution in transportation and may not reduce private car ownership rates. Increase of traffic safety and transport to desired level; Balanced distribution of transportation modes and integration are important for the transportation system to operate efficiently. Furthermore; the governance of consumption culture and transportation master plan should be integrated into each other. The preference of public transportation can be done according to; supply-demand management and orientation, the ability of the consumption culture to be channeled in the right direction, innovative and technical equipment, and service parameters (punctuality, comfort, safety, cost). Example of consumer culture in Japan; a business man usually tolerates the use of metro as a public transportation vehicle. This is because that the service parameters of Japan, particularly comfort and safety, are provided at a high level in public transportation. In Istanbul the crossings from Asia to Europe are examined by several researchers and, it is seen that 81% of the transportation carried by bridges and only 19% carried by sea.

Development Trends In Istanbul

From a broader perspective; In the crossings of the Bosphorus bridges, 90% of the vehicles are occupied by private cars, while 24% of the passengers are transported by tires and 10% of them are transported by 37% of the passengers. Private automobiles, which are the most important factor of the traffic jam on the bridge, only meet a very limited part of the passengers carried from the bridges as a result of the increase in private car ownership rates and as a result of having an average of 1-1.2 passengers on almost every private car. From here; It is also possible to reach from the bridges the passage of very special automobiles from people. In this context; It is seen that public transportation priority approaches should be developed in the transportation investments to be realized. Figure 1 below shows the variation of the urban distribution of Istanbul between 1996 and 2006. As can be seen in Figure 1, the variation in the distribution of urban transportation was mainly realized in the post-1996 period, and there was a significant increase in the number of private automobiles and service vehicles.

Especially in the last decade, investments in urban rail systems have made significant progress in balancing this table.

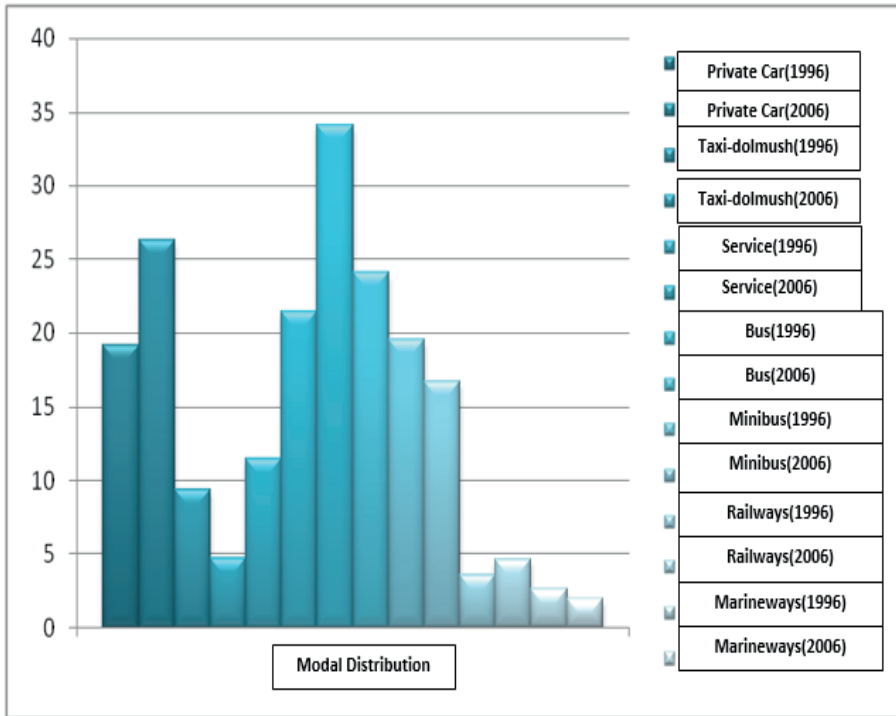


Figure 1. Modal Distribution in the 1996-2006 Istanbul Urban Transportation

Below on Table 1, it has seen that the informations about yearly population growth and volume of increase. A partial decrease is seen for last years on the population increase acceleration of Istanbul and also high amount of population increases are continuing as it is seen from the tables.

	2009-2010	2010-2011	2011-2012	2012-2013	2013-2014	2014-2015
Increase	340.527	368.555	230.500	305.727	216.551	280.416
Increase Rate(%)	26,0	27,4	16,8	21,8	15,2	19,3

Table 1. Yearly Population Growth and Acceleration On The Years Of 2009-2015

At this point, another affect is accelerating of urbanization on both sides of the city, along the Marmara coasts and inner regions of the city by the construction of three Bosphorus bridges. Below on Table 2 is illustrated the general values of Istanbul. It can be said that the rate of square measures between two sides of the city is similar to the rate of population distribution of two sides of the city.

It has been estimated that the number of vehicle accesses in bosphorus bridges is approximately 250.000/day. But at this point, totally 600.000 vehicles/day have been accessed by the 1st and 2nd bosphorus bridges.

Data	Unit	Value
Square Measure (Lakes included-118 Km ² -)	Km ²	5.461
AnatolianSide (%35)	Km ²	1.898
EuropeanSide (%65)	Km ²	3.563
Population	Person	14.657.434
Men Population	Person	7.360.499
Women Population	Person	7.296.935
Yearly Population Increase Rate Of Istanbul (2015)	%	19,3
Yearly Population Increase Rate Of Turkey (2015)	%	13,4
The Population Rate Of Istanbul/Turkey	%	18,6
The Number Of Districts	Item	39
The Number Of Quarters	Item	959*
The Number Of Residences	Item	3.886.890**

Table 2. The General Values Of Istanbul

The construction of 1st and 2nd Bosphorus bridges in Istanbul has led changings at significant scales in urban structure and transportation system that is expected to emerge important affects on urban traffic and bosphorus bridges accesses because of the Marmaray operation which has been opened in 29th October 2013.

Urban Rail Systems

The transportation values in Istanbul reveal the necessity to use and use public transportation in a higher level than the present situation. For this, Diversification of transport types and balancing of mode distribution, integration between modes (integration between different types of public transportation, integration between different types of transportation, integration between public transportation and individual transportation, etc.) is necessary. The rail system and especially the metro investments have a vital proposition when the traffic congestion in Istanbul is brought to bearable levels. Construction of the metro and light rail system line is continuing in Istanbul in 2004 and the operation of Kadıköy-Kartal Metro line has been operated as of last year. Interms of travel values in Istanbul in 2010, the road transport ratio is 78.4% in terms of type distribution and it is 67.7% in 2014, 50.7% in 2018, 26.5% in 2023, a reduction is anticipated. Marmaray, which was partially opened as of October 29, 2013, is 7.4% in terms of diversification as of 2014; 7.9% in 2018; In 2023 it is predicted to reach 5.7% share. Another main determinant of the traffic congestion problem in Istanbul is the relocation of the railway system lines to the bearable point. As for the urban railway system lines, it is necessary to make metro lines as a common investment

area and it is necessary that these lines should be realized in an integrated manner with each other. The Metrobüsline (BRT), which has been operating for the first time in Istanbul for the first time as a sole example, is a system that has successful examples in the world especially in Latin America and it is a transportation type that is preferred especially in terms of time in Istanbul. The Metrobus line connects the two distant points of the city on the east-west axis and the regions with intense travel demands. This line, which provides significant savings in terms of working and full capacity, is also discussed on the other side in terms of comfort and safety parameters.

Istanbul Urban Transportation Survey

- The survey was conducted with 850 people aged 16-63 with an average age of 24.

- 59% of the participants were male and 41% were female.

- Questionnaire; Technicians, lawyers, administrators, technicians, accountants, members of the military, architects, housewives, technicians, designers, engineers, technicians, teachers, self-employed persons, Trader, public official, operator, chemist, driver, heavy worker, tourist, modelist, landscape architect, printer, security personnel, tradesman, laborant, public relations, makinist, coach, municipality staff, marketer, captain, service personnel, writer, academician Dentist, international relations specialist, crane operator, banker, banker, baker, contractor, photographer, pdr, financial advisor, doctor, business man, archivist, bookstore, real estate consultant, religious officer, cashier, Hairdresser, project manager, as well as people from many professional branches.

- About 2/3 of the respondents are undergraduates (associate degree students) while 70% of them are graduates with graduate degrees (or students). Therefore, the educational status of the participants is clearly above the average of Turkey and Istanbul.

- Those who participated in the survey were mainly Kartal, Esenyurt, Fatih, Güngören, Pendik, Esenler, Avcılar, Sultangazi, Sarıyer, Zeytinburnu, Üsküdar, Kagithane, Beykoz, Basaksehir, Beyoglu, Eyüp, Silivri, Beşiktaş, Beylikdüzü, Gaziosmanpaşa, Bahçelievler, Şişli, Bağcılar, Maltepe, Ümraniye, Küçükçekmece, Çekmeköy, Bayrampaşa, Sultanbeyli, Ataşehir, Bakırköy, Kadıköy, Tuzla and Arnavutköy.

- Those who participated in the survey were mostly Fatih, Üsküdar, Kagithane, Şişli, Avcılar, Esenyurt, Sarıyer, Pendik, Tuzla, Güngören, Bağcılar, Bakirkoy, Beyoglu, Kartal, Eyüp, Beşiktaş, Beykoz, Esenler, Zeytinburnu, Maltepe, Beylikdüzü, Bahçelievler, Başakşehir, Silivri, Küçükçekmece, Buyukcekmece, Ümraniye, Sultangazi, Gaziosmanpaşa, Bayrampaşa, Arnavutköy, Sancaktepe, Ataşehir.

About one-third of the participants live in Anatolia, while two-thirds live in Europe. 7.8% of the participants are traveling every day for work-school trips. The rate of those who pass from Anatolia to Europe is 4.2% whereas this rate is 3.6% for those who pass from Europe to Anatolia. While the majority of the respondents (92.2%) resided in the area where they had business trips, it was 29.0% compared to the participants in Anatolia - 63.2% for Europe. These results tell us; The city is rapidly becoming a multi-center city, Istanbul is a city far away from the sea. The overall distribution of the participants' cohesion is largely in line with the Istanbul population employment. Also, 33.1% of the participants are carrying out Daily home-work / schooltrips on existing Marmaray and connection lines (also Gebze-Halkalı full capacity Marmaray route).

More than 53% of respondents use more than two times a day on public transport, compared to 8% for those who use it once a day. Therefore, approximately 2 out of every 3 participants use public transportation (intensive) every day. This is remarkable and striking when it is taken into consideration that Istanbul is above the public transportation use and the participants' education level is above the Istanbul average. This; It is understood that they need to be analyzed in a socio-economic perspective rather than merely a conscious choice. It is roughly possible to make roughly one in every 1 out of 3 participants, mainly using public transport several times a week, several times a week, several times a week, most of them using private cars on their home-business / school trips and therefore having a private car. However, it is thought that the rate of preference of public transport from time to time for private vehicle owners should be examined separately in what direction and at what moment during the last ten years.

Participants stated that they use a system of more than 50% urban railway systems when they are asked what vehicles they use on their home-business / school trips, and 18.5% of them said that they use Marmaray. Participants stated that they used İETT and private public buses with 58% more and again stated that 42.1% used metrobus. On these trips, participants stated that they use 11% of the sea transportation, and about 1 out of 3 participants stated that they use minibus-minibuses in their home-business / school trips. This rate is 10.6% for service vehicles, approximately 10% for taxis and 22.8% for private vehicles. The conclusions that can be drawn from this are: people are satisfied with the investment of the generic city rail system (metro, tramway etc.) and believe that as the investments are maintained in functional terms, the transportation opportunities will increase and also the traffic congestion can be controlled and this is revealed with the interest shown to Marmaray. However, taking full capacity operation of Marmaray 's and good management of this process is important in this point. Again, it is understood that there is an animal that has attracted special vehicles from home, on business trips and

school trips, especially in recent years, and that there is an increase in this population. However, it is understood that the problem of increasing fuel prices and traffic congestion, which is not the only reason for this, is also effective. While it is seen that sea transport is preferred by most of the participants compared to Istanbul, the answers to the other questions of the questionnaire are not permanent and insistent. While the choice for IETT and private public buses is still at the top, it is partly a compulsory choice (investments in tracked system investments are still on the rise) - as is clear from other survey questions - partly improved fleets Renewal, line optimizations, stall applications, partial improvements in integration with other systems). Taxis and service vehicles also take a considerable share in home-business / school trips, and the future course of these types will also include smart taxi applications-such as the orientation of audits and service vehicles in traffic, and the location of traffic in transit. The current share of minibus-dolmuş is a completely compulsory preference, and in the other questions of the questionnaire the approach to the service parameters is more clear that the minibus-minibuses will not be in the mid-range in public transport.

More than 36% of respondents stated that they were satisfied with 'speed' from the service parameters of public transportation, followed by 26% with punctuality, frequency with 23%. The users (and therefore the participants) say that the city rail system lines have 'high speed' they understand as they travel along their route without encountering traffic congestion they know from the highway. Higher values in urban traffic congestion also increased the sensitivity of public transport to detecting 'speed' parameters. Here; IETT and special public buses in recent years, fleet and operational re-related to the need to mention worthwhile.

Approximately 30% of respondents indicated that the most inadequate service of public transport was 'comfort', followed by 24.9% with punctuality and 24.4% wage. For security, this rate is 13.8% and if it is considered that comfort and safety should be assessed together in a certain extent, this ratio is approaching 44% and it is prevalent as one of the most urgent issues of mass transportation in Istanbul. This; There is an indirect link with selected routes and pedestrian accessibility at certain points, such as direct connection with capacity overruns and traffic accident rates. At this point; Metrobus and minibus-minibus modes should be mentioned first. Although the tariff seems to be a point in terms of its share in both questions, it can be considered that a relative decrease in costs is likely to significantly affect satisfaction in this direction, and this point can be handled coincidentally with the strategy of raising the system investments. The change in the punctuality-frequency parameter is essentially; The investments in the system of railway systems in the country - a process that goes on the minibus-minibus axis.

Most of the participants think that the 3rd bridge is going to affect Istanbul traffic positively. 3. The bridge is also equipped with a rail system line. The third bridge is a positive view, special vehicle usage habits and point of view, satisfaction and expectation from the investments of the railway system in the city are the issues to be evaluated together. Available tablodan; It is clear that the third link - publicly - on all sides - can not be dismissed enough from 'political engagement'.

2 out of 5 respondents expressed their overall satisfaction as 'good' from public transport. 28% of those who give the 'normal' answer to this question are about '1/3', 'inadequate-very inadequate'.

Results

In cities, even if a large part of the capacity of the roads is used by automobiles, most of the journeys are carried out by means of public transport, which uses only a fraction of the road capacity. Therefore, in order to increase the efficiency in public transport, regulations should be made to ensure that operators do not damage, and that users get comfortable, cheap and fast service. In order to increase the commercial speed especially at peak hours, special bus routes should be put into service firstly and high speed bus routes should be planned in the main arteries that the road platform allows.

Another main determinant in eliminating the traffic congestion problem in Istanbul is the extension of urban railway system lines. Istanbul Metropolitan Municipality has increased the metro and light rail system lines of the city geometrically with the investments of the metro that it made during the last ten years. But; There is a need for a metro line which is already important for a city on Istanbul scale. Projects for construction, construction and operation for metro lines in 2014, 2019 and 2019 have been put forward in Istanbul with the targets set for Istanbul's 10th and 11th Maritime Communication Committees' It is fore seen to be among the cities with its network.

In Istanbul, the distribution of roads has an overloaded share, while the share of usage of 'private cars' on the highways is also very high. It; While leading to consequences that threaten road traffic safety, it forces all Istanbul people to constantly waive parameters such as comfort, security, punctuality as much as possible. Public transportation; To approach all modes of transport and to offer a more integrated, comfortable, punctual, safe service in this sense will enable us to receive visible returns in the short term. As we can see from this whole table; In order to minimize the traffic congestion and the problems caused by urban transportation in Istanbul, it is necessary to provide modal distribution and intergral integration. Marmaray Project, subway planning, 3rd bridge, rubber wheeled tube passage etc. It is useful to evaluate the projects in this framework.

In this sense; the development of technology, the orientation of investments, the development strategies of cities and the improvement of transportation systems should be seen and acted with a 'human-focused' perspective.

REFERENCES

- M.İlçali, N. Çatbaş, A. Öngel, M. Ç. Kızıldaş, 'Multimodal Transportation Issues in Istanbul: A Case Study for Traffic Redistribution Due to Long Span Bridge Rehabilitation', Hong Kong, 2013.
- M.Ç.Kızıldaş, 'Ulaştırma Yatırımları ve Marmaray-1', Available: <http://www.ulastirmadunyasi.com/index.php/2013/12/ulastirma-yatirimlari-ve-marmaray-1/> (24.04.2014).
- M.Ç.Kızıldaş, 'Ulaştırma Yatırımları ve Marmaray-7', Available: <http://www.ulastirmadunyasi.com/index.php/2013/12/ulastirma-yatirimlari-ve-marmaray-7/> (24.04.2014).
- M.Ç.Kızıldaş, 'Ulaştırma Yatırımları ve Marmaray-4', Available: <http://www.ulastirmadunyasi.com/index.php/2013/12/ulastirma-yatirimlari-ve-marmaray-4/> (24.04.2014).
- G.Tzeng, T.Shiau, 'Multiple Objective Programming For Bus Operation: A Case Study For Taipei City, Transportation Research Part B 22 (3), 195-206, 1988.
- M.Ç.Kızıldaş, 'Yüksek Hızlı Demiryolu Politikaları-1', Available: <http://www.ulastirmadunyasi.com/?p=824> (01.10.2014).
- J.Rawls, 'A Theory Of Justice', HarwardUniversityPress, Cambridge, 1971.
- Dill, J., Rose, G., (2012) E-Bikes and transportation policy: insights from early adopters. In: Transportation Research Board 91st Annual Meeting, Washington DC.
- García-Palomares, J.C., Gutiérrez, J., Latorre, M., (2012) Optimizing the location of stations in bike-sharing programs: a GIS approach. *Appl. Geogr.* 35, 235e246.
- Theurel, J., Theurel, A., Lepers, R., (2012) Physiological and cognitive responses when riding an electrically assisted bicycle versus a classical bicycle. *Ergonomics* 55, 773e781.
- Kızıldaş, M, Ç, 2018. Küresel Örnekleri ile Toplu Ulaştırma, Transist 2018, İstanbul Ulaşım Kongresi ve Fuarı, İstanbul, 8-10 Kasım
- Diaz, M., Soriguera, F., Autonomous Vehicles: Theoretical and Practical Challenges, 2018, *Transportation Research Procedia*, Vol. 33, 275,282.
- Rueda, D., Nieuwenhuijsen, M., Khreis, H., Frumkin, H. Autonomous Vehicles and Public Health, 2019, *Annual Review Of Public Health*.
- Nurumbayeva L.M., Badanin A.N. (2014) Justification for determination of the depth of an active zone based on the ii group of limiting states *Applied Mechanics and Materials*. Vol. 580-583.Pp. 98-104.
- Dianov V.N., Gevondian T.A. (2014) Parking system of high reliability innovation technologies. Vol. 2. pp 531-535.
- A. Vaibhav, D. Shukla, S. Das, S. Sahana, P. Johri, Security challenges, authentication, application and trust models for vehicular Ad Hoc network-a survey, *Int. J.*

Wirel. Microw. Technol. 3 (2017) 36–48, doi:10.5815/ijwmt.2017.03.04.

- J. Fujie, “An advanced arrangement of the combined propulsion, levitation and guidance system of superconducting Maglev,” *IEEE Trans. Magn.*, vol. 35, no. 5, pp. 4049–4051, Sep. 1999.
- P. Burke, R. Turton, and G Slemmon, “The calculation of eddy losses in guideway conductors and structural members of high-speed vehicles,” *IEEE Trans. Magn.*, vol. MAG-10, no. 3, pp. 462–465, Sep. 1974.
- B.-T. Ooi, “Electromechanical dynamics in superconducting levitation systems,” *IEEE Trans. Magn.*, vol. MAG-11, no. 5, pp. 1495–1497, Sep. 1975.
- G. Bohn, “Calculation of frequency responses of electro-magnetic levitation magnets,” *IEEE Trans. Magn.*, vol. MAG-13, no. 5, pp. 1412–1414, Sep. 1977.
- Amendo, C., Hamm, P., Kelly, J., Maerz, L., Brunette, K., Scrudato, M., Finley, G. & Greene, L., 2016. *Autonomous*
- Wang, F.Z., Google released the product of smart home: Google Home. Available from <http://tech.163.com/16/0519/01/BND3AHMH000915BD.html> (in Chinese) (2016)
- Sak, H., Senior, A., Beaufays, F., (2014) Long short-term memory recurrent neural network architectures for large scale acoustic modeling. *INTERSPEECH*, p.338-342.
- Langford, B., Cherry, C., Yoon, T., Worley, S., Smith, D., (2013) North America’s first ebike share: a year of experience. *Transport. Res. Record: J. Transport. Res. Board* (In Press)
- Takatsu T, (2007) “The history and future of high-speed railways in Japan”. *Japan Railway & Transport Review*, 48, 6-21
- TÜİK verileri, 2015
- Golobič, M., & Marot, N., (2011) Territorial impact assessment: Integrating territorial aspects in sectoral policies. *Evaluation and program planning*, 34(3), 163–173. doi:10.1016/j.evalprogplan.2011.02.009
- Steer Davies Gleave. (2006). *Air and rail competition and complementarity*. Report for European Commission DG TREN.
- Kızıldaş, Mehmet Çağrı (2013), *Şehir, Şehirleşme ve Ulaştırma, Ulaştırma Dünyası Gazetesi*
- TR 10. Government Plan Transportation and Traffic Safety Ö.İ.K. Report, 2012, Ankara
- Wang, Y., “Remote sensing and modeling in regional land cover change study,” *International Society for Photogrammetry and Remote Sensing*, 34(4), 22-26, 2002.
- Lobb, B., Harré N., Terry, N., 2003, ‘An Evaluation of Four Types of Railway Pedestrian Crossing Safety Intervention’
- Congalton R.G., and Green K., *Assessing the accuracy of remotely sensed data: principle and practices*, CRC Press; 2 edition, December 12, 2008

The graphic features a central white circle with a green semi-circle at the top. The text 'Chapter 14' is written in a black, stylized font on the green background. Below this, the title 'THE ROLE OF GEOPOLYMERS IN MINING AND THEIR CONTRIBUTIONS TO A SUSTAINABLE FUTURE' is written in a bold, black, sans-serif font. The author's name 'Kemal ŞAHBUDAK¹' is centered below the title. The entire graphic is surrounded by a glowing yellow and green aura with a green line that loops around it.

Chapter 14

THE ROLE OF GEOPOLYMERS IN MINING AND THEIR CONTRIBUTIONS TO A SUSTAINABLE FUTURE

Kemal ŞAHBUDAK¹

¹ Metallurgy and Materials Engineering / Sivas Cumhuriyet University Faculty of Engineering,
kemalsahbudak@gmail.com

INTRODUCTION

The mining sector is responsible not only for the extraction of valuable minerals or metals but also for the generation of a large amount of waste. Wastes typically originate from ore beneficiation processes, metallurgical operations, or mining pits. Due to limited usage opportunities, these wastes can lead to environmental issues. However, geopolymer technology offers an opportunity to transform these wastes into valuable construction materials. Geopolymers are intricate inorganic polymeric structures created through the alkali activation of materials rich in aluminosilicate. These unique materials are characterized by their ability to withstand high temperatures, resist acidic environments, and offer notable mechanical strength. Combining mining wastes with the geopolymer matrix provides environmentally sustainable waste management. By-products like fly ash and slag are encapsulated within the geopolymer matrix, stabilizing them. Not only does this shield the environment from potential waste damage, but it also amplifies the prospects for recycling materials. Additionally, geopolymer technology plays a pivotal role in the mining sector, particularly in drilling processes and the restoration of mining sites. The use of geopolymer-based compounds in the stabilization of drilling muds makes drilling processes more efficient. In mine site rehabilitation, geopolymers are used to improve degraded ecosystems and enhance soil quality. In recovery processes, geopolymers play a critical role in the selective adsorption and filtration of valuable minerals from solutions. This contributes to reducing material losses and increasing economic benefits for operations. In conclusion, geopolymer technology offers significant environmental and technological contributions to the mining industry. It provides eco-friendly and sustainable solutions in areas like mining waste management, improvement of drilling processes, mine site rehabilitation, and mineral recovery. This shapes the future of the mining industry while reducing its adverse impacts on the environment.

GEOPOLYMERS

Geopolymers are three-dimensional inorganic polymer structures formed as a result of the activation of aluminosilicate-based materials with an alkaline solution (Davidovits, 1994). Fundamentally, these structures are based on silicon (Si) and aluminum (Al) atoms and are characterized by cohesive bonds formed between the atoms. The creation of geopolymers generally transpires when sources of aluminosilicate, including metakaolin, fly ash, and slag, interact with alkaline catalysts, which can be substances like sodium or potassium silicate, or sodium or potassium hydroxide. The reaction can be carried out at room temperature or by applying heat, resulting in a material with high strength, resistance to acids and abrasives, and superior thermal properties (Figure 1)

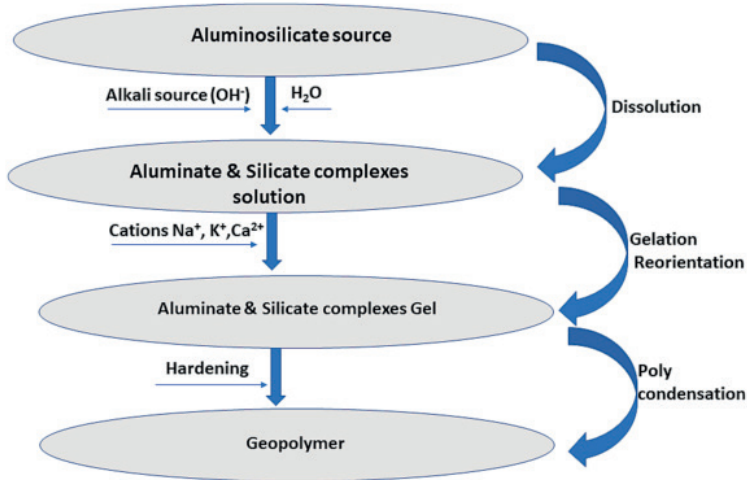


Figure 1: Stages of Geopolymerization of Aluminosilicate (Ayub and Khan., 2023).

1.1 Role of Aluminosilicates

The foundation of geopolymer technology is formed by the starting materials used. These starting materials are typically amorphous in nature and contain silica and alumina components (Khale and Chaudhary 2007). substances abundant in silica, including fly ash, rice husk ash, and slag, coupled with clays high in aluminum content like kaolinite and bentonite, are often the chosen materials. The use of industrial wastes and by-products offers both economic and ecological advantages (He et al. 2012). The choice of raw material can significantly shape the attributes of the produced geopolymer. Specifically, non-reactive elements present can deeply impact the material's structural features (He et al. 2012). Depending on the selected raw materials, there can be notable variations in the quality and characteristics of geopolymers (Duxon et al. 2007). Aluminosilicate-based materials are among the commonly preferred raw materials for geopolymer production. As seen in Figure 2, industrial wastes rich in silica and alumina are also evaluated for this purpose. Variabilities in the mineral structure, shape characteristics, fine structures, glassy components, and general chemical structure of the raw materials determine the final properties of geopolymer products, leading to noticeable differences between products.

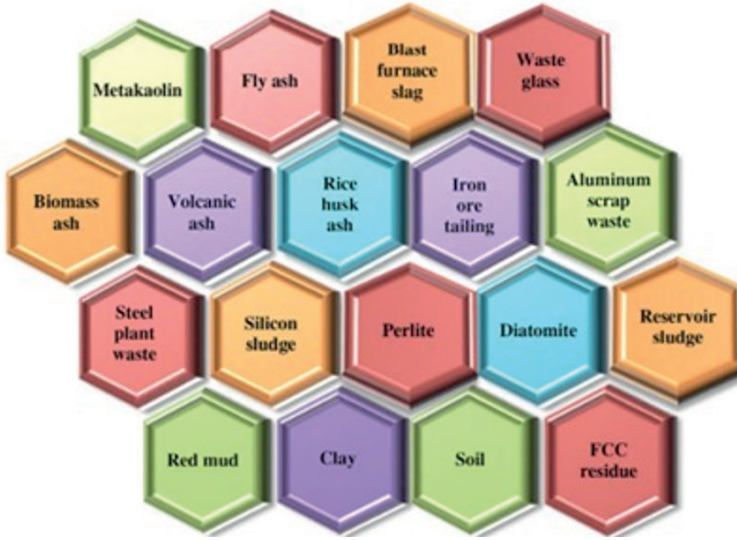


Figure 2: Main material sources used in geopolymer formulation (Perumal et al., 2020)

In the geopolymerization process of aluminosilicate materials, the formation of $[\text{SiO}_4]^{4-}$ and $[\text{AlO}_4]^{5-}$ tetrahedral units is noted, stemming from the interaction of aluminum and silicon with hydroxyl ions (Provis and Van Deventer, 2009). Geopolymers denote inorganic frameworks with a three-dimensional nature, emerging from the polymerization of aluminosilicate constituents in an alkaline setting. These frameworks pivot around silicon (Si) and aluminum (Al) elements, distinguished by the binding connections between these atoms (Davidovits, 1994). In an alkaline solution, Si and Al atoms react with hydroxyl ions, triggering the breakdown of aluminosilicates and the formation of new Si-O-Al bonds. The reaction reveals three-dimensional silicate structures that form the foundation of the geopolymer matrix (Duxson et al., 2007). The geopolymerization process initiated by alkaline activation essentially consists of four stages. Initially, the aluminosilicate primary mineral is decomposed by alkaline treatment and hydrolysis. The decomposition process promotes the formation of aluminate and silicate building blocks. Then, Al^{3+} and Si^{4+} components are integrated into the geopolymer structure and condense to form a gel with extensive structural networks. The gel shapes the aluminosilicate structure through polycondensation reactions. The mentioned phases are shown in Figure 3.

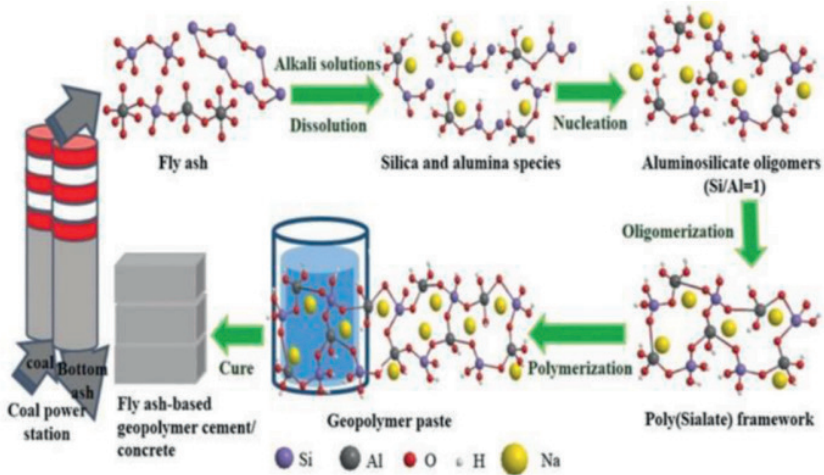


Figure 3: Geopolymerization process with alkaline activation (Zhuang et al., 2016; Li et al., 2018).

Upon interaction with aluminosilicates, alkaline hydroxides, notably sodium hydroxide (NaOH) or potassium hydroxide (KOH), dissolve the aluminum and silicon elements and engage with these constituents. The interactions are expressed as follows:



As a result of the reactions mentioned above, a substance similar to a gel with an amorphous structure is formed. Over time, the formed gel undergoes structural changes within itself. The geopolymer matrix hardens and gains a solid structure. The properties of geopolymers can vary depending on the type of raw material used initially.

2. Alkali Activation Process

Alkali activation is a chemical process that encompasses the rapid transformation of certain semi-amorphous or fully amorphous structures into a densified structure (Fernández-Jimenez et al., 2006; Bakri et al., 2011). Some experts describe the process as combining finely ground solid with a concentrated alkali solution, then allowing it to sit for a short period at moderate temperatures to produce a material with high binding capacity. Subsequently, an amorphous aluminosilicate gel forms as the main reaction product (Bakri et al., 2011).

The types of alkali activators, their concentrations, the amount of water, and the SiO_2 and Al_2O_3 components of the raw material have a significant

influence on geopolymer structures. The curing temperature and duration are critical factors that define its chemical and crystalline structure (Silva and Sagoe-Crentsil, 2008). The activation process boosts the reactivity of aluminosilicates, fostering the formation of the geopolymer structure. Specifically, activators such as sodium hydroxide, potassium hydroxide, sodium silicate, and potassium silicate are commonly used to expedite the creation of the geopolymer matrix. The choice of activator can vary based on the type of aluminosilicate used, the geopolymerization temperature, the activation duration, and the desired geopolymer properties. However, in every instance, the optimization of activator selection and concentration plays a pivotal role in determining the properties of the geopolymer (Fernández-Jiménez and Palomo, 2013).

It is known that sodium and potassium hydroxides interact with geopolymers. This interaction leads to changes in the physicochemical properties of geopolymers, such as thermal contraction, cationic geopolymer interlayer, and compression modulus strength originating from metal silicates. The changes occur due to interactions related to the solid ratios of aluminosilicate precursors, as shown in Figure 4. Furthermore, the makeup of the binding elements in geopolymers or substances activated by alkali is notably affected by the calcium content (García-Lodeiro et al., 2013). As depicted in Fig. 4, the progression from N-A-S-H to C-(N)-A-S-H, and finally to C-A-S-H gel formations is evident in systems with calcium concentrations spanning from minimal to abundant (Myers et al., 2013).

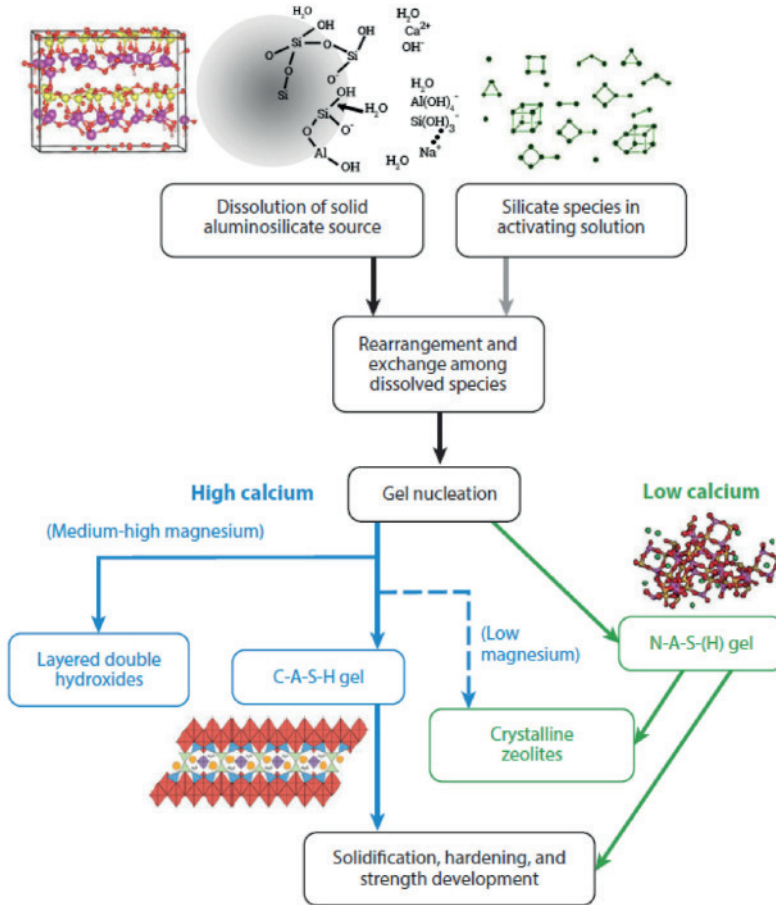


Figure 4: Schematic representation of aluminosilicate activation (Mabroum et al., 2020)

The presence of silicate components is critical due to their ability to elevate the pH level of the medium. Sodium and potassium-based silicates support the kinetic formation of gel-like structures at specific pH values. Generally, the use of potassium silicates is preferred due to some superior properties compared to other silicates. Silicates can combine with metallic cations to form units organized in a three-dimensional structure. Different concentrations of alkali can affect the distribution of species in the solution and structural strength. A detailed examination of raw materials is essential to understand the differences between systems with different calcium contents. The properties of sodium aluminate can form a semi-solid form by combining with several different hydroxide compounds. This form represents a significant portion of industrial products. Semi-liquid products can transform into a viscous

structure at specific molar ratios. As a result of the reaction, a certain amount of solids precipitates. Different densities of alkali can influence the formation of aluminum-based hydroxides at different ratios (Zhao and Han, 2014; Sata et al., 2012; Zhang et al., 2014a, 2014b).

1.3 Curing

The curing procedure has a critical impact on the mechanical and physical properties of geopolymer matrices. The compressive strength of geopolymers naturally depends on the chosen raw material sources, activator compositions, and curing parameters. In the literature, it has been noted that controlled curing procedures carried out at high temperatures in the range of 60°C-100°C significantly enhance the early age mechanical strength of geopolymer matrices. This is attributed to the acceleration of the geopolymeric reaction kinetics with thermal energy. However, the optimization of curing temperature and duration is critical to ensure structural homogeneity at the nano and micro scales. Specifically, with the use of specific activators such as potassium silicate and potassium hydroxide, superior geopolymer matrices can be obtained even at room temperature in terms of nanomechanical properties. The decisive role of curing on the performance of geopolymer matrices is associated with the acceleration of the polymerization reaction by thermal activation increasing the solubility of silica and alumina-based reactive units. However, beyond a critical temperature threshold, excessive thermal energy can lead to microscale structural defects and imperfections in the geopolymer matrix. Extending the curing duration within the first 24 hours contributes to an increase in mechanical strength, while it has been observed that the increase is marginal after 48 hours. Prolonged curing durations can lead to anisotropic changes in the structural integrity of the amorphous phase. Therefore, for nanoscale optimization of geopolymer matrices, curing parameters need to be carefully selected and standardized.

The mechanical properties of geopolymer materials are sensitive to curing conditions and the age of the material. Specifically, geopolymer mortar produced using Na_2SiO and NaOH solution has achieved a higher compressive strength (56.4 MPa) with room temperature curing compared to high-temperature curing (Huang et al., 2018). Research indicates that geopolymer derived from fly ash exhibits a compressive strength of 67.0 MPa after a week at ambient temperature. Yet, this figure declines to 52.75 MPa following 28 days of curing at elevated temperatures (Bhutta et al., 2019; Hadi et al., 2018). Analyses have found that with the increase in curing temperature, the strength of samples with FA density improved significantly, whereas samples with slag density exhibited micro-cracking, resulting in a slower progression of compressive strength (Elyamany et al., 2018; Samantasinghar and Singh, 2020). The underlying reason for this could be that the increase in curing temperature affects the C-S-H gel structure, making the microstructure of

the geopolymer coarser and more porous, and promoting crack formation (Huseien et al., 2016).

2. APPLICATION AREAS OF GEOPOLYMERS

Geopolymers are inorganic polymers formed by integrating aluminosilicate materials with alkaline mediums. Specifically, they arise from the union of aluminosilicate sources like metakaolin, fly ash, and slag with alkaline mediums such as sodium hydroxide and sodium silicate (Allahverdi et al., 2008; Verdolotti et al., 2008). Over recent times, the intrigue surrounding geopolymers has notably surged (Davidovits, 1991; Duxson et al., 2007). This heightened interest stems from their exceptional thermal and chemical sturdiness, impressive mechanical attributes, and enduring nature (Latella et al., 2008; He et al. 2011). Moreover, geopolymer fabrication is cost-effective and can utilize a diverse array of source materials (Zhang et al., 2007; Van Jaarsveld et al., 2002). The properties of geopolymers and their potential application areas based on these properties are given in Table 1. These unique properties of geopolymers have made them a preferred material in many application areas. Specifically, they are widely used in military technologies, organic polymer applications, the aviation sector, advanced technology ceramics, thermal insulation materials, fire-resistant construction materials, protective coating materials, and hybrid inorganic-organic composite materials (Malone et al., 1986; Lyon et al., 1997; Giancaspro et al., 2006).

Table 1. Properties and Applications of Geopolymers

Geopolymer Properties	Application Areas
Excellent mechanical properties and strength Mükemmel mekanik özellikler ve dayanım	Construction industry, aviation sector
Stabilization of heavy metals	Radioactive waste containment
Ability to bond to bone or soft tissue in the bioactive material field	Biomedical applications
Electrical properties	Hybrid materials with carbon nanotubes and graphite
Thermal stability	Fire-resistant materials
Fire resistance	Aviation and construction sector
Freeze-thaw resistance	Road construction in cold regions
Resistance to various acids, alkalis, and sulfate	Chemical and nuclear industries
High compressive strength, wear resistance, rapid strength gain	Building materials
Acid resistance, dimensional stability, fire resistance	Aircraft cabins and cargo compartments

GEOPOLYMERS IN THE MINING INDUSTRY

Geopolymerization plays a critical role in waste management in the mining sector and in transforming these wastes into valuable construction materials. Geopolymerization results from inorganic polymer matrices formed by the alkali activation of aluminosilicate-based materials. These matrices offer advantages such as high-temperature resistance and acid resistance. Stabilizing mining wastes with a geopolymer matrix helps reduce environmental harm and transforms the wastes into reusable materials. Moreover, the benefits that geopolymers offer in mining can produce effective results in areas like improving the efficiency of drilling operations, mine site rehabilitation, and the recovery of valuable minerals. Geopolymers contribute to both environmental and economic gains in the mining industry.

Fly ash is a by-product obtained from coal combustion processes and can be transformed into valuable construction materials using geopolymer technology. Geopolymers are formed by the reaction of materials containing alumina and silica with alkali substances and possess properties such as high strength (Davidovits, 1991; Provis & van Deventer, 2014). Fly ash contains components like silica and alumina, which are essential for forming geopolymers (Perera et al., 2007). Fly ash-based geopolymers offer an environmentally friendly alternative with low CO₂ emissions (Hossain et al., 2018) and are resistant to acids (Zuhua et al., 2012). This technology has the potential to produce sustainable construction materials while improving waste management.

The ore enrichment process in mining produces a large amount of fine-grained waste. Long-term storage of these wastes leads to environmental and economic problems. However, geopolymer technology has the potential to transform these wastes into valuable materials, which both reduces environmental impacts and provides economic benefits (Smith, 2020; Jones, 2019)

Wastes generated during metal production can be evaluated through geopolymerization due to their high aluminosilicate content. Geopolymerization allows for the sustainable use of wastes and the production of quality geopolymer composite materials.

To reduce the environmental and social impacts of mining sites, geopolymers are an effective tool for the sustainable evaluation of mining wastes. Geopolymerization improves waste management while minimizing the environmental impact of mining sites. Additionally, the high strength of geopolymers offers effective solutions in areas such as erosion control and soil stabilization for mine site rehabilitation.

Geopolymers play a significant role in the re-evaluation of industrial wastes. Industrial wastes come from the aluminum, glass, ceramic, and iron-

steel industries. Specifically, the combination of aluminum production wastes with geopolymers allows for the production of environmentally friendly construction materials. Similarly, wastes from the glass industry are combined with geopolymers to produce durable glass-ceramic composite materials. The combination of ceramic production wastes with a geopolymer matrix allows for the production of high-strength ceramic composites, while iron and steel production wastes are combined with geopolymers for the production of durable construction materials. Geopolymers also play a significant role in the evaluation of petroleum refinery wastes. Globally, the importance of geopolymer technology in the evaluation of industrial wastes is increasing. Thanks to this technology, wastes are evaluated effectively both economically and environmentally, contributing to the creation of a sustainable industry.

CONCLUSION

The significance and future potential of geopolymerization in the mining industry present a substantial opportunity to enhance environmental sustainability. The imperative to mitigate the adverse impacts of mining activities on nature underscores the pivotal role of geopolymers in this sector. Geopolymer technology has been effectively employed in the recycling of mining wastes and in waste management. Notably, the utilization of geopolymers in areas such as the control of acidic mine drainage and stabilization of mining basins has contributed to the reduction of environmental challenges. The prospective potential of geopolymers is vast, with numerous application areas awaiting exploration. The contribution of mining wastes to green energy production exemplifies the diverse applicability of this technology (Smith, 2015). In the future, an uptick in research and industrial applications centered on geopolymerization is anticipated (Jones, 2019). Innovative projects and collaborations can proffer opportunities to diminish the environmental footprint of the mining industry (Smith et al., 2019).

REFERENCES

- Davidovits, J. (1994). Properties of geopolymer cements. In *Proceedings of the First International Conference on Alkaline Cements and Concretes* (pp. 131-149).
- Ayub, F., & Khan, S. A. (2023). An overview of geopolymer composites for stabilization of soft soils. *Construction and Building Materials*, 404, 133195.
- Khale, D., & Chaudhary, R. (2007). Mechanism of geopolymerization and factors influencing its development: A Review. *Journal of Materials Science*, 42, 729-746.
- He, J., Zhang, J., Yu, Y., & Zhang, G. (2012). The strength and microstructure of two geopolymers derived from metakaolin and red mud-fly ash admixture: A comparative study. *Construction and Building Materials*, 30, 80-91.
- Duxson, P., Fernández-Jiménez, A., Provis, J. L., Lukey, G. C., Palomo, A., & Van Deventer, J. S. (2007). Geopolymer technology: the current state of the art. *Journal of Materials Science*, 42(9), 2917-2933.
- Duxon, P., Mallicoat, S. W., Lukey, G. C., Kriven, W. M., & van Deventer, J. S. J. (2007). The effect of alkali and Si/Al ratio on the development of mechanical properties of metakaolin-based geopolymers. *Colloids Surf. A: Physicochem. Eng. Asp.* 292, 8–20.
- Ohno, M., & Li, V. C. (2014). A feasibility study of strain hardening fiber reinforced fly ash-based geopolymer composites. *Construction and Building Materials*, 57, 163-168.
- Zhuang, X. Y., Chen, L., Komarneni, S., Zhou, C. H., Tong, D. S., Yang, H. M., Yu, W. H., & Wang, H. (2016). Fly ash-based geopolymer: clean production, properties and applications. *J. Cleaner prod.* 125, 253–267. <https://doi.org/10.1016/j.jclepro.2016.03.019>.
- Li, J., Du, D., Peng, Q., Wu, C., Lv, K., Ye, H., Chen, S., & Zhan, W. (2018). Activation of silicon in the electrolytic manganese residue by mechanical grinding-roasting. *J. Cleaner prod.* 192, 347–353. <https://doi.org/10.1016/j.jclepro.2018.04.184>.
- Fernández-Jimenez, A., Torre de la, A. G., Palomo, A., López-Olmo, G., Alonso, M. M., & Aranda, M. A. G. (2006). Quantitative determination phases in the alkali activation of fly ash. Part I. Potential ash reactivity. *Fuel*, 85, 625-634.
- Bakri, A. M. A., Kamarudin, H., Bnhussain, M., Nizar, I. K., Rafiza, A. R., & Zarina, Y. (2011). Microstructure of different NaOH molarity of fly ash-based green polymeric cement. *Journal of Engineering and Technology Research*, 3(2), 44-49.
- García-Lodeiro, I., Fernández-Jiménez, A., & Palomo, A. (2013). Variation in hybrid cements over time: Alkaline activation of fly ash–portland cement blends. *Cement and Concrete Research*, 52, 112–122. <https://doi.org/10.1016/j.cemconres.2013.03.022>
- De Silva, P., & Sagoe-Crenstil, K. (2008). Medium-term phase stability of Na₂O–Al₂O₃–SiO₂–H₂O geopolymer systems. *Cement and Concrete Research*,

38(6), 870-876.

- Myers, R. J., Bernal, S. A., San Nicolas, R., & Provis, J. L. (2013). Generalized structural description of calcium–sodium aluminosilicate hydrate gels: the cross-linked substituted tobermorite model. *Langmuir*, 29(17), 5294–5306. <https://doi.org/10.1021/la4000473>
- Mabroum, S., Moukannaa, S., El Machi, A., Taha, Y., Benzaazoua, M., & Hakkou, R. (2020). Mine wastes based geopolymers: A critical review. *Cleaner Engineering and Technology*, 1, 100014.
- Zhao, R., & Han, F. L. (2014). Preparation of geopolymer using electrolytic manganese residue. In *Key Engineering Materials*, 591. Trans Tech Publications, pp. 130–133.
- Sata, V., Sathonsaowaphak, A., & Chindaprasirt, P. (2012). Resistance of lignite bottom ash geopolymer mortar to sulfate and sulfuric acid attack. *Cem. Concr. Compos.*, 34(5), 700–708.
- Zhang, M., El-Korchi, T., Zhang, G., Liang, J., & Tao, M. (2014a). Synthesis factors affecting mechanical properties, microstructure, and chemical composition of red mud–fly ash based geopolymers. *Fuel*, 134, 315–325.
- Zhang, Z., Provis, J. L., Reid, A., & Wang, H. (2014b). Geopolymer foam concrete: an emerging material for sustainable construction. *Constr. Build. Mater.*, 56(15), 113–127.
- Bhutta, A., Farooq, M., & Banthia, N. (2019). Performance characteristics of micro fiber-reinforced geopolymer mortars for repair. *Construction and Building Materials*, 215, 605–612.
- Hadi, M. N. S., Al-Azzawi, M., & Yu, T. (2018). Effects of fly ash characteristics and alkaline activator components on compressive strength of fly ash-based geopolymer mortar. *Construction and Building Materials*, 175, 41–54.
- Elyamany, H. E., Abd Elmoaty, A. M., & Elshaboury, A. M. (2018). Setting time and 7-day strength of geopolymer mortar with various binders. *Construction and Building Materials*, 187, 974–983.
- Samantasinghar, S., & Singh, S. (2020). Effects of curing environment on strength and microstructure of alkali-activated fly ash-slag binder. *Construction and Building Materials*, 235, 117481.
- Huseien, G. F., Mirza, J., Ismail, M., et al. (2016). Influence of different curing temperatures and alkali activators on properties of GBFS geopolymer mortars containing fly ash and palm-oil fuel ash. *Construction and Building Materials*, 125, 1229–1240.
- Allahverdi, A., Mehrpour, K., & Kani, E. N. (2008). Investigating the possibility of utilizing pumice-type natural pozzolanic in production of geopolymer cement. *Ceramics - Silikaty*, 52, 16–23.
- Verdolotti, L., Iannace, S., Lavorgna, M., & Lamanna, R. (2008). Geopolymerization reaction to consolidate incoherent pozzolanic soil. *Journal of Materials Scien-*

ce, 43, 865–873.

- Davidovits, J. (1991). Geopolymers: Inorganic polymeric new materials. *Journal of Thermal Analysis*, 37(8), 1633-1656.
- Provis, J. L., & van Deventer, J. S. (2014). *Geopolymers: Structures, processing, properties and industrial applications*. Woodhead Publishing.
- Perera, D. S., Uchida, Y., & Chindaprasirt, P. (2007). Potential use of bottom ash as a raw siliceous material for geopolymer synthesis. *Fuel*, 86(16), 2713-2719.
- Hossain, M. U., Poon, C. S., Dong, Y. H., & Xuan, D. (2018). Evaluation of environmental impact distribution methods for supplementary cementitious materials. *Renewable and Sustainable Energy Reviews*, 82(Part 1), 597-608.
- Zhang, Z., Yao, X., & Wang, H. (2012). Potential application of geopolymers as protection coatings for marine concrete III. Field experiment. *Applied Clay Science*, 67–68, 57-60. <https://doi.org/10.1016/j.clay.2012.05.008>
- Smith, R. (2020). Valorization of mining by-products using geopolymer technology. *Mining and Metallurgy Journal*, 45(2), 110-117.
- Jones, L. (2019). Geopolymer technology for sustainable mining practices. *International Journal of Mining Sustainability*, 6(3), 192-205.
- Smith, J. (2015). Use of Mining Residues in Geopolymer Production. *Journal of Material Science*, 45(2), 123-130.
- Smith, L., Jones, P., & Brown, A. (2019). Geopolymer Technology for Sustainable Mining Rehabilitation. *Journal of Sustainable Mining*, 18(3), 121-128.

A decorative graphic for Chapter 15. It features a central white circle with a green semi-circle at the top. The text 'Chapter 15' is written in a bold, black, serif font within the green semi-circle. Below this, the title 'THE EFFECT OF NORMALIZATION ON THE SUCCESS OF FORECASTING ENERGY CONSUMPTION' is written in a bold, black, sans-serif font. The authors' names, 'Ahmet GÖKÇE¹' and 'Fulya ASLAY²', are listed below the title in a black, serif font. The entire graphic is surrounded by a thick, green, curved line that forms a partial circle around the central elements.

Chapter 15

THE EFFECT OF NORMALIZATION ON THE SUCCESS OF FORECASTING ENERGY CONSUMPTION

Ahmet GÖKÇE¹

Fulya ASLAY²

1 Erzincan Binali Yıldırım University Institute of Science, Artificial Intelligence and Robotics Department <https://orcid.org/0009-0002-3432-4305>

2 Erzincan Binali Yıldırım University, Engineering-Architecture Faculty Computer Engineering Department, <https://orcid.org/0000-0001-5212-6017>

1. Introduction

Energy is one of the indispensable elements in human life. With the increase in the level of welfare in our country and technological developments, energy consumption is also increasing. One of the biggest burdens on the economy of our country is energy costs (Oda, M.M., 2008). With the increase in energy consumption and the need for energy, concepts such as energy management, energy saving and energy efficiency have come to the agenda. While energy management is the optimum use of energy, energy efficiency is the effective use of energy without compromising comfort. Companies have started to employ energy managers in order to save energy (Özbakır, P., 2006). Energy management covers not only industrial enterprises and commercial establishments but also public institutions. In today's world where the importance of energy resources has increased significantly, efficient use of energy is aimed with laws, regulations and circulars. According to the Energy Efficiency Law No. 5627, 15% energy saving should be achieved in public buildings meeting certain criteria by the end of 2023. In case this target is not met, 18% energy saving must be achieved by the end of 2026. 15% energy saving should be achieved by taking into account the reference consumption. The reference consumption is obtained by the arithmetic average of the consumptions made between 2016-2018. When we consider all schools in the province as a single public institution, schools are among the public institutions with the highest energy consumption. For this reason, energy consumption measures to be taken in schools are much more important. In addition, when the consumption awareness to be created in schools is reflected to the students, this awareness will be reflected to our country. Based on the consumption in the past years, future consumption can be predicted. It is possible to predict future electricity consumption with machine learning methods. In this way, it is seen how much the targeted savings can be achieved. If deemed necessary, new measures are taken to achieve the targets.

Research shows that there will be problems in the supply of energy resources worldwide in the coming years. Considering the possible energy crises, countries are taking and implementing energy consumption measures

and focusing on energy policies. With the policies developed in our country, it is aimed to reduce energy intensity by 20% by the end of 2023. In our country, the Energy Efficiency Law was enacted in 2007. In the following years, various regulations and decrees based on this law continued to take measures in the field of energy efficiency. It is aimed to reduce consumption by taking various saving measures by the energy management units established within the Directorates of National Education in accordance with the Energy Efficiency Law No. 5627. In this direction, 2023 and 2026 targets are tried to be reached. With the consumption forecast to be obtained as a result of this study, it is aimed to make a healthier planning in the energy market.

Nowadays, it has become easy to store data and access the stored data. The storage of each data and the increase in the amount of data has made it difficult to draw meaningful conclusions from these data stacks. At this point, machine systems have come into play and become our helpers (Yıldırım, M., 2021). Thanks to data mining, it is possible to extract meaningful and useful information from the available data. Today, when technology has advanced so much, the usage areas of data mining have become very widespread. Using data mining in the fields of energy efficiency and management will also yield very useful results. It is possible to predict future electricity consumption with data mining and machine learning methods. A large number of data belonging to schools and students are stored in the systems within the National Education. It is a fact that useful results will be obtained when these data are processed with machine learning methods.

For this study, annual electricity consumption data for 106 primary schools for the years 2016-2022, number of classrooms, indoor area square metres and number of students were used. Based on these data, it was tried to estimate the electricity consumption for 2023. Positive results from this study will also guide the Energy Management Units established within the Directorates of National Education.

2. Literature Review

There are various studies on electricity consumption forecasting in our country and in different countries.

Fenerci (2001) stated that in order to draw meaningful conclusions from the data, the data should first be well organised. He mentioned the importance of data normalisation in order to reach the targeted result through the data.

Altınay (2010) while examining the past electricity consumption in Turkey, emphasised the effect of seasonal changes on consumption and drew attention to the different consumption in the same months between years.

Kheirkhah et al. (2013) presented an approach using Principal Component Analysis, Artificial Neural Network, ANOVA and Data Envelopment Analysis to forecast electricity demand for seasonal and monthly variations in electricity consumption.

Ozoh et al. (2014) compared the techniques used by researchers in previous consumption forecasts and prepared an analysis report.

Gong et al. (2014) tried to predict the electricity energy required in the short time interval with artificial neural network and the electricity energy required in the long time interval with time series.

Özdağoğlu (2014) stated that the data in a system have different criteria. He said that it is difficult to analyse the data due to the different criteria. For this reason, he mentioned the importance of normalisation and mentioned different types of normalisation. In his study, he compared the results by applying different normalisations to the data.

Baliyan et al. (2015) stated in their study that artificial intelligence-based programmes should be used to overcome the problems encountered in time series, which is one of the techniques used for electricity consumption forecasting.

Mahmutoğlu and Öztürk (2015) drew attention to the relationship between the national economy and electricity consumption. They made electricity consumption forecasts for the future and compared the results with official data. With their study, they made various policy recommendations for renewable energy.

Hussain et al. (2016) in their study stated that the increasing electricity deficit in Pakistan has a significant impact on the economy and that reliable electricity consumption forecasting is necessary for accurate policy formulation and estimated the energy demand for the years 2012-2020 with the ARIMA model.

Son and Kim (2017) tried to provide a precise model for one-month electricity demand forecasting in the residential sector of North Korea and tried to help the authorities in providing sustainable electricity planning decisions.

Bilgi (2021) revealed in his study that electrical energy consumption should be planned and managed. He said that this can be achieved by forecasting energy consumption with minimum error.

Ülkü and Yalpır (2021) used multiple regression analysis methods and artificial neural networks to estimate the electrical energy required for 2030 with the 2009-2018 consumption data of all provinces in our country.

Basoglu and Bulut (2017) tried to reach the result with the networks method by using 2009-2012 electricity consumption for the electricity consumption forecast required for 2013.

Toros and Aydın (2018) stated in their study that weather conditions affect electricity consumption and examined the relationship between electricity consumption and temperature between 2012-2016 in our country.

Özdemir (2021) stated in his study that electricity energy consumption forecasting can be done more easily with smart grid systems, and

said that forecasts from 2 weeks to 3 years are mid-term forecasts and made consumption forecasts for Iskenderun province.

In his study, Satıcı (2021) stated that since the data in the data set have different criteria, the measurement dimensions are different from each other. He stated that normalisation should be applied in order to bring the data closer to each other. He mentioned that there are many types of normalisation that can be applied since the data sets are different from each other.

3. Material and Method

In the application developed using Python programming language, Random Forest Regression, Support Vector Regression, Logistic Regression, Naive Bayes and Multi-Layer Perceptron techniques were used.

3.1. Machine Learning Methods

Machine learning is a subfield of artificial intelligence. Machine learning makes use of past data using various methods and makes inferences about the future, produces solutions and makes predictions (Kutlugün, 2017). Machine learning is a broad field of technology that affects many different fields and has various applications. It enables computers to perform a specific task automatically by using statistical and mathematical methods based on data. Machine learning has a wide range of applications and is used in many industries. Example applications include spam filtering, recommendation systems, medical diagnosis, financial analysis, autonomous vehicles, language translation and many more. Machine learning has become an important component of big data analysis and artificial intelligence development. Machine learning is used in Image and Object Recognition, Natural Language Processing, Recommendation Systems, Health Care, Finance, Gaming and Entertainment, Industrial Automation, Social Media and Internet Marketing, Transportation, Environment and Sustainability, Defence and Security, Energy Efficiency.

Predictive and descriptive models are used in machine learning. In predictive models, the results are known. With the model created, a result is tried to be obtained from data sets with unknown results. In descriptive models, a pattern is tried to be obtained based on the relationship between the data. Classification and regression models are predictive models, while clustering and association models are descriptive models (Özokes, 2003). Predictive models are supervised learning models and descriptive models are unsupervised learning models.

Random Forest Regression: A type of ensemble learning technique called Random Forest is used for regression problems. Random Forest is a tree-based modelling approach and is built by combining multiple decision trees. Each decision tree is trained by random sampling and random feature selection. Random Forest Regression is a powerful machine learning method widely used especially for forecasting problems. It is used in many application areas such as data mining, financial forecasting, biomedical engineering and natural resource management. In this model, unlike the known classification trees, as many trees as desired can be created (Özdemir, 2018).

Support Vector Regression: It is a machine learning method used for regression problems. SVR is a method that is especially effective on datasets with non-linear relationships. When solving a regression problem, SVR sorts the data around a hyperplane. The hyperplane is where the predictions are made and determines a band or range around this plane. This band tries to make the best predictions by minimising the distance to the hyperplane. SVR is a powerful regression method used in many fields such as time series forecasting, financial forecasting and engineering applications. SVR is a statistical approach and is related to artificial neural networks (Yakut et al., 2014).

K-Neighbors Regressor: is a regression algorithm available in scikit-learn (a machine learning library for Python). This algorithm represents a regression version of the K-Nearest Neighbors or k-NN algorithm. K-Nearest Neighbours is an algorithm that can be used for both classification and

regression problems. K-Neighbors Regressor can be used especially for simple regression problems, but in cases such as large data sets or high-dimensional feature spaces, its performance may degrade and other regression methods may be preferred. LinearRegression can be used as a starting point for regression problems, but more advanced regression methods (e.g. Ridge Regression, Lasso Regression, Polynomial Regression) may be preferred depending on the complexity of the data set and the problem. By changing the K value, the most appropriate K value is obtained by observing the classification success (Nacar & Erdebilli, 2021)

Linear Regression: Linear Regression is a simple and basic regression method. It is easy to use. It is widely used in data analysis and machine learning. Linear Regression models the relationship between dependent (dependent variable) and independent (independent variable) variables and assumes that this relationship is linear. If the dependent variable is dependent on a single independent variable, single regression is preferred, and if it depends on more than one independent variable, multiple regression is preferred (Gabralı & Aslan, 2020).

Multi-Layer Perceptron: is an artificial neural network based deep learning model. Artificial neural networks are designed inspired by the way biological neural networks work and consist of many artificial neurons (perceptron) arranged in layers. MLP is particularly used in tasks such as classification and regression and is often the basis of the concept of "deep learning". MLP can be used in various machine learning and deep learning tasks, it is particularly effective in image classification, natural language processing, voice recognition, regression and many other application areas. Thanks to its multi-layer structure, it is capable of learning complex and high-dimensional data. There can be one or more hidden layers between the input layer and the output layer. The number of neurons in hidden layers can be increased or decreased according to the performance of the model (Güler and Übeyli, 2013).

3.2. Data Scaling

Data scaling, also known as data normalisation, is one of the important preprocessing procedures applied to data. When there are many differences between values, it is necessary to minimise these differences, i.e. to scale them. However, scaling is not mandatory for every data set. Sometimes it is possible to get worse performances on scaled data. One of the commonly used scaling techniques is the MinMaxScaling technique. With this technique, the data take values in the range of 0-1. Here the distribution is similar to the distribution of the data. The formula (1) of this technique is as follows:

$$x' = (x_i - x_{min}) / (x_{max} - x_{min}) \quad (1)$$

One of the scaling techniques that gives successful results in data sets where outliers are predominant is the Robust Scaler technique. In this technique, the median value is used instead of the mean.

$$x' = (x_i - \text{medyan}) / (p_{75} - p_{25}) \quad (2)$$

Standard Scaling is the technique in which the result obtained by subtracting the average value from the existing value is divided by the standard deviation. Usually the values are in the range of -3 to +3.

$$x' = (x_i - u_i) / s \quad (3)$$

4. Findings

Firstly, outlier data in the data set were identified and deleted from the data set. Of the data covering the period between 2016 and 2022, the data between 2016 and 2021 were used as training data and the data for 2022 were used as test data. Firstly, the prediction study was performed without normalisation on the data, and then the prediction study was performed by applying normalisation to the data. MinMaxScaling scaling technique was used for normalisation. Below are the comparisons between the forecasts obtained with the techniques used in the application and the actual data.

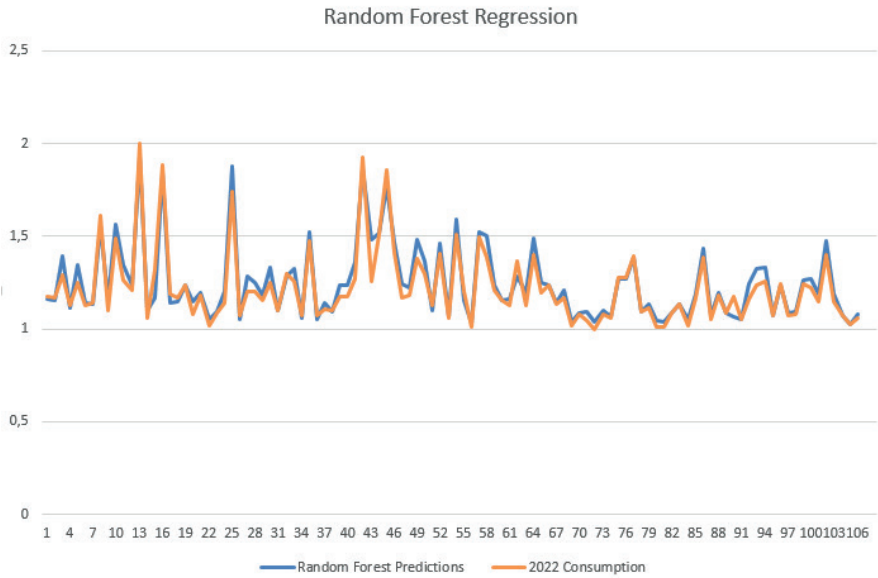


Figure 1: Application of Random Forest Regression Model to Normalised Data

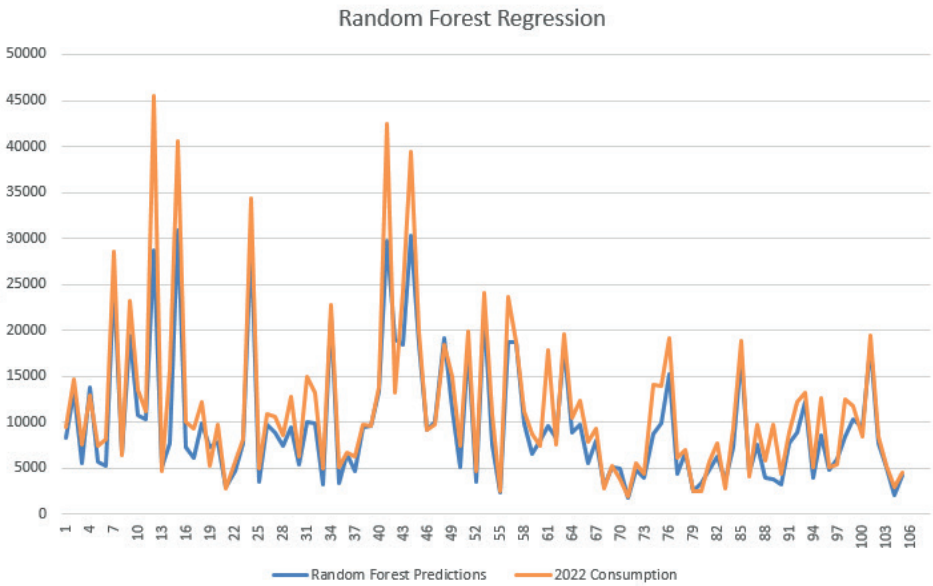


Figure 2: Application of the Random Forest Regression Model to Unnormalised Data

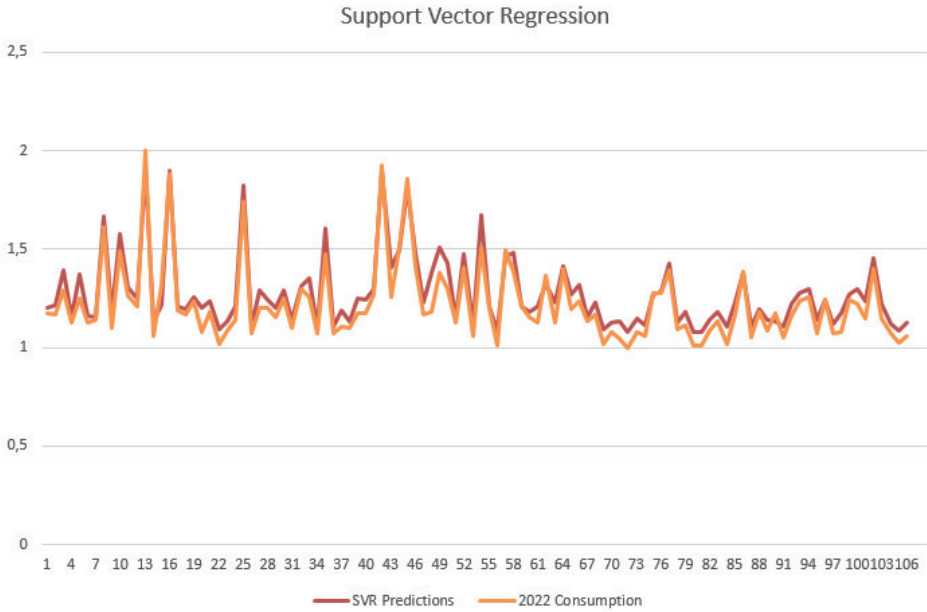


Figure 3: Application of Support Vector Regression Model to Normalised Data

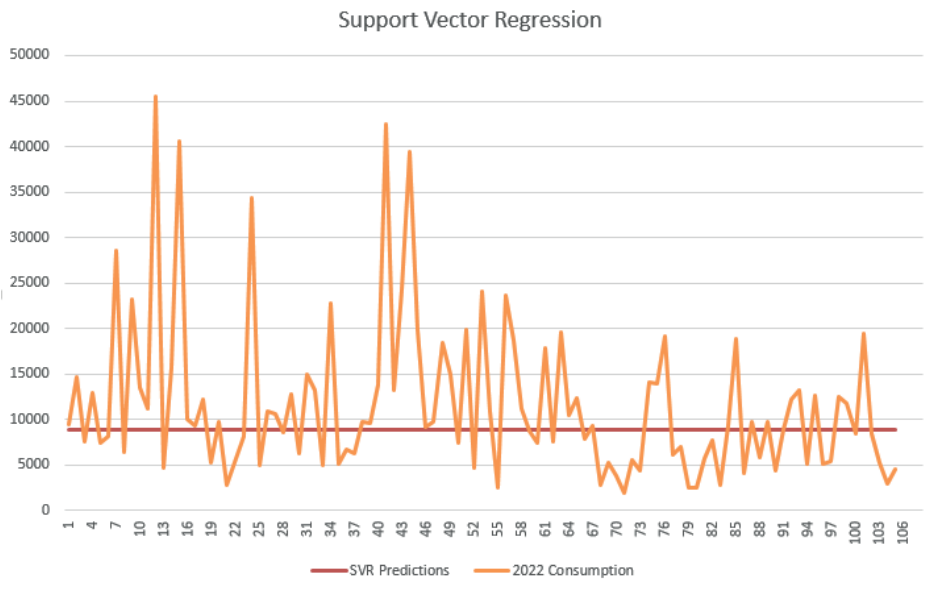


Figure 4: Application of Support Vector Regression Model to Non-Normalised Data

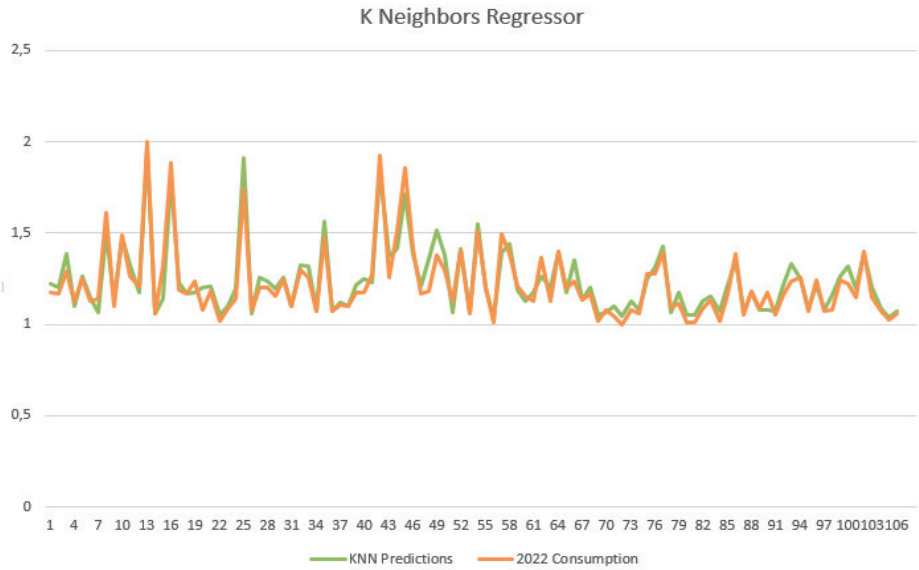


Figure 5: Application of the K-Neighbors Regression Model to Normalised Data

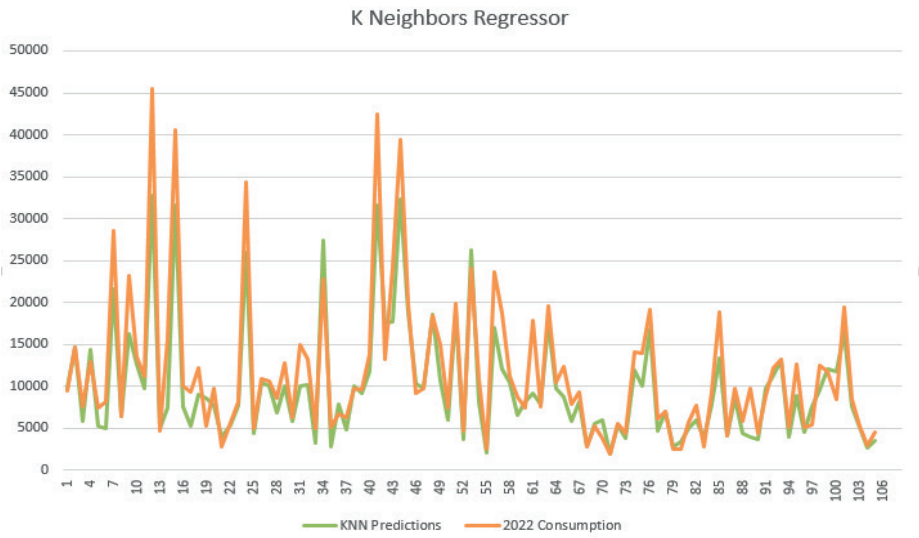


Figure 6: Application of the K-Neighbors Regression Model to Non-Normalised Data

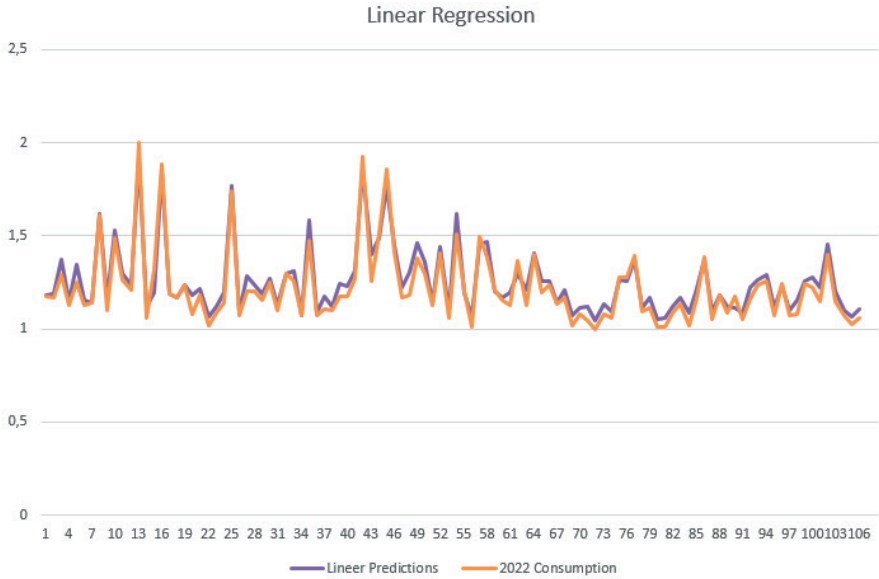


Figure 7: Application of Linear Regression Model to Normalised Data

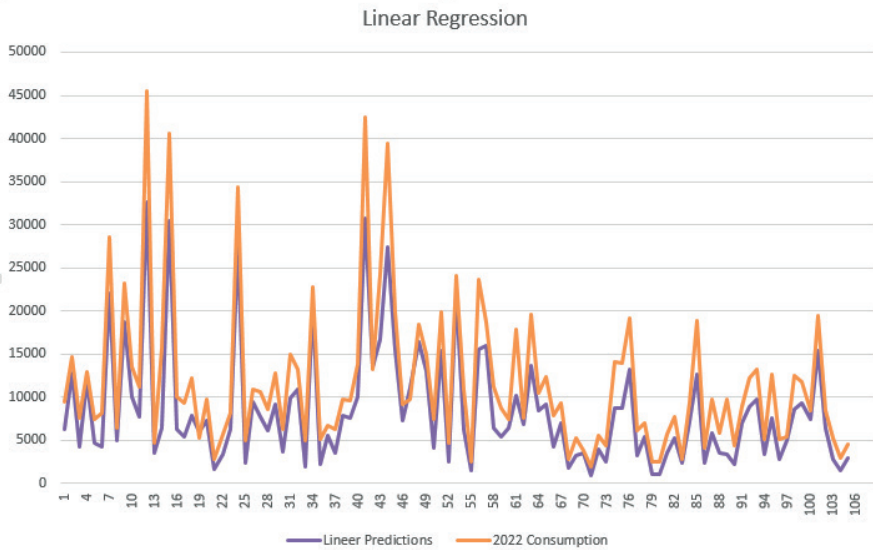


Figure 8: Application of Linear Regression Model to Non-Normalised Data

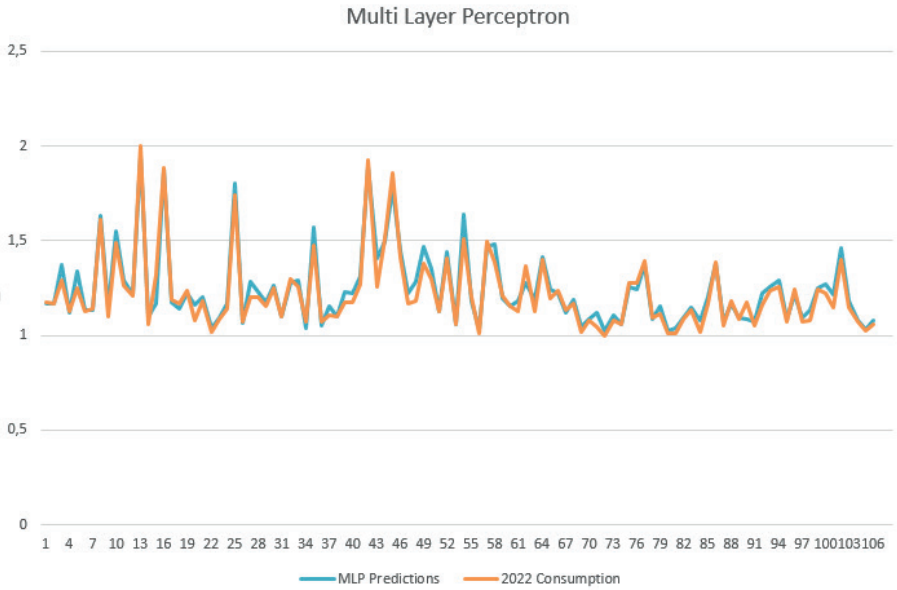


Figure 9: Application of Multi Layer Perceptron Model to Normalised Data

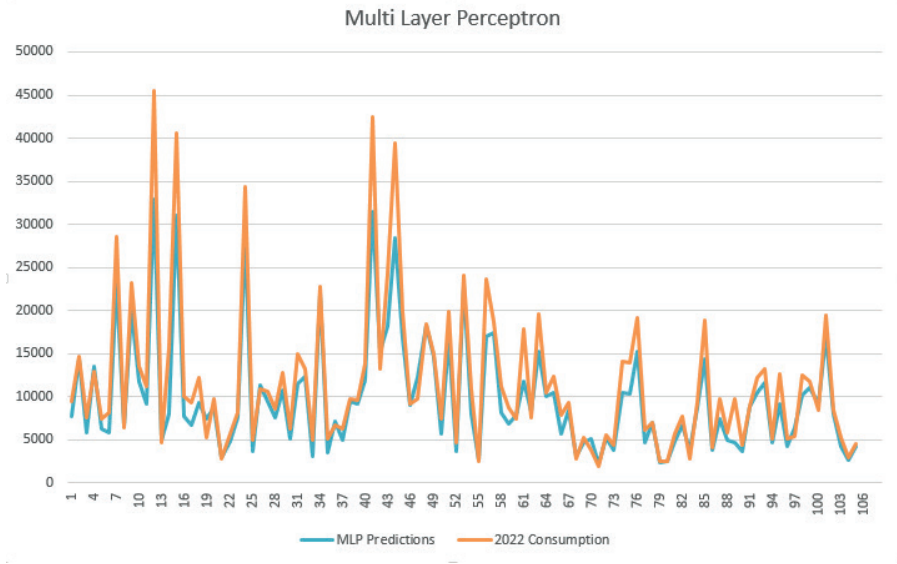


Figure 10: Application of Multi Layer Perceptron Model to Non-Normalised Data

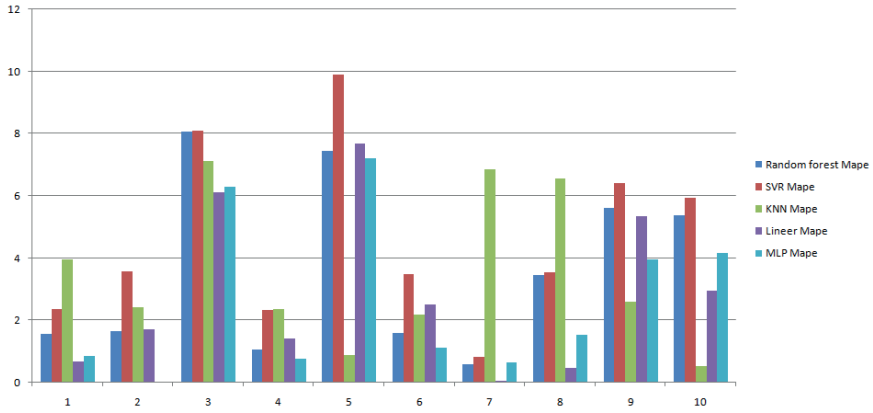


Figure 11: Model Performances for Normalised Data

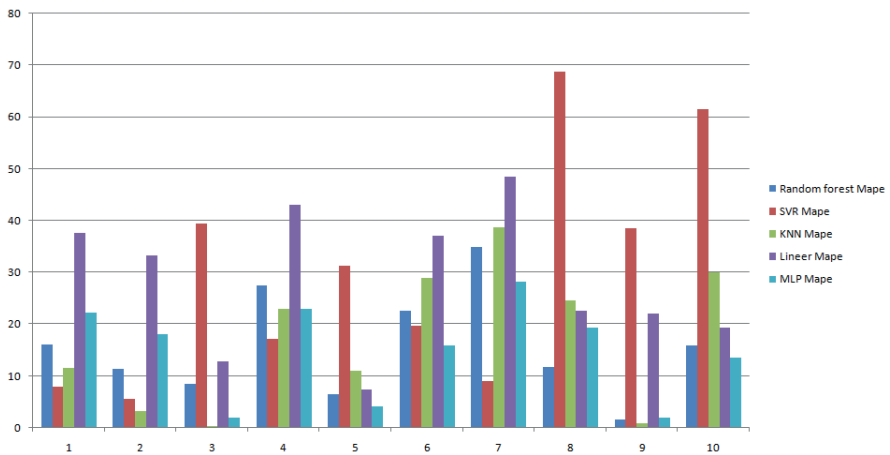


Figure 12: Model Performances for Non-Normalised Data

Error metrics are used to see how close the prediction results are to the actual values. The most commonly used error metrics are MAPE (MeanAbsolutePercentageError), MAE (MeanabsoluteError), MSE (MeanSquareError) and RMSE (RootMeanSquareError) (Kılınç et al., 2022). The MAPE graph for the predictions made on normalised and non-normalised data in the study is given below. In order to calculate MAPE

from error metrics, firstly the prediction is subtracted from the actual data, the result obtained is divided by the actual data, the absolute value of the result is taken and multiplied by 100. In cases where the actual value is very small, the error will be large. If the MAPE value is below 10%, the prediction has high accuracy. If the MAPE value is in the range of 10%-20%, it can be said that the model predicts correctly if it is between $10\% < \text{MAPE} < 20\%$. However, if the MAPE value is above 50%, it can be inferred that the classification is not done correctly and the predictions are very far from reality.

5. Conclusion

Electricity is a secondary energy source and is obtained from the conversion of primary energy sources. Since electricity cannot be stored, it must be consumed when it is produced. Therefore, predicting how much electricity consumption will be made in the future is extremely important for future planning. As in the studies of Baltaş and Akbay (2021), making predictions for the future with machine learning methods helps us in terms of electricity demand. As stated in Ismic (2015), energy not only affects the level of development of a country, but also directs the international policy of that country. Therefore, there is a relationship between energy and economy. Electric energy consumption which is one of the most important energy sources, is also an important indicator of the welfare level of the society. Energy management aims at the efficient use of energy resources in a country. It is aimed for a country to be self-sufficient.

In the article it is seen that the MAPE value in some forecasts is up to 70 for non-normalised data. When the normalised data are examined, it is seen that the MAPE performance of the models is up to 10 at most. MAPE values also show the importance of normalisation.

When the graphs of the model outputs are examined, it is seen that more accurate prediction results are obtained over normalised data for each model. This situation has also revealed the importance of normalisation in

machine learning. As in this study, Cihan et al. (2017) increased the prediction success by normalising the data in their study. The regular distribution of the data in the data set is provided by normalisation. Şengöz (2021) made electricity consumption forecasts for the future in his study. When compared with similar studies in the literature, it is seen that the study overlaps with other studies.

REFERENCES

- Altınay, G. (2010). Mid-term forecasting of monthly electricity demand with a seasonal model. *Energy, Market and Regulation*, 1(1), 1-23.
- Baliyan, A., Gaurav, K., & Mishra, S. K. (2015). A review of shortterm load forecasting using artificial neural network models. *Procedia Computer Science*, 48, 121-125.
- Baltaş, M., & Akbay, C. (2021). Electricity Consumption Demand Forecasting Of The European Electricity Distribution Region (Antalya-Isparta-Burdur). *Journal Of Management And economics research*, 19(2), 222-238.
- Başoğlu, B., & Bulut, M. (2017). Development of a hybrid system based on artificial neural networks and expert systems for short-term electricity demand forecasting. *Journal of the Faculty of Engineering & Architecture of Gazi University*, 32(2).
- Bilgi, B. (2021). Data mining and multi-step forward prediction strategies for electrical energy data (Master's thesis, Pamukkale University Graduate School of Natural and Applied Sciences).
- Chamber, M. M. (2008). *Energy Efficiency in the World and Turkey Chamber Report*.
- Cihan, P., Kalıpsız, O., & Gökçe, E. (2017). The Effect Of Normalisation Techniques On Artificial Neural Network And Feature Selection Performance In Animal Disease Diagnosis. *Electronic Turkish Studies*, 12(11).
- Fenerci, T. (2001). The Importance of Database Design and Normalisation Process. *Türk Kütüphaneciliği*, 15(2), 123-135.
- Gabrali, D., & Aslan, Z. (2020). Modelling of solar energy potential with multiple linear regression and artificial neural networks. *AURUM Journal of Engineering Systems and Architecture*, 4(1), 23-36.
- Güler, İ., & Übeyli, E. (2013). Diabetes Diagnosis Diagnosis Diagnosis Diagnosis Diagnosis With Multi Layered Perseptron Neural Networks. *Journal of Gazi University Faculty of Engineering and Architecture*, 21(2), 319-326.
- Gong, Y., Liu, L., Yang, M., & Bourdev, L. (2014). Compressing deep convolutional neural networks using vector quantisation. arXiv preprint arXiv:1412.6115.
- Harika, Ü. L. K. Ü., & Yalpır, Ş. (2021). Methodology development for energy demand forecasting: 2030 Turkey case. *Niğde Ömer Halisdemir University Journal of Engineering Sciences*, 10(1), 188-201

- Hussain, A., Rahman, M., & Memon, J. A. (2016). Forecasting electricity consumption in Pakistan: The way forward. *Energy Policy*, 90, 73-80.
- Ismic, B. (2015). Electricity consumption, economic growth and population relationship in developing countries. *Journal of Çankırı Karatekin University Faculty of Economics and Administrative Sciences*, 5(1), 259-274.
- Kheirkhah, A., Azadeh, A., Saberi, M., Azaron, A., & Shakouri, H. (2013). Improved estimation of electricity demand function by using of artificial neural network, principal component analysis and data development analysis. *Computers & Industrial Engineering*, 64(1), 425-441.
- Ozoh, P., Abd-Rahman, S., Labadin, J., & Apperley, M. (2014). A comparative analysis of techniques for forecasting electricity consumption. *International journal of computer applications*, 88 (15).
- Kılınç, G., Karaatlı, M., & Ömürbek, N. (2022). Prediction Of Container And Cargo Handling Volumes In Turkey's Ports With Ann Narx Model. *Journal of Productivity*, (2), 251-266.
- Kutlugün, M. A. (2017). Text-to-speech synthesis by genre through supervised machine learning (Master's thesis, Istanbul Sabahattin Zaim University, Istanbul Sabahattin Zaim University, Institute of Science and Technology, Department of Computer Engineering).
- Mahmutoğlu, M., & Öztürk, F. (2015). Turkey electricity consumption forecasting and policy recommendations that can be developed in this context. In *EY International Congress on Economics II (EYC2015)*, November 5-6, 2015, Ankara, Turkey (No. 239). Economic Approximation Association.
- Hussain, A., & Rahman, M., & Memon, J. A., 2016, "Forecasting electricity consumption in Pakistan: the way forward," *Energy Policy*, Elsevier, vol. 90(C), pages 73-80.
- Nacar, E. N., & Erdebilci, B. (2021). Sales Forecasting With Machine Learning Algorithms. *Industrial Engineering*, 32(2), 307-320.
- Ozoh, P., Abd-Rahman, S., Labadin, J., & Apperley, M. (2014). A comparative analysis of techniques for forecasting electricity consumption. *International journal of computer applications*, 88(15).
- Özbakır, P. (2006). Energy management. (Master's thesis, Yıldız Technical University, Institute of Science and Technology).
- Özdağoğlu, A. (2014). The Effect of Normalisation Methods on Multi-criteria Decision Making Process-Moora Method Investigation. *Ege Academic Review*, 14(2).

- Özekes, S. (2003). Data mining models and application areas.
- Özdemir, S. (2018). Potential distribution modelling and mapping using RandomForest Method: The case of Yukarıgökdere Region. *Turkish Journal of Forestry*, 19(1), 51-56.
- Özdemir, M. E. (2021) Medium Term Electricity Consumption Forecasting by Using Artificial Neural Networks: Iskenderun Case. *European Journal of Science and Technology*, (28), 489-492.
- Satici, S. (2021). The Effect Of Different Normalisation Techniques On Multi-Criteria Decision Making Methods: *Journal of Business, Economics and Management Research*, 4(2), 350-361.
- Son, H., & Kim, C. (2017). Short-term forecasting of electricity demand for the residential sector using weather and social variables. *Resources, conservation and recycling*, 123, 200-207.
- Şengöz, M. (2021). National energy management. *Journal of International Political Research*, 7(1), 73-85.
- Toros, H., & Aydın, D. (2018). Prediction of Short-Term Electricity Consumption by Artificial Neural Networks Using Temperature Variables. *European Journal of Science and Technology*, (14), 393-398.
- Yakut, Y. B. E. T. Y., YAKUT, E., & Yavuz, S. (2014). Stock Market Index Forecasting with Artificial Neural Networks and Support Vector Machines. *Journal of Süleyman Demirel University Faculty of Economics and Administrative Sciences*, 19(1), 139-157.
- Yıldırım, M. (2021). Electricity Consumption Forecasting With Some Data Mining Methods (Doctoral dissertation).

A circular graphic with a green top half and a white bottom half, framed by a green outline. The text is centered within the circle.

Chapter 16

RENEWABLE ENERGY AND SUSTAINABLE LIVING

Abdullah YİNANÇ¹

¹ Doç, Dr. Tekirdağ Namık Kemal Üniversitesi, Teknik Bilimler Meslek Yüksekokulu, ayinanc@nku.edu.tr, ORCID: 0000-0002-8144-8266

INTRODUCTION

Our modern world faces unique environmental challenges and increasing energy demands. To meet these challenges and build a sustainable future, it is essential to effectively integrate renewable energy sources and adopt sustainable living principles. Technological progress and industrialisation have enabled us to make great strides in meeting our energy needs. However, this process has brought along problems such as overuse of natural resources, environmental destruction and climate change. The basis of sustainability is the efficient use of natural resources, recycling and minimising waste (Nemli, 2007). In this context, renewable energy resources are of great importance.

Economic and social development is directly related to the level of development of a country. Energy serves as one of the most important factors in achieving this level of development. Energy is a necessity for sustainable development, but it can make significant contributions to industrialisation and the overall development of communities when reliable economic conditions and environmental factors are taken into account (Kok and Benli, 2017). Energy, which constitutes the basic dynamics of an economy, has an important place in the growth and development of countries. Countries can achieve this with the right, strategic and sustainable growth policies. At this point, renewable energy, which is environmentally friendly, whose installation costs are decreasing day by day with the developing technology and has an inexhaustible resource, is the right alternative to the use of non-renewable energy resources. With the 1973 global oil crisis, the importance of renewable energy has come to the fore (Sevim, 2012: 4384).

In this section, renewable energy sources will be discussed in detail. It will also emphasise on sustainable living. This chapter will enlighten the readers to understand and apply these concepts in depth in this era when renewable energy and sustainable living are of critical importance.

RENEWABLE ENERGY

Renewable energy sources are defined as natural and self-renewable energy sources. Renewable energy sources can be expressed as solar energy, wind energy, biomass energy, geothermal energy, hydroelectric energy, wave and tidal energy. The source of renewable energy is natural resources such as sunlight, wind, rain, geothermal heat and currents (Karagöl and Kavaz 2017: 7). Renewable energy sources are a type of energy that is inexhaustible and easily replaced (Smith & Taylor, 2008). Figure 1 shows the world renewable energy consumption rates by years.

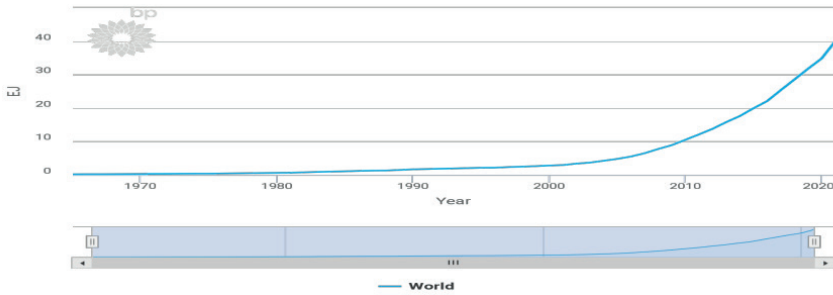


Figure 1: *World Renewable Energy Consumption Rates*

Source: *BP, 2023*

According to the figure, it is seen that the use of renewable energy has increased significantly in the world in the 2000s. These resources pollute the environment less than non-renewable energy resources. In addition, the fact that they are accessible and sustainable all over the world attributes great importance to these resources (Kumbur et al., 2005: 3). In general, renewable energy sources can be classified as solar energy, wind energy, biomass energy, hydraulic energy, geothermal energy and ocean energy (Bhattacharya et al., 2016: 734).

Solar Energy

Solar energy is the world's most fundamental energy source, which is kilometres away from the earth, provides heat and light to the earth and is an alternative to fossil fuels. Solar energy, which enables energy reflections in the world, can undergo variations and transform into different types of energy such as ocean temperature difference, wind, sea wave and biomass energies. Solar energy, which is utilised for heating and electricity generation, provides water transformation and creates current potential (Varınca and Gönüllü, 2006: 270). Sunlight is converted into electricity and can power everything. Solar energy can be used in a wide variety of areas such as heating buildings, heating water and powering our devices. While roof panels can power a house, projects using mirrors to concentrate sunlight and solar farms can create much larger resources. In addition to being renewable, solar systems are also clean energy sources as they do not produce air pollutants or greenhouse gases (Twi-global, 2021). Solar energy applications are very popular in national and international energy policies at the point of achieving the goal of sustainable energy (Koçaslan 2020). Among the advantages of solar energy are that it is produced using natural materials, does not harm the environment, is economical and not dependent on foreign energy. However, its low efficiency and seasonal and daily interruptions negatively affect the use of this type of energy (Öztürk, 2013: 52). Solar energy is a clean, abundant,

quiet and beautiful, unlimited and sustainable energy source, and it is also environmentally friendly as it has no polluting emissions (Camacho and Berenguel, 2012).

Solar energy and different technologies can be considered as an important source in meeting a large part of the country's energy needs (Kılıçkaplan et al., 2017). Solar energy, which is a mandatory power source for living things to sustain their lives, does not require any energy in its use because it is an infinite energy source. A significant portion of the energy sources used today have been shaped as a result of different reactions caused by the sun. In addition to these positive contributions, large areas are required for the installation of power plants. In addition, stocking this energy source causes a high level of cost (Kaynar, 2020: 50).

The most important advantages of solar energy are that it is a renewable resource, it is ready for energy production without requiring any pre-production process in nature, it does not leave any waste during or at the end of the production process, it allows the use of large and idle facility roofs and inefficient lands such as factory warehouses, etc., and it is noiseless. Dependence on meteorological conditions (such as summer and winter difference, sunny and overcast weather difference), high initial installation costs, mirror reflections in concentrated thermal power plants pose a danger to insects and birds, leakage of toxic substances during the production of photovoltaic cells, low mechanical resistance to harsh weather conditions such as snowstorms, hail, etc. can be considered as weaknesses of solar energy systems (Kádár, 2014: 221-222).

Wind Energy

While the meaning of wind in the dictionary is “revolution”, its meaning in meteorology is defined as a displaced air flow. Wind energy, which is formed by the conversion of 1-2% of solar energy into wind energy, is a clean, renewable, endless and natural resource. Wind formation is based on temperature and pressure differences. The winds moving from high-pressure areas to low-pressure areas differ depending on geographical differences and temperature changes on the earth (Akova, 2008: 24). Among the advantages of wind energy is that it is renewable, has no transport problem, does not require very high technology for energy production, reduces dependence on foreign countries and is an energy source that allows production with domestic resources. Wind energy, which does not cause environmental pollution, is abundant in the atmosphere (Şenel and Koç, 2015). Wind energy was recognised as one of the new and renewable resources by the UN in 1961, and it was accepted to be the most advanced and commercially efficient energy type among renewable energies (Yapraklı, 2013: 40). Wind energy is preferred at a higher rate than alternative renewable energy sources. In addition to its features such as being

completely free and abundant in connection with natural events, it is highly preferred due to factors such as being completely environmentally friendly, not having high power plant installation costs, not emitting any gas emissions and having very low energy production costs (Oskay, 2014).

The use of renewable energy sources, especially wind energy, has attracted intense interest from governments and private organisations, as it is considered one of the best and most competitive alternative energy sources in the current energy transition adopted by many countries around the world. In addition, wind energy plays an important role in mitigating global warming as it reduces greenhouse gas emissions (Vargas et al., 2019). In short, wind energy is a clean, reliable, stable, independent energy source that reduces the unit cost of energy produced with the developing technology. The biggest disadvantage of wind energy is the time difference between production and consumption times. If the system in question is provided, it is predicted that wind energy can be obtained in approximately 95% of the earth (Öztürk, 2013: 23). In addition, wind energy has many advantages such as being a renewable resource, being ready for continuous use in nature, not turning into any waste during and after the electricity generation process, and low power plant maintenance and operation (electricity generation) costs. Since wind energy is mainly dependent on meteorological factors, the amount and quality of electricity produced from wind power plants vary with weather conditions. In addition, noisy operation of turbines and high investment costs can be shown among the disadvantages (Kádár, 2014: 215).

Geothermal Energy

Geothermal energy, which can be defined as heat energy obtained from underground hot water and water vapour, is considered as an alternative energy source in reducing the environmental damage of fossil fuels, ensuring the sustainable development of energy, and increasing the efficiency of energy use (Liu et al. 2022). Geothermal energy can be defined as energy consisting of hot water, steam and gas, which is formed by the heat in different layers of the earth's crust, which has a temperature higher than the air temperature and can contain minerals, salts and gases that are more valuable than the water resources fed in the basins in the world. Geothermal energy is formed by the thermal energy accumulated in the earth. Since the inner layers of the earth are too hot, heat transfer takes place towards the surface and the heat increases as you go from the surface to the centre. Some hard rocks, whose underground temperature is utilised, are considered as geothermal energy sources although they do not contain liquid in their structures (Etemoğlu et al., 2004: 93-94). Geothermal energy is a type of energy originating from the internal temperature of the Earth. This energy is expressed as thermal energy in the form of hot liquid (vaporised water, gas) and hot, dry rock forms, which are collected under pressure in the deep regions of the earth's crust (Koç and Kaya, 2015).

Geothermal energy resources are defined as the total amount of thermal energy (heat) accumulated in the earth's crust to a certain depth, according to a certain area where calculations are made and average annual temperatures in the earth's surface groups. Traditionally, geothermal resources are hydrothermal resources containing reservoirs of hot water and/or steam and are classified as vapour- or liquid-dominated resources. Geothermal energy has three main uses: electricity generation, direct use applications and for heating and cooling buildings with geothermal heat pumps. In addition to these, there are a wide variety of uses such as aquaculture, drying crops, growing plants and vegetables in greenhouses, paper and cement industry, food processing and health spas (Sowizdzal, 2018).

The proportional distribution of geothermal energy resources in the world and the fact that it is an energy type that is less affected by climatic conditions have the advantage of being preferred as a renewable energy source. The geothermal system consists of the heat source deep in the earth's crust, the heat-carrying fluid, the reservoir rock containing the fluid, and the cover rock that prevents heat loss. Magma activities reaching shallow depths in the earth's crust and reaching the earth's surface from the fractured zones formed by tectonism in the centre of the earth constitute the heat source of the geothermal system. Deeply heated water is collected in the porous and permeable reservoir rock (Arslan et al., 2001). Geothermal energy, whose production cost is cheaper than other energy sources, is used in chemical production, drying, thermal tourism, electricity generation, heating and plant and aquaculture (Kaymakçioğlu and Çirkin, 2020: 1-2).

Biomass Energy

Biomass energy is one of the oldest energy sources and is among the natural energy sources that are widely consumed worldwide, protect nature and do not create waste. Biomass is derived from other fuels such as firewood, animal, urban, agricultural and urban wastes of biological origin, which are used to obtain energy. Items that can be used to explain biomass can be listed as animal droppings, food and fruit juice, trees, business and domestic wastes (Toklu, 2017: 236). Biomass is defined as a renewable energy source gained through living resources such as wood, charcoal, animal and construction excrement; agricultural products and forest sector organic residues, alkon and methane fermentation, different water information (Gürsoy, 2004: 127). Biogas is a renewable energy source produced by anaerobic digestion of biomass. There are at least five main biomass resource areas where biomass can be used. These are sewage, landfill, animal manure, organic waste and energy crops. In terms of its origin, biogas consists of methane (40-75%), carbon dioxide (20-45%) and some other compounds, usually in trace amounts (Budzianowski, 2012: 343).

The production and conversion technologies of biomass energy need to be well understood. The advantages of biomass are that it is suitable for energy efficiency at all scales, low light intensities are sufficient and continuous. On the other hand, it also has disadvantages such as low conversion efficiency, high transport and labour costs, high water content, low thermal value compared to fossil fuels and competition for agricultural areas. Biomass, which can be grown in any environment, is shown as a strategic energy source that provides socio-economic progress, can be stored, can generate electricity without harming the environment, can be obtained as fuel for vehicles and contributes significantly to the revival of the rural economy (Öztürk, 2013). Throughout the world, biomass energy is gaining importance as a strategic and environmentally friendly energy source. Many studies are carried out in this field. The most advanced technologies are found in European countries, and studies on energy obtained from garbage wastes are carried out primarily in big cities. In the studies carried out, the total potential power is estimated to be approximately 23,000,000 MW, and it has been revealed that the largest part of this is a resource that can be obtained from garbage waste (Alemdaroğlu, 2007: 27). This type of energy contributes to sustainable waste management while helping to reduce energy dependence on fossil fuels (Yi et al., 2018).

In addition to the economic benefits derived from energy and fuel production, biomass energy provides additional environmental benefits such as anaerobic digestion facilities, reductions in water, soil and air pollution, etc. Traditionally, manure is used directly as fertiliser in agriculture without treatment. This can cause environmental problems, water pollution. Natural degradation of manure leads to methane and carbon dioxide emissions during storage. Anaerobic digestion contributes to the reduction of odours associated with manure storage and decomposition. It therefore eliminates pathogens that may pose a risk to human and animal health. The digestate from biogas production can be used as fertiliser with the same nutrient content as manure. This provides economic benefits by reducing the use of chemical fertilisers on farms and prevents methane emissions by reducing nutrient run-off (Scarlat et al., 2018).

Hydroelectric Energy

Hydroelectric energy is a type of energy generated by converting the potential energy of water into kinetic energy. The sea, lakes and rivers evaporate under the influence of the sun, the evaporated water condenses and falls on the mountain slopes in the form of rain or snow and feeds the rivers. With this cycle, hydraulic energy constantly renews itself (Özdemir, 2020: 118). People have used hydroelectric energy for a long time, mostly for agricultural or irrigation purposes. The first hydroelectric power plant was built in 1902 and quickly became an important domestic energy source for Turkey. Hydroelectric power plants were initiated by the Ministry of Public Works

in the 1930s and the Electrical Works Planning and Survey Administration (EIE) was established in 1935 to assess Turkey's energy demand and to develop hydroelectric and other resource potential (Erdoğan, 2011). Hydroelectric power is a consolidated technology for generating electricity from water resources and is considered as a clean method. Although there are some controversies in the environmental dimension, the HEPP profile of countries has a very strategic importance in terms of both short-term development and the dissemination of sustainable energy resources due to the improvements it offers to the economy on a regional and global basis (Catolico et al., 2021). Hydraulic energy is generated by installing dams on rivers, collecting and accumulating water in large reservoirs and converting the potential energy of this accumulated water into electricity. It is a natural energy source that does not create environmental pollution, can be activated very quickly in case of excessive energy demand, can be deactivated very quickly in emergencies and is not dependent on foreign energy. On the other hand, the investment costs of hydraulic energy are high and the total construction period is very long. In addition, dams can change the ecological characteristics of the region around them and cause flooding of residential areas and ancient sites. In addition, there may be fluctuations in the production of hydroelectric power plants (in total production shares every year) depending on rainfall conditions (Öztürk, 2013).

Since the main factor in the formation of hydroelectric energy is water, this energy source has the advantage of being both more sensitive to the environment in the process of electricity generation and the cheapest source in the long term. In addition, hydroelectric power plants producing electrical energy; low power hazard emission, long life span, being in a natural energy production position and undertaking similar tasks are the reasons that make hydroelectric power plants favourable (Başkaya, 2010: 669). Being a clean and renewable energy, being stable and reliable in terms of electricity generation, being in a structure that can operate for many years, reducing foreign dependency in energy due to the fact that it can be built on a country's own rivers, being able to be used against hazards such as floods and overflows by providing control of rivers as well as electricity generation, and needing very little personnel during operation (commissioning and production process) are among the main advantages of hydraulic energy. The main disadvantages of hydraulic energy include long installation processes (especially in dam-type HEPPs), evacuation of settlements during the installation phase, causing effects such as flooding of the natural environment, restricting transportation on the river, having negative effects on aquatic creatures such as fish, etc., having the possibility of bad consequences in case of damage in possible earthquakes or terrorist attacks, and decreasing capacity during drought periods (Kádár, 2014: 212-213).

Wave and Tidal Energy

Since wave energy occurs as a result of surface movements, it is also called tidal energy in the literature (Bekar, 2020). Wave energy is the obtaining of energy from the use of waves formed in the sea through the wind formed as a result of the heating of the Earth's surface at different levels. Tidal energy is generated by the rise or fall of the water level in the oceans as a result of the spatial proximity or distance of the moon and the sun to the earth (Özdemir, 2020: 130). Considering that 70% of the world is water, it is possible to meet a high portion of the energy need from wave energy. However, wave and tidal energy is known as the least used energy type in the world (Bayraç et al., 2018: 71). It is a type of energy generated directly from the surface of the waves or by capturing the pressure differences under the surface. This energy from the waves is converted into usable energy with systems installed on the coastline, near the coast or far from the coast. The power source of wave energy, whose potential is available in the regions where seas and oceans are located, is infinite and abundant. It provides the opportunity to utilise the potential technology in other researches to be carried out in the ocean and sea. It helps to turn salt water into fresh water and pump it to the areas where it is needed. Wave energy is seen as one of the energy sources of the future within the framework of new technological developments. In addition, it has negative aspects such as the inability to create a design to utilise each wave size, the high costs of feasibility studies, installation and maintenance, and the dependence of energy production on natural conditions (Yapraklı, 2013: 43-44). In addition, it is possible to obtain infinite energy at the desired limit from the seas by utilising wave power. As a clean energy source, it does not cause soil loss and provides positive effects on the natural balance. When the use of energy obtained from this source becomes widespread, the advantage of utilising it for heating purposes also emerges. If used for this purpose, it will increase the quality of the atmosphere by reducing the effect of carbon and similar harmful gases in the atmosphere (Çokan, 2004: 3-4).

Wave energy is a renewable and clean energy source. The power plants established offshore or on the coast also provide benefits as natural breakwaters as they break the kinetic energy of the waves. Since it is installed on the sea surface, fertile inefficient soil is not used and in this way a protection is provided. For sea creatures, power plants can provide an artificial habitat and provide a breeding and shelter environment. Besides its advantages, wave energy also has some disadvantages. For example, there are some disadvantages such as the fact that the power plants established on the shore and close to the shore cause noise pollution, the stagnation caused by the power plants far from the shore has negative effects on living things and the possibility of creating a risk for sea traffic, although it is a renewable and clean energy in terms of carbon dioxide emission, there is a little carbon dioxide emission during installation,

and very high powers cannot be reached with current technologies (Ün, 2013: 7).

SUSTAINABLE LIFE

Sustainability is the use of environmental values and natural resources in a way that does not lead to wastefulness in environmental values and natural resources, taking into account the rights of present and future generations, and ensuring economic development (Keleş, 1998: 17-18). Sustainability aims to protect the existing resources of the world and ensure that they are transferred to future generations (Karabıçak and Özdemir, 2015: 44). From another perspective, sustainability is a process of change in which the use of resources, investment targets, technological developments and institutional changes are made consistent with the needs of the future as well as the present (Camagni et al., 1998: 105). Ehrenfeld (2005) defines sustainability as the possibility of infinite development of all forms of life. Sustainable consumption is a form of consumption that ensures the use of existing resources within sustainability and tries to minimise the damage to natural life (Pir, 2022: 7).

Sustainable built environment is defined as an environment that, on the one hand, maintains the quality of human life at an acceptable level and preserves the carrying capacity of ecosystems on a regional and global scale, on the other hand, conserves non-renewable energies, materials and ecological resources; reuses and recycles materials and outputs within the built environment; minimises toxic substance emissions and reintegrates them with the environment throughout the life cycle of building systems; and reintegrates with the environment in harmony and flawlessly at the end of its life cycle. Human health depends on the continuity of the health of the natural environment (Yeang, 2012: 438). As an increasing number of consumers are interested in social and environmental issues related to what they eat and wear, a new trend has emerged to explain these conscious lifestyle choices: the lifestyle of health and sustainability (LOHAS). These consumers are characterised as valuing quality of life with an emphasis on health and sustainability, and as a result, they prefer environmentally friendly locally produced products that can help sustain their communities (Sung and Woo, 2018: 120). Consumers with LOHAS are characterised as valuing quality of life with an emphasis on health and sustainability, and as a result, these consumers prefer environmentally friendly locally produced products that can help sustain their communities (Sung and Woo, 2018: 120). As consumers with this awareness increase, a wide customer profile is formed for businesses. However, for businesses, such consumers or environmentalist consumers are seen as a customer group that can be persuaded quite difficult (Özdemir et al., 2010: 256; Pir, 2019: 1556).

RENEWABLE ENERGY AND SUSTAINABILITY

Sustainable development faces three critical challenges: rapidly growing world population, energy scarcity, and ever-increasing environmental pollution. Currently, many countries around the world are interested in new energy research, especially renewable energy, to gradually reduce their dependence on traditional fossil fuels (Zhu et al., 2015). With the developments in recent years, the risk and reality of environmental degradation have become more apparent. Increasing evidence of environmental problems has necessitated potential long-term actions for development. In this regard, renewable energy sources are seen as one of the most efficient and effective solutions. Therefore, there is a strong link between renewable energy and sustainable development (Kaygusuz & Kaygusuz, 2002).

Renewable energy resources, which do not create environmental pollution problems, are inexhaustible and distributed over a wide geography because they take their source from nature. These resources are rapidly renewed in natural processes. The main advantage of renewable resources is that they can be used throughout the year and with a one-time investment, they can meet energy needs for decades without affecting the environment (Alrikabi, 2014). Environmental awareness means that individuals recognise environmental problems, actively participate in the solution of these problems and accept their responsibilities towards the environment. In order to reach such a level of maturity, it is very important to maintain a human-centred approach when addressing environmental concerns and to avoid endangering the environment for personal interests (Cansaran, 2015: 70). Due to social responsibility in organisations, environmental pollution is reduced, vegetation is protected, cultural assets are preserved, cleaner production processes and energy savings are ensured (Aktan & Börü, 2007; Yılmaz, 2018).

CONCLUSION

Renewable energy sources, which are called energy sources that exist in nature and have the ability to constantly renew themselves, have an environmentally friendly feature compared to fossil fuels. As a result of the use of fossil fuels, carbon dioxide gas released into the world atmosphere causes an increase in global warming and as a result of this, it causes the emergence of world climate changes, the melting of the glaciers in the poles, thus increasing sea levels and flooding of agricultural lands. For this reason, it is emphasised how important it is for the infrastructures of the existing energy sources used by the states around the world to switch to renewable energy sources. It has started to be emphasised on every platform that the fossil fuels they are using should be reduced and thus it is necessary to prevent global warming in the world we live in (Keleş and Hamamcı, 2002: 105). Energy is at the forefront of economic development. However, countries

have to determine policies on the use of energy resources according to their economic, cultural and geographical conditions. In addition to the distance and cost of the energy produced from the source to the place of use, it is also desired to be environmentally friendly. Therefore, energy use should be shaped and developed according to the validity of market conditions, environmental health protection and technological innovations (Atilgan, 2000).

The environmental dimension of sustainability is based on the idea of improving or at least preserving the ecological environment for future generations. Reducing the pressure on natural resources and not damaging the ecological environment while maintaining development is necessary to ensure environmental sustainability. Reducing resource consumption, utilising materials from recycled or renewable resources, recycling wastes, conserving energy resources and meeting energy demand from renewable resources are the main objectives of environmental sustainability (Akgül, 2010: 155-156). Sustainable development aims to ensure environmental quality of life, social quality of life and economic viability (Tosun, 2009). This, in turn, will bring sustainable life. Sustainable life refers to a situation where these three basic components come together in a balanced way. In this model, economic growth aims to use natural resources without depleting them, to support social justice and equality and to realise them without harming the environment. Thus, while meeting the needs of today, it also considers the needs of future generations. Sustainable living is an important approach to ensure that future generations have the same opportunities while improving the quality of life of people today. In this way, sustainable use of natural resources, sustainability of economic development, ensuring social justice and preservation of environmental balance are possible.

According to the principles of urban sustainability in the Aalborg Charter; environmental approach should be integrated into urban management tools in order to ensure sustainability. It is emphasised that the only sustainable way for the world is the use of renewable energy sources. The increase in pollution should be stopped and pollution should be prevented at its source. The effective participation of citizens is important in this process (European Conference on Sustainable Cities & Towns, 1994: 2-6). The stock of renewable resources should not decrease over time, and in case of depletion of exhaustible resources, the amount of renewable resources and man-made capital should be increased, and thus depleted resources should be compensated” (Çetin, 2006: 4). In order to ensure sustainable life design, ecological systems must be protected

Sustainable development necessitates meeting the rapidly increasing energy need with economic growth and population increase in order to realise economic activities and raise living standards and is considered as one of the most basic inputs of development. Both in the world and in Turkey, the need

for energy is increasing day by day, on the other hand, due to the limited and constantly decreasing energy resources in the world, countries should review their energy policies and turn to ways of using energy in the most efficient ways possible (Seydioğulları, 2013). Renewable energy reduces external dependence (Karagöl and Kavaz 2017: 7). Unlike other energy sources, there is no risk of supply problems caused by international problems (Akova, 2008: 24), which is another important issue for sustainable life in the long term.

The most important advantage of renewable energy sources is that they reduce carbon dioxide emission levels and thus improve air quality (Aydın 2010: 319). When all studies are reviewed, it reveals the importance of renewable energy potentials of countries for sustainable use of energy, reduction of carbon emissions and increasing development levels (Leng and Zhang 2023). Turkey signed the Paris Climate Agreement in 2016, one of the global steps taken on climate change, and the agreement officially entered into force with the adoption of the agreement in the parliament in 2020. By committing to zero carbon emissions by 2053, Turkey will increase the share of renewable energy sources in energy production, reduce the proportion of fossil resources or reduce the pressure of carbon emissions on the natural environment by reducing the proportion of fossil resources or implementing processes such as making waste from fossil resources safe. Thus, important steps will be taken for sustainable life. In order to achieve these goals, Turkey can invest in energy efficiency projects, increase forest cover and promote sustainable practices in the agricultural sector. It should also aim to improve the air quality of cities by promoting environmentally friendly transport systems and expand public transport. By raising public awareness on environmental issues through education and awareness campaigns, Turkey can support the development of green technologies and promote environmentally friendly industrial practices. Turkey can also contribute to the fight against climate change through international co-operation and technology transfer and should strive for a globally sustainable future.

REFERENCES

- Akgül, U. (2010). Sürdürülebilir kalkınma: Uygulamalı antropolojinin eylem alanı, Ankara Üniversitesi Dil Tarih Coğrafya Fakültesi Antropoloji Dergisi, 24, 133-164.
- Akova, İ. (2008). Yenilenebilir enerji kaynakları, Ankara: Nobel Yayınevi.
- Aktan, C. C., & Börü, D. (2007). Kurumsal sosyal sorumluluk, işletmeler ve sosyal sorumluluk. İstanbul: İgiad Yayınları.
- Alemdaroğlu, N. (2007). Enerji sektörünün geleceği: Alternatif enerji kaynakları ve Türkiye'nin önündeki fırsatlar. İstanbul Ticaret Odası, Prive Grafik Matbaacılık, İstanbul, 26-27.
- Alrikabi, N. K. M. A. (2014). Renewable energy types. Journal of Clean Energy Technologies, 2(1), 61-64.
- Arslan, S., Mustafa, D., & Çetin, K. (2001). Türkiye'nin jeotermal enerji potansiyeli. Jeotermal Enerji Semineri, Ankara, 21-28.
- Atılğan, I. (2000). Türkiye'nin enerji potansiyeline bakış. Gazi Üniversitesi Mühendislik Mimarlık Fakültesi Dergisi, 15, 31-47.
- Aydın, F. F. (2010). Enerji tüketimi ve ekonomik büyüme. Erciyes Üniversitesi İktisadi ve İdari Bilimler Fakültesi Dergisi, 35, 317-340.
- Başkaya, Ş. (2010). Hidroelektrik santralleri ve rüzgâr enerjisi santrallerinde çevresel etki değerlendirmesi. III. Ulusal Karadeniz Ormanlık Kongresi, 2, 668-676.
- Bayraç, N., Çelikay, F., & Çildir, M. (2018). Küreselleşme sürecinde sürdürülebilir enerji politikaları. Bursa: Ekin Basım Yayın Dağıtım.
- Bekar, N. (2020). Yenilenebilir enerji kaynakları açısından Türkiye'nin enerji jeopolitiği. Türkiye Siyaset Bilimi Dergisi, 3(1), 37-54.
- Bhattacharya, M., Paramati, S. R., Ozturk, I., & Bhattacharya, S. (2016). The effect of renewable energy consumption on economic growth: Evidence from top 38 countries. Applied Energy, 162(15), 733-741. <https://doi.org/10.1016/j.apenergy.2015.10.104>
- BP. (2023). BP Energy Graphic Tools. <https://www.bp.com/en/global/corporate/energy-economics/statisticalreview-of-world-energy/energy-charting-tool-desk-top.html>, (12.08.2023).
- Budzianowski, W. (2012, January). Sustainable biogas energy in Poland: Prospects and challenges. Renewable and Sustainable Energy Reviews, 16(1), 342-349.
- Camacho, E. F., & Berenguel, M. (2012). Control of solar energy systems. IFAC Proceedings Volumes, 45(15), 848-855.
- Camagni, R., Capello, R., & Nijkamp, P. (1998). Towards sustainable city policy: An economy-environment technology nexus. Ecological Economics, 24(1), 103-118.

- Cansaran, D. (2015). Çevre bilinci düzeyini belirlemeye yönelik uygulamalı bir çalışma: Merzifon Meslek Yüksekokulu örneği. *Aksaray Üniversitesi İktisadi ve İdari Bilimler Fakültesi Dergisi*, 7(2), 69-74.
- Catolico, A. C. C., Maestrini, M., Strauch, J. C. M., & Giusti, F., Hunt, J. (2021). Socioeconomic impacts of large hydroelectric power plants in Brazil: A synthetic control assessment of Estreito hydropower plant, 151, 111508.
- Çetin, M. (2006). Teori ve uygulamada bölgesel sürdürülebilir kalkınma. C.Ü. İktisadi ve İdari Bilimler Dergisi, 7(1), 1-20.
- Çokan, M. (2004). Dalga enerjisi (dalga elektrik santralleri). V. Ulusal Temiz Enerji Sempozyumu Bildiri Kitabı, 2.
- Ehrenfeld, J. R. (2005). The roots of sustainability. *MIT Sloan Management Review*, 46(2), 23-33.
- Erdoğan, E. (2011). The regulation of natural gas industry in Turkey. *The Political Economy of Regulation in Turkey* (ss. 145-176). Springer, New York.
- Etemoğlu, A. B., Can, M., & Kılıç, M. (2004). Ülkemiz jeotermal kaynaklarının ikinci kanun verim değerlerine bağlı sınıflandırılması. *Uludağ Üniversitesi Mühendislik-Mimarlık Fakültesi Dergisi*, 9(1), 93-101.
- European Conference on Sustainable Cities & Towns. (1994). Charter of European Cities & Towns Towards Sustainability. https://sustainablecities.eu/fileadmin/repository/Aalborg_Charter/Aalborg_Charter_English.pdf, (16.12.2022).
- Gürsoy, U. (2004). Enerjide toplumsal maliyet ve temiz ve yenilenebilir enerji kaynakları (Birinci baskı). Ankara: Türk Tabipleri Birliği Yayınları.
- Kádár, P. (2014). Pros and cons of the renewable energy application. *Acta Polytechnica Hungarica*, 11(4), 211-224.
- Karabıçak, M., & Özdemir, M. B. (2015). Sürdürülebilir kalkınmanın kavramsal temelleri. *Süleyman Demirel Üniversitesi Vizyoner Dergisi*, 6(13), 44-49.
- Karagöl, E. T., & Kavaz, I. (2017). Dünyada ve Türkiye'de yenilenebilir enerji. *Siyaset, Ekonomi ve Toplum Araştırmaları Vakfı*, 197, 1-32.
- Kaygusuz, K., & Kaygusuz, A. (2002). Renewable energy and sustainable development in Turkey. *Renewable Energy*, 25(3), 431-453.
- Kaymakçioğlu, F., & Çirkin, T. (2005). Jeotermal enerjinin değerlendirilmesi ve elektrik üretimi. III. Yenilenebilir Enerji Kaynakları Sempozyumu ve Dergisi Bildiriler Kitabı, 19-21.
- Kaynar, N. K. (2020). Yenilenebilir enerji kaynaklarından güneş enerjisinin amasya ilindeki potansiyeli. *Bilge International Journal of Science and Technology Research*, 4(2), 48-54.
- Keleş, R., & Hamamcı, C. (2002). Çevrebilim. *İmge Kitabevi*, Ankara.
- Keleş, R. (1998). *Kentbilim Terimleri Sözlüğü*, 2. Baskı. *İmge Kitabevi Yayınları*, Ankara.

- Kılıçkaplan, A., Bogdanov, D., Peker, O., Caldera, U., Aghahosseini, A., & Breyer, C. (2017). An energy transition pathway for Turkey to achieve 100% renewable energy powered electricity, desalination and non-energetic industrial gas demand sectors by 2050. *Solar Energy*, 158, 218-235.
- Koç, E., & Kaya, K. (2015). Enerji kaynakları-yenilenebilir enerji durumu. *Mühendis ve Makina*, 56(668), 36-47.
- Koçaslan, G. (2020). Dünyada ve Türkiye’de güneş, rüzgar ve jeotermalde güncel iktisadi görünümü. *Ömer Halisdemir Üniversitesi İktisadi ve İdari Bilimler Fakültesi Dergisi*, 13(2), 213-226.
- Kok, B., & Benli, H. (2017). Energy diversity and nuclear energy for sustainable development in Turkey. *Renewable Energy*, 111, 870-877.
- Kumbur, H., Özer, Z., Özsoy, H. D., & Avcı, E. D. (2005). Türkiye’de geleneksel ve yenilenebilir enerji kaynaklarının potansiyeli ve çevresel etkilerinin karşılaştırılması. III. Yenilenebilir Enerji Kaynakları Sempozyumu Bildirileri.
- Leng, Y. J., & Zhang, H. (2023). Comprehensive evaluation of renewable energy development level based on game theory and TOPSIS. *Computers & Industrial Engineering*, 175, 108873.
- Liu, G., Zhao, Z., Xu, H., Zhang, J., Kong, X., & Yuan, L. (2022). A robust assessment method of recoverable geothermal energy considering optimal development parameters. *Renewable Energy*, 201, 426-440.
- Nemli, E. (2007). Sürdürülebilir gelişme: Ekonomi ile çevre arasındaki denge. İstanbul, Kalder-Çevre Uzmanlık Grubu. (Erişim Tarihi: 24. 08. 2023).
- Oskay, C. (2014). Sürdürülebilir kalkınma çerçevesinde rüzgâr enerjisinin önemi ve Türkiye’de rüzgâr enerjisi yatırımlarına yönelik teşvikler. *Niğde Üniversitesi İİBF Dergisi*, 80.
- Özdemir, H. Ö., Karaarslan, M. H., & Altuntaş, B. (2010). Tüketicilerin çevreci işletmelere ve ürünlere karşı tutumları: Ankara, İstanbul ve Kırşehir illerinde bir uygulama. *E-Journal of New World Sciences Academy*, 5(4), 353-366.
- Özdemir, Y. (2020). Türkiye’nin enerji stratejisi. Ankara: Atlas Akademik Basım Yayın Dağıtım.
- Öztürk, H. (2013). Yenilenebilir enerji kaynakları. İstanbul: Birsen Yayınevi.
- Pir, E. Ö. (2019). Yeşil tüketim ve gönüllü sade tüketim davranışlarının tüketici haklarının farkındalığı üzerine bir araştırma. *Business & Management Studies: An International Journal*, 7(4), 1555-1572.
- Pir, E. Ö. (2022). Sürdürülebilir pazarlama. Çanakkale: Paradigma Akademi.
- Scarlat, N., Dallemand, J.-F., & Fahl, F. (2018). Biogas: Developments and perspectives in Europe. *Renewable Energy*, 129, 457-472.
- Sevim, C. (2012). Küresel enerji jeopolitiği ve enerji güvenliği. *Yaşar Üniversitesi E-Dergisi*, 7(26), 4378-4391.
- Seydioğulları, H. S. (2013). Sürdürülebilir kalkınma için yenilenebilir enerji. *Planlama*

Dergisi, 23(1), 19-25.

- Smith, Z. A., & Taylor, K. D. (2008). *Renewable and alternative energy resources: A reference handbook*. Bloomsbury Publishing Usa.
- Sowizdzal, A. (2018). Geothermal energy resources in Poland—overview of the current state of knowledge. *Renewable and Sustainable Energy Reviews*, 82, 4020-4027.
- Sung, J., & Woo, H. (2019). Investigating male consumers' lifestyle of health and sustainability (LOHAS) and perception toward slow fashion. *Journal of Retailing and Consumer Services*, 49, 120–128.
- Şenel, M. C., & Koç, E. (2015). Dünyada ve Türkiye'de rüzgâr enerjisi durumu-genel değerlendirme. *Mühendis ve Makina*, 56(663), 46-56.
- Toklu, E. (2017). Biomass energy potential and utilization in Turkey. *Renewable Energy*, 107, 235-244.
- Tosun, K. E. (2009). Sürdürülebilirlik olgusu ve kentsel yapıya etkileri. *Paradoks, Ekonomi, Sosyoloji ve Politika Dergisi*, 5(2).
- TWI-Global. (2021, January). What is renewable energy? Retrieved from <https://www.twi-global.com/technical-knowledge/faqs/renewable-energy> (Erişim Tarihi: 10.08.2023).
- Ün, Ü. T. (2003). *Dalga Enerjisi: Teknolojisi, ekonomisi, çevresel etkisi ve dünyadaki durumu*. II. Yenilenebilir Enerji Sempozyumu.
- Vargas, S. A., Esteves, G. R. T., Maçaira, P. M., Bastos, B. Q., Oliveira, F. L. C., & Souza, R. C. (2019). Wind power generation: A review and a research agenda. *Journal of Cleaner Production*, 218, 850-870.
- Varınca, K. B., & Gönüllü, M. T. (2006). Türkiye'de güneş enerjisi potansiyeli ve bu potansiyelin kullanım derecesi, yöntemi ve yaygınlığı üzerine bir araştırma. I. Ulusal Güneş ve Hidrojen Enerjisi Kongresi, Eskişehir.
- Yapraklı, S. (2013). *Enerjiye dayalı büyüme Türk sanayi sektörü üzerine uygulamalar*. İstanbul: Beta Yayıncılık.
- Yeang, K. (2012). *Ekotasarım Rehberi*. Yem Yayın, İstanbul.
- Yılmaz, F. (2018). Corporate social responsibility. In K. Özdaşlı, et al. (Eds.), *Innovative Approaches in Social, Human and Administrative Sciences*. Ankara: Gece Kitaplığı.
- Zhu, J., et al. (2015). A review of geothermal energy resources, development, and applications in China: Current status and prospects. *Energy*, 93, 466-483.

Chapter 17

GREEN BUILDING CONCEPT: AN OVERVIEW FROM THE WORLD AND TURKEY PERSPECTIVE

Mirac Nur CİNER¹

Emine ELMASLAR ÖZBAŞ²

H. Kurtulus OZCAN³

1 Arş. Gör. Environmental Engineering Department, Engineering Faculty, Istanbul University-Cer-
rahpasa, Istanbul, Turkey

2 Doç. Dr., Environmental Engineering Department, Engineering Faculty, Istanbul University-Cer-
rahpasa, Istanbul, Turkey

3 Prof. Dr., Environmental Engineering Department, Engineering Faculty, Istanbul University-Cer-
rahpasa, Istanbul, Turkey

Introduction

Green buildings are defined as structures constructed and operated by implementing principles of environmental sustainability. Such buildings aim to reduce their environmental impacts by utilizing energy, water, and other resources more efficiently. The primary objectives of green buildings are to decrease carbon footprints, prevent the depletion of natural resources, and enhance indoor air quality (Komnitsas 2011). To achieve these goals, strategies such as energy efficiency, waste management, water conservation, and the utilization of renewable energy are employed. Green buildings not only provide environmental benefits but also reduce operational costs and offer healthier living spaces for occupants (Zhang et al. 2018).

The increasing popularity of green buildings has gained momentum alongside the rise in environmental issues and escalating energy costs. Green building certifications are utilized to attest that such structures conform to sustainability standards and promote various industry benchmarks for green building design and construction. Green buildings provide both building owners and users with greater satisfaction and value (Pitt et al. 2009). Simultaneously, they play a significant role in the overall environmental and economic well-being of society. Therefore, green building practices and technologies will form the cornerstone of a sustainable and environmentally friendly construction sector in the future.

The damage caused to the environment by climate change and the rapid pollution of nature have brought the issue of long-term preservation of the environment and resources to the forefront. The International Union for Conservation of Nature (IUCN) adopted the World Conservation Strategy in 1982, which is when the notion of sustainability was first articulated (Gezen 2015). The plan underscores the need of managing ecosystems, organisms, terrestrial and marine resources, and the atmosphere for human use in a way that maximizes sustainability, as long as it doesn't compromise the integrity of ecosystems and species.

One of the main components of sustainable design is environmentally aware architecture design, which is sustainable through reducing resource use and utilizing renewable resources. Put differently, examples of sustainable architecture are built in harmony with the natural world and do not endanger the environment in which they are situated, either in their active or passive states. Maintaining continuity via the use of non-depletable and renewable resources is one of the main goals of sustainable design. Of special importance is preventing the depletion of essential energy resources needed for homes, such natural gas, electricity, and water. The primary goal of sustainable architecture is to enable a structure to obtain the resources it needs on its own from the surrounding environment. It is thought that the widespread use of

this architectural type will prevent energy supplies from being depleted (URL 1).

Green buildings are a part of the global response that recognizes the increasing role of human activity in causing global climate change. Green buildings are technologically advanced properties that take into account the environmental and human health impacts of buildings. They are designed to be powered by renewable energy sources, facilitate the recycling of wastewater, maximize the use of natural daylight, employ effective thermal insulation, and aim for self-sufficiency in energy production. These objectives can be achieved through better site orientation, design, material selection, construction, operation, maintenance, transportation, and, to the greatest extent possible, reuse (Yudelson 2010). Today, green buildings, known under various names such as sustainable, ecological, and environmentally friendly, are characterized as structures designed with a holistic understanding that encompasses social and environmental responsibility. They are evaluated within the framework of their lifecycle, starting from site selection, and are tailored to climate data and site-specific conditions. These buildings are designed to be in harmony with their surroundings, consume only what is necessary, harness renewable energy sources, utilize natural and non-waste-generating materials, and exhibit sensitivity to ecosystems (Sur 2012).

According to the Ministry of Development's 2019–2023 Sustainable Management of Environment and Natural Resources report, 52%, or half, of production in 2016 came from fossil fuels (URL 2). These include coal, oil, and its derivatives, as well as natural gas. On the other hand, non-renewable and ecologically hazardous resources make up the remaining 48% of energy sources.

Advantages of Green Building

By adopting sustainable techniques and ecologically friendly design, green buildings provide a number of benefits (Figure 1). The fundamental ideas of energy efficiency and environmental sustainability underpin these advantages. Energy-saving techniques that preserve natural resources include installing air and vapor barriers on building walls and surfaces, installing daylight-controlled lighting systems, installing water-efficient fixtures, and collecting rainwater (URL 3). Furthermore, by recycling and recovering garbage, waste management also follows sustainable principles. Meanwhile, green infrastructure such as green roofs and greenery protects natural ecosystems. Cogeneration and renewable energy sources, such as solar panels and mini wind turbines, can reduce energy reliance and reduce carbon footprint. Water conservation is aided by low-pressure water systems and the recycling of greywater and blackwater. Moreover, ventilation systems, natural lighting, and LED lighting improve energy efficiency. In addition to being environmentally

benign, green construction features save operating costs, improve interior air quality, and raise occupant comfort levels. Green building techniques therefore provide long-term benefits for both the environment and public health (URL 3).



Figure 1. Advantages of Green Building (URL 4)

Benefits of Green Buildings

Green buildings offer significant advantages as environmentally friendly and sustainable structures. These advantages not only facilitate the creation of reliable and healthy living spaces but also reduce energy dependency and provide economic benefits. Additionally, they minimize negative impacts on the environment and enhance worker productivity. In a more detailed examination, green buildings have the following benefits:

- Reliable living spaces are established. Green buildings enhance indoor air quality, providing residents with a healthy living environment.
- Comfortable living spaces are created. Well-designed green buildings offer improved thermal insulation, sound insulation, and natural lighting.
- Reduced dependence on energy sources. Green buildings contribute to sustainable energy usage by promoting energy savings and reducing energy costs.
- Significant reduction in heating expenses. Well-insulated and energy-efficient buildings result in significantly lower heating and cooling costs, with

energy savings reaching up to 70%.

- Minimal environmental impact during construction. Green building construction offers a sustainable approach to minimizing harm to the environment through the selection of materials and optimization of construction processes.

- Excavation waste is repurposed. Green building construction minimizes waste and encourages recycling.

- Purification and utilization of rainwater. Green building design includes systems for the collection, purification, and reuse of rainwater.

- Making use of natural light and solar energy. Renewable energy sources like solar panels and natural lighting are used in green buildings.

- Green buildings lower greenhouse gas emissions, which helps in the fight against climate change.

- Gives local materials more importance. Green building techniques promote the utilization of regional resources, which boosts the regional economy (URL 5).

- Increases worker productivity by up to 16%, positively impacting workplace performance (URL 6).

For these reasons, green building practices offer long-term advantages for both the environment and human health. These benefits are encouraging the increasing prevalence of green building design and construction.

The Most Commonly Used Technologies in Green Buildings

The goal of green buildings is to encourage resource efficiency and lessen environmental effect while adhering to environmental sustainability principles. To achieve this goal, various technologies are integrated into green buildings, such as energy-efficient fluorescent lighting, double-pane glass windows, water-conserving toilets, water-saving faucets, water-saving urinals, motion-activated lighting, LED lighting, geothermal heat pumps, solar panels, energy-efficient hand dryers, exhaust heat recovery systems, airtight entrances, solar daylight tubes, rain gardens, induction lighting, solar water heaters, wind power technology, and gray water systems. Thus, the objectives include energy conservation, water conservation, resource efficiency, improved indoor air quality, and reduced environmental impacts.

Abdallah et al. (2013) focused on the feedback and experiences of personnel implementing green technologies in a study they conducted. Within the scope of this study, Figure 2 illustrates the ranking of green measures implemented in various government buildings based on the reported number of participants (Abdallah et al. 2013). According to the survey participants'

responses, energy efficient fluorescent lighting, double-pane glass windows, water conserving toilets, water conserving faucets, water conserving urinals, motion activated lighting, LED lighting, and geothermal heat pumps are among the most commonly used green technologies. Solar daylight tubes, rain gardens, induction lighting, solar water heaters, wind power technology, and gray water systems, on the other hand, fall within the category of less frequently utilized green technologies.

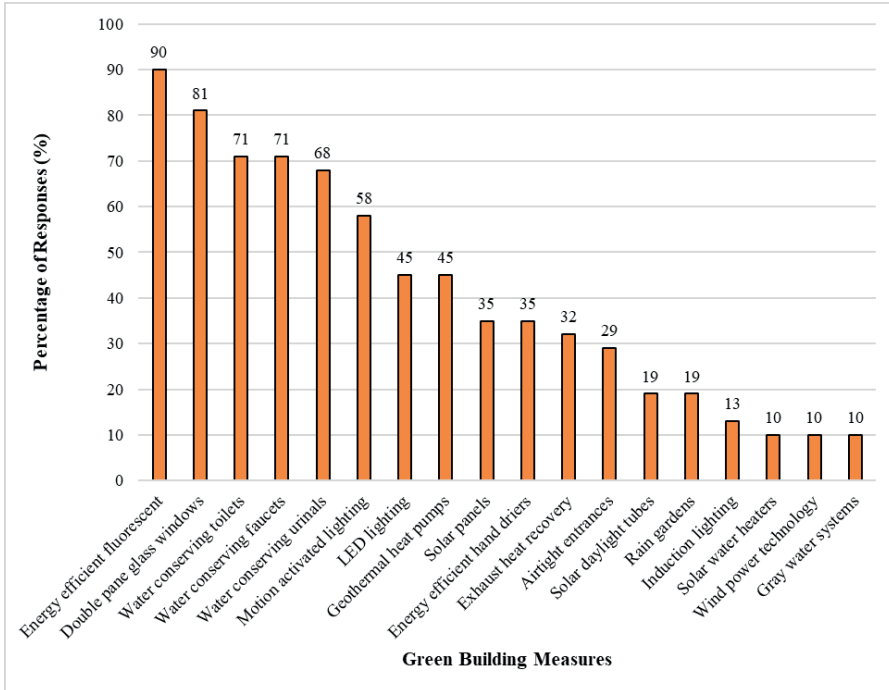


Figure 2. Percentage of Responses Implementing Various Green-Building Measures (Abdallah et al. 2013)

Disadvantages of Green Buildings

Sustainable buildings bring about an increase in investment cost ranging from 1% to 7%. A significant portion of this cost is attributed to specialized architectural design and innovative energy modeling. Additionally, the cost of a sustainable building varies based on the building's location, function, and local climate conditions, in addition to consultancy fees. The earlier sustainable building criteria are incorporated into the design process, the lower the cost becomes. In fact, the financial advantages of a sustainable building far exceed the structure's cost when considering original investment, operating, and maintenance costs. These benefits also show that this situation is not first seen as a disadvantage (URL 7).

However, green buildings may need to meet various specific requirements to directly comply with national regulations in some countries (Wei et al. 2015). In such cases, this may require more planning, monitoring, and cost. Additionally, retrofitting older buildings with green practices may not be practical in some technical and administrative circumstances. Green building technologies are continuously evolving and changing. Therefore, green buildings may require regular updates and improvements (Doan et al. 2017).

What is the Difference of Green Buildings from Other Buildings?

Green buildings exhibit a distinct difference from traditional buildings in terms of environmental and sustainability aspects. High criteria are set for these buildings in areas including indoor air quality, resource efficiency, energy efficiency and water conservation (Seif 2023). Green buildings contribute to energy and resource savings with features like high-quality insulation, energy-efficient lighting, environmentally friendly materials, and renewable energy sources. Moreover, they prioritize health and comfort by enhancing indoor air quality. Subjecting green buildings to certification programs allows for the standardization of these sustainable practices (Seif 2023).

The goals of designing green buildings are to maximize occupant productivity, preserve occupant health, and use energy, water, and other resources effectively. Studies on environmentally friendly buildings have shown that when these buildings are planned and run this way, energy use can be reduced by up to 50%, carbon dioxide emissions by up to 39%, water use by up to 50%, solid waste generation by 70%, and maintenance costs by 13% when compared to average buildings planned and run with traditional methods (URL 8). According to data released by the United States Green Building Council (USGBC), a green building typically uses 32% less power, which results in an annual reduction of 350 metric tons of CO₂ emissions. (URL 8).

Green Building International Certification Systems

Certification systems aimed at reducing the environmental impact of buildings provide an unbiased assessment of a building's effects. The first building certification system was introduced by the Building Research Establishment (BRE) in 1990 in the United Kingdom, known as BREEAM. Following this system, the Leadership in Energy and Environmental Design (LEED) system was established by the United States Green Building Council (USGBC) in 1998. Subsequently, certification systems such as the German Sustainable Building Council (DGNB), Comprehensive Assessment System for Built Environment Efficiency (CASBEE) in Japan, and GREEN STAR in Australia were developed. In addition to these, other countries have also developed their own certification systems in accordance with their standards. Table 1 lists certification systems by country (Gökçen 2020).

Table 1. Certification Systems by Country (Gökçen 2020)

Certificate System	Country
BREEAM	United Kingdom
LEED	United States
DGNB	Germany
CASBEE	Japan
GREEN STAR	Australia
VERDE	Spain
LEED Brasil	Brazil
HQE	France
ESTÍDAMA	United Arab Emirates
BREEAM Netharlands	Netherlands
GREEN Star SA	South Africa
LEED Mexico	Mexico
Teri GRÍHA	India
LEED Canada	Canada
Minergie	Switzerland

Established in the United Kingdom in 1990, the Green Building Certificate, also known as BREEAM (Building Research Establishment Environmental Assessment Method), establishes best practices for buildings' environmental performance in terms of design, specifications, construction, and operation. The first green building evaluation system was developed in 1990 and was called BREEAM. By 1990, it was in use in 77 countries around the Persian Gulf, the United Kingdom, EU, and EFTA (European Free Trade Association) member nations (URL 9). But as time went forward, the LEED Certification in particular became well-known around the world and developed a robust online infrastructure. As a result, BREEAM was still applicable in the UK. With the USGBC, the US Green Building Council, the topic of green building certification became more widely available (URL 9).

The United States Green Building Council created the LEED (Leadership in Energy and Environmental Design) certification for environmentally friendly buildings. The most well-known green construction certification in the world today is the LEED certification, which has been granted since 1998 and is also used in our nation (URL 10). Buildings that have achieved LEED certification are guaranteed to be economically, ecologically, and health-wise designed. Buildings thus consume less energy and water, affect the environment less, and produce healthier, more habitable places. The building's worth is raised by the LEED certification, which also improves the building's international recognition and the standing of the businesses and organizations who constructed it. Buildings that already exist can get certified LEED®. The LEED® for Existing structures certification is awarded to existing structures that have not reached the end of their economic life but nonetheless strive for energy efficiency, health, and low environmental impact (URL 10).

The Australia Green Building Council (GBCA) created the Green Star rating system in 2003 to evaluate buildings for their environmental design and construction (Anbarcı et al. 2012). Green Star measures the environmental potential of a building's design, construction, and management processes under ideal conditions. The Green Star certification system has been created to establish a common language for the environmental assessment of buildings and to increase public awareness to lead to sustainable design, like in other certification systems. As in other certification systems, categories such as energy, emissions, materials, management, indoor environmental quality, land use and ecology, water, and transportation have been defined for assessment. The points collected for these specified categories are multiplied by weighting factors considering the conditions of the region where the assessed building is located. Innovation points are also added to create the final assessment score (Anbarcı et al. 2012).

Casbee is a thorough evaluation system for a building's environmental performance. The Japanese Sustainable Building Consortium first presented Casbee, an environmental labeling system for buildings, in 2004 (Endo et al. 2005). Casbee has developed four assessment tools related to the life cycle of buildings. The collective name for these four tools is 'Casbee Family,' and it is customized for specific purposes. Casbee for Pre-Design, Casbee for New Buildings, Casbee for Renovation, and Casbee for Existing Buildings are the evaluation tools that comprise the Casbee Family. Every tool is made to fulfill a variety of user needs and serve distinct functions (Casbee 2007).

Situation in Turkey

To address this need, Turkey has established the YeS-Tr certification within the scope of 6 international and 2 national certifications. YeS-Tr certification is a system that conducts the certification process online for the national green certification system. It includes information and document entry, review and evaluation stages, and concludes with approval and certification. on June 12, 2022, the Regulation on Green Certification for Buildings and Settlements was published, and a guide for buildings and settlements was released for the **YeS-Tr** certification. According to the guide, the evaluation categories for green buildings are as follows;

- » Integrated Construction Management and Building Design
- » Quality of Indoor Environment
- » Building Materials: Life Cycle Analysis
- » Energy Use and Efficiency
- » Management of Water and Waste
- » Produced by modules of innovation.

The Integrated Building Design and Construction Management module ensures the creation of a delivery process involving all stakeholders for both new and existing buildings, ensuring that the building is designed, constructed, and managed to meet expectations. Indoor environmental quality ensures a healthy indoor environment and comfort. Building material and life cycle support health, comfort, and safety conditions through the use of environmentally friendly materials. Energy use and efficiency provide energy-efficient buildings supported by renewable energy sources. Water and waste management ensure sustainable planning for efficient water use and waste management. The innovation module for the building vision offers innovative solutions that provide users with a high quality of life, as well as social and health benefits (URL 11).

Conclusions

The increasing global population, along with global warming, environmental pollution, water scarcity, and the rapid depletion of natural resources on a global scale, has brought ecological buildings into the construction sector. Consequently, constructions called “green buildings” have surfaced. By promoting sustainability features including resource efficiency, interior environmental quality, and energy efficiency, these structures hope of reducing their negative effects on the environment. The advantages of green buildings include energy and water savings, reduced operating costs, healthier indoor environments, and minimized environmental impacts. However, the construction and maintenance costs of green buildings can be higher than those of conventional buildings, and the rapidly changing nature of green technologies may necessitate updates. While green building practices are becoming increasingly widespread worldwide, countries like Turkey are also promoting sustainable construction practices.

The global proliferation of green buildings encourages more efficient resource utilization and reduced environmental impacts while offering economic and health benefits. Countries like Turkey contribute to this global trend by supporting green building practices and promoting green building projects through local regulations and certification programs. This way, the sustainability of green buildings can be enhanced, and environmental impacts can be reduced. New developments in the construction sector conforming to global standards will play a significant role in preserving natural resources. The importance of certification systems that assess and evaluate buildings reliably and accurately in this regard is increasing. Finally, the most crucial factor in ensuring sustainability is environmental awareness. These certification systems aim not only to promote sustainability but also to increase environmental consciousness among individuals.

REFERENCES

- Abdallah, M., El-Rayes, K., & Liu, L. (2013). Operational Performance of Sustainable Measures in Public Buildings. *Journal of Construction Engineering and Management*, 139(12), A4013008.
- Anbarcı, M., Giran, Ö., & Demir, İ. H. (2012). Uluslararası Yeşil Bina Sertifika Sistemleri ile Türkiye'deki Bina Enerji Verimliliği Uygulaması (in Turkish). *Engineering Sciences*, 7(1), 368-383.
- Casbee, (2007). Comprehensive Assessment System for Built Environment Efficiency. CASBEE for Urban Development: Technical manual 2007 Edition.
- Doan, D. T., Ghaffarianhoseini, A., Naismith, N., Zhang, T., Ghaffarianhoseini, A., & Tookey, J. (2017). A Critical Comparison of Green Building Rating Systems. *Building and Environment*, 123, 243-260.
- Endo, J., Murakami, S., Ikaga, T., Iwamura, K., Sakamoto, Y., Yashiro, T., and Bogaki, K. (2005) Extended Framework Of Casbee; Designing An Assessment System Of Buildings For All Lifecycle Stages Based On The Concept Of Eco-Efficiency, The 2005 World Sustainable Building Conference, Tokyo.
- Gezen, A. F. (2015). İnşaat Sektöründe Sürdürülebilir Kent Yaşamı ve Karayollarında Uygulama Alanları. Beykent Üniversitesi, Fen Bilimleri Enstitüsü, İnşaat Mühendisliği Ana Bilim Dalı, Yüksek Lisans Tezi, Bursa (In Turkish).
- Gökçen, T. (2020). Yeşil Bina Sertifikasyon Sistemlerinde Yapı Malzemesi Alt Kategorisinin Araştırılması ve Türkiye'deki Durum. Bursa Uludağ Üniversitesi, Fen Bilimleri Enstitüsü, Mimarlık Anabilim Dalı, Yüksek Lisans Tezi, Bursa (In Turkish).
- Komnitsas, K. A. (2011). Potential of Geopolymer Technology Towards Green Buildings and Sustainable Cities. *Procedia Engineering*, 21, 1023-1032.
- Pitt, M., Tucker, M., Riley, M., & Longden, J. (2009). Towards Sustainable Construction: Promotion and Best Practices. *Construction Innovation*, 9(2), 201-224.
- Seif, H. A. (2023). Review on the Interrelations Between Commissioning and Green Buildings Contributed to Energy Savings. 7th International Conference on Applied Researches in Science and Engineering.
- Sur, H. (2012). Çevre Dostu Yeşil Binalar, Yeşil Binalar Referans Rehberi, İstanbul (In Turkish).
- URL 1 Ekolojist.com (in Turkish) Website [Online].
<https://www.ekolojist.com/ekoloji-ve-yasam/surdurulebilir-mimari-nedir/>
- URL 2 T.C. Kalkınma Bakanlığı, on Birinci Kalkınma Planı (2019-2023) (in Turkish)
https://www.sbb.gov.tr/wp-content/uploads/2020/04/Cevre_ve_DogalKaynaklarınSurdurulebilirYonetimiCalismaGrubuRaporu.pdf
- URL 3 (2019) Çevre Bilinci Platformu (in Turkish) Website [Online].

(<http://www.cevrebilinci.com/yesil-bina-nedir/>

URL 4 (2013) Bam Website [Online].

<https://sustainability.bam.co.uk/insights/2013-09-20-greener-buildings-better-places-healthier-people>

URL 5 (2018) Malzeme Bilimi.Net (in Turkish) Website [Online].

<https://malzemebilimi.net/yesil-bina-nedir-faydalari-nelerdir.html>

URL 6 (2023) Green Building Industry Statistics [Fresh Research] Website [Online].

<https://blog.gitnux.com/green-building-industry-statistics/>

URL 7 (2012) Sürdürülebilir Mimari (in Turkish) Website [Online].

<http://surdurulebilir-mimari.blogspot.com/2012/08/surdurulebilir-binalarn-avantajlar-ve.html>

URL 8 (2020) Baret Dergisi (in Turkish) Website [Online].

<https://www.baretdergisi.com/yesil-binalarin-diger-binalardan-farki-nedir/18420/>

URL 9 (2020) ECOBUILD Website [Online].

<https://www.ecobuild.com.tr/post/2019/08/20/breem-sertifikas-c4-b1-nedir>

URL 10 (2019) ECOBUILD Website [Online].

<https://www.ecobuild.com.tr/post/2019/08/10/leed-sertifikas-c4-b1-nedir>

URL 11 (2023) T.C. Çevre, Şehircilik ve İklim Değişikliği Bakanlığı (in Turkish) Website [Online]. <https://yestr.csb.gov.tr>

Wei, W., Ramalho, O., & Mandin, C. (2015). Indoor Air Quality Requirements in Green Building Certifications. *Building and Environment*, 92, 10-19.

Yudelson, J. (2010). *The Green Building Revolution*, Island Press, Washington.

Zhang, L., Wu, J., & Liu, H. (2018). Turning Green into Gold: A Review on the Economics of Green Buildings. *Journal of Cleaner Production*, 172, 2234-2245.

Chapter 18

A MACHINE LEARNING BASED RECEIVER SCHEME FOR VARIABLE ON-OFF KEYING MODULATION TECHNIQUE

Methmet SÖNMEZ¹

¹ Doç. Dr., Osmaniye Korkut Ata Üniversitesi, Mühendislik Fakültesi, Elektrik-Elektronik Mühendisliği Bölümü

1. Introduction

The VLC systems have been investigated from many researchers since they can support very high speed data transmission when consider the hybrid communication systems (Hu et al., 2023; Shukla et al., 2022; Zhang, et al., 2023). Specifically, it is considered that VLC is a preferable indoor communication technology because it supports both the data transmission and the lighting at the same time (Inn et al., 2023; Younus and Hussein, 2021). Therefore, optical communication technologies must serve major options such as variable dimming level in the future. The target dimming level can ensure both an effective user connection and a requested lighting level. In this context, it seems important to adjust the dimming level in VLC systems.

Due to providing both lighting and data transmission at the same time, the majority of dimming methods have been investigated in VLC systems (Belli et al., 2022; Guo et al., 2020; Yoo et al., 2015; Zhu and Zhang, 2020). The brightness of LEDs can usually be adjusted using two techniques, typically through digital and analog methods (Yang et al., 2017; Zafar et al., 2015a). The analog dimming methods are used to change signal amplitude while digital dimming techniques are achieved adjusting duty cycle of the modulated signal. In the literature, adjusting the brightness of LEDs using digital dimming techniques has better performance compared to analog dimming methods because it can be asserted that the change in brightness is much more linear with digital dimming (Feng et al., 2018; Zafar et al., 2015b).

The VLC technologies have utilized many modulation methods to provide data transmission via optical links (Lee and Park, 2011; Li et al., 2013; Salmento et al., 2019; Sönmez, 2018; Yoo et al., 2015). Additionally, these transmission methods can be employed to adjust LED brightness for indoor systems. Since wireless data sharing and network systems have been expanding exponentially, modulation schemes used in VLC links have been investigated in terms of data rate, spectrum efficiency (Li et al., 2019), energy efficiency (Kumari and Arya, 2023), and complexity (Miriayala and Mani, 2021). With the promise of the sixth generation (6G)/VLC, higher efficiency will be achieved, where it can be considered recent optical technologies as a complementary technology in the scope of a heterogeneous wireless communication networking system (Sharma and Jha, 2022). Specifically, these wireless technologies will provide the transmission for extremely high data

rate services, where there are requirements for a substantial communication bandwidth (Bravo et al., 2023).

One of these methods is Pulse Amplitude Modulation (PAM). Although the PAM scheme allows multilevel data transmission (Belli et al., 2022), it can support the binary level data transmission that is referred to as On-Off Keying (OOK) (X. Li et al., 2019; Sönmez, 2020). This modulation scheme is spectrum-efficient technique when compared with other methods (Mahdiraji and Zahedi, 2006). However, the mobility supporting is very complex in Multilevel PAM systems. This is because M-PAM consists of many threshold levels. To ensure the variable dimming support, the Pulse Width Modulation (PWM) scheme is employing for OOK and Pulse Position Modulation (PPM) that is a position-based transmission scheme (Lee and Park, 2011; Ozaki et al., 2014). The modified modulation schemes are defined as VOOK (Variable OOK) and VPPM (Variable PPM), respectively.

In VLC technology, the machine learning and the deep learning schemes have been widely used to the threshold detection (Ayten and Sönmez, 2021), the modulation classification (Ağır and Sönmez, 2023), the design of equalizer (Chen et al., 2021; Pouralizadeh, Baghersalimi, et al., 2022; Rajalakshmi, et al., 2023), the reducing of signal distortion (Lin, et al., 2021), indoor positioning (Wang and Shen, 2019), and etc. Specifically, the SVM method has been used to detect the threshold level of received signal and classify the modulation order of PPM signals (Ağır and Sönmez, 2023; Yuan et al., 2017). In the literature, a SVM based receiver scheme has been employed for 8-Superposed Pulse Amplitude Modulation (8-SPAM) scheme (Yuan et al., 2017). The results have been obtained by considering the data transmission rate. Another paper focused on modulation classification by using machine learning techniques such as K-nearest neighbor (KNN), SVM and Decision Tree Model (Ağır and Sönmez, 2023). Moreover, the SVM method was used for signal detection and Light Emitted Diode (LED) selection for generalized spatial modulation scheme (Sun, et al., 2021; Zhang et al., 2021). Addition to these, IoT (Internet of Things)-VLC systems consist of SVM based receiver structure in the literature (Khadr et al., 2021).

As mentioned above, many papers focused on SVM based receiver scheme, including the detecting, the estimation and the classification. Furthermore, the threshold detection for OOK transmission scheme has been investigated

in the literature (Li et al., 2016; Li et al., 2017; Sönmez, 2020). In this paper, the main objective is summarized as follows:

- A threshold detection method is implemented on VOOK transmission scheme. The BER performance of receiver system is investigated by considering the distance between receiver and transmitter under user mobility condition.
- A data transmission structure is employed to detection threshold using the machine learning techniques including SVM and Tree models. This transmission scheme consists of a calibration signal which is used to classify the logical levels by the SVM and Tree.

The calibration signal may include either full filled slot or signal with target dimming level. Therefore, a comparison of BER performance is obtained by using two calibration signals. In these cases, it is investigated which the threshold is being level. Addition to these, it is given a comparison between traditional system and ML based receiver schemes.

2. VOOK Scheme

In this paper, we give the VOOK transmission method which provides the dimming supporting for the VLC systems. The VOOK transmission method is achieved by implementing of PWM technique on OOK scheme. While the pulse width of filled slot is regulated by PWM, the logical level of modulated signal is determined by the OOK scheme. The disadvantage of amplitude based transmission method is required a detection threshold method to estimate the logical level of received signal. Specifically, it is very crucial under mobility condition which causes dynamic threshold level since the distance between receiver and transmitter is changing.

The bandwidth efficiency of VOOK-VLC system can be decreased while the PWM method provides an advantage in terms of adjusting of brightness level. Moreover, the BER performance of VOOK-VLC system is decreasing while the target dimming level is moving away from 50% of dimming level. Hence, transmission performance further falls when compared to traditional OOK scheme that is 50% of average dimming level. In Fig. 1, it can be shown VOOK signal versus bit time. According to the figure, each bit period is divided by 10 slots to detect the transition of VOOK signal. The number of filled slot is equal to 6 for data bit '1' under 30% dimming level of VOOK signal. For data bit '0', all slots are empty. Under 70% of dimming level, the all slots are filled for data bit '1'

while the number of filled slot is equal to 4. Hence, the term of average dimming level can be used for the VOOK transmission scheme. The average dimming level for VOOK scheme can be expressed by,

$$\delta = \frac{1}{2} \frac{(d_0 + d_1)}{S_n} \quad (1)$$

where, δ is dimming level of VOOK signal. The d_0 and d_1 are explained as the number of filled slot for data bit '0' and data bit '1', respectively. For instance, the number of filled slot is equal to 10 for 70% of dimming level while the VOOK signal fills 4 slots.

We define the VOOK signal as follows:

$$s(t) = \sum_{i=-\infty}^{\infty} d_i g(t - iT_b) \quad (2)$$

where, $d_i T_b$ and $g(t)$ are expressed as binary codeword, bit time, and a basis function of which duty cycle can be adjusted by considering target dimming level, respectively. A framework of VOOK signal can be given by taking into account two cases: Firstly, the dimming level is 50% or lower. Other case is more than 50% of brightness level.

First Case: The dimming level is 50% or lower:

In this case, the basis function can be defined by considering the target dimming level. According to Table 1, the duty cycle of Logical '1' and Logical '0' levels can be changed according to target dimming level. The basis function $g(t)$ can be given by,

$$g(t) = \text{rect}\left(\frac{t - \delta T_b}{2\delta T_b}\right) \quad (3)$$

where, δ can be expressed as target dimming level of VOOK signal. The width of filled slot is equal to twice of δT_b as shown in the Table 1.

Second Case: The dimming level is more than 50%:

According to the table of VOOK codeword, both data bit '1' and data bit '0' consists of filled slot under more than %50 dimming level. Hence, the VOOK

signal can be defined by considering conditions of these two logical levels.

$$g(t) = \underbrace{(1-d_i) \operatorname{rect}\left(\frac{t-(1-\delta)T_b}{2(1-\delta)T_b}\right)}_{\text{Part-1}} + \underbrace{\operatorname{rect}\left(\frac{t-(\delta-\frac{1}{2})T_b}{(2\delta-1)T_b}\right)}_{\text{Part-2}} \quad (4)$$

In this case, we define the VOOK signal by considering two parts. The part-1 shows filled slot for data bit '1' in which the all slots of VOOK signal are filled as logical '1'. If the optical received VOOK signal is expressed by $y(t)$, it is given as follows:

$$y(t) = s(t) \otimes h(t) + n(t) \quad (5)$$

where, ' \otimes ' is defined as convolution operator. The $h(t)$ and $n(t)$ denote the impulse response of optical channel and noisy signal.

After the received signal is passed through the integral processing, it is applied on SVM input to train the learning system. The trained SVM system can detect the data signal from received VOOK signal. At the receiver side, we can define the output of integrator as follows (Lee and Park, 2011):

$$I(t) = \int_0^{2\delta T_b} y(t) dt \quad ; \quad \text{if } \delta \leq 0.5$$

$$I(t) = \int_0^{2(1-\delta)T_b} y(t) dt \quad ; \quad \text{if } \delta > 0.5 \quad (6)$$

where, $I(t)$ is output of integral block. According to the Eq. (6), the output of integrator is given by considering the the dimming level of received VOOK signal. In training stage, we apply the $I(t)$ to the SVM system. Afterwards, a threshold level is determined by SVM to detect the data bits.

Table 1. Codewords for VOOK scheme according to dimming level (δ)

δ (%)	VOOK codeword
1	1111111111
0.9	dd11111111
0.8	ddd1111111
0.7	dddd111111
0.6	dddddd1111
0.5	ddddddddd
0.4	ddddddd00
0.3	dddddd0000
0.2	ddd000000
0.1	dd0000000
0	000000000

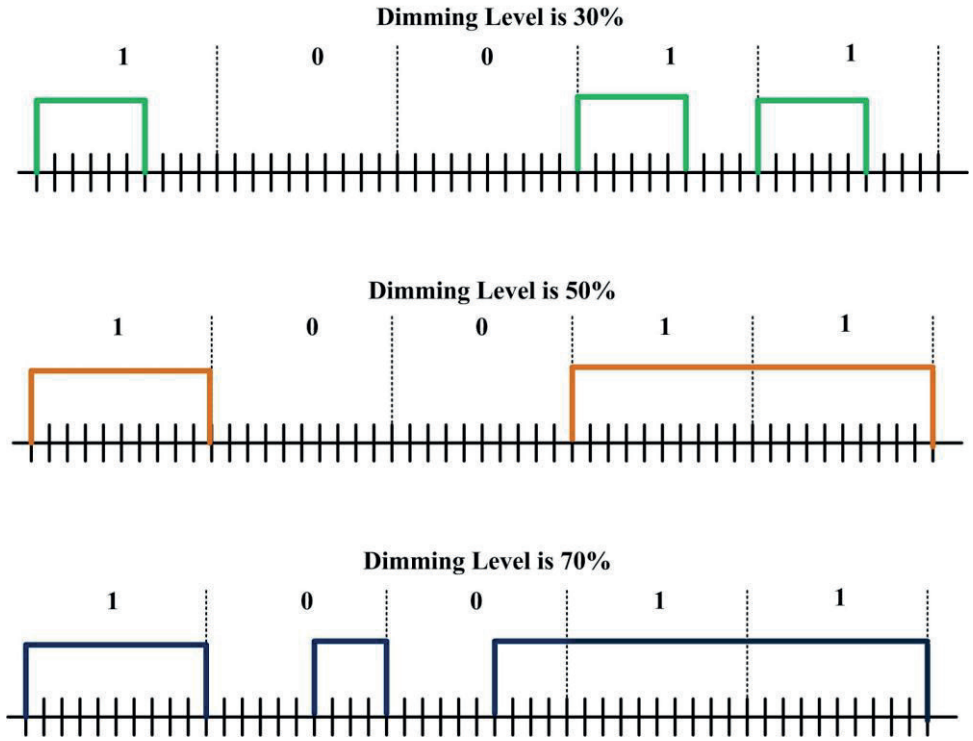


Figure 1. The changing of VOOK signal according to time under variable dimming levels

3. Machine Learning Based Demodulator

In the literature, machine learning based systems has been attracted attention from many researchers since variable conditions can't be severally modelled. Hence, a prediction can be computed by using Machine learning systems after a learning process. In this section, we give SVM technique and Tree model based demodulator architecture for VOOK signal.

It is considered an indoor communication media and a user that is a mobility condition. Because of mobility condition, transmitted signal has variable power at the receiver side. Under the case of using position based modulation schemes such as PPM method, the variable power at the receiver side don't effect the demodulation process due to waveform of position based signal. However, the power level of received signal is very crucial where modulation methods that require a threshold level have been employed. In particular, OOK scheme that allows data transmission at logical '1' and logical '0' levels requires using of a variable threshold level at the receiver side. It must be used an adaptive threshold system since variable OOK scheme is one of types of OOK techniques. The adaptive threshold system can be designed by using Machine Learning Methods such as Support Vector Machine, and Tree model.

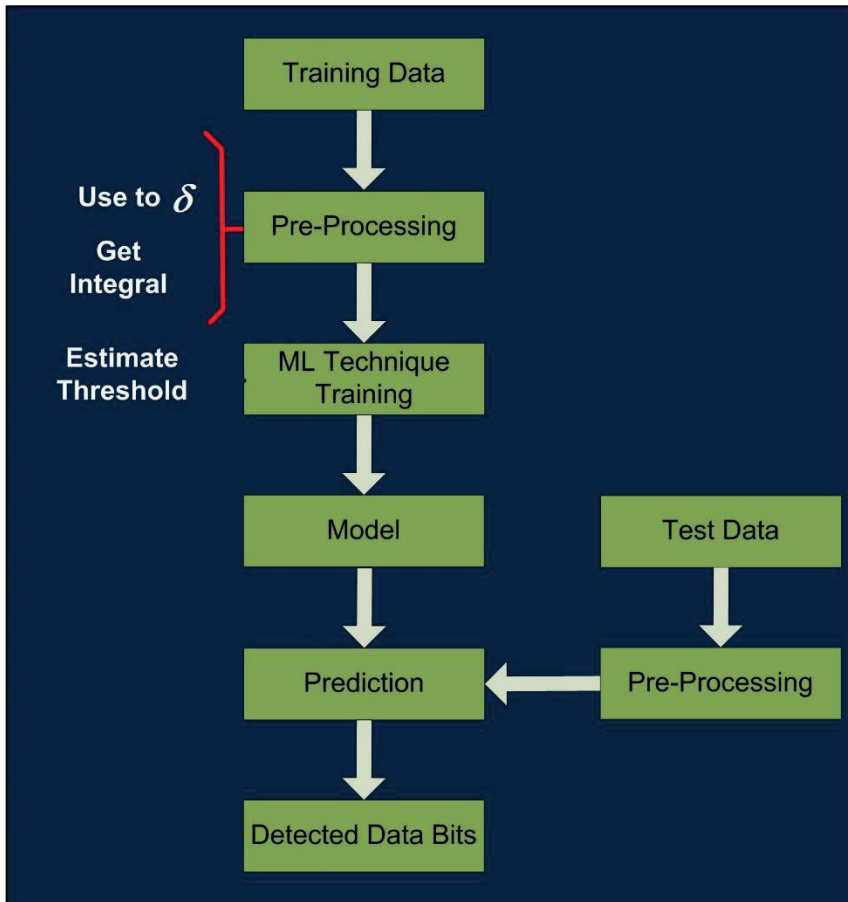


Figure 2. A flowchart for Machine Learning Based Receiver

Fig. 2 gives a flowchart for machine learning based receiver model to present the design of VOOK demodulator scheme. Training data is applied for learning stage before pre-processing level that consists of an integration process. It is required the dimming level information of VOOK signal to get the integral because the dimming level of received VOOK signal determines the boundary of integral operation. To detect data bits received signal by using estimated threshold value, test data is firstly applied to Pre-processing stage where received signal is passed through an integrator. The optimum threshold value can be obtained for distance between receiver and transmitter by using machine learning techniques. The received signal consists of two amplitude level: logical '0' and logical '1'. Hence, it is necessary to detect a threshold value that can separate the logical '1' and logical '0' levels.

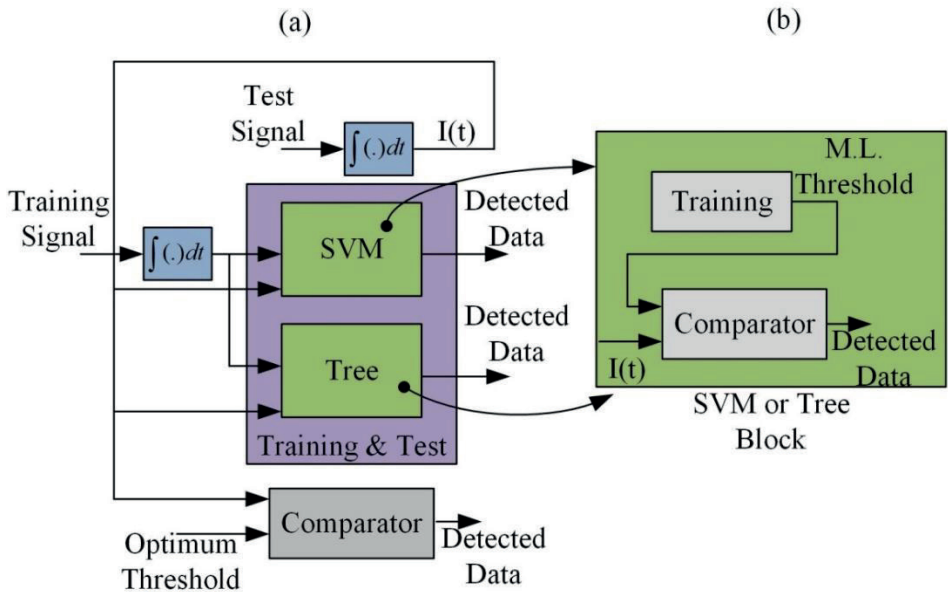


Figure 3. ML based VOOK demodulator

The Fig. 3 demonstrates a block scheme to represent the ML based VOOK demodulator. It can be reported that the training signal aids to estimate the threshold level of VOOK signal for the first time. The detected threshold, which is referred to as M.L. Threshold in the figure, is implemented to SVM or Tree blocks to detect the data signal from received Test Data. Optimum threshold is determined by traditional technique. It can be considered that optimum threshold is equal to mean of filled and empty slot. By using Eq. (6), the optimum threshold can be defined follow as:

$$\begin{aligned}
 th &= A\delta Tb \quad ; \quad \text{if } \delta \leq 0.5 \\
 th &= A(1-\delta)Tb \quad ; \quad \text{if } \delta > 0.5
 \end{aligned}
 \tag{7}$$

where, th is threshold level for VOOK receiver. In the equation, A can be defined as peak value of received VOOK signal at the any distance between receiver and transmitter. It is assumed that VOOK is noiseless signal at the output of photodiode for this threshold value. However, we apply the modulated signal with noise for classification under training stage.

4. Simulation Results

In this section, it is introduced simulation results by using main simulation results that are given in Table 2. As mentioned previous section, SVM and Tree methods that are defined as machine learning techniques are applied to VOOK receiver scheme to demodulate received signal. It can be characterized as a basic demodulator scheme since the improved receiver structure has based on logical '0' and logical '1' levels. We obtained the simulation results by taking into account dimming levels of 30%, 40%, and 50% because modulated signal at 30% and 40% of dimming levels has same BER performance as signals at 70% and 60% dimming levels, respectively. In the simulation results, it is employed Tree and SVM algorithms as machine learning techniques. Addition to this, a traditional receiver scheme that have optimum threshold value is used to compare with machine learning methods. Other scheme is referred to as traditional scheme that uses threshold value for the distance of 2.35m.

Table 2. Main Simulation Parameters

Parameters	Values
Room Dimension	5x5x3m
Semiangle Half Power	60°
Order of the Lambertian emission	1
Physical area of the PD	0.0001 m ²
Optical filter gain of the PD	1
Concentrator gain of the PD	2.548
Field of View (FOV) Angle of the PD	70°
Semiangle Half Power	70°

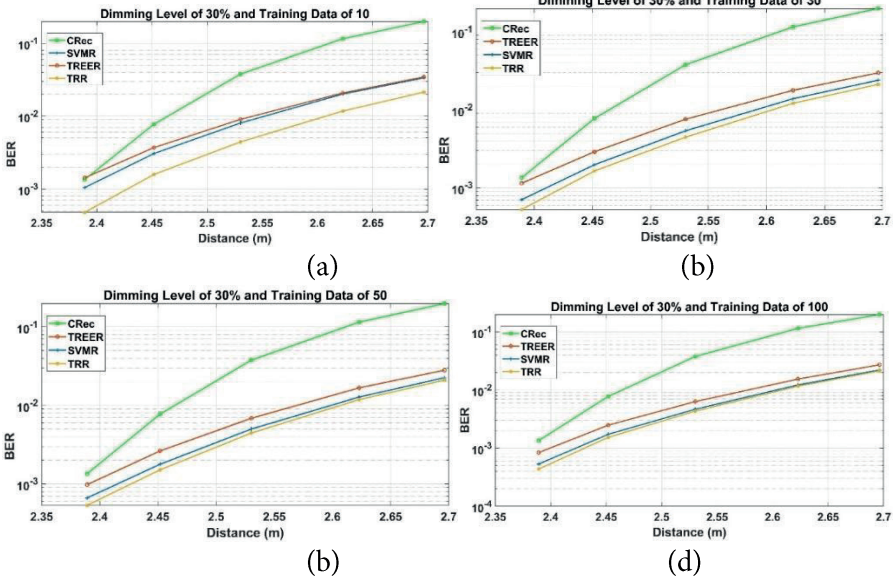


Figure 4. Simulation results for dimming level of 30%

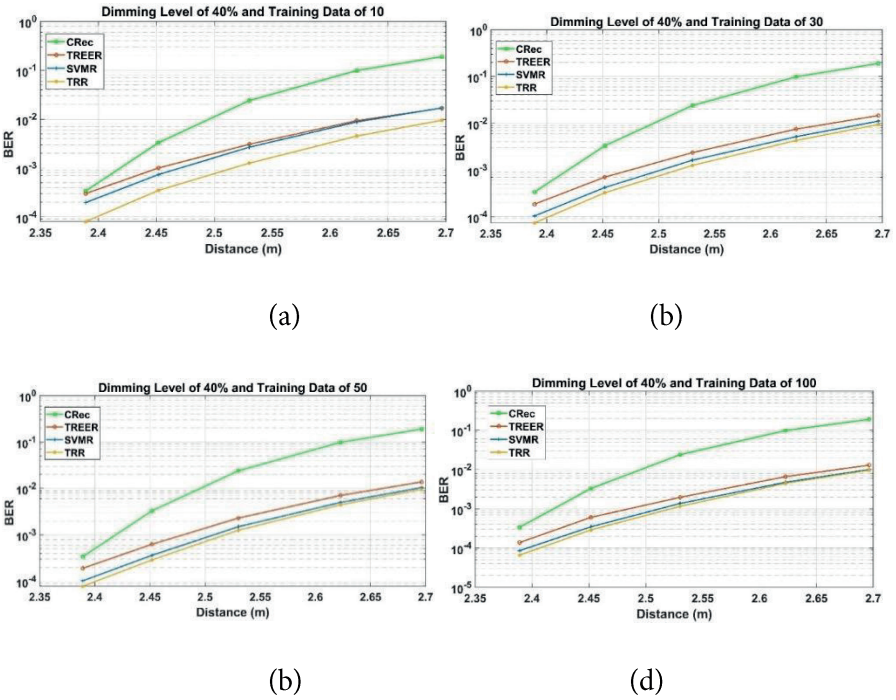


Figure 5. Simulation results for dimming level of 40%

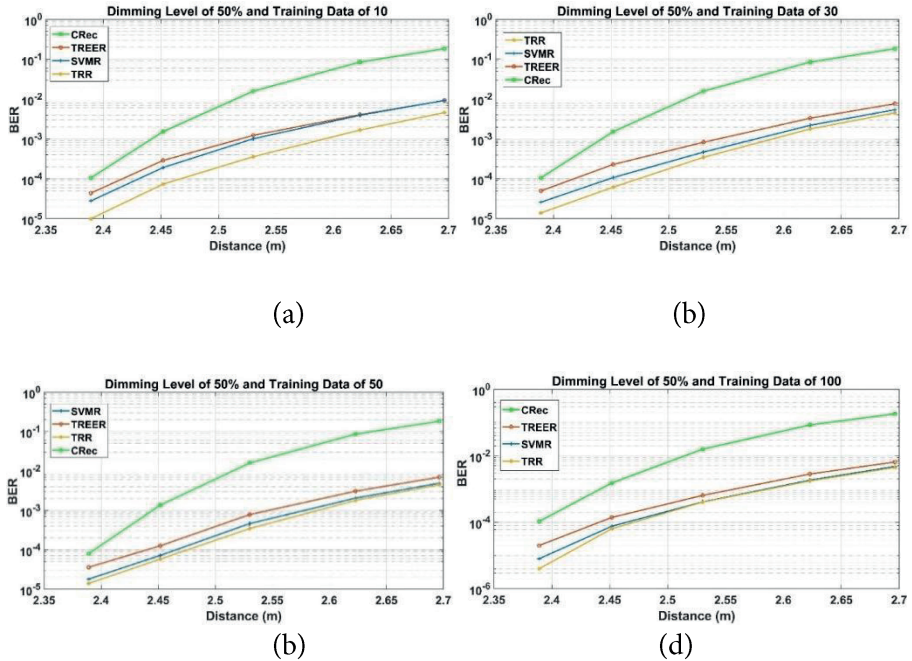


Figure 6. Simulation results for dimming level of 50%

Other performance comparison is obtained by considering the variable training data set. Training data of 10, 30, 50, and 100 is used to observe the BER performances of Tree and SVM algorithms under variable distance between receiver and transmitter. In Figure 4, simulation results are obtained at 30% of dimming level by considering variable training data size. The CRec represents traditional receiver that uses threshold value for distance of 2.35m. According to simulation results, TRR has the best performance compared with others since this scheme has optimum threshold value for all distances between transmitter and receiver. The SVMR which referred to as SVM based receiver gives better BER performance than that of Tree-based receiver model TREER. It is shown from simulation results that the BER performance is increasing while the training data size is extended. Similar BER performances are obtained from 40% and 50% of dimming levels that are given in Figure 5 and Figure 6, respectively. TRR method gives lower BER than that of others for both 40% of dimming level and 50% of dimming level. Addition to this, the SVM technique is superior when compared with Tree model.

When evaluated aspect of dimming level of received signal, it is shown that the duty cycle is crucial for BER performance of VOOK transmission method. The best BER performance is obtained at the 50% of dimming level. It is illustrated that the performance is gradually increasing while dimming level is approaching to 50%. The simulation results show machine learning based receiver models is preferable methods in terms of variable threshold level when compared to traditional method that uses static threshold level.

5. Conclusion

It is expected that visible light communication system has low power communication technology due to usage of prominent LED lighting systems. Addition to this, power consumption can be maintained by using modulation method that adjusts LED brightness. The VOOK transmission method is one of these dimmable modulation schemes. Hence, this chapter has reported a threshold challenges under user mobility condition. The detected threshold level must be chosen very close to optimum threshold level that cannot obtain for experimental system since BER performance of VOOK method can be target limits. Therefore, it is shown that machine learning based receiver models can be given acceptable results in terms of BER performance of VOOK technique. Specifically, simulation results have illustrated that the threshold level can be effected from the type of Machine Learning method. It is observed that SVM-based ML method has better BER performance than that of Tree-based technique for design of VOOK receiver. In future, it is considered that ML methods will be widely used to solve many challenges in experimental visible light communication systems.

REFERENCES

- Ağır, T. T., & Sönmez, M. (2023). The modulation classification methods in PPM-VLC systems. *Optical and Quantum Electronics*, 55(3), 223.
- Ayten, K., & Sönmez, M. (2021). Threshold detection and slot clustering algorithms in DPIM-VLC systems. *Optik*, 248, 168085.
- Belli, R., Runge, C., Portugheis, J., & Finamore, W. (2022). A capacity-approaching coding scheme for M-PAM VLC systems with dimming control. *Optics Communications*, 509, 127891.
- Bravo Alvarez, L., Montejo-Sánchez, S., Rodríguez-López, L., Azurdia-Meza, C., & Saavedra, G. (2023). A Review of Hybrid VLC/RF Networks: Features, Applications, and Future Directions. *Sensors*, 23(17), 7545.
- Chen, H., Niu, W., Zhao, Y., Zhang, J., Chi, N., & Li, Z. (2021). Adaptive deep-learning equalizer based on constellation partitioning scheme with reduced computational complexity in UVLC system. *Optics Express*, 29(14), 21773-21782.
- Feng, Z., Guo, C., Ghassemlooy, Z., & Yang, Y. (2018). The Spatial Dimming Scheme for the MU-MIMO-OFDM VLC System. *IEEE Photonics Journal*, 10(5), 1-13.
- Guo, J.-N., Zhang, J., Zhang, Y.-Y., Li, L., Zuo, Y., & Chen, R.-H. (2020). Multilevel transmission scheme based on parity check codes for VLC with dimming control. *Optics Communications*, 467, 125733.
- Hu, Q., Gan, C., Liu, X., Gong, G., & Zhu, Y. (2023). Dynamic handover cost modeling in hybrid VLC/RF networks. *Ad Hoc Networks*, 146, 103174.
- Inn, A., Hassan, R., Hasan, M. K., Latiff, L. A., & Deriche, M. (2023). Analyzing the maximum angle of light-emitting diodes for indoor visible light communication. *Electronics Letters*, 59(18), e12951.
- Khadr, M. H., Walter, I., Elgala, H., & Muhaidat, S. (2021). Machine Learning-Based Massive Augmented Spatial Modulation (ASM) for IoT VLC Systems. *IEEE Communications Letters*, 25(2), 494-498.
- Kumari, M., & Arya, V. (2023). Integrated long reach and energy-efficient NGPON-VLC system with OCDM/WDM for smart green buildings. *Optik*, 289, 171280.
- Lee, K., & Park, H. (2011). Modulations for Visible Light Communications With Dimming Control. *IEEE Photonics Technology Letters*, 23(16), 1136-1138.
- Li, H., Huang, Z., Xiao, Y., Zhan, S., & Ji, Y. (2019). A Power and Spectrum Efficient NOMA Scheme for VLC Network Based on Hierarchical Pre-Distorted LACO-OFDM. *IEEE Access*, 7, 48565-48571.
- Li, J. F., Huang, Z. T., Zhang, R. Q., Zeng, F. X., Jiang, M., & Ji, Y. F. (2013). Superposed pulse amplitude modulation for visible light communication. *Optics Express*, 21(25), 31006-31011.

- Li, S., Pandharipande, A., & Willems, F. M. J. (2016). Unidirectional Visible Light Communication and Illumination With LEDs. *IEEE Sensors Journal*, 16(23), 8617-8626.
- Li, S., Pandharipande, A., & Willems, F. M. J. (2017). Adaptive visible light communication LED receiver. *2017 IEEE SENSORS*, 1-3. Glasgow: IEEE.
- Li, X., Min, C., Gao, S., Sun, G., Chen, X., & Chen, H. (2019). A CDMA-based high-speed multi-access VLC system with OOK modulation. *Optics Communications*, 451, 147-152.
- Lin, B., Lai, Q., Ghassemlooy, Z., & Tang, X. (2021). A Machine Learning Based Signal Demodulator in NOMA-VLC. *Journal of Lightwave Technology*, 39(10), 3081-3087.
- Mahdiraji, G. A., & Zahedi, E. (2006). Comparison of Selected Digital Modulation Schemes (OOK, PPM and DPIM) for Wireless Optical Communications. *2006 4th Student Conference on Research and Development*, 5-10.
- Miriyala, G., & Mani, V. V. (2021). A nonlinear modelled low-complex ADO-OFDM for Visible light communication systems. *Optik*, 246, 167831.
- Ozaki, T., Kozawa, Y., & Umeda, Y. (2014). Variable multi-pulse PPM using new dimming control method for visible light communications. *2014 International Symposium on Information Theory and its Applications*, 80-84.
- Pouralizadeh, A., Baghersalimi, G., Ghassemlooy, Z., & Nassiri, M. (2022). Performance improvement of a CAP VLC system employing a deep learning-based post equalizer. *Optics Communications*, 524, 128741.
- Rajalakshmi, R., Pothiraj, S., Mahdal, M., & Elangovan, M. (2023). Adaptive Fuzzy Logic Deep-Learning Equalizer for Mitigating Linear and Nonlinear Distortions in Underwater Visible Light Communication Systems. *Sensors*, 23(12), 5418.
- Salmento, M. L. G., Soares, G. M., Alonso, J. M., & Braga, H. A. C. (2019). A Dimmable Offline LED Driver With OOK-M-FSK Modulation for VLC Applications. *IEEE Transactions on Industrial Electronics*, 66(7), 5220-5230.
- Sharma, H., & Jha, R. K. (2022). VLC Enabled Hybrid Wireless Network for B5G/6G Communications. *Wireless Personal Communications*, 124(2), 1741-1771.
- Shukla, N. K., Mayet, A. M., Vats, A., Aggarwal, M., Raja, R. K., Verma, R., & Muqet, M. A. (2022). High speed integrated RF-VLC data communication system: Performance constraints and capacity considerations. *Physical Communication*, 50, 101492.
- Sönmez, M. (2018). Simplified and accelerated PPM receivers for VLC systems. *IET Optoelectronics*, 12(1), 36-43.
- Sönmez, M. (2020). Artificial neural network-based threshold detection for OOK-VLC Systems. *Optics Communications*, 460, 125107.

- Sun, H., Zhang, Y., Wang, F., Zhang, J., & Shi, S. (2021). SVM Aided Signal Detection in Generalized Spatial Modulation VLC System. *IEEE Access*, 9, 80360-80372.
- Wang, X., & Shen, J. (2019). Machine Learning and its Applications in Visible Light Communication Based Indoor Positioning. *2019 International Conference on High Performance Big Data and Intelligent Systems (HPBD&IS)*, 274-277. Shenzhen, China: IEEE.
- Yang, Y., Zeng, Z., Cheng, J., & Guo, C. (2017). A Novel Hybrid Dimming Control Scheme for Visible Light Communications. *IEEE Photonics Journal*, 9(6), 1-12.
- Yoo, J., Kim, B. W., & Jung, S. (2015). Modelling and analysis of M-ary variable pulse position modulation for visible light communications. *IET Optoelectronics*, 9(5), 184-190.
- Younus, S. H., Al-Hameed, A. A., & Hussein, A. T. (2021). Novel handover scheme for indoor VLC systems. *IET Communications*, 15(8), 1053-1059.
- Yuan, Y., Zhang, M., Luo, P., Ghassemlooy, Z., Lang, L., Wang, D., Han, D. (2017). SVM-based detection in visible light communications. *Optik*, 151, 55-64.
- Zafar, F., Kalavally, V., Bakaul, M., & Parthiban, R. (2015). Experimental investigation of analog and digital dimming techniques on photometric performance of an indoor Visible Light Communication (VLC) system. *Fourteenth International Conference on Solid State Lighting and LED-based Illumination Systems*, 9571, 59-66. SPIE.
- Zafar, F., Karunatilaka, D., & Parthiban, R. (2015). Dimming schemes for visible light communication: The state of research. *IEEE Wireless Communications*, 22(2), 29-35.
- Zhang, F., Wang, F., Zhang, J., & Zuo, T. (2021). SVM aided LEDs selection for generalized spatial modulation of indoor VLC systems. *Optics Communications*, 497, 127161.
- Zhang, W., Zhao, X., Zhao, Y., & Sun, J. (2023). On security performance analysis of IRS-aided VLC/RF hybrid system. *Physical Communication*, 61, 102176.
- Zhu, J., Mu, L., & Zhang, X. (2020). PWM-based dimmable hybrid optical OFDM for visible-light communications. *IET Communications*, 14(6), 930-936.



Chapter 19

A COMPREHENSIVE REVIEW ON THE DESIGN AND PERFORMANCE OF SOLAR DRYING METHODS

Mesut YAZICI¹

Ramazan KÖSE²

1 Kutahya Dumlupinar University, Faculty of Simav Technology, Mechanical Engineering, Kutahya, Turkiye, mesut.yazici@dpu.edu.tr, ORCID ID: 0000-0001-6379-8396

2 Kutahya Dumlupinar University, Faculty of Engineering, Mechanical Engineering, Kutahya, Turkiye, ramazan.kose@dpu.edu.tr, ORCID ID: 0000-0001-6041-6591

1. INTRODUCTION

Drying is a process that consumes very high amounts of energy. Many sectors, especially food, benefit from the drying. In recent years, negative situations such as pandemics, natural disasters, wars, and regional conflicts have caused disruptions in the supply chain on a global scale. The areas most affected by these disruptions were the food and energy sectors. So much so that the difficulties experienced in these sectors have placed the concepts of energy and food supply security at the focal point of governments and scientific circles in every country of the world.

Drying is defined as the removal of water from a solid, liquid, or gas. Drying food products means reducing the moisture level in them to a level where microbial activities will not occur. Food drying has been one of the most preferred food preservation methods from ancient times to the present. This method has been adopted so much that, in addition to basic food products, various food products are also dried.

Fresh vegetables and fruits, which are food products, should be consumed within a short time after harvesting. Otherwise, spoilage such as rotting and mold may occur in food products. If a very high amount of product is harvested during harvest periods, the market price is low. In this case, if these products are dried, their deterioration will be prevented and their value in the market will increase even more in their dried form. Drying reduces the volume of food products. Thus, there is a decrease in storage and transportation costs. In addition, the color of dried products may change and their nutritional value may decrease. On the other hand, it is desired that the color and nutritional values of food products change minimally after a drying process. Considering the commercial objectives, the main ones are to complete the drying process in the shortest time and thus keep energy costs low.

Around the world, especially in underdeveloped and developing countries, drying is done using traditional methods. With this method, the products are dried in the open sun on platforms such as sheets, brands, exhibitions, crates, etc. In the traditional drying process, very large amounts of product can be dried without energy costs. However, this requires huge amounts of space. The drying time in this method is much longer than the drying process using technical methods. However, a large number of human workforce is needed for the processes of laying, inspecting, and collecting the products. Since the products dried in this method are open to the atmosphere, they may be exposed to the negative effects of dust, garbage, pests, birds, and other animals. In this regard, it is very difficult to say that the product dried in this method is hygienic. The biggest disadvantage of this method is that it depends on meteorological conditions and the products are open to the atmosphere. Namely, if the weather becomes cloudy during drying, the drying time is

prolonged and, moreover, in case of possible rain, significant product loss may occur.

Solar energy can be used in the drying process using more technical methods. There are many drying styles and methods for this. With these methods, it is possible to obtain dried products of the desired quality under more hygienic conditions and by keeping the drying parameters under control. In addition, by making the necessary arrangements, a larger amount of product can be obtained in a shorter time, and the final product with the desired properties. However, in these methods, the heat provided for the drying process has an energy cost. Energy cost has a significant proportion in the unit cost of the dried product. Upward fluctuations in energy costs are the most important disadvantage of these methods. There is a trend towards renewable energy sources in order to minimize energy costs in drying processes. Solar energy has become the most used renewable energy source.

2. SOLAR DRYING METHODS

The solar drying method is the oldest known drying method. Beyond solar drying using technical methods, even open sun drying is still preferred today. Solar dryers are classified according to criteria such as their design, solar utilization, drying air circulation method, etc. Kumar and Singh (2020), classified solar drying methods for crop drying as the open sun and solar dryer in the first stage (Figure 1). Solar dryer is divided into two different methods according to active and passive mode. These two methods are divided into three sub-branches (direct, indirect, and mixed).

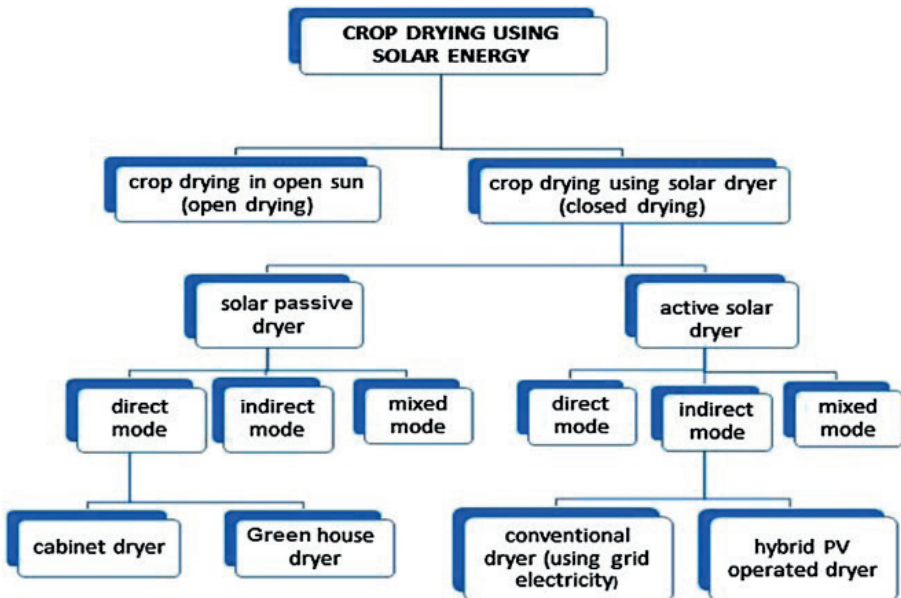


Figure 1. Crop drying methods using solar energy (Kumar & Singh, 2020)

Solar dryers are typically designed as direct, mixed, and indirect according to how they benefit from solar radiation. In addition, according to the circulation method of the drying air in the dryer, it is divided into two types: passive and active convection. In direct-mode, products are directly exposed to solar radiation. The design, manufacture, and operation of this type of dryer is simpler than other modes. Additionally, the initial installation cost is lower. These types of dryers are preferred for drying products that are not adversely affected when exposed to sunlight. Indirect-mode solar dryers are preferred for drying products that are negatively affected by solar radiation. Solar dryers in this mode are more complex and difficult to design, manufacture, and operate compared to direct-mode solar dryers. Additionally, the initial investment cost is high. In this mode, the heat source is heat generated from solar energy in an external unit. This generated heat is transferred to the environment where the products are located through a channel or a direct connection. Mixed-mode solar dryers are designed by combining direct and indirect-mode solar dryers. As can be understood, the part where the products are placed is made of completely or partially transparent material, the products are exposed to solar radiation, and the heat obtained from the water or air-heated solar collector is also transferred to this part.

The solar dryer can be designed with natural convection, in which the heated air rises as a result of the density difference or circulates under the influence of winds. There are no energy costs in this type of application. On the other hand, it can also be arranged in forced convection, where the air inside the dryer is moved by a fan. In such an application, an electrical grid or a photovoltaic system is needed. As a result, such a mechanism increases both the initial installation cost and the operating cost of the solar dryer. However, compared to passive mode, active mode reduces drying duration and increases the efficiency of the dryer.

2.1. Open Sun Drying

It is possible to say that this drying method has been the most preferred drying method in the world for centuries. It is especially preferred in underdeveloped and developing countries around the world. Although this method does not require a high initial investment and energy consumption costs, it also brings with it many drawbacks. The most important disadvantage is that it has a long drying time. In particular, farmers are most concerned about adverse weather conditions (clouding, rain, etc.) during the drying process. Because the weather remains cloudy for long periods of time, which significantly extends the drying time. Moreover, there is a risk of spoilage of products in case of rain. In addition, disadvantages such as requiring very large areas, requiring a greater number of workers, and being exposed to external environmental effects (bird, rodent, fungal attack, dust, garbage, etc.)

can be listed. Open sun drying is not currently the subject of any scientific study. However, in scientific studies, the designed dryers are compared with the open sun drying to evaluate their performance (Rabha, Muthukumar, & Somayaji, 2017; Chauhan, Kumar, Nuntadusit, & Banout, 2018; Fadhel, Charfi, Balghouthi, & Kooli, 2018). Figure 2 shows a schematic diagram of a typical open sun drying method (Bhardwaj, Kumar, Kumar, Goel, & Chauhan, 2021). After the short wavelength of solar radiation from the sun hits the products, the wavelength increases and is reflected into the atmosphere. Dried products lose the heat obtained from solar radiation by conduction to the base on which they are placed and to the atmosphere in high amounts through convective and evaporative means.

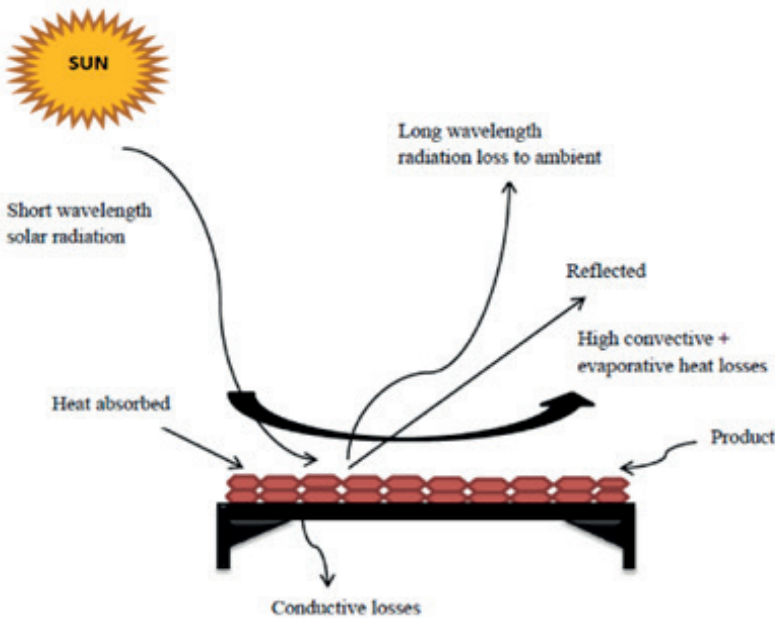


Figure 2. Schematic diagram of a typical open sun drying method (Bhardwaj et al., 2021)

2.2. Solar Dryers

Solar dryers, which include a technical system, have many advantages over open sun drying. Its most important advantage is that it allows drying under more hygienic conditions. In addition, they occupy a small area, making it easier for producers. The drying process takes less time and is more controllable than open sun drying. It is minimally affected by adverse weather conditions.

2.2.1. Direct Mode

Direct-mode dryers are generally designed as greenhouse and cabin types. Additionally, it can be manufactured in tunnel form with different designs.

According to the classification, this type of dryer does not have an external heater. To make these dryers more efficient, which are generally operated in passive mode, and to reduce drying times, the effect of active mode supported by photovoltaic systems is also being investigated.

2.2.1.1. Greenhouse Dryers

One of the solar dryers in direct type is the greenhouse dryers. Greenhouses are structures created from glass or plastic covers. Generally, they are also known as structures that protect agricultural products from the effects of adverse weather conditions in order to ensure that they grow earlier. These structures are also used in drying processes after the necessary transformations are made (Figure 3). These; It has wooden floors (Badaoui, Hanini, Djebli, Haddad, & Benhamou, 2019), north wall insulation (Chauhan & Kumar, 2018), indirect type arrangement (Mehta, Samaddar, Patel, Markam, & Maiti, 2018), and tunnel type (Morad, El-Shazly, Wasfy, & El-Maghawry, 2017).



Figure 3. A typical greenhouse dryer view (Kaewkiew et al., 2012)

When literature studies are examined, researchers make various modifications and innovations on typical greenhouse-type dryers. Tiwari and Tiwari (2016) integrated a PV-T (photovoltaic-thermal system) into a single-pitched roof greenhouse-type dryer in natural and forced modes and investigated this dryer's performance under India's climatic conditions. Thermal modeling of the PV-T system in natural and forced mode without load conditions has been experimentally verified. Additionally, the impact of characteristic curves, mass flow rate, and packing factor were also evaluated on some thermodynamic criteria. Solar cells, total thermal, thermal, and overall exergy efficiency were taken into account as criteria. With the rise in the packaging factor of the PV module, thermal energy was reduced, and electrical energy production rose by 76.39 and 88.73%, respectively. It was determined that the increase in mass flow rate increased thermal energy by 65.7 and 89.44% for forced and natural modes, respectively.

Chauhan et al. (2017) manufactured a greenhouse dryer with a PV-integrated solar collector and examined it in ventilated mode at no load. Different significant thermal performance parameters including convective heat transfer coefficient, COP, heat usage factors, and net heat gain percentage were evaluated for the effectiveness of the modifications. The energy, electricity, and exergy efficiency of the PV system installed for the exhaust fan were also analyzed. Greenhouse dryer experiments were carried out with and without solar air heater. The increase in peak convection heat transfer coefficient for the greenhouse dryer with the solar air heater was 150% compared to the absence of the solar collector.

Azaizia et al. (2017) modeled a new greenhouse dryer for drying red peppers. A mathematical model was improved with the packet program (TRNSYS). This model estimated the alteration in drying kinetics throughout the drying process. The experimental part of the investigation was created to investigate the solar air heater's performance. Testing revealed that the efficiency of this air-heated solar collector ranges from 0.5% to 0.65%. The model was confirmed with the obtained outcomes. Obtained modeling results demonstrated good agreement with test data. The effects of dried product area, air flow rate, moisture content, and collector area changes on air moisture and temperature distribution in the greenhouse were examined.

In another study, Eltawil et al. (2018) examined the performance of a PV-supported tunnel greenhouse dryer suitable for potato drying. The dryer's performance was calculated with and without load. Additionally, the use and non-use of thermal curtains on potato slices on sunny days were also examined. In the study, performance changes for distinct air flow rates (4.18, 3.12, and 2.1 m³/min) and pre-treatment of samples were examined. The system operated with PV reached the safe humidity level of the products in 6 and 7 hours, respectively, with and without using the thermal curtain at an airflow rate of 3.12 m³/min. The highest drying efficiency was recorded as 28.49% and 34.29% at 0.0786 kg/s air flow for using and not using thermal curtains, respectively.

Hamdi et al. (2018) compared the numerical and experimental results of grape drying using a greenhouse-type solar dryer. The experimental setup mainly comprises a chapel-shaped greenhouse and an air-heated solar collector. The experiments were conducted in two stages, firstly, the performance analysis was made for the case where the solar collector was not integrated. Finally, drying experiments were made. The changes in the moisture content and main drying parameters of the product were analyzed. The grapes' moisture content reached the target level from the initial level within 128 h. A model was created in the TRNSYS program to simulate the system. Simulation outcomes were compared with experimental values. Additionally, comparisons were made with the classical model to validate the new model.

El Kahdraoui et al. (2019) carried out red pepper drying experiments using a new forced convection greenhouse-type dryer. To evaluate the dryer's performance, open sun drying was made under same conditions. Experimental drying values were placed into eight distinct thin-layer drying models. The compatibility of data with these models was evaluated using chi-square, coefficient determination, and RMSE (Root Mean Square Error). The outcomes obtained demonstrated that there was no constant rate time in the experimental drying curves. The proposed system dropped the drying duration by one day compared to the open sun method. Finally, an economic evaluation was made. It has been determined that the system's payback period is 1.02 years.

Khanlari et al. (2020a) improved the thermal performance of the greenhouse dryer by integrating a cost-effective and easy-to-implement tube-type solar air heater (T-SAH). As the first step of the research, the authors numerically analyzed the dryer's thermal performance. In the next stage of the study, a dryer was manufactured based on the results obtained. To see the performance of the dryer, apricot samples were dried at flowrates of 0.015, 0.013, and 0.010 kg/s. Findings of the investigation have shown that T-SAH's contribution to greenhouse dryer significantly reduces drying time.

Heat loss from the north wall of greenhouse-type dryers is one of the most important problems to be overcome. To solve this problem and increase the performance of the dryer, researchers are looking for innovative solutions.

2.2.1.2. Cabinet-Type Solar Dryers

The structural features of this type of dryers vary according to the designs in the studies in the literature. However, it generally has a wooden or metal case and its upper part is inclined and covered with a transparent material. Depending on the design, drying air enters through holes opened at the bottom of the cabinet or on the sides, and exits from the top of the cabinet through a chimney or from the side surfaces if it has a fan. This type of dryer has a simple structure, is easy to manufacture, and has low cost. The difficulties that must be overcome are that the drying air in the cabin is not distributed evenly and the moist air is insufficient to be expelled. Figure 4 shows a typical cabinet-type solar dryer (Bhardwaj et al., 2021). By using a transparent material in the part where solar radiation enters the cabin, the amount of heat loss to the atmosphere is minimized.

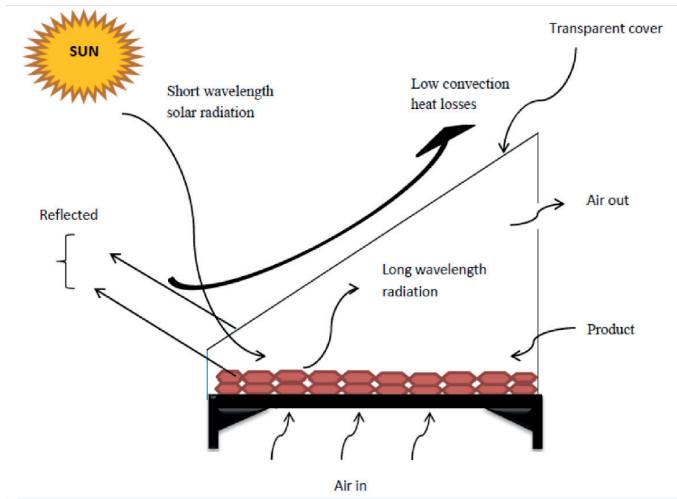


Figure 4. Typical cabinet-type solar dryer (Bhardwaj et al., 2021)

Tunde-Akintunde (2011) examined the chili peppers' drying characteristics using an open sun drying and solar dryer. The peppers to be dried have been pre-treated. Additionally, some peppers were not pretreated as a control variable. Pre-treated chili peppers dried faster than non-pre-treated peppers. To select an appropriate drying equation, four mathematical models (Henderson and Pabis, Newton, Logarithmic, and Page) were fitted to the test values. It was determined that the Page model best describes the drying behavior of chili peppers for drying in both dryers.

Sallam et al. (2015) aimed to dry mint in two identical indirect and direct solar dryers for the same dimensions. Both dryers were run in forced and natural convection modes. The impact of working mode and solar dryer type on the mint's drying kinetics was examined. Ten thin-layer drying models were employed to fit the drying curves. Only one of them did not comply. The outcomes showed that mint drying under both operating conditions happened in the falling rate period. Additionally, the results show that mint's drying rate for forced convection was higher than natural convection, especially in the first hours of drying.

Singh and Sethi (2018) proposed a new direct-type cabinet dryer (Inclined Solar Cooker-Cum-Dryer). To develop the drying performance of this dryer, a single reflector north face booster mirror has been integrated into the dryer (Figure 5). Tempered double glass with 10 mm between two layers is used to reduce heat loss. Jangawang (2017) designed a compact solar cabin dryer for drying meat and measured its performance. The solar cabinet comprises a transparent cube-shaped drying chamber made of acrylic material and a trapezoidal roof. The drying chamber has dimensions of 120 x 120 x 120 cm.

During the two-day drying process, the mean temperature on the shelves varied between 45.75°C and 48.63°C. The temperature at the lower shelf level remained lower than the upper shelves.

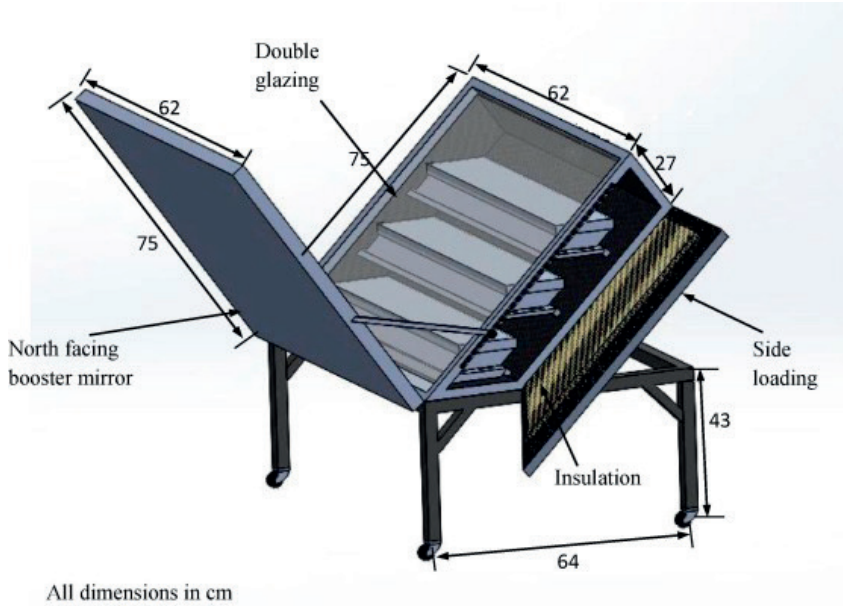


Figure 5. Technical drawing view of Inclined Solar Cooker-Cum-Dryer

2.2.2. Indirect Solar Dryers

Figure 6 shows a typical indirect solar dryer design. Solar dryers in indirect-mode, food samples are placed in the drying chamber. Heat is produced in an external unit and sent to the drying room. Heat is generally produced in air-heated solar collectors. Solar air collector can be either directly connected to the drying room or connected through a channel, depending on the design. In this regard, the units where heat is produced become important for this type of dryers. For this reason, many researchers have focused on air-heated solar collectors with different design features to increase the efficiency of this type of dryers (Khanlari et al., 2020b; Potgieter, Bester, & Bhamjee, 2020; Hassan et al. 2022; Heydari, 2022).

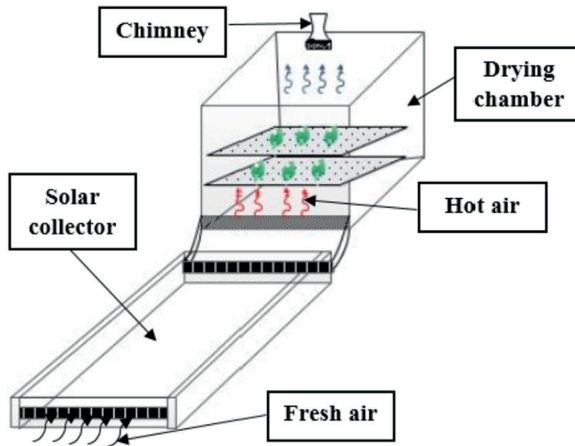


Figure 6. A typical indirect solar dryer design (Zoukit et al., 2019)

When the literature is examined, indirect-mode solar dryers are generally operated with forced convection (Janjai, Srisittipokakun, & Bala, 2008; Akpınar, 2010; Sami, Etesami, & Rahimi, 2011). On the other hand, there are also designs where performance research is carried out by operating with natural convection (Pangavhane, Sawhney, & Sarsavadia, 2002; Romero, Cerezo, Garcia, & Sanchez, 2014; Lingayat, Chandramohan, & Raju, 2017). In addition, many researchers have compared the performance changes of these types of dryers in natural and forced convection modes (Bhavsar & Patel, 2021; Gilago & Chandramohan, 2022; Mugi & Chandramohan, 2022). Varun et al (2012) have aimed to improve a solar dryer with natural convection and an indirect type for drying horticultural products. In this study, the authors also investigated the performance change compared to natural convection by operating the dryer under forced convection conditions. Air mass flowrates of 0.019 and 0.00653 kg/s were acquired for forced and natural convection, respectively. The heated air increased a mean temperature of 40°C and 45°C for natural and forced mode, respectively. Moreover, the outcomes acquired were compared with open sun drying outcomes. For indirect solar dryers, a balanced temperature distribution is expected in the drying room. Zoukit et al (2019) modeled the temperature distribution inside the drying room for forced and natural convection. They used the Takagi-Sugeno fuzzy logic model to estimate. Firstly, some tests were conducted on the dryer to find out its dynamic and static properties for distinct climatic conditions. Secondly, the temperature measurements inside the drying room were carried out around some locations under both convection modes. Linear transfer functions are defined around some selected operating points. The estimates agree with the experimental results with the RMSE remaining below 1.94% (0.52°C) and 0.81% (0.4°C) in forced and natural convection.

El Sebai and Shalaby (2013) purposed to design and manufacture a solar dryer in the ventilated and indirect type. The system's thermal performance in the prevailing climatic conditions of Tanta was investigated experimentally. The setup consists of drying room and double-pass V-groove solar air heater. Thymus and mint drying tests were employed to observe the dryer's performance. Mint and thymus were dried in 5 and 34 hours, respectively. Fourteen thin-layer drying models were employed to detect the appropriate model to explain the drying action of the examined samples.

Kabeel and Abdelgaied (2016) presented theoretical analysis results the impact of the rotary dryer wheel on the solar dryer's thermal performance. As seen in Figure 7a, the dryer comprises a rotary dryer wheel, a solar air heater, and a drying room. Figure 7b shows a solar dryer without the rotary desiccant wheel. Theoretical models of the dehumidifying wheel and the solar air heater are confirmed using experimental outcomes. Additionally, the impact of the rotation velocity of the dryer wheel on this system's performance was examined. Moreover, the findings show that the optimum rotation velocity of the dryer wheel, which achieves the maximum drying air temperature and minimum moisture content of the dryer unit, is 15 rph. By integrating the rotary dryer wheel into the solar drying unit, a useful heat gain of 153% was achieved.

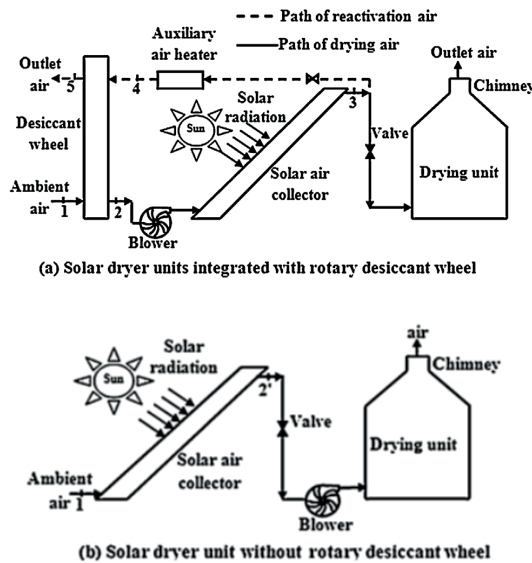


Figure 7. a) Solar dryer units integrated with rotary desiccant wheel, b) Solar dryer units without rotary desiccant wheel

Benhamou et al. (2014) aimed to detect the solar drying curve and drying change rate on olive pomace and colonite relying on solar radiation. A

solar dryer with ventilated and indirect mode was used to detect the drying dynamics of these products. In the study, the impact of some criteria on drying kinetics was evaluated. To verify the reliability of the dryer for drying products with different moisture values, the variation of drying rate, solar radiation, and variable outdoor temperatures were examined.

Chandrasekar et al. (2018) used the heated air coming out of the condenser unit of a split air conditioner in a solar dryer with an indirect mode. Thus, an established mechanism was employed to rise the temperature and speed of the drying air. The drying behavior of this dryer for Sultana grapes was examined. The tests were conducted in India in spring climatic conditions. The use of condenser-exit drying air from the split air conditioner dropped the drying duration of samples by 16.7% compared to the open sun drying. By integrating the air conditioning condenser into the indirect solar dryer, a 13% rise for dryer efficiency was achieved. From the results, it was determined that the exponential model could describe the drying characteristics of samples. The predicted humidity values were found to be compatible with the experimental findings. Exergy analysis showed increased heat accessibility within the drying room.

2.2.3. Mixed-Mode Solar Dryers

Figure 8 shows the technical drawing and real view of a mixed-mode cabin solar dryer (Da Silva et al., 2021). A solar dryer in mixed mode is a type of dryer created by combining the characteristics of direct and indirect solar dryers. Namely, the foods in the drying chamber are exposed to both direct sunlight and hot air sent by heating the air in the heated solar collector. The manufacture of this type of dryer is more difficult, complex, and expensive than direct and indirect dryers. On the other hand, drying performance is higher.

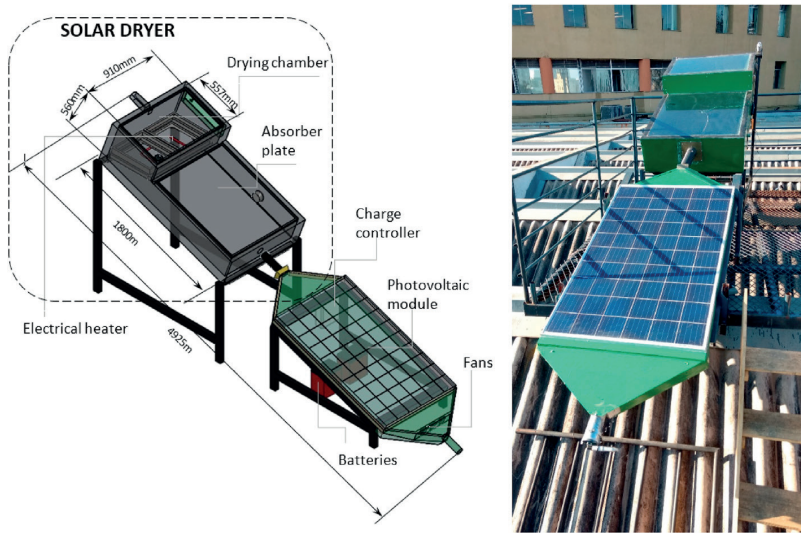


Figure 8. Technical drawing and real view of a mixed-mode cabin solar dryer (Da Silva et al., 2021)

Singh and Kumar (2012) designed a solar dryer with mixed-mode to dry potato products such a cylindrical. Sixteen drying mathematical models were obtained for an extensive range of drying process variables. Loading density, food sample thickness, air mass flow rate, and absorbed thermal energy were the investigated criteria. A testing methodology in a new concept is proposed to evaluate the dryer's performance. This methodology is based on drying time and moisture component ratio. The proposed methodology is described to a dimensionless parameter called the dryer performance index that characterizes the efficiency of the drying setup. To verify the proposed methodology, potatoes, bananas, and wheat were dried in different solar dryers under actual climatic conditions.

Singh and Kumar (2013) conducted experiments drying cylindrical potato slices in a solar dryer in mixed-mode to determine an extensive range of process variables. Here, air flow rate, absorbed thermal energy, and sample loading density and thickness are the variables investigated. A numerical methodology has been improved to predict various performance index. These are CO₂ emissions reduction, SEC, drying efficiency, carbon credits earned, and the quantity of distinct hydrocarbons saved due to the use of solar drying. The hydrocarbons including LPG, coal, natural gas, and diesel are investigated in this study. Research results show that for all conditions, dryer can reduce maximum CO₂ emissions by replacing coal with solar energy. There was a significant increase in absorbed energy and charge density, resulting in SEC and possible CO₂ reduction, while the opposite tendency was seen for product thickness. But, the effect of airflow

rate on these parameters was discovered to be quite distinct. A correlation was improved using the Levenberg-Marquart algorithm to establish the functional relationship between process variables and SEC.

Frerich et al. (2018) presented the tomato drying performance results of a forced convection solar dryer in mixed mode. The examined system comprises a PV-T (photovoltaic-thermal) collector and a drying chamber. Airflow enters the aluminum tube channels at the bottom of the PV panel and simultaneously spreads into an overhead space. As a result, it supplies heat exchange on both faces of the PV, which helps in cooling the PV cells and transporting thermal energy to the drying room. Using the prototype, the sample's moisture content was declined from 91.94% to 22.32% for shelf-1, and 28.9% for shelf-2. In contrast, it dropped to only 30.15% for open sun drying.

Cesar et al. (2020) presented to design, and test results a solar dryer in passive mode. The dryer (Figure 9) was operated in mixed mode (MSD) and indirect mode (ISD). Drying efficiency, energy efficiency, and drying kinetics were selected as the performance examination parameters for the dryer. Throughout the experiments, the temperature in the drying room during sunny noon hours varied between 65-70°C for MSD, and 55-60°C for ISD. ISD and MSD dried tomatoes in 26 and 17 hours, respectively. The solar air heater's efficiency varied between 52.3% and 55.45%. The efficiency of the dryer in ISD and MSD mode was between 8.8% and 10.6%, respectively, whereas the drying efficiency was 5.47 and 4.48%, respectively. Investigation outcomes on sample drying kinetics were fitted to five thin-layer drying models. The modified Henderson and Pabis model demonstrated a good fit as R^2 for MSD and ISD was 0.9888 and 0.9996, respectively, while for RMSE it was 0.0027 and 0.008, respectively.

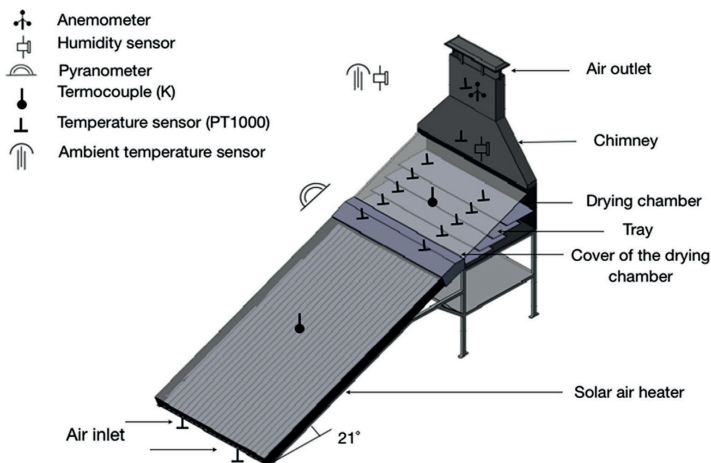


Figure 9. Technical drawing of passive solar dryer in mixed type and placement of measuring devices on it (Cesar et al., 2020)

Djebli et al. (2020), presented the potato drying performance results of ventilated solar dryers in mixed and indirect modes. Figure 10 shows indirect, and mixed mode solar dryers. Mixed-mode is also in the form of a greenhouse-type dryer and the products are placed on the shelves. The drying temperature in the indirect mode was lower than in mixed mode. Mixed mode dried the products 65 minutes later than the indirect mode. Laplace transforms and Fourier series were employed to figure out the diffusivity equation. Seven mathematical models were examined and their relative correctness was verified against test outcomes. Two new models were determined to good agreement the drying curve of samples for both working mode.

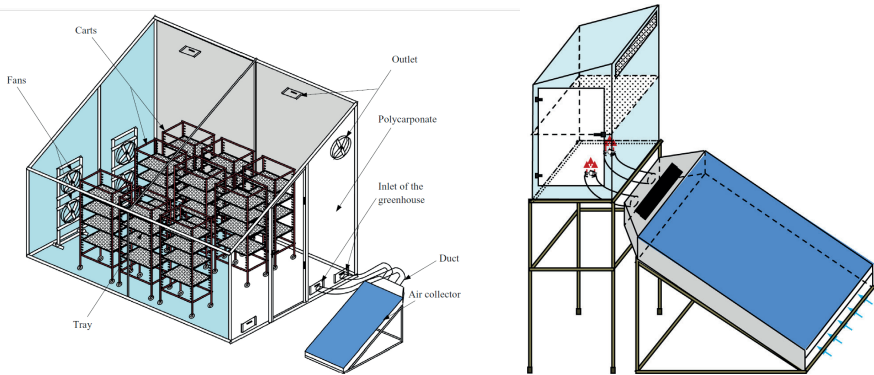


Figure 10. *The ventilated mixed solar dryer (left), the indirect solar dryer (right) (Djebli et al., 2020)*

2.2.4. Solar Dryers With Integrated Heat Storage System

Although each drying method has some advantages, it also has some limitations. While solar dryers can dry during periods when solar radiation is active, they cannot dry during periods outside of this. While some fruits, vegetables, medicinal and aromatic plants, etc. dry in a short time, some of them dry in more than one day. Solar dryers are insufficient to provide continuous drying. Heat storage systems are used to benefit more from solar energy throughout the daytime and increase the time the solar dryer is active. In this application, the stored heat can be utilized in cloudy weather when solar radiation is ineffective and after sunset. Heat storage systems increase the reliability of solar energy.

Heat storage systems can be indexed as low-, medium-, and high-temperature heat storage systems. Low-temperature heat storage systems are divided into two: sensible and latent heat storage systems. It is possible to perform low-temperature heat storage in liquids or solids in isolated environments. The heat stored in this process can be used again in thermal applications. However, its conversion into energy types such as electricity and mechanics is quite inefficient.

The impact of heat storage systems on solar dryers' performance has been focused intensively by researchers for several decades. Phase change materials are extensively preferred in heat storage systems. Vasquez et al. (2019) aimed to model product drying kinetics in a solar dryer with a PCM heat storage medium. Additionally, thermal modeling of this dryer was done. The results obtained were confirmed by experimental outputs. Paraffin wax was preferred as PCM material. In many studies, paraffin wax is preferred as a heat storage medium (Jain, & Tewari, 2015; Raj, Srinivas, & Jayaraj, 2019; Arun et al., 2020). Energy balances were created for the system components and heat transfer coefficients were determined.

Bhardwaj et al. (2019) explored the performance of forced convection indirect solar dryer integrated with phase change material (PCM) and sensitive heat storage material (SHSM). Both gravel iron scrap mixture and engine oil SHSM were preferred in the solar air heater. Paraffin RT-42 was placed in the unit where the products were placed. Drying experiments were made for a medicinal plant of the *Valeriana Jatamansi* species and the moisture content was dropped from 89% to 9%. When SHSM and PCM were used at the same time, the total drying rate was determined as 0.051 kg/h. These values are 0.028 and 0.018 kg/h without using thermal storage media and in conventional shade drying, respectively. In the recommended dryer, it took 120 hours for the products to reach the final moisture level. Drying without thermal storage and conventional shade drying took 216 and 336 hours, respectively. While the solar collector without SHSM had a mean exergy and energy efficiency of 0.14%, and 9.8% respectively, in the presence of SHSM, these parameters were determined as 26.1% and 0.815%, respectively.

Iranmanesh et al. (2020), aimed to evaluate the performance of a cabin-type solar dryer with a thermal storage system (PCM). The solar collector is in the form of an evacuated tube heat pipe. In the study, drying efficiency, quality evaluation of dried samples, CFD modeling of the system, and thermal analysis of the solar collector, were investigated. The dryer's performance was simulated and verified with experimental values. Experiments with and without using PCM were carried out at different air flow rates (0.09, 0.05, and 0.025 kg/s) for the drying system, to dry 5 mm thick apple slices. Thermal investigation outcomes demonstrated that using PCM increased the inlet heat energy by 5.12% and 1.72% for airflow rates of 0.05 and 0.025 kg/s, respectively. However, it has been understood that an excessive rise in air flow rate reduces the inlet heat energy. The maximum total drying efficiency was figured out to be 39.9% at 0.025 kg/s when associated with the PCM system. Experimental and simulation outcomes of the dryer and heat storage unit confirmed each other.

2.2.5. Solar-Assisted Heat Pump Dryers

Heat pump drying systems can be used to utilize an existing heat source at low temperatures. The humid air leaving the drying room can be dehumidified by the heat pump system and reintroduced into the drying system. In a closed circuit system, moist drying air is passed through the evaporator of the heat pump system and both its heat and humidity are removed. Afterward, this drying air is passed through the condenser, its temperature is increased, and given back to the drying room. Fresh air can be added to the drying air at certain rates with different designs.

Solar systems are inadequate for drying applications outside the summer season. For heat pump dryers, a higher temperature heat source may be advantageous during these periods. In such cases, a solar collector with air heating can be integrated into the heat pump drying system. Thus, the low-temperature heat produced from solar energy becomes more useful for heat pump dryer applications.

Studies on solar energy-assisted heat pump dryers have been continuing for many years. As seen in Figure 11, Şevik (2014) designed a new solar dryer comprises a heat pump, a double-pass solar air collector, and photovoltaic units. Carrot drying tests were applied to determine the solar dryer's performance. In the drying system, a double-pass solar air collector provided heat for the drying process. The recommended dryer dried carrot slices at variable air speed and 50°C temperature. They were brought from an initial moisture content of 7.76 g water/g dry matter (d.b.) to a target moisture content of 0.1 g water/g dry matter (d.b.). The air velocity was varied depending on the air inlet temperature of the drying room. The thermal efficiency of the double-pass collector was calculated to be between 60-78% based on experimental outcomes. Samples were dried for 220 minutes in a solar-assisted heat pump dryer using a double-pass solar air collector. Mohanraj (2014) investigated a SAHSHPD's performance (Solar-Ambient Air Source Hybrid Heat Pump Dryer) for drying in hot humid atmosphere conditions. Performance criteria including condenser heat capacity, COP, and SMER were examined. The findings revealed that the COP value of SAHSHPD was 2.54 on average and varied between 2.31 and 2.77. The heating capacity of the condenser varied range 2.9 kW and 3.75 kW, with a mean value of 3.290 kW. SMER was 0.79 kg/kWh. The moisture content of the dried product decreased from approximately 52% (w.b.) to approximately 9.2 and 9.8% in 40 hours in the lower and upper trays, respectively.

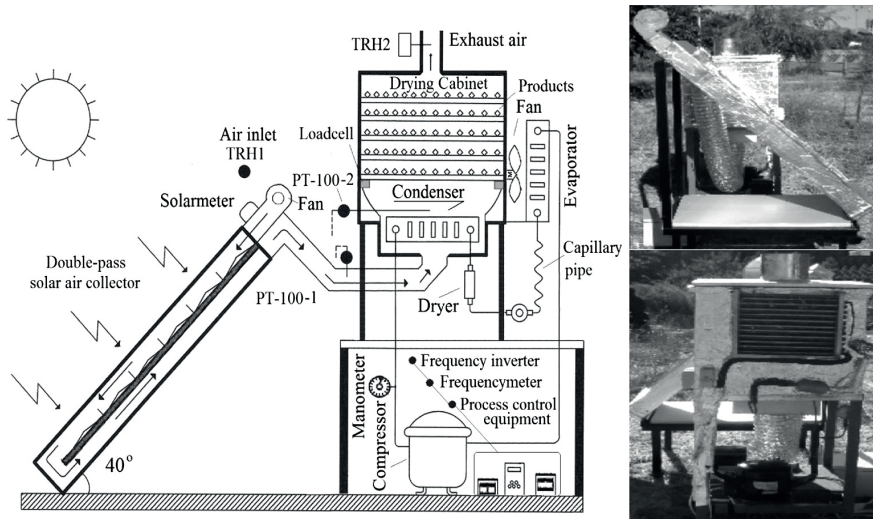


Figure 11. Schematic view of double-pass solar air heater integrated heat pump dryer (Şevik, 2014)

Yahya et al. (2016) aimed to compare the drying performance of solar-assisted heat pump dryer (SAHPD) and SD (solar dryer) on cassava sawdust. SD and SAHPD reduced cassava mass from 30.8 kg to 17.4 kg in 13 and 9 hours, respectively, at mean temperatures of 40°C and 45°C. The mean thermal efficiencies for SD and SAHPD were calculated as 25.6% and 30.9%, respectively. While SMER for SD and SAPD were 0.38 and 0.47 kg/kWh, respectively, the average drying air flow rate for SD and SAHPD were 1.33 and 1.93 kg/h and, respectively. Average solar fractions were determined as 44.6% for SAHPD and 66.7% for SD. The mean COP value of the heat pump was 3.38 and varied between 3.23-3.47.

In some studies, heat storage systems have been integrated into solar-assisted heat pump dryers as an innovation. Qiu et al. (2016) suggested a new solar-assisted heat pump drying system with thermal storage and heat recovery. Additionally, the impact of distinct economic parameters on the payback period was determined. The condenser and evaporator are integrated into the drying room, and a water storage tank is installed in the setup. It is aimed to improve the practice of solar energy and effectively recover heat in performing these operations. Depending on the total heat of 23,157 MJ required to dry 10 kg of radish, numerical investigation findings showed that the system operates in solar dryer mode when the daily mean radiation intensity is 0.48 kW/m². When this value is between 0.43 and 0.48 kW/m², the system operates in solar-assisted heat pump drying mode. Additionally, it was determined that the setup operates in heat pump drying mode when this value is less than 0.43 kW/m². The drying system's COP varied between 3.21

and 3.49 for solar-assisted heat pump dryer mode. It has also been reported that SAHPD reduces energy consumption by 40.53% with regard to thermal storage and heat recovery. The payback period for drying radishes, peppers, and mushrooms throughout the system life is calculated as 6, 4, and 2 years, respectively.

Khouya (2020) proposed a new concentrated photovoltaic thermal energy-powered water/air heat pump dryer to realize the softwood drying process. The proposed system comprises a concentrated photovoltaic/thermal system, closed supply air heater, us/air heat pump, and drying chamber, (Figure 12). Numerical and experimental analysis was performed to estimate the drying system's performance. The test findings demonstrated good agreement with the numerical analysis outcomes. The COP value ranged from 3.91 to 7.2. When the heat pump set value was decreased from 75°C to 65°C, there was an increase of at least 17% in the COP value. The combined use of concentrated photovoltaic thermal systems and heat pump declined the energy consumption rate by up to 86%. The dryer's thermal performance has been developed with the proposed system.

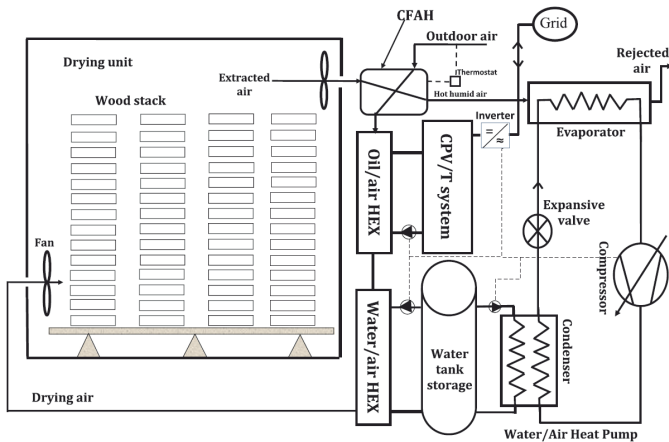


Figure 12. Schematic diagram of concentrated photovoltaic thermal energy-powered water/air heat pump dryer (Khouya, 2020)

2.2.6. Geothermal Energy Assisted Solar Dryers

Hybrid energy drying mechanisms are designed for uninterrupted drying of foods with long drying times. The dryer is operated with solar energy during the day and a second energy source such as geothermal is used at night. In addition, in case the weather becomes cloudy or rainy during the day, geothermal energy is activated and solar energy is supported. These energy source changes can be made manually or controlled by automation systems. Studies on this subject remain very limited. Ivanova and Andonov

(2001) carried out unloaded and apricot drying experiments in a hybrid-type dodecahedral sharp pyramid-shaped dryer with solar and geothermal energy. Temperature distribution and thermal efficiency in the drying room were determined in no-load experiments conducted during the day. Additionally, a drying model based on temperature and humidity was created. In apricot drying experiments, solar energy throughout the day and geothermal energy at night were used. In another study on the same dryer, Ivanova et al. (2003) carried out an energy and economic analysis based on data obtained from the previous study. In this study, the dryer examined was compared with different energy-based drying applications in terms of parameters such as payback period and savings. The dryer's payback period was determined 2.4 years.

In order to develop the thermal performance of the solar dryer in direct mode, Sandali et al. (2019) integrated a double-level tube heat exchanger in which geothermal hot water circulates into the system. The heat exchanger is placed on the absorber plate. The temperature of the water circulating in the heat exchanger was fixed at 70°C with an electric heater to simulate the temperature of geothermal water in the southern region of Algeria. Numerical simulation was also performed and the findings were compared with test data. The outcomes demonstrated that integrating the heat exchanger importantly improved the solar dryer's performance. With heat exchanger, the lowest and highest temperature value was 46°C and 58°C, respectively. At night, the drying temperature remained at an average of 46°C. Hadibi et al (2021) dried tomato pastes simultaneously in two natural convection direct-type solar dryers, one with a geothermal heat exchanger and the other without. The drying performance, economic analysis, and drying kinetics of the dryers were compared. Insulation was added to the dryer with the geothermal heat exchanger to prevent heat loss after sunset. By integrating the geothermal heat exchanger into the system, a temperature increase of 11.5°C was achieved. In the night, the difference between the cabin interior temperature and the outdoor temperature at night reached 30.8°C. While tomato paste was dried for 22 consecutive hours with the hybrid dryer, without a heat exchanger took a total of three days. According to the outcomes of the economic analysis, the hybrid dryer's payback period was determined as 2.21 years.

In these studies, natural convection conditions were evaluated. However, studies have also been conducted on how ventilation will contribute to the performance of the hybrid dryer. Hadibi et al. (2022) compared the drying performance of four different dryers (solar direct mode (SDM), solar geothermal direct mode (SGD), ventilated direct solar dryer mode (CVD), and ventilated direct solar geothermal dryer mode (VHD)) for tomato paste. The effects of these drying modes on product quality, economic analysis, and exergy efficiency were investigated. As a result of the experiments, the drying time of tomato paste in SDM, SGD, CVD, and VHD modes was determined as

10, 9, 8, and 4.5 hours, respectively. The highest specific energy consumption value and drying efficiency were obtained in VHD mode with 3.21 kWh/kg, and 68.27%, respectively. The highest exergy efficiency was obtained in VHD and SGD modes as 54%. The payback period of SDM, SGD, CVD, and VHD modes was found to be 0.28, 0.325, 0.3, and 0.169 years, respectively. It has been stated that solar drying, in which geothermal energy and ventilation are integrated, shows the best performance with regard to energy, drying time, exergy efficiency, quality features, and economic analysis.

CONCLUSIONS and FUTURE PROSPECTS

Solar energy has become more preferred in electricity generation and space heating processes in recent years. In addition to these two areas of use, solar energy is used extensively in the drying of many products, especially agricultural products, wood, paper, textile products, etc. Significant increases in the prices of fossil fuels in recent years have directed consumers to solar energy. However, a decrease in these prices again in the coming years may reverse this trend of consumers towards solar energy. The most important reason behind this is that energy production stops when there is no sun.

Studies on solar dryers have been ongoing for many years. Researchers working in this field generally focus on designs and applications to increase the solar dryer's performance (direct, indirect, and mixed-mode). However, in recent years, there has been a tendency to make solar dryers capable of working day and night. For this reason, many studies are being carried out on integrating heat storage systems into solar dryers. The most notable trend has been the use of phase change materials. In addition to this subject, solar energy-assisted heat pump dryers and hybrid dryers using more than one energy source have become popular research topics. With these two methods, drying processes as highly efficient as possible were conducted, especially during periods when the sun was absent or had low influence. However, it is not possible to say that the point reached is sufficient.

The designs discussed are generally applications where efficiency was achieved by testing on a pilot scale, and it is a matter of curiosity how they can be adapted to industrial or mass drying processes. Of course, such applications will not be easy to implement as they will take a long time and involve high costs. Studies on this subject are important so that the gains obtained can compete with fossil-based industrial drying systems in which very high amounts of products are dried at the same time.

Acknowledgment

This research has been supported by Kutahya Dumlupınar University Scientific Research Projects Coordination Office under grant number #2021-

REFERENCES

- Akpinar, E.K. (2010). Drying of mint leaves in a solar dryer and under open sun: Modelling, performance analyses. *Energy Conversion and Management*, 51, 2407-2418. doi:10.1016/j.enconman.2010.05.005
- Arun, K.R., Kunal, G., Srinivas, M., Kumar, C.S.S., Mohanraj, M., & Jayaraj, S. (2020). Drying of untreated Musa nendra and Momordica charantia in a forced convection solar cabinet dryer with thermal storage. *Energy*, 192, 116697. https://doi.org/10.1016/j.energy.2019.116697
- Azaizia, Z., Kooli, S., Elkhadroui, A., Hamdi, I., & Guizani, A. (2017). Investigation of a new solar greenhouse drying system for peppers. *International Journal of Hydrogen Energy*, 42, 8818-8826. http://dx.doi.org/10.1016/j.ijhydene.2016.11.180
- Badaoui, O., Hanini, S., Djebli, A., Haddad, B., & Benhamou, A. (2019). Experimental and modelling study of tomato pomace waste drying in a new solar greenhouse: Evaluation of new drying models. *Renewable Energy*, 133, 144-155. https://doi.org/10.1016/j.renene.2018.10.020
- Benhamou, A., Fazouane, F., & Benyoucef, B. (2014). Simulation of solar dryer performances with forced convection experimentally proved. *Physics Procedia*, 55, 96-105. doi: 10.1016/j.phpro.2014.07.015
- Bhardwaj, A.K., Kumar, R., & Chauhan, R. (2019). Experimental investigation of the performance of a novel solar dryer for drying medicinal plants in Western Himalayan region. *Solar Energy*, 177, 395-407. https://doi.org/10.1016/j.soler.2018.11.007
- Bhardwaj, A.K., Kumar, R., Kumar, S., Goel, B., & Chauhan, R. (2021). Energy and exergy analyses of drying medicinal herb in a novel forced convection solar dryer integrated with SHSM and PCM. *Sustainable Energy Technologies and Assessments*, 45, 101119. https://doi.org/10.1016/j.seta.2021.101119
- Bhavsar, H.P., & Patel, C.M. (2021). Performance investigation of natural and forced convection cabinet solar dryer for ginger drying. *Materials Today: Proceedings*, 47, 6128-6133. https://doi.org/10.1016/j.matpr.2021.05.050
- Cesar, L.E., Lilia, C.A., Octavio, G., Isaac, P.F., & Rogelio, B.O. (2020) Thermal performance of a passive, mixed-type solar dryer for tomato slices (*Solanum Lycopersicum*). *Renewable Energy*, 147, 845-855. https://doi.org/10.1016/j.renene.2019.09.018
- Chandrasekar, M., Senthilkumar, T., Kumaragurubaran, B., & Fernandes, J.P. (2018). Experimental investigation on a solar dryer integrated with condenser unit of split air conditioner (A/C) for enhancing drying rate. *Renewable Energy*, 122, 375-381. https://doi.org/10.1016/j.renene.2018.01.109
- Chauhan, P.S., & Kumar, A. (2018). Thermal modeling and drying kinetics of gooseberry drying inside north wall insulated greenhouse dryer. *Applied Thermal Engineering*, 130, 587-597. https://doi.org/10.1016/j.applthermaleng.2017.11.028

- Chauhan, P.S., Kumar, A., & Nuntadusit, C. (2017). Heat transfer analysis of PV integrated modified greenhouse dryer. *Renewable Energy*, 121, 53-65. <https://doi.org/10.1016/j.renene.2018.01.017>
- Chauhan, P.S., Kumar, A., Nuntadusit, C., & Banout, J. (2018). Thermal modeling and drying kinetics of bitter melon slices drying in modified greenhouse dryer. *Renewable Energy*, 118, 799-813. <https://doi.org/10.1016/j.renene.2017.11.069>
- Da Silva, G.M., Ferreira, A.G., Coutinho, R.M., & Maia, C.B. (2021). Energy and exergy analysis of the drying of corn grains. *Renewable Energy*, 163, 1942-1950. <https://doi.org/10.1016/j.renene.2020.10.116>
- Djebli, A., Hanini, S., Badaoui, O., Haddad, B., & Benhamou, A. (2020). Modeling and comparative analysis of solar drying behavior of potatoes. *Renewable Energy*, 145, 1494-1506. <https://doi.org/10.1016/j.renene.2019.07.083>
- El Khadraoui, A., Hamdi, I., Kooli, S., & Guizani, A. (2019). Drying of red pepper slices in a solar greenhouse dryer and under open sun: Experimental and mathematical investigations. *Innovative Food Science and Emerging Technologies*, 52, 262-270. <https://doi.org/10.1016/j.ifset.2019.01.001>
- El-Sebaï, A.A., & Shalaby, S.M. (2013). Experimental investigation of an indirect-mode forced convection solar dryer for drying thymus and mint. *Energy Conversion and Management*, 74, 109-116. <https://doi.org/10.1016/j.enconman.2013.05.006>
- Eltawil, M.A., Azam, M.M., & Alghannam, A.O. (2018). Solar PV powered mixed-mode tunnel dryer for drying potato chips. *Renewable Energy*, 116, 594-605. <https://doi.org/10.1016/j.renene.2017.10.007>
- Fadhel, A., Charfi, K., Balghouthi, M., & Kooli, S. (2018). Experimental investigation of the solar drying of Tunisian phosphate under different conditions. *Renewable Energy*, 116, 762-774. <https://doi.org/10.1016/j.renene.2017.10.025>
- Gilago, M.C., & Chandramohan, V.P. (2022). Performance evaluation of natural and forced convection indirect type solar dryers during drying ivy gourd: An experimental study. *Renewable Energy*, 182, 934-945. <https://doi.org/10.1016/j.renene.2021.11.038>
- Hassan, A., Nikbahkt, A.M., Welsh, Z., Yarlagadda, P., Fawzia, S., & Karim, A. (2022). Experimental and thermodynamic analysis of solar air dryer equipped with V-groove double pass collector: Techno-economic and exergetic measures. *Energy Conversion and Management: X*, 16, 100296. <https://doi.org/10.1016/j.ecmx.2022.100296>
- Hadibi, T., Boubekri, A., Mennouche, D., Benhamza, A., & Kumar, A. (2021). Economic analysis and drying kinetics of a geothermal-assisted solar dryer for tomato paste drying. *Journal of the Science of Food and Agriculture*, 101, 6542-6551. DOI 10.1002/jsfa.11326
- Hadibi, T., Boubekri, A., Mennouche, D., Benhamza, A., Kumar, A., Bensaci, C., & Xiao, H-W. (2022). Effect of ventilated solar-geothermal drying on 3E (exergy, energy, and economic analysis), and quality attributes of tomato paste. *Energy*,

243, 122764. <https://doi.org/10.1016/j.energy.2021.122764>

- Hamdi, I., Kooli, S., Elkhadraoui, A., Azaizia, Z., & Abdelhamid, F. (2018). Experimental study and numerical modeling for drying grapes under solar greenhouse. *Renewable Energy*, 127, 936-946. <https://doi.org/10.1016/j.renene.2018.05.027>
- Heydari, A. (2022). Experimental analysis of hybrid dryer combined with spiral solar air heater and auxiliary heating system: Energy, exergy and economic analysis. *Renewable Energy*, 196, 1162-1175. <https://doi.org/10.1016/j.renene.2022.08.110>
- Iranmanesh, M., Akhijahani, H.S., & Jahromi, M.S.B. (2020). CFD modeling and evaluation the performance of a solar cabinet dryer equipped with evacuated tube solar collector and thermal storage system. *Renewable Energy*, 145, 1192-1213. <https://doi.org/10.1016/j.renene.2019.06.038>
- Ivanova, D., & Andonov, K. (2001). Analytical and experimental study of combined fruit and vegetable dryer. *Energy Conversion and Management*, 42, 975-983.
- Ivanova, D., Enimanev, K., & Andonov, K. (2003). Energy and economic effectiveness of a fruit and vegetable dryer. *Energy Conversion and Management*, 44, 763-769.
- Jain, D., & Tewari, P. (2015). Performance of indirect through pass natural convective solar crop dryer with phase change thermal energy storage. *Renewable Energy*, 80, 244-250. <http://dx.doi.org/10.1016/j.renene.2015.02.012>
- Jangswang, W. (2017). Meat products drying with a compact solar cabinet dryer. *Energy Procedia*, 138, 1048-1054. [10.1016/j.egypro.2017.10.103](https://doi.org/10.1016/j.egypro.2017.10.103)
- Janjai, S., Srisittipokakun, N., & Bala, B.K. (2008). Experimental and modelling performances of a roof-integrated solar drying system for drying herbs and spices. *Energy*, 33, 91-103. [doi:10.1016/j.energy.2007.08.009](https://doi.org/10.1016/j.energy.2007.08.009)
- Kabeel, A.E., & Abdelgaied, M. (2016) Performance of novel solar dryer. *Process safety and environmental protection*, 102, 183-189. <http://dx.doi.org/10.1016/j.psep.2016.03.009>
- Kaewkiew, J., Nabnean, S., & Janjai, S. (2012) Experimental investigation of the performance of a large-scale greenhouse type solar dryer for drying chilli in Thailand. *Procedia Engineering*, 32, 433-439. [doi:10.1016/j.proeng.2012.01.1290](https://doi.org/10.1016/j.proeng.2012.01.1290)
- Khanlari, A., Sözen, A., Şirin, C., Tuncer, A.D., & Gungor, A. (2020a). Performance enhancement of a greenhouse dryer: Analysis of a cost-effective alternative solar air heater. *Journal of Cleaner Production*, 251, 119672. <https://doi.org/10.1016/j.jclepro.2019.119672>
- Khanlari, A., Güler, H.Ö., Tuncer, A.D., Şirin, C., Bilge, Y.C., Yılmaz, Y., & Güngör, A. (2020b). Experimental and numerical study of the effect of integrating plus-shaped perforated baffles to solar air collector in drying application. *Renewable Energy*, 145, 1677-1692. <https://doi.org/10.1016/j.renene.2019.07.076>
- Khouya, A. (2020). Performance assessment of a heat pump and a concentrated photovoltaic thermal system during the wood drying process. *Applied Thermal Engineering*, 180, 115923. <https://doi.org/10.1016/j.applthermaleng.2020.115923>

- Kumar, P., & Singh, D. (2020). Advanced technologies and performance investigations of solar dryers: A review. *Renewable Energy Focus*, 35, 148-158. <https://doi.org/10.1016/j.ref.2020.10.003>
- Lingayat, A., Chandramohan, V.P., & Raju, V.R.K. (2017). Design, development and performance of indirect type solar dryer for banana drying. *Energy Procedia*, 109, 409-416. doi: 10.1016/j.egypro.2017.03.041
- Mehta, P., Samaddar, S., Patel, P., Markam, B., & Maiti, S. (2018). Design and performance analysis of a mixed mode tent-type solar dryer for fish-drying in coastal areas. *Solar Drying*, 170, 671-681. <https://doi.org/10.1016/j.solener.2018.05.095>
- Mohanraj, M. (2014). Performance of a solar-ambient hybrid source heat pump drier for copra drying under hot-humid weather conditions. *Energy for Sustainable Development*, 23, 165-169. <http://dx.doi.org/10.1016/j.esd.2014.09.001>
- Morad, M.M., El-Shazly, M.A., Wasfy, K.I., & El-Maghawry, H.A.M. (2017). Thermal analysis and performance evaluation of a solar tunnel greenhouse dryer for drying peppermint plants. *Renewable Energy*, 101, 992-1004. <http://dx.doi.org/10.1016/j.renene.2016.09.042>
- Mugi, V.R., & Chandramohan, V.P. (2022). Comparison of drying kinetics, thermal and performance parameters during drying guava slices in natural and forced convection indirect solar dryers. *Solar Energy*, 234, 319-329. <https://doi.org/10.1016/j.solener.2022.02.012>
- Pangavhane, D.R., Sawhney, R.L., & Sarsavadia, P.N. (2002). Design, development and performance testing of a new natural convection solar dryer. *Energy*, 27, 579-590.
- Potgieter, M.S.W., Bester, C.R., & Bhamjee, M. (2020). Experimental and CFD investigation of a hybrid solar air heater. *Solar Energy*, 195, 413-428. <https://doi.org/10.1016/j.solener.2019.11.058>
- Qiu, Y., Li, M., Hassanien, R.H.E., Wang, Y., Luo, X., & Yu, Q. (2016). Performance and operation mode analysis of a heat recovery and thermal storage solar-assisted heat pump drying system. *Solar Energy*, 137, 225-235. <http://dx.doi.org/10.1016/j.solener.2016.08.016>
- Rabha, D.K., Muthukumar, P., & Somayaji, C. (2017). Experimental investigation of thin layer drying kinetics of ghost chilli pepper (*Capsicum Cinense* Jacq.) dried in a forced convection solar tunnel dryer. *Renewable Energy*, 105, 583-589. <http://dx.doi.org/10.1016/j.renene.2016.12.091>
- Raj, A.K., Srinivas, M., & Jayaraj, S. (2019). A cost-effective method to improve the performance of solar air heaters using discrete macro-encapsulated PCM capsules for drying applications. *Applied Thermal Engineering*, 146, 910-920. <https://doi.org/10.1016/j.applthermaleng.2018.10.055>
- Romero, V. M., Cerezo, E., Garcia, M.I., & Sanchez, M.H. (2014) Simulation and validation of vanilla drying process in an indirect solar dryer prototype using CFD fluent program. *Energy Procedia*, 57, 1651-1658. doi: 10.1016/j.egypro.2014.10.156

- Sallam, Y.I., Aly, M.H., Nassar, A.F., & Mohamed, E.A. (2015). Solar drying of whole mint plant under natural forced convection. *Journal of Advanced Research*, 6, 171-178. <http://dx.doi.org/10.1016/j.jare.2013.12.001>
- Sami, S., Etesami, N., & Rahimi, A. (2011). Energy and exergy analysis of an indirect solar cabinet dryer based on mathematical modeling results. *Energy*, 36, 2847-2855. <https://doi.org/10.1016/j.energy.2011.02.027>
- Sandali, M., Boubekri, A., Mennouche, D., & Gherraf, N. (2019). Improvement of a direct solar dryer performance using a geothermal water heat exchanger as supplementary energetic supply. An experimental investigation and simulation study. *Renewable Energy*, 135, 186-196. <https://doi.org/10.1016/j.renene.2018.11.086>
- Singh, S., & Kumar, S. (2012). New approach for thermal testing of solar dryer: Development of generalized drying characteristic curve. *Solar Energy*, 86, 1981-1991. <http://dx.doi.org/10.1016/j.solener.2012.04.001>
- Singh, S., & Kumar, S. (2013). Solar drying for different test conditions: Proposed framework for estimation of specific energy consumption and CO₂ emissions mitigation. *Energy*, 51, 27-36. <http://dx.doi.org/10.1016/j.energy.2013.01.006>
- Singh, M., & Sethi, V.P. (2018). On the design, modelling and analysis of multi-shelf inclined solar cooker-cum-dryer. *Solar Energy*, 162, 620-636. <https://doi.org/10.1016/j.solener.2018.01.045>
- Şevik, S., Aktaş, M., Doğan, H., & Koçak, S. (2013). Mushroom drying with solar assisted heat pump system. *Energy Conversion and Management*, 72, 171-178. <http://dx.doi.org/10.1016/j.enconman.2012.09.035>
- Şevik, S. (2014). Experimental investigation of a new design solar-heat pump dryer under the different climatic conditions and drying behavior of selected products. *Solar Energy*, 105, 190-205. <http://dx.doi.org/10.1016/j.solener.2014.03.037>
- Tiwari, S., & Tiwari, G.N. (2016). Thermal analysis of photovoltaic-thermal (PVT) single slope roof integrated greenhouse solar dryer. *Solar Energy*, 138, 128-136. <http://dx.doi.org/10.1016/j.solener.2016.09.014>
- Tunde-Akintunde, T.Y. (2011). Mathematical modeling of sun and solar drying of chili pepper. *Renewable Energy*, 36, 2139-2145. doi:10.1016/j.renene.2011.01.017
- Varun, S., Sharma, A., & Sharma, N. (2012). Construction and Performance Analysis of an Indirect Solar Dryer Integrated with Solar Air Heater. *Procedia Engineering*, 38, 3260-3269. doi: 10.1016/j.proeng.2012.06.377
- Vasquez, J., Reyes, A., & Pailahueque, N. (2019). Modeling, simulation and experimental validation of a solar dryer for agro-products with thermal energy storage system. *Renewable Energy*, 139, 1375-1390. <https://doi.org/10.1016/j.renene.2019.02.085>
- Yahya, M., Fudholi, A., Hafizh, H., & Sopian, K. (2016). Comparison of solar dryer and solar-assisted heat pump dryer for cassava. *Solar Energy*, 136, 606-613. <http://dx.doi.org/10.1016/j.solener.2016.07.049>

Zoukit, A., El Ferouali, H., Salhi, I., Doubabi, S., & Abdenouri, N. (2019). Takagi Sugeno fuzzy modeling applied to an indirect solar dryer operated in both natural and forced convection. *Renewable Energy*, 133, 849-860. <https://doi.org/10.1016/j.renene.2018.10.082>

A large, stylized graphic for Chapter 20. It features a central circle with a green upper half and a white lower half. The text 'Chapter 20' is written in a black, cursive font on the green background. Below it, 'BIOCOMPUTING AND BIOCOMPUTERS' is written in a bold, black, sans-serif font on the white background. At the bottom, 'Esra ŞATIR 1' is written in a black, italicized font. The entire graphic is surrounded by a glowing yellow aura and a green line that curves around it.

Chapter 20

BIOCOMPUTING AND BIOCOMPUTERS

Esra ŞATIR ¹

1. Introduction

Silicon-based computer systems play a dominant role in technology. Therefore, modern computing is based on the Boolean logic operations which are executed by binary numbers. Binary numbers are used to perform logical operations that assigned “true” to “1” in bit form and “false” to “0”. As the result of limited capacity of silicon and increasing computational demands alternative solutions for building computer systems are investigated. Thus, biomolecules are expected to solve these demands and additionally, complex problems that are difficult to handle by traditional silicon-based computers (Geng et al., 2020).

Bioelectronics is a multidisciplinary research field that combines biology and electronics for implementing electronic functions on the chip using biomolecules. Biomolecules are the essential mediums for development of bioelectronic devices since they have inherent properties like redox properties of metalloproteinase and catalytic reaction of the enzymes. Bioelectronics is being recognized that is able to overcome the current limitations of conventional silicon-based devices by taking advantage of the unique characteristics of nanometer-sized biomolecules (Yoon et al., 2022).

Because of these discoveries, the biochemical systems performing various logic operations like AND, OR, XOR, simple computing steps like full-adder/full-subtractor and auxiliary computing processes like molecular multiplexing/demultiplexing have been formulated. However, there are two major problems in this area: 1) There are still a few biomolecular computer systems in practice. So, a real biocomputer or a biocomputing system is not feasible in today’s level of technology except some simple logic games like tic-tac-toe. 2) Biomolecular systems should have enough number of individual logic elements connected in complex computing networks, similar to electronic systems. This will allow to perform real computational tasks as it is done in computers (Guz et al., 2016).

Biological materials, such as DNA fragments, RNA fragments and even whole cells are targeted to be employed for computational tasks. The concerning approaches in this field are various since the biological systems are highly complex. Due to these factors, the suggested approaches for designing bio-computational systems can be sought in living systems at various levels of their organization. On the other hand, multicellular systems are capable of acting as computational instruments where brain itself is the most efficient example (Gotovtsev et al., 2020).

This study has been organised as follows: In section 2, biocomputaion concept has been investigated with the possible biologic mediums for biocomputation. In section 3, the concept of biocomputer has been evaluated by considering

the traditional computer systems. Finally, a general outcome has been reached in section 4.

2. Biocomputation

The most simple bioinformatics components are enzymes and antibodies. Since they recognize self-molecules, they can be considered as bioelectronics preprocessors. The antigenic molecule, which is a non-self material for the body, is taken as an input signal. The chemical transformation as the result of chemical reactions to protect the body, can be considered as the output. Structural genes store the strict work-flows of antibodies, enzymes, ribosomes and etc. Since these work-flows are defined as sequential nucleotides and they are not trained, the term “preprocessor” is proven. Various levels of organisations for designing biological systems is shown in Fig.1.

The weight of a biological molecule is of the order of 10^5 . The weight of amino acids part is of the order of 10^3 . The active section which indirectly interacts input molecule section contains 3-10 amino acids. There is no energetic pumping in antibodies and enzymes which is significant for genome and ribosomes. Atoms are in basic state in the beginning and so it is possible to substitute Josephson oscillator model by the simplest one that is the combination of one dimensional electronic oscillators. It can be interpreted as the simplest coherent process because of the synchronisation of atom-electron oscillator with zero vibration. From quantum theory of dispersion forces, the vibration between the atoms are additive with good accuracy. Thus, the total interaction of N atoms will be N^2 . This interaction energy will be nearly $1eV$ if N is kept at 30 (Bannikov, 1996). In this section, we are going to investigate the biological materials with the aim of computing.

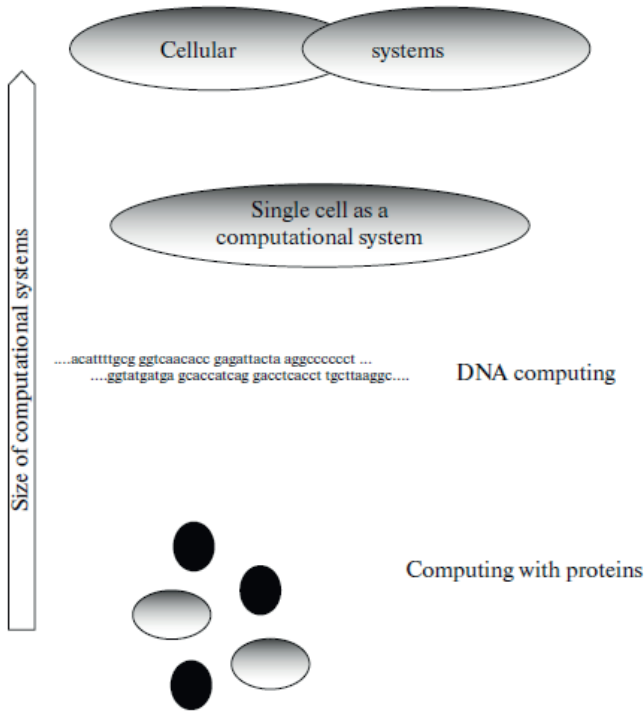


Figure 1. Various levels of organisations for designing biological systems (Gotovtsev et al., 2020).

2.1. Computations via protein molecules

Because of their multiplicity of structural variants, catalytic properties, and capability of playing a role in electrochemical processes proteins provide broad opportunities for designing biocomputer components. However, protein structures are difficult to predict from the amino acid sequence. But several recent studies were aimed at creating the biological components that could be used as components of computational systems, focusing primarily on transistors. In the beginning of 2000s, application of metalloproteins as transistors is a promising field. But it was noted that such a transistor could work only in an aqueous medium of a certain chemical compositions and its operating efficiency was highly limited by oxidation rate and reduction processes. Nowadays, this issue is investigated in the scope of synthetic biology.

Another biological component showing characteristic of a transistor is an antibody conjugated with two gold nanoparticles. In addition to this, it was noted

that the designed biotransistor was shown to be gated by an optical signal when a quantum dot was attached to the antibody.

If we consider logic gates as another issue, Cascades of enzymatic reactions can be employed. Fig.2 shows a few of the simplest logical elements based on enzymatic reactions.

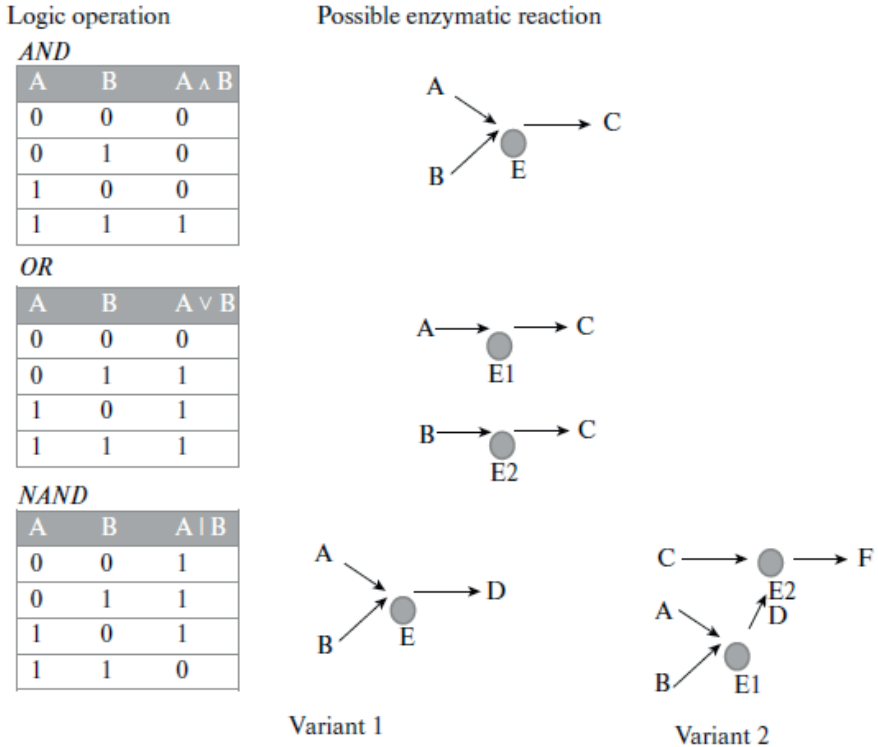


Figure 2. Logic gates based on enzymatic reactions(Gotovtsev et al, 2020).

AND can be represented by a simple synthetic or an ATP-dependent enzymatic reaction. In the latter case, an enzyme converts the substance A to substance C by utilizing Adenosine Triphosphate (ATP), which can be taken to be the substance B. *OR* can be designed using two reactions which use similar substrates to yield the same product. *NAND* can be designed the same way as *AND* but the product D is taken to be zero. In spite of these developments, a protein based functional computational instrument has not been constructed (Gotovtsev et al., 2020).

2.2. Nucleic Acid based computers

In recent years, DNA logical circuits are constructed to implement multiple functions based on functional DNA structures and DNA-based hybridizations as seen in Figure 3. Many basic/advanced logical DNA operations or even functional logic circuits were designed and carried out in the literature. Despite significant advancements in DNA computing, there are still a range of restrictions like producing undetectable optical signals, being incapable of realizing complex mathematical operations and the lack of a whole platform to integrate multiplex logic operations (Geng et al., 2020). That's why we are going to investigate DNA in terms of its usage for information processing.

During information processing process, information is firstly encoded in the primary structure of the molecule thus the code is rendered to be simple to read. Then, information of one molecule will be possible to read from at several locations simultaneously. And finally, a DNA molecule is possible to cut at certain sites with restriction enzymes to produce fragments with sticky ends. Theoretically, this makes DNA possible to perform a large number of computations in parallel by using many molecules. That's why the most impressive demonstrations of biocomputing systems were consequently made with DNA computers. Accordingly, the first DNA computers included the following steps:

- An encoding method and DNA molecules which were synthesized by considering this encoding method,
- Determination of biochemical methods to perform the necessary reactions and ligases and restriction nucleases,
- Reactions carried out in parallel
- PRC and electrophoresis to read the computation results.

The most popular implementation of DNA computers, is the traveling salesman problem. Calculation of the square root (Gotovtsev et al., 2020).

2.3. Human Brain

The mystery of how brain works is fascinating. The human brain is an enormous neural network where billions of neurons make connection with each other via synapses as indicated in Fig. 3a-d. The human brain can perform complex computation tasks in parallel with low power consumption, significant fault tolerance and strong robustness by means of its complicated connectivity and the systematic hierarchy. As denoted in Fig. 3e, a high-performance AI chip is needed to obviate the gap between artificial computing platforms and the human brain.

From an algorithmic point of view, scientists generally interested in brain-like computing. Artificial Neural Networks (ANNs) is the concrete example of this field.

From a hardware point of view, synaptic and neuronal computations are critical. Traditional implementation of synaptic plasticity and neuronal dynamics based on nonbiomimetic complementary metal–oxide–semiconductor transistor (CMOS) circuits require higher power consumption and larger chip space. However, the developments in microelectronics and materials science made novel functional devices possible to perform (Yang et al., 2020).

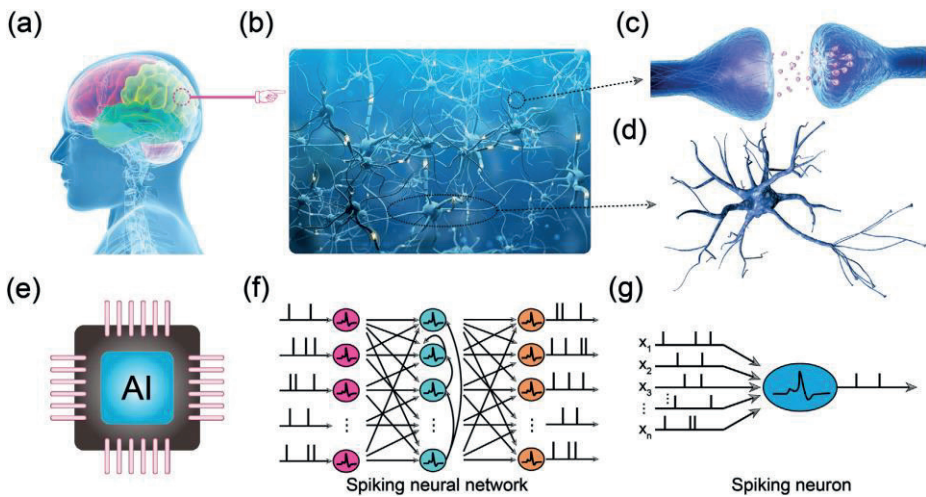


Figure 3. Demonstration of biological and artificial computing systems. a) Human brain. b) Biological neural network. c) Biological synapse. d) Biological neuron. e) AI chip. f) Spiking neural networks. g) An artificial spiking neuron (Yang et al., 2020).

3. Closer to Biocomputer

Several important features distinguish modern computers from biocomputers in terms of information input and output, random access memory and the most important issue; the capability of executing a broad variety of algorithms. A biocomputer should have all of these elements in order to be classified as a computer (Gotovtsev et al., 2020). Namely, the ultimate goal of combining molecular biology and engineering is to form a biocomputer. Synthesis of fundamental Boolean logic gates and design of genetic oscillator, have been partly succeeded. However, the rapid development in synthetic biology made development a class of combinational and sequential genetic logic circuits for specific applications possible since most of the biochemical reactions can be

described in terms of mathematical models. Besides, employing computer simulation before conducting real-world experiments is a confirmation stage (Lin et al., 2018).

To build up a functional bio-computer there should be a universal coding style, a memory, a processing unit (CPU) and peripheral devices. In this section, we are going to discuss whether adaptation of these mentioned components of traditional computer systems starting from coding styles to peripheral devices is possible to biocomputer systems.

3.1. Arithmetic coding via genetic codes

Information systems are produced by arithmetic coding. Numeration system is necessary for arithmetic calculations. Genetic code is a *sui generis* alphabet of genetic texts. Nature of these texts has been investigated but computing has not been clearly performed in genetic text since their digital nature is not clear. However, amino acids can hardly be digitized because of their hydrophobicity. Thus, the nucleons in amino acids seem more suitable for arithmetic operations.

Accordingly, we can make an assumption that some organelles of a cell could work as biocomputers. The only essential thing which has to be done is to discover their number systems. It is reported that the genetic code has many similarities with the ASCII code (shCherbak, 2003).

3.2. A simple biocomputer model

The biocomputing system should perform the similar tasks of conventional computing system using biomolecules instead of silicon- or inorganic-based components. Although bioelectronic functions are conducted at the protein or nucleic acid level in nowadays' conditions, it is expected that the development of a biocomputing system could be ultimately possible in the near future via the convergence of different functional bioelectronic devices and demonstration of electronic functions at the cellular level (Yoon et al., 2022).

A prototype bio-arithmetic architecture is proposed by Kuo et al. in 2016 which forms a fundamental development for the biocomputer. The simplified architecture is shown in Fig. 4. There are minimally four genetic regulatory circuits connected consequently. There are a trigger, a four bit genetic full adder and a two four bit parallel input and parallel output (PIPO) genetic registers. One of these registers is served as a temporary register and while another one is being served as a genetic accumulator.

Here, this simple construction is enough to perform three fundamental operations; fetching, arithmetic addition and data storing. In the design of a biocomputer, all functional modules should be realised by gene circuits (Kuo et al., 2017).

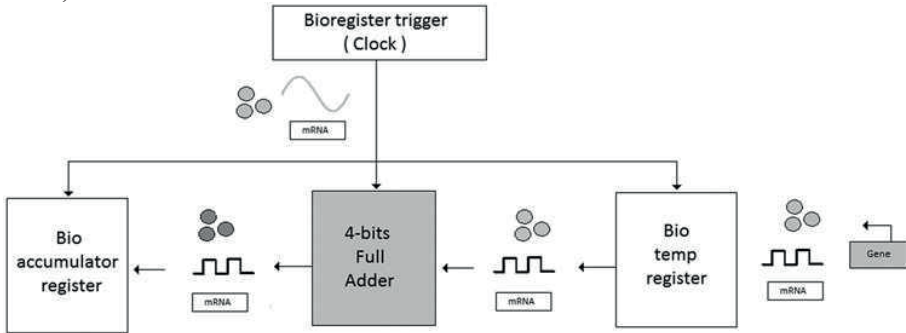


Fig 4. Schematic diagram of a simplified biocomputer (Kuo et al., 2017).

3.3. Biomemory

Memory is one of the most important components of computer systems where storing is performed. Many significant researches have been performed to develop efficient memory functioning devices by controlling two distinct states; “0” and “1” in conventional silicon-based electronic memory devices. However, the main limitations of semiconductor oriented computing systems are the thickness limitation of silicon-based circuits and the occurrence of errors or malfunctions due to the increased degree of integration in the circuit.

In biomemories where the unique characteristics of biomolecules are used, memory functions can be conducted at the nanometer scale. Metalloproteins offer great advantages for biomemory because the state of the metal ions (oxidation and reduction) can be controlled by external electrical or electrochemical stimulation. Nucleic acid, especially DNA, is another molecule that has also attracted attention for the development of biomemory. At the same time, DNA has been widely used to develop the biomemristor, known as the resistive random-access memory (ReRAM) device, which has been researched for commercialization because of its rapid processing, high storage density, and low energy consumption. The biomemristor is recognized as the next standard for biomemory. In addition to DNA, some researches have been conducted by developing metalloproteins, and nucleic acids by combining novel nanomaterials with RNA, chitosan, and viruses (Yoon et al., 2022).

3.4. Bioprocessing device

Processing is the essential task in all electronic systems that processes and converts input information to output data. Conventional silicon-based electronic processing devices have reached physical and technological limitations since the number of electronic elements are concentrated in a limited area. This results in problems, such as high energy consumption and heat generation. Moreover, the electrical current often leaks and flows to adjacent electronic elements value due to the excessive miniaturization of the processing devices. This causes unstable processing functions and errors in the output. Therefore, there is a strong need to find new materials to overcome these issues.

Biomolecules can be used to realize the processing function. Here, DNA provides a great alternative medium that shows excellent characteristics, like massive parallel data processing, simple design of relatively complex circuits and affordability. As a concrete example, DNA switching circuits based on the DNA strand displacement reactions were developed for the implementation of arbitrary Boolean functions (Yoon et al., 2022).

Enzymes are another alternative of biomolecules employed for developing bioprocessing devices. When compared to DNA-based bioprocessing, they have several advantages like highly selective reaction with various substances and rapid response. As a different approach, bioprocessing inside living organisms has been suggested using the DNA origami technique. In this study, various logic functions were emulated inside cockroaches (Amir et al., 2014).

3.5. Peripheral bioelectronic components

In addition to the biodevices discussed above, there are some attempts to develop the peripheral components such as bioantenna and biokeypad lock. In the design of a bioantenna; only a signal of a desired type is received and then the received information is transmitted to another medium, as similar to the operation principle of a conventional antenna. This task can be provided by utilizing the specific binding properties between biomolecules. Enzyme is the most broadly used material for this purpose.

Biokeypad lock system is another peripheral component that is studied to demonstrate the molecular keypad system functions using biomolecules. Here, the biokeypad lock can suggest a more secure lock system when compared to the other simple molecular keypad systems since a correct combination of biomolecular inputs (such as biomolecules or enzymatic reactions) is enable to grant the secure and classified passwords (Yoon et al., 2022).

4. Conclusion

Although nature and computers seems to be unrelated concepts, the reached point of today's technological conditions made researchers to combine them in order to develop a new design that is tiny, has lower energy consumption and massive parallelism. Nature has significant components for realizing such design. DNA, proteins with RNA and enzymes are the most evaluated components of nature for biocomputing and designing a biocomputer.

There are many significant studies in the literature which focus on coding information in biological molecules, the design of biologic gates, biotransistor, biomemory and bioprocessing unit. Additionally, some researches focus on the design of peripheral components like bioantenna or biokeypad. Also, a simple biocomputer model has been proposed (refer to subsection 3.2).

However, these studies are not enough if we consider the traditional computer system with its all tasks from presenting the input to taking storing or taking the output. This problem originates from the unpredictable and unstable structure of biomolecular components in the nature. Despite this undesired specification for traditional computer systems, biocomputation and development of the design of a biocomputer is gaining a huge attraction.

REFERENCES

- Amir, Y., Ben-Ishay, E., Levner, D., Ittah, S., Abu-Horowitz, A., Bachelet, I., (2014). *Nat. Nanotechnol.* 9: (5), 353–357.
- Bannikov, V., S., (1996). Bioelectronic information-computing mediums, *Biosensors and Bioelectronics*, 11: (9): 933-945
- Geng, H., Yin, Z., Zhou, C., Guo, C., (2020). Construction of a simple and intelligent DNA-based computing system for multiplexing logic operations, *Acta Biomaterialia*, 118: 44-53
- Gotovtsev, P., M., Kirillova, D., A., Vasilov, R., G., (2020). Biocomputers: Problems They Solve, State of the Art, and Prospects. *Nanotechnol Russia* 15: 3–12
- Guz , N., Fedotova, T., A., Fratto, B., E., Schlesinger, O., Alfonta, L., Kolpashchikov, D., Katz, E., (2016). Bioelectronic interface connecting reversible logic gates based on enzyme and DNA reactions, *ChemPhysChem* 17:2247–2255
- Kuo, T., Y., Lin, C., L., Charoenkit, N., Chen, Y., Y., Preuksakarn, C., (2017). Toward theoretical synthesis of biocomputer. *IET Syst Biol.*, 11: (1), 36-43
- Lin, C., L., Kuo, T., Y., Li, W., X., (2018). Synthesis of control unit for future biocomputer, *Journal of Biological Engineering*, 12: (14), <https://doi.org/10.1186/s13036-018-0109-4> PMID: 30127848
- shCherbak, V., I., (2003). Arithmetic inside the universal genetic code, *Biosystems*, 70: (3), 187-209, doi: 10.1016/s0303-2647(03)00066-2
- Yang, J., Q. Wang, R., Ren, Y., Mao, J., Y., Wang, Z., P., Zhou, Y., Han, S., T., (2020). Neuromorphic engineering: from biological to spike-based hardware nervous systems, *Adv. Mater.* 32, 2003610 (2020).
- Yoon, J., Lim, J., Shin, M., Lee J, Y., Choi, J., W., (2022). Recent progress in nano-material-based bioelectronic devices for biocomputing system, *Biosensors and Bioelectronics*, 212, <https://doi.org/10.1016/j.bios.2022.114427>

The title 'Chapter 21' is written in a large, bold, black, cursive font. It is centered within a green semi-circular shape that is part of a larger circular graphic. The graphic consists of a white circle with a green semi-circle on top and a green line that curves around the bottom and sides, creating a frame-like effect. The background of the circle has a subtle radial gradient.

Chapter 21

MATLAB/SIMULINK SUPPORTED ANALYSIS OF RL AND RC CIRCUITS

Hilmi ZENK¹

Birol ERTUĞRAL²

1 Assoc. Prof. Dr. Hilmi ZENK, <https://orcid.org/0000-0002-1653-8580>, Department of Electrical and Electronics Engineering, Giresun University, 28200 Giresun, Turkey.

2 Prof. Dr. Birol ERTUĞRAL, <https://orcid.org/0000-0002-4376-3476>, Department of Physics, Giresun University, 28200 Giresun, Turkey.

RL and RC circuits are electrical circuits that contain resistors (R), inductors (L) and capacitances (C). It is important that these circuits explain the complex dimensions of electric current and voltage and use them in various applications. In this study, scientific analysis of RL and RC circuits was made, then numerical data was produced on theoretical examples and tried to be proven through the MATLAB/Simulink computer program.

I. ANALYSIS OF RL CIRCUITS

If we examine the transient regime of a simple series circuit consisting of resistance and inductance in Figure-1, let's find the change of $i(t)$ assuming that $i(0) = I_0$ at time $t=0$; Based on the circuit equation;

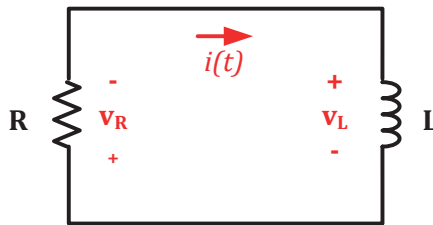


Figure-1. Simple RL circuit and definition of electrical parameters.

$$\begin{aligned}
 V_R + V_L &= R \cdot i + L \cdot \frac{di}{dt} = 0 \\
 \frac{di}{dt} + \frac{L}{R} \cdot i &= 0
 \end{aligned}
 \tag{1}$$

$$\frac{di}{dt} = -\frac{R}{L} \cdot dt
 \tag{2}$$

$$\begin{aligned}
 \int_{I_0}^{i(t)} \frac{di}{i} &= \int_0^t -\frac{R}{L} dt \\
 \ln i \Big|_{I_0}^1 &= -\frac{R}{L} t \Big|_0^t = \ln i - \ln I_0 = -\frac{R}{L} t \\
 i(t) &= I_0 \exp\left(-\frac{R}{L} t\right)
 \end{aligned}
 \tag{3}$$

The result is found. In another solution method, assuming that the solution of equation (1) is in exponential form;

$$i(t) = A \cdot \exp(s_1 t)$$

The constants A and s_1 need to be determined. For this reason, if it is substituted in expression (1);

$$(s_1 + \frac{R}{L}) \cdot A \cdot \exp(s_1 t) = 0$$

For the solution to be different from zero;

$$s_1 = -R/L \quad (4)$$

It should be;

$$i(t) = A \cdot \exp(-\frac{R}{L} t) \quad (5)$$

Initial conditions for finding constant A ;

$$t = 0 \text{ 'da} \quad i(0) = I_0 \quad \text{ile} \quad I_0 = A$$

is found and,

$$i(t) = I_0 \cdot \exp(-\frac{R}{L} t)$$

The same expression is obtained as . Now let's think about the power and energy relations for this circuit; power consumed in resistance;

$$P_R = R \cdot i^2 = R \cdot I_0^2 \cdot \exp(-\frac{2R}{L} t) \quad (6)$$

It is calculated as and the energy converted to heat in the resistance is;

$$w_R = \int_0^\infty P_R \cdot dt = \frac{1}{2} \cdot L \cdot I_0^2 \quad (7)$$

It is found as . Initially, the energy of the inductance is; It is $\frac{1}{2} \cdot L \cdot I_0^2$ and after infinite time, this energy becomes zero and all of it turns into heat in the resistor [1]. From expression (3) in the free behavior of the series connected RL stream;

$$\frac{i(t)}{I_0} = \exp\left(-\frac{R}{L}t\right) \quad (8)$$

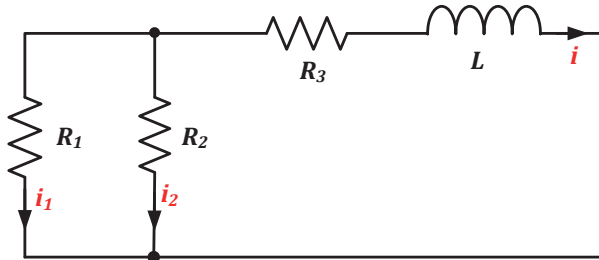
The change of the function for a constant R/L ratio is certain. The

slope of $i(t)/I_0$ at time $t = 0$; $\frac{d}{dt}\left(\frac{1}{I_0}\right)\Big|_{t=0} = -\frac{R}{L}$.

$$\exp\left(-\frac{R}{L}t\right)\Big|_{t=0} = -\frac{R}{L} \quad (9)$$

is available. The L/R ratio is called the time constant and is denoted by τ [2-12].

Example 1: In the circuit in Figure-2, if $i(0) = I_0$ at time $t = 0$, find $i_2(t)$ for $t \geq 0$.



Şekil-2.

Solution: In the circuit in Figure 2, all resistors can be represented with an R_{eq} equivalent resistance.

$$R_{eq} = R_3 + \frac{R_1 R_2}{R_1 + R_2}$$

Time constant of the circuit;

$$\tau = \frac{L}{R_{eq}}$$

is calculated. The current passing through L is,

$$i(t) = i(0) \cdot \exp(-t/\tau) \quad (10)$$

It is defined by equation (10). Current equation for the node in the circuit;

$$i_1(t) + i_2(t) = -i(t) \quad (11)$$

At time $t = 0$;

$$i_1(0) + i_2(0) = -i(0)$$

Voltage at the ends of R_1 ve R_2 resistors;

$$R_1 i_2(t) = R_2 i_1(t) \quad (12)$$

is calculated . From equations (11) and (12);

$$i_2(t) = -\frac{R_1}{R_1+R_2} i(t)$$

If the expression above is substituted,

$$i_2 = -\frac{R_1}{R_1+R_2} \cdot i(0) \cdot \exp(-t/\tau) \quad (13)$$

equation is reached.

Example 2: In the circuit in Figure-3, the initial currents of the inductances are akımları $i_1(0) = i_{10}$, $i_2(0) = i_{20}$. Find $i_1(t)$, $i_2(t)$ and $i(t)$

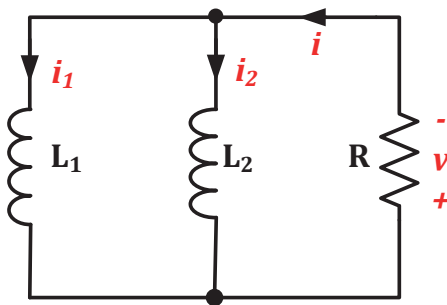


Figure-3

Solution: Equivalent of parallel inductances

$$L_{eq} = \frac{L_1 L_2}{L_1 + L_2} \quad (14)$$

Starting current of the resistor;

$$i(0) = i_1(0) + i_2(0) = i(0) = i_{10} + i_{20}$$

equations can be established. Current flowing through the resistor and voltage across its terminals;

$$i(t) = i_0 \exp\left(-\frac{R}{L}t\right)$$

$$V(t) = R \cdot i_0 \cdot \exp\left(-\frac{R}{L}t\right)$$

and the voltage V in terms of the currents of the inductances;

$$-V = L_1 \cdot \frac{di_1}{dt} = L_2 \cdot \frac{di_2}{dt}$$

equation is established. From here the i_0 current is;

$$\int_{i_{10}}^{i_1} di_1 = -\frac{1}{L_1} \int_0^t R \cdot I_0 \cdot \exp\left(-\frac{R}{L_e}t\right) \cdot dt$$

$$i_1(t) = i_{10} + \frac{L_e}{L_1} \cdot i_0 \cdot [\exp\left(-\frac{R}{L_e}t\right) - 1] \quad (15)$$

Similar to the above expression for $i_2(t)$;

$$i_2(t) = i_{20} + \frac{L_e}{L_2} \cdot i_0 \cdot [\exp\left(-\frac{R}{L_e}t\right) - 1] \quad (16)$$

can be written.

Example 3: In the circuit shown below, the switches are opened at time $t = 1$ after being closed for a long time. According to this;

- $i(1)$ currents when the switch is opened,
- Calculate the $V(1^+)$ voltages for the time value immediately after the switch is opened.
- Design the circuit of the Simulink environment and obtain the desired graph.

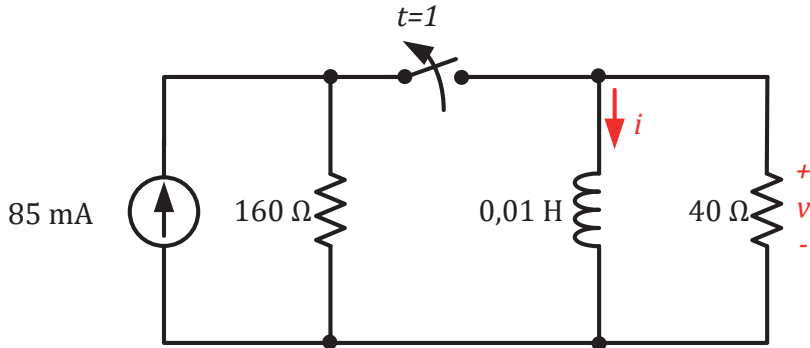


Figure-4.

Solution:

- a) If the initial conditions of the inductance are examined to find the $i(1)$ current when the switch is opened, since the switch remains closed for a long time; Since it will act as a short circuit element, all welding current will pass through it;

$$i(0) = 85 \text{ mA}$$

It is found as.

- b) When the switches are opened at time $t = 1$, two separate independent cells are formed in the circuit. Since the coil current will pass through the eye on the right side with an inductance of 0.01 H and 40 Ohms, the voltage is;

$$V(0^+) = 85 \cdot 10^{-3} \cdot 40 = 3,4 \text{ V}$$

value is calculated.

- c) The equivalent of the circuit in the Matlab/Simulink environment is given in Figure 5. Figure-6 shows the change in inductance current and voltage V on the output resistor immediately after the desired switch position changes in options a and b of the problem.

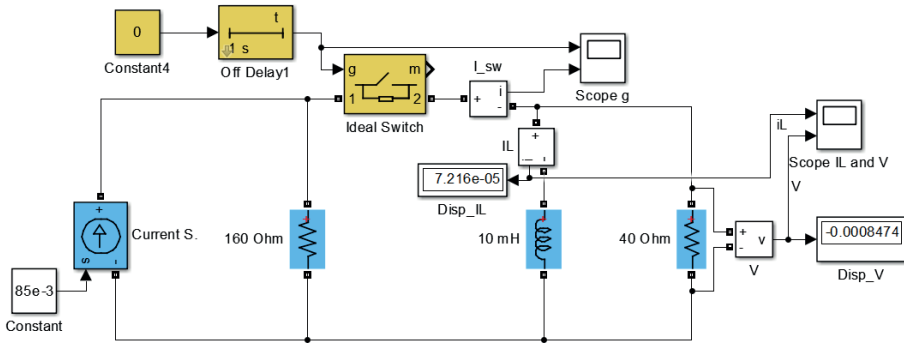


Figure-5.

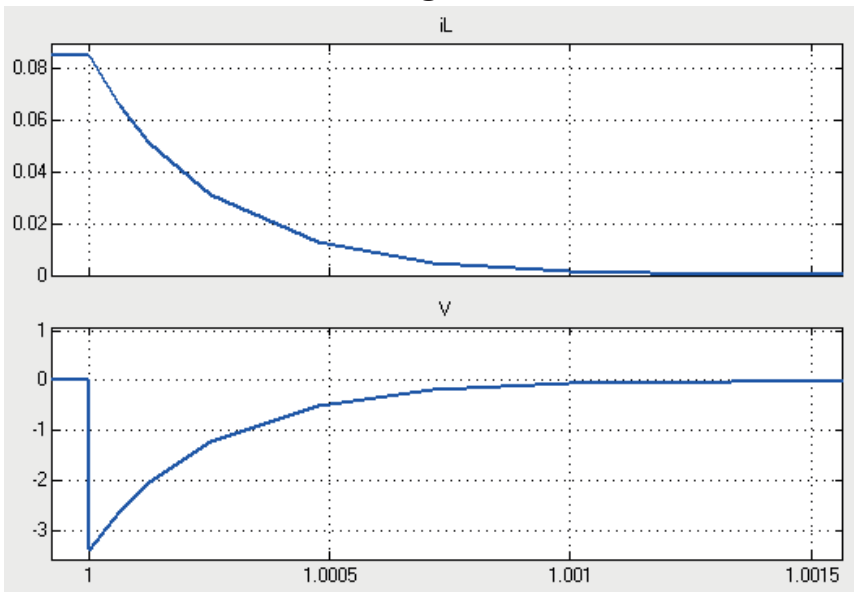


Figure-6.

Example 4: In the circuits shown in Figure-7, the switches are opened at $t = 2$ after being closed for a long time. According to this;

- a) $i(2)$ currents when the switch is opened,
- b) Calculate the $v(2^+)$ voltages immediately after the switch is opened.
- c) Design the circuit of the Simulink environment and obtain the desired graph.

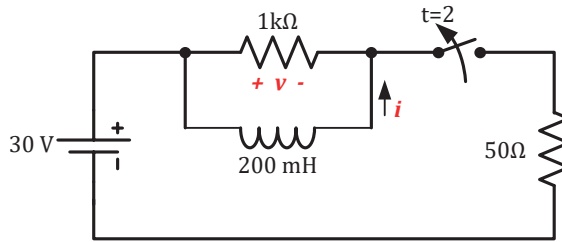


Figure-7.

Solution:

- a) To find the $i(2)$ currents when the switch is opened, consider the inductances as short circuit elements (since the switch remains closed for a long time) and the currents passing through it are;

$$i(2) = 30/50 = 0,6 \text{ A}$$

- b) When the switches are opened at $t = 2$, 200 mH inductance and 1k Ohm coil current will pass in the circuit, and the voltage v on the 1k Ohm resistor is;

$$v(2^+) = 0,6 \cdot 1 \cdot 10^{-3} = 600 \text{ V}$$

is available.

- c) The equivalent of the circuit in the Matlab/Simulink environment is given in Figure-8. Figure-9 shows the change in inductance current and voltage v on the output resistor immediately after the switch changes position.

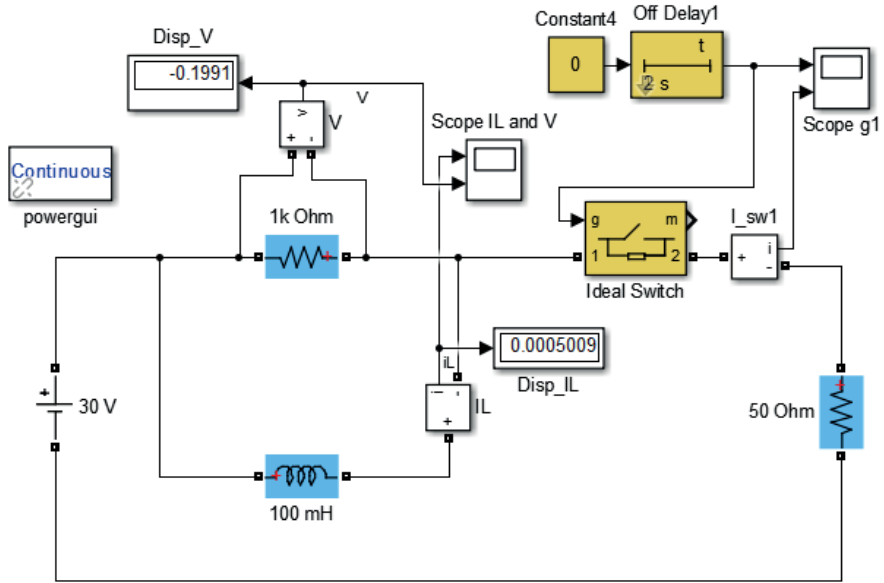


Figure-8.

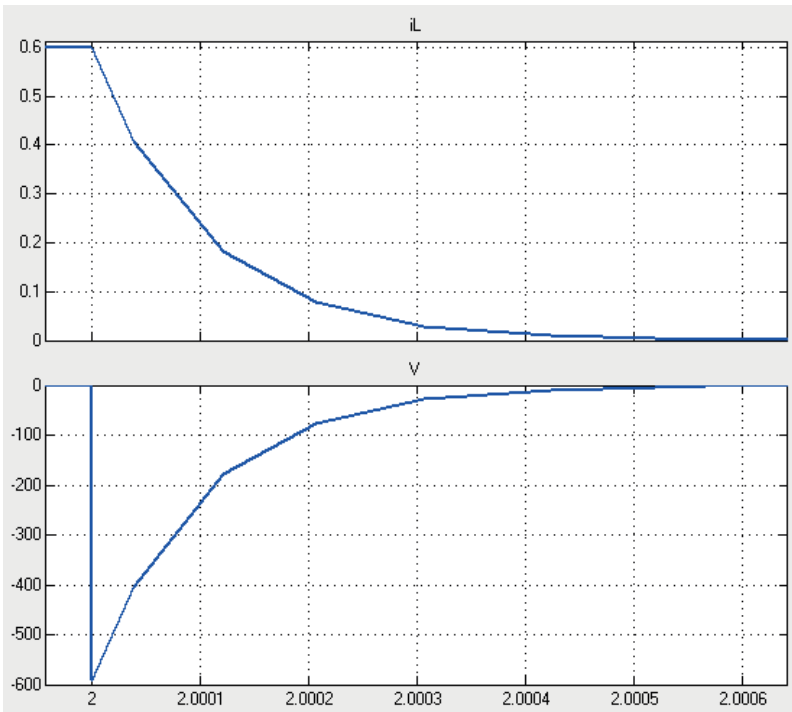


Figure-9.

Example 5: In the circuit in Figure-10, after the switch contact number 4 remained in position a for a long time, it was moved to b at time $t = 1,5$, and to c at $t = 3$ seconds. According to this;

- Find the expression $i(t)$ for the time intervals $t \leq 1,5$, $1,5 \leq t \leq 3$ sec and $t \geq 3$ sec.
- Calculate the values of $i(2)$, $i(2,5)$ and $i(3,5)$.
- Design the circuit of the Simulink environment and obtain the desired values.

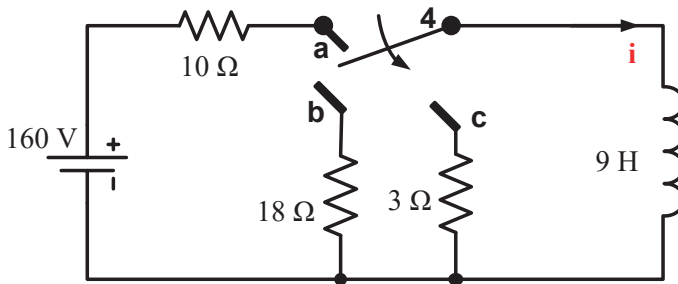


Figure-10.

Solution:

- Since the switch remained in position a for a very long time, the inductance of 9 H was accepted as a short circuit and at the moment $i(1,5^-)$;

$$i(1,5^-) = \frac{160}{10} = 16 \text{ A} \quad (t \leq 1,5)$$

is available. $1,5 \leq t \leq 3$ for the time period;

$$i(t) = i(1,5) \cdot \exp\left(-\left(t - 1,5\right) \frac{R}{L}\right) = 16 \cdot \exp\left(-\left(t - 1,5\right) \frac{18}{9}\right) \text{ A}$$

$$t = 3 \text{ for; } i(3) = 16 \cdot \exp(-2 \cdot 1,5) = 0,796 \text{ A}$$

$t \geq 3$ for; time constant; $\tau = 9/3$ (1/s) is the current;

$$i(t) = i(3) \cdot \exp\left(-\left(t - 3\right) \cdot \frac{3}{9}\right) = 0,796 \cdot \exp\left(\frac{-t-3}{3}\right) \text{ A is available.}$$

- b) The current passing through the inductor is 2nd and 2.5th. value per second;

$$i(t) = 16 \cdot \exp\left(-\left(t - 1,5\right) \frac{18}{9}\right) \text{ A}$$

from equality;

$$i(2) = 16 \cdot \exp\left(-\left(2 - 1,5\right) \frac{18}{9}\right) = 5,886 \text{ A}$$

$$i(2,5) = 16 \cdot \exp\left(-\left(2,5 - 1,5\right) \frac{18}{9}\right) = 2,165 \text{ A}$$

It is found and the current passing through the inductance is 3.5. The value per second is;

$$i(t) = 0,796 \cdot \exp\left(\frac{-t - 3}{3}\right) \text{ A}$$

from equality;

$$i(3,5) = 0,796 \cdot \exp\left(\frac{-3,5 - 3}{3}\right) = 0,673 \text{ A}$$

is calculated.

- c) The equivalent of the circuit in Matlab/Simulink environment is given in Figure-11. Figure-12 shows the change in the inductance current and the voltage V on the output resistor immediately after the switch changes position in parts a and b of the problem..

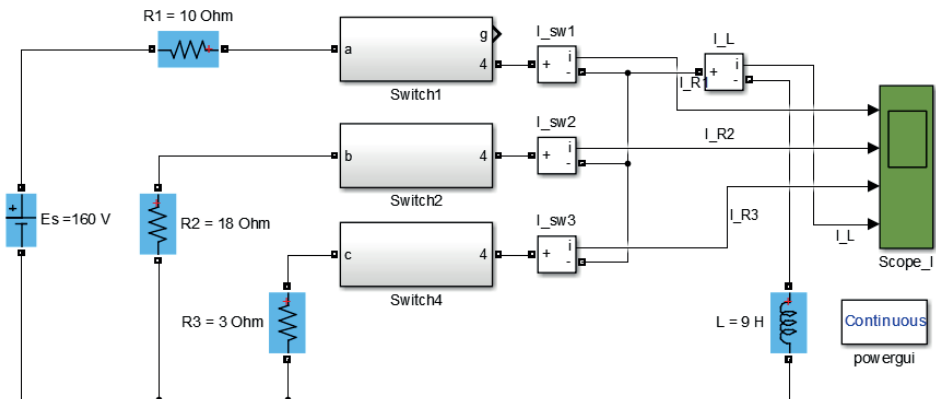


Figure-11.

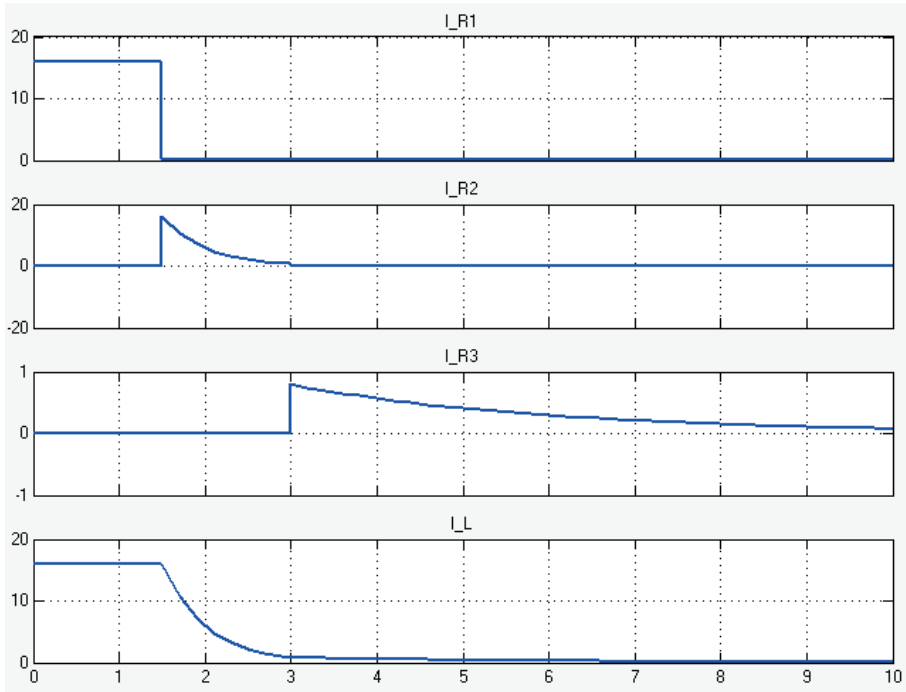


Figure-12.

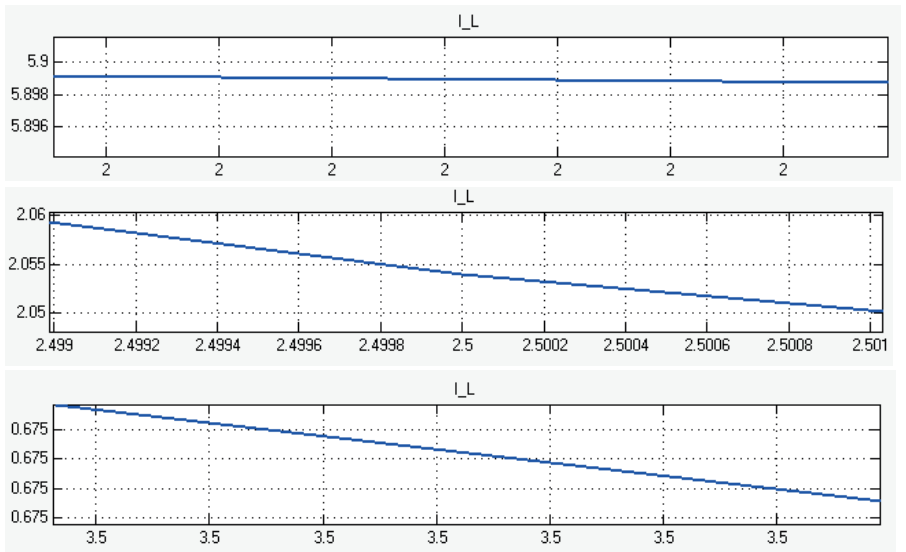


Figure-13.

Example 6: In the circuit in Figure 14, the switch was opened at $t = 0$ after being closed for a long time. According to this;

- a) Find $i_L(t)$ and $i_1(t)$ for $t < 0$ and $t > 0$.

- b) Find the values of $i_L(0,0002)$ and $i_1(0,003)$.
 c) Design the circuit of the Simulink environment and obtain the change graph of i_L and i_1 currents.

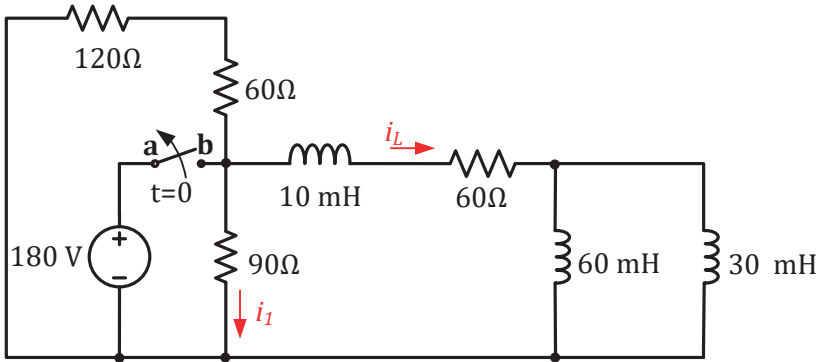


Figure-14.

Solution:

- a) First, if we consider the circuit in Figure 15 a) to calculate $i_L(0^-)$ and $i_1(0^-)$ at time $t = 0^-$

$$i_L(0^-) = \frac{180}{60} = 3 \text{ A} \quad i_1(0^-) = \frac{180}{90} = 2 \text{ A} \quad (t < 0)$$

For $t > 0$; As can be seen in Figure 15 b), if the time constant of the series circuit consisting of an R and L is found;

$$\frac{L}{R} = \frac{30 \cdot 10^{-3}}{120} = \frac{1}{4} \cdot 10^{-3} \text{ (1/sn)}$$

$$i_L(t) = 3 \cdot \exp(-4000t) \text{ A} \quad (t > 0)$$

(13) considering 14 equations;

$$i_1(t) = -\frac{180}{90+180} \cdot 3 \cdot \exp(-4000t) = -2 \cdot \exp(-4000t) \text{ A} \quad (t > 0)$$

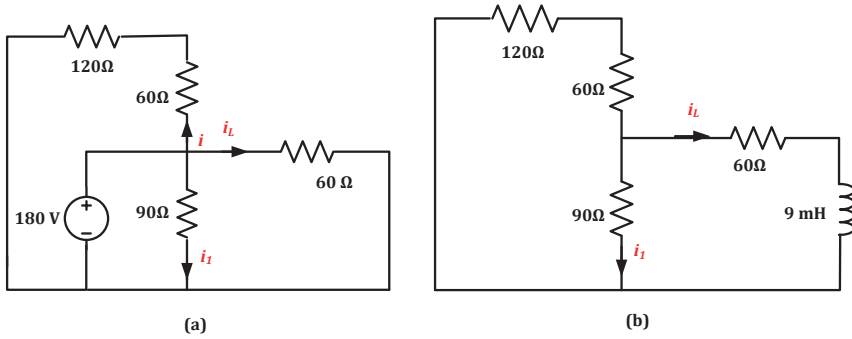


Figure-15.

b) To find $i_L(t)$ values, $i_L(t) = 0,36 \cdot \exp(-4000t)$ A; ($t > 0$) ifadesinden hareketle;

$$i_L(2) = 3 \cdot \exp(-4000 \cdot 0,002) = 3 \cdot \exp(-8) = 1,006 \text{ mA}$$

$i_1(t)$ değerlerini bulmak için; $i_1(t) = -2 \cdot \exp(-4000t)$ A ; based on the expression ($t > 0$);

$i_1(2) = -2 \cdot \exp(-4000 \cdot 0,002) = -0,03$ A, is calculated.

c) The equivalent of the circuit in Matlab/Simulink environment is given in Figure-16. Figure-17 shows the change in the L_1 inductance current and the current of the R_3 resistor immediately after the desired switch position changes in part b of the question

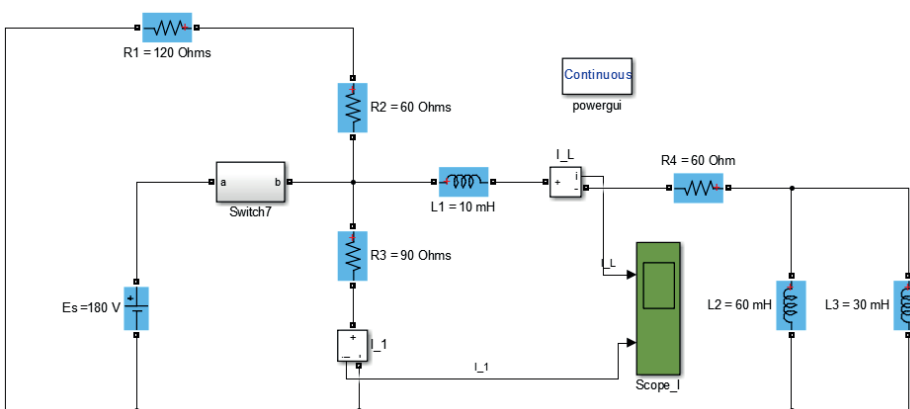


Figure-16.

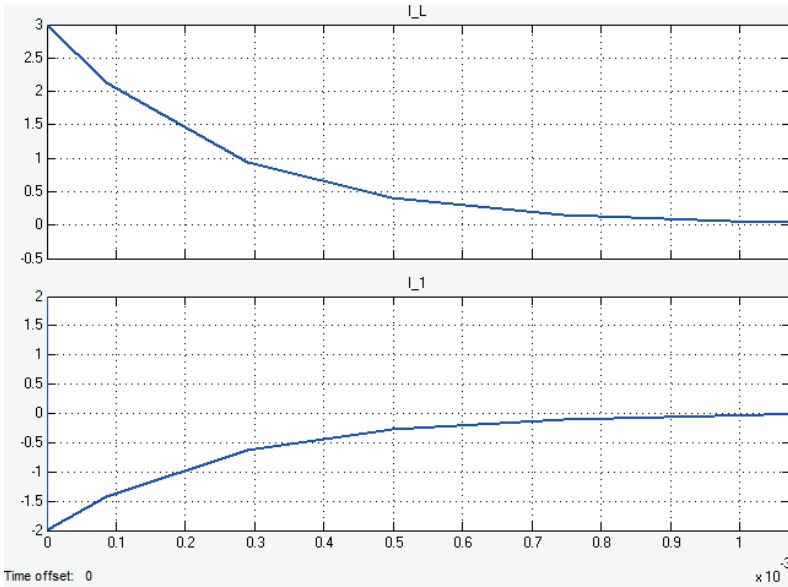


Figure-17

II. ANALYSIS OF RC CIRCUITS

For the closed circuit consisting of resistance and capacitance in Figure-18, let's find the voltage at the capacitance terminals for $t > 0$, assuming that the voltage at the capacitance terminals at $t = 0$ is V_0 , that is, energy has already been stored in the capacity; Current equation for a node;

$$i_C + i_R = 0 \tag{17}$$

is calculated [1-12]. For R and C elements;

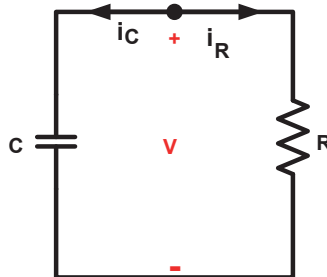


Figure-18. Simple RC circuit and definition of electrical parameters.

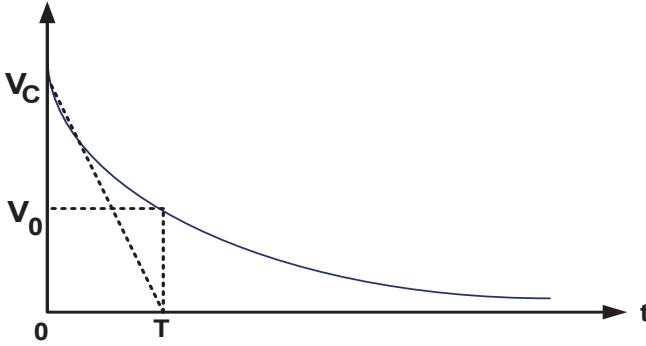


Figure-19.

$$i_R = V/R$$

$$i_C = C \frac{dv}{dt}$$

If the definition relations are replaced in expression 17 and edited;

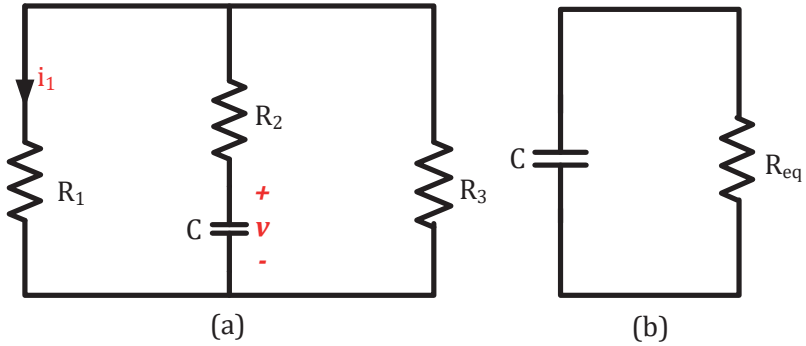
$$\frac{dv}{dt} + \frac{v}{RC} = 0 \quad (18)$$

is available. This expression has the same form as expression (1). In this situation; i and V_0 L/R and RC are replaced, the solution is; Similar to expression (3)

$$V(t) = V(0). \exp\left(-\frac{t}{RC}\right) \quad (19)$$

and time constant is $\tau = RC$. The details of the theorem are explained in Example 7.

Example 7: Şekil 2.11 'deki devrede $t = 0$ anındaki kapasite uçlarındaki gerilim V_0 'dır. $t \geq 0$ için $v(t)$ 'yi ve $i_1(t)$ 'yi bulunuz.

**Figure-20.**

Solution: Equivalent of R_1 and R_3 connected in parallel and R_2 connected in series;

$$R_{eq} = R_2 + \frac{R_1 R_3}{R_1 + R_3} \quad (20)$$

Voltage at capacitance ends for $t \geq 0$ için kapasite uçlarındaki gerilim;

$$v(t) = V_0 \cdot \exp(-t/R_{eq} C)$$

To find the change in the current passing through R_1 , let's first find the initial current.;

$$i(0) = -\frac{V(0)}{R_{eq}} \quad (21)$$

$$R_1 \cdot i_1(0) = \frac{R_1 \cdot R_3}{R_1 + R_3} \cdot i(0) \quad (22)$$

From equations (21) and (22), the current passing through R_1 at $t = 0$;

$$i_1(0) = -\frac{V(0)}{R_{eq}} \cdot \frac{R_3}{R_1 + R_3} \quad (23)$$

becomes and the expression $i_1(t)$ for $t \geq 0$; It is found a; $i_1(t) = i_1(0) \cdot \exp(-t/R_{eq} C)$

Example 8: Calculate $v(0^+)$, $i_2(0^+)$ and $i_4(0^+)$ for the circuit in Figure 21. Show the changes of the parameters examined in the Simulink environment over time.

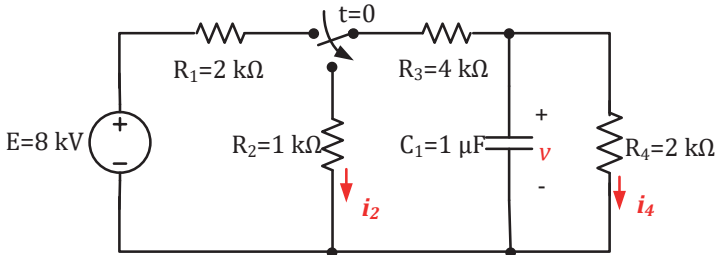


Figure-21

Solution:

In the circuit in Figure-21, for the moment $t = 0^-$, the current passing through the $R_4 = 1\text{ k}\Omega$ resistor connected in parallel to the capacity (considering the capacity as an open circuit);

$$i_4(0^-) = 8 \text{ kV} / 8 \text{ k}\Omega = 1 \text{ A}$$

It is found. For $t < 0$, the voltage on resistor R_4 will be the same as the voltage v ;

$v(0^-) = i_4(0^-) \cdot R_4 = 2000 \cdot 1 = 2000 \text{ V}$ and $v(0^-) = v(0^+) = 2 \text{ kV}$ It is found.

Immediately after the moment $t = 0$, when the switch changes position, the currents in the circuit will be shaped by the capacitor voltage. According to this; The current of the eye formed by C_1 , R_3 and R_2 ;

$$i_2(0^+) = \frac{v(0^+)}{R_3 + R_2} = \frac{2000}{4000 + 1000} = 0,4 \text{ A}$$

It is found. Similarly;

$$i_4(0^+) = \frac{v(0^+)}{R_4} = \frac{2000}{2000} = 1 \text{ A}$$

It is found. The equivalent of the circuit in Matlab/Simulink environment is given in Figure-22. Figure-23 shows the change in the L_1 inductance current and the current of the R_3 resistor immediately after the desired switch position changes in part b of the question.

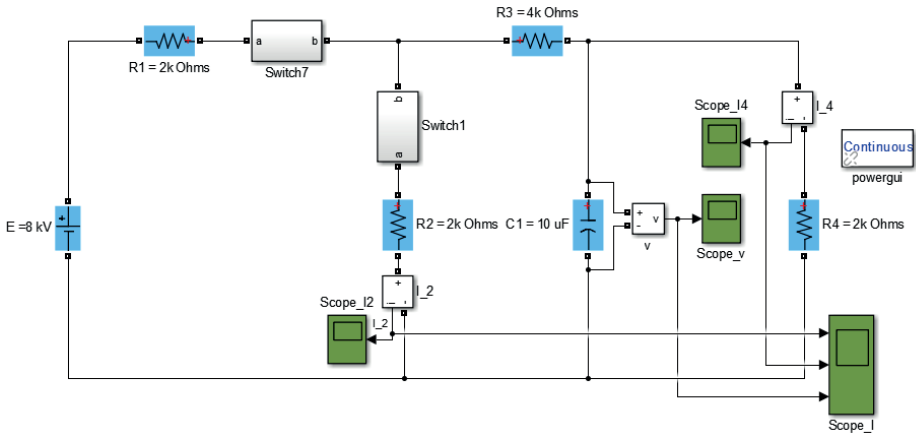


Figure-22.

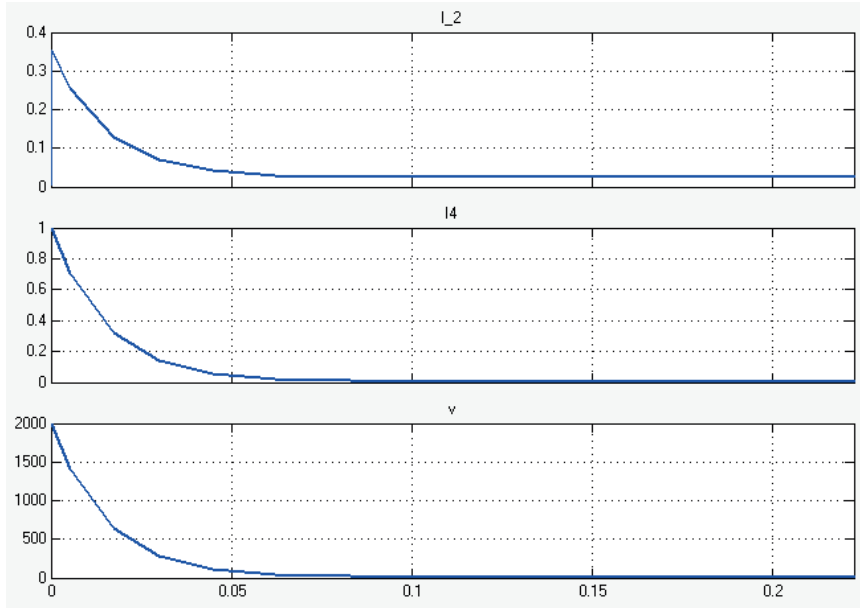


Figure-23.

Example 9: In the circuit in Figure 22, the switch was moved from position b to position a at $t=0$.

- a) Calculate $v(0^+)$ and $i(0^+)$
- b) Show the changes of the parameters examined in the Simulink environment over time.

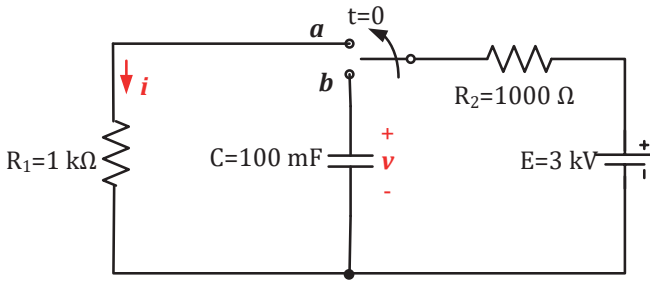


Figure-24.

Solution: Figure-22 for the circuit; $v(0^-) = v(0^+) = 3 \text{ kV}$

$t = 0^+$ for $i(0^+)$;

$$i(0^+) = \frac{v(0^+)}{R_1} = \frac{3000}{1000} = 3 \text{ A} \quad \text{It is found.}$$

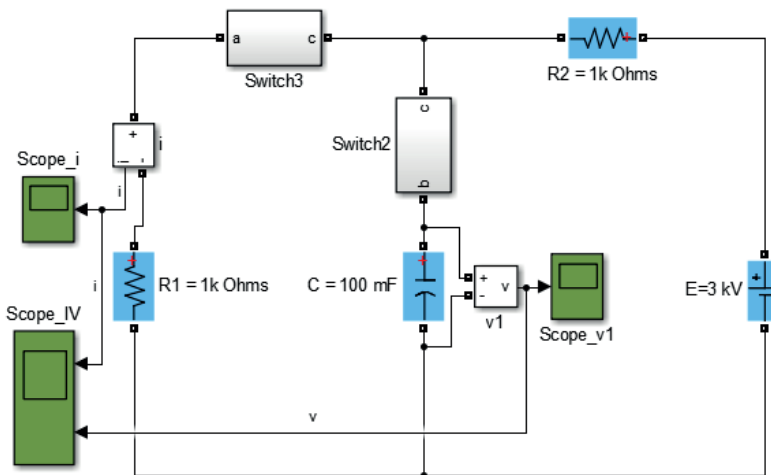


Figure-25.

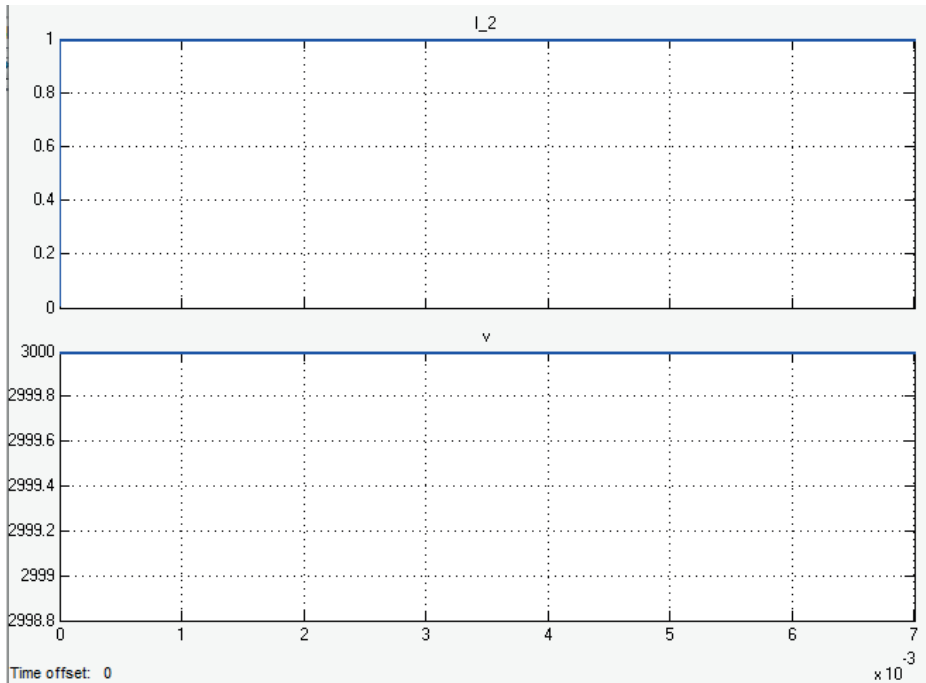


Figure-26.

Example 10: In the circuit in Figure 27, the switch opens at $t = 1$ per second. Calculate $v(1^+)$ and $i(1^+)$ accordingly. Show the change of Simulink software and parameters of this circuit over time.

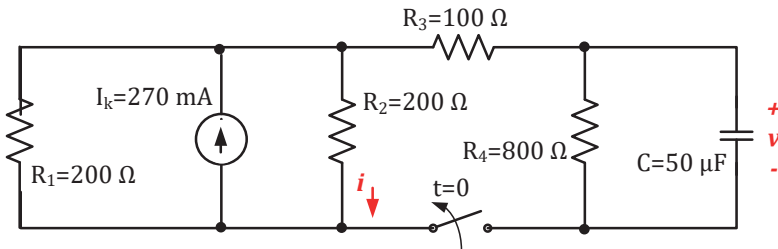


Figure-27.

Solution: For the circuit in Figure-27; To find the capacitance voltage at $t = 0^+$, based on the knowledge that the capacitance is open circuit at $t < 0$, the current passing through resistors R_3 and R_4 is found by using the current division rule. If the current passing through resistor R_3 is i_{R_3} ;

$$i_{R_3}(0^-) = I_k \frac{R_{12}}{R_3 + R_4} = 270 \cdot 10^{-3} \cdot \left(\frac{100}{100 + 900} \right)$$

$$iR_3(0^-) = 27 \cdot 10^{-3} \text{ A}$$

$$v(0^-) = v(0^+) = 800 \cdot iR_3(0^-) = 800 \cdot 27 \cdot 10^{-3} = 21,6 \text{ V}$$

The $i(0^+)$ current is separated from the capacitance and the current I_k is; Since the current will be distributed between the resistors R_1 and R_2 within the framework of the division rule;

$$i(0^+) = I_k \frac{R_1}{R_1 + R_2} = 270 \cdot 10^{-3} \frac{200}{200 + 200} = 135 \text{ mA} \quad \text{It is found.}$$

Matlab / Simulink simulation of the circuit is given in Figure-28, and the change of v and i parameters with time is given in Figure-29.

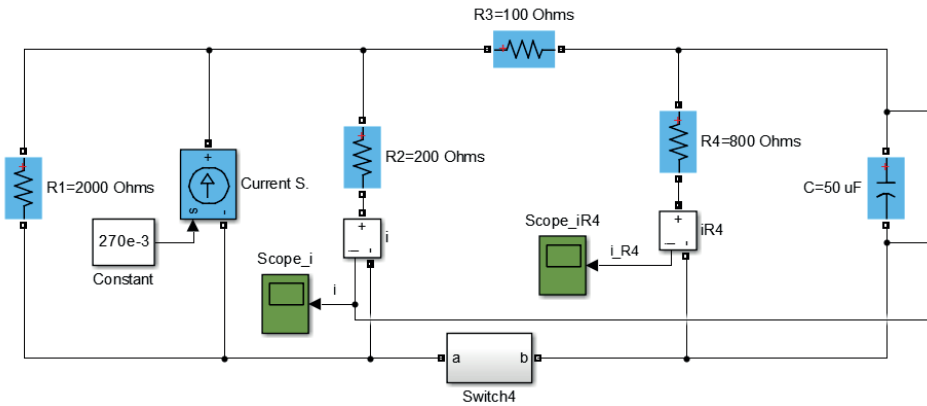


Figure-28.

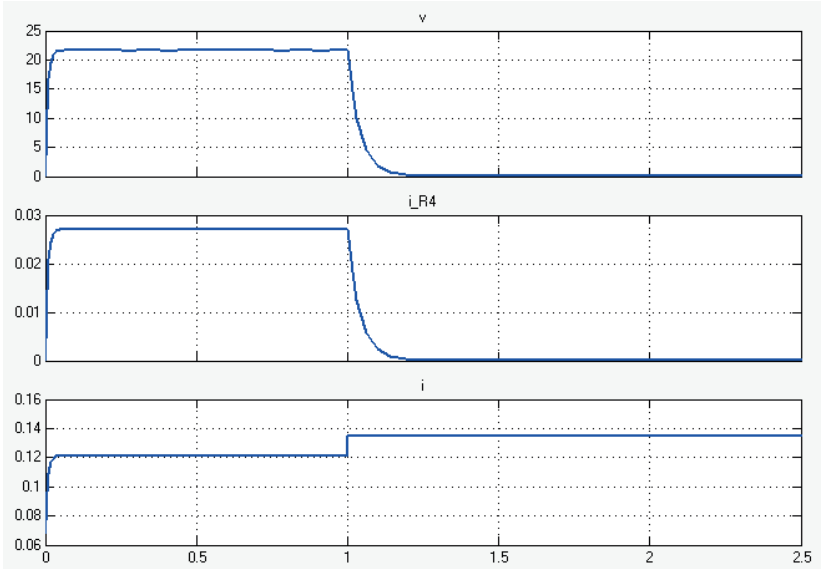


Figure-29.

Example 11: In the circuit shown in Figure-30, after the switch remained in position A for a long time, it was moved to position B at time $t = 2$.

- a) Calculate $V_{C1}(2^-)$, $V_{C2}(2^-)$, $V_{C1}(2^+)$, $V_{C2}(2^+)$ and $V_R(2^+)$.
- b) Find $V_R(t)$ and $i(t)$ for $t > 0$.

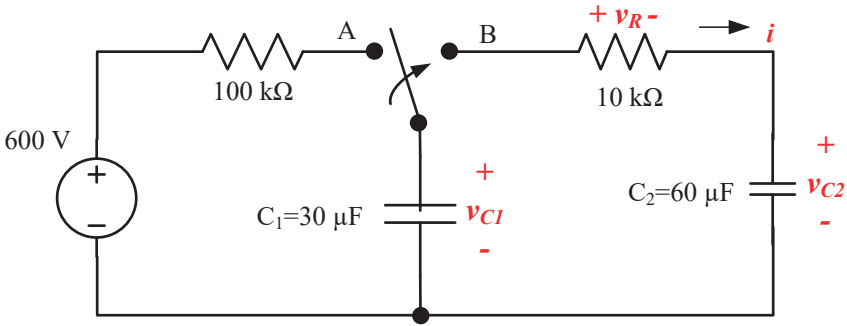


Figure-30.

Solution:

$$\mathbf{a)} \quad V_{C1}(2^-) = 600 \text{ V} = V_{C1}(2^+) \text{ and } \quad V_{C2}(2^-) = 0 = V_{C2}(2^+)$$

From the environmental equation for the moment $t = 2^+$;

$$V_R(2^+) = V_{C1}(2^+) - V_{C2}(2^+) = 600 \text{ V} \quad \text{It is found.}$$

$$\mathbf{b)} \quad C_e = \frac{30 \cdot 60}{30 + 60} = 20 \text{ } \mu\text{F} \text{ and } \quad R \cdot C_e = 10 \cdot 10^3 \cdot 20 \cdot 10^{-6} = 0,2 \text{ (1/sn)}$$

$$V_R(t) = V_{C_e}(t) = 60 \cdot \exp\left(-\frac{1}{0,2}t\right) = 60 \cdot \exp(-5t) \text{ V and } i(t) = \frac{V_R(t)}{R} = 6 \cdot \exp(-5t) \text{ mA}$$

It is found.

REFERENCES

1. KASAPOĞLU, A. (1996). *Devre Analizi*. Yıldız Teknik Üniversitesi Elektrik-Elektronik Fakültesi.
2. BOYLESTAD, R. L., & NASHELSKY, L. (2012). *Electronic devices and circuit theory*. Prentice Hall.
3. ALEXANDER, C. K., & SADİKU, M. N. (2000). *Fundamentals of electric circuits*. McGraw-Hill Education.
4. IRWIN, J. D., & NELMS, R. M. (2010). *Basic engineering circuit analysis* (Vol. 900). John Wiley & Sons.
5. ZENK, H., & GÜNER, F. (2022). ELECTRICAL CIRCUIT THEOREMS AND SIMULINK ANALYSIS. *International Research in Engineering*, 279.
6. FLOYD, T. L. (2012). *Electronic devices: conventional current version*. Pearson.
7. NİLSSON, J. W. (2008). *Electric circuits*. Pearson Education India.
8. ZENK, H. (2022). RESONANCE IN ELECTRICAL CIRCUITS. *International Research in Engineering*, 383.
9. HAYT, W. H., KEMMERLY, J. E., & DURBİN, S. M. (1986). *Engineering circuit analysis* (p. 74). New York: McGraw-Hill.
10. BOYLESTAD, R. L. (2010). *Introductory circuit analysis*. Pearson Education.
11. ZENK H., (2015). *Elektrik Mühendisliğine Giriş, Ders Notları*, Giresun Üniversitesi.
12. ZENK H., (2015). *Elektrik Devre Teorisi, Ders Notları*, Giresun Üniversitesi.